

Connecting Large and Small Vessels in Cerebrovascular Disease



Maarten Zwartbol

ISBN

978-94-93330-80-1

Cover illustration

Ammarens Lycklama à Nijeholt

Design, lay-out and print

Promotie In Zicht | www.promotie-inzicht.nl

© Maarten H.T. Zwartbol, 2024

All rights are reserved. No part of this book may be reproduced, distributed, stored in a retrieval system, or transmitted in any form or by any means, without prior written permission of the author. The copyright of the articles that have been published has been transferred to the respective journals.

Connecting Large and Small Vessels in Cerebrovascular Disease

Verbinding van grote en kleine vaten in cerebrovasculaire ziekten

(met een samenvatting in het Nederlands)

Proefschrift

ter verkrijging van de graad van doctor aan de
Universiteit Utrecht
op gezag van de
rector magnificus, prof. dr. H.R.B.M. Kummeling,
ingevolge het besluit van het college voor promoties
in het openbaar te verdedigen op

dinsdag 14 mei 2024 des middags te 2.15 uur

door

Maarten Hendrik Teunisz Zwartbol

geboren op 2 oktober 1985
te Meppel

Promotor

Prof. dr. J. Hendrikse

Copromotoren

Dr. M.I. Geerlings

Dr. A.G. van der Kolk

Beoordelingscommissie

Prof. dr. G.J. Biessels

Prof. dr. M.H. Emmelot-Vonk (voorzitter)

Prof. dr. ir. M.J.P. van Osch

Prof. dr. B.K. Velthuis

Prof. dr. A. van der Zwan

This research was supported by the European Research Council (grant agreement numbers 637024 and 66681).

Financial support by the Dutch Heart Foundation for the publication of this thesis is gratefully acknowledged.

Additional financial support was provided by Alzheimer Nederland (Amersfoort) and Noord Negentig.

"Do it. Just. Do. It."

- Shia LaBeouf

Contents

| | | |
|---|--|-----|
| Chapter 1 | General introduction | 9 |
| Part I. Vessel Wall Lesions and Intracranial Atherosclerosis on 7T MRI | | 19 |
| Chapter 2 | Intracranial vessel wall lesions on 7T MRI | 21 |
| Chapter 3 | Intracranial atherosclerotic burden on 7T MRI is associated with markers of extracranial atherosclerosis – the SMART-MR study | 45 |
| Chapter 4 | Intracranial atherosclerosis on 7T MRI and cognitive functioning: the SMART-MR study | 65 |
| Chapter 5 | Intracranial vessel wall lesions on 7T MRI and MRI features of cerebral small vessel disease – the SMART-MR study | 89 |
| Part II. Cerebral Microinfarcts on 7T MRI | | 107 |
| Chapter 6 | Cortical cerebral microinfarcts on 7T MRI: risk factors, neuroimaging correlates and cognitive functioning – the Medea-7T study | 109 |
| Chapter 7 | Microinfarcts in the deep gray matter on 7 Tesla MRI: risk factors, MRI correlates and relation to cognitive functioning. The SMART-MR study | 131 |
| Part III. White Matter Lesions, Cerebral Blood Flow and Brain Atrophy | | 151 |
| Chapter 8 | White matter hyperintensity shape is associated with cognitive functioning – the SMART-MR study | 153 |
| Chapter 9 | Reduced parenchymal cerebral blood flow is associated with greater progression of brain atrophy. The SMART-MR study | 175 |
| Chapter 10 | General discussion | 197 |
| Appendices | Nederlandse samenvatting | 213 |
| | About the author | 217 |
| | List of publications | 219 |
| | Dankwoord | 223 |



1

General introduction

General introduction

Cerebrovascular disease encompasses a variety of disorders affecting the cervical and intracranial blood vessels and cerebral blood flow.¹ The most severe outcome of these disorders is stroke, a leading global cause of death and long-term disability.² In the year 2019 alone, stroke was linked to 6.5 million deaths and accounted for 143 million disability-adjusted life years.² Moreover, cerebrovascular disease is a major contributor to cognitive decline and dementia, one of the major public health concerns of our time.^{3,4} Approximately 20% of stroke patients are diagnosed with dementia within a year of their stroke event.⁵ The global number of strokes, deaths and disability-adjusted life years has increased sharply in the past decades, and this trend is expected to continue in the coming decades.² This is attributed to growing and aging populations and rising adverse lifestyle factors in low and middle-income countries.²

Cerebrovascular disease: large and small vessel disease

The diseases of the cerebral vasculature are often divided into large vessel disease and small vessel disease (CSVD).^{6–8} Large vessel disease includes disorders affecting the large to middle-sized intradural arteries. Conversely, small vessel disease encompasses a diverse array of disorders that affect the smaller arteries, arterioles, capillaries and venules of the brain.⁹ In the aging brain, intracranial atherosclerosis (ICAS) represents the predominant type of large vessel disease, whereas and vascular risk factor–associated CSVD is the most common form of CSVD.¹⁰ Of note, in this thesis the term “large vessel disease” is used interchangeably with ICAS, as is “small vessel disease” with vascular risk factor–associated CSVD.

The main clinical manifestations of ICAS and CSVD are stroke and TIA.¹¹ However, there are significant differences between the two. The presentation of CSVD can vary, from clinically “silent” to overt ischemic or hemorrhagic stroke.¹² Moreover, CSVD is thought to contribute to 45% of all dementia cases.¹³ In contrast, ICAS has a higher risk of recurrent stroke and TIA and does not lead to hemorrhagic stroke. While ICAS is linked to cognitive decline and dementia, the exact attributable risk is still not known.

The difference in clinical presentation is largely mirrored in their MRI appearance. Namely, CSVD is correlated with various MRI markers, such as white matter hyperintensities (WMH) and lacunes of presumed vascular origin, recent small subcortical infarcts, microbleeds, enlarged perivascular spaces, cerebral atrophy and microinfarcts.^{9,14} Of note, the actual small vessels cannot yet be accurately visualized on MRI. ICAS is primarily characterized by arterial stenosis and cortical and subcortical infarcts.¹⁵

ICAS and CSVD both compete for the leading global cause of stroke. ICAS is likely the most frequent cause, although this is mainly because of a dominance in Asian populations, where it is implicated in 30-50% of all strokes.¹⁶ In White populations, ICAS is implicated in approximately 10% of strokes.¹⁶ CSVD is thought to account for around 20% of strokes worldwide with less regional variety.⁷

Large and small vessel disease: an outdated dichotomy?

Although in neuroimaging studies ICAS and CSVD are almost solely examined as distinct entities, post-mortem studies have revealed a significant overlap between these disorders.¹⁰ This overlap is mainly seen in terms of their co-occurrence, shared risk factors and pathological findings.¹⁰ A few *in vivo* studies have found similar associations, mainly between large vessel disease and small infarcts, i.e. cerebral microinfarcts and lacunes.^{17,18} However, their relation remains under debate.¹⁹

In our view, the relationship between ICAS and CSVD requires further investigation, because it may explain some of their heterogeneity. For example, the etiology and cognitive correlates of CSVD are heterogeneous and not fully understood.^{20–22} This heterogeneity might partially be caused by co-occurrence of ICAS, having parallel effects on cognitive functioning or causing CSVD-associated lesions. A better understanding of their relationship can help clarify this. One of the aims of this thesis is to study the relation between MRI markers of ICAS and CSVD.

Cognitive correlates of MRI markers of cerebrovascular disease

In recent decades, extensive research has been performed to understand the link between MRI markers of cerebrovascular disease and cognitive decline.^{23–25} As cerebrovascular disease, a significant contributor to cognitive decline, is potentially preventable, further understanding of their association is essential.²⁶ Studies have identified several MRI markers of CSVD, e.g. lacunes and WMH, that associate with cognitive dysfunction.^{17,23,24} Furthermore, neuroimaging studies on ICAS have shown associations between >50% arterial stenosis and cognitive dysfunction.^{20,27,28} These results emphasize the significance of identifying MRI markers that are associated with cognitive functioning.

Advancements in MRI technology, specifically on 7 Tesla (7T) MRI, in the prior decade have led to the development of several novel MRI markers of cerebrovascular disease, such as intracranial vessel wall lesions and cerebral microinfarcts.^{29–31} However, the cognitive implications of these novel MRI markers remain incompletely understood.

Intracranial vessel wall lesions are a novel marker of cerebral large vessel disease that can be visualized with vessel wall MR imaging (VW-MRI) on 7T brain MRI.^{30,32} In contrast to MR or CT angiography, VW-MRI enables imaging “beyond the lumen”, allowing visualization of the actual pathology in the vessel wall.^{30,33} Furthermore, it enables visualization of the smallest plaques, even those that do not cause stenosis.³³ Consequently, VW-MRI enables a more complete assessment of ICAS burden than conventional methods. A few neuroimaging studies have found that ICAS, defined as arterial stenosis, is correlated with cognitive impairment and dementia.^{27,28,34} However, this relationship has not yet been found in premorbid cognitive functioning. Vessel wall lesions — being a more comprehensive measure of ICAS burden — may facilitate the estimation of this relationship.

Cerebral microinfarcts have long been referred to as the “invisible lesion” because of their elusive presence on neuroimaging.³⁵ In 2013, these small ischemic lesions were first

recognized in living subjects using 7T brain MRI, which led to their identification on lower field strengths.³⁶ A few studies have shown a relation between microinfarcts and cognitive functioning.^{37–39} However, these findings are hard to generalize because of sample sizes or specific setting, e.g. memory clinics. Additional clarification in more diverse settings is warranted. Furthermore, the *in vivo* relationship between subcortical microinfarcts and cognitive functioning has not yet been studied.

WMH is an MRI marker of CSVD with an established detrimental effect on cognitive functioning.²¹ However, the overall correlation between WMH and cognitive function is weak.²¹ A possible explanation could be that conventional measures of WMH, such as WMH volume, do not correlate well with the severity of underlying brain pathology. Notably, histopathology studies have shown that the pathology underlying WMH is very heterogeneous, ranging from subtle gliosis to subtotal brain infarction.²² WMH shape features are a novel MRI marker that might be a better descriptor of the underlying pathological severity.^{40,41} The added value of WMH shape features over WMH volume in relation to cognitive functioning has not yet been studied.

Determinants of MRI markers of cerebrovascular disease

Understanding the cognitive correlates of MRI markers is vital to better comprehend the impact of cerebrovascular disease on cognitive functioning. However, it is equally important to identify their determinants, as they could offer potential opportunities for intervention.

Vessel wall lesions are thought to be the MRI correlate of atherosclerotic plaques.^{30,32} However, radiopathologic correlation studies are lacking.⁴² Furthermore, it would be erroneous to presume that the determinants of vessel wall lesions are equal to those of arterial stenosis. As mentioned previously, VW-MRI — especially on 7T MRI — visualizes much smaller lesions, including those without stenosis, possibly unrelated to conventional vascular risk factors. Correlation with known cardiovascular risk factors and other markers of atherosclerosis would further validate their potential as a novel MRI marker of ICAS.

The main etiological mechanisms associated with cerebral microinfarcts are thought to be CSVD, microemboli and hypoperfusion.¹⁴ Associations with cardiovascular risk factors, however, have been inconsistent.¹⁴ In addition, the correlation with other MRI markers that could aid in understanding their etiology, has been understudied. Furthermore, studies on the frequency and determinants of subcortical microinfarcts are non-existent.

Although not a novel MRI marker, cerebral atrophy is an MRI correlate of cerebrovascular disease of which the vascular etiology is unclear. Cerebral hypoperfusion is currently regarded as the most likely potential mechanism.^{43,44} However, it is unclear if hypoperfusion is a cause or a consequence, since atrophy may lower metabolic demand, thereby leading to reduced cerebral perfusion. The only longitudinal study on this relationship found that reduced brain volume preceded reduced cerebral perfusion.⁴⁵

Outline of this thesis

This thesis aims to study several emergent MRI markers of cerebrovascular disease, with a focus on their characteristics, determinants, and cognitive correlates, seeking to explore the relationship between ICAS and CSVD.

Part I of this thesis is focused on intracranial vessel wall lesions observed on 7T VW-MR imaging as a marker of ICAS. In **Chapter 2**, we describe their frequency, morphology, distribution and explore their association with vascular risk factors. Next, in **Chapter 3**, we look at their relationship with several markers of extracranial atherosclerosis (e.g., ankle-brachial index). In **Chapter 4**, we report on their association with cognitive functioning. In **Chapter 5**, we move beyond the dichotomy of large and small vessel disease and propose a more comprehensive approach. This chapter focuses on the relationship between intracranial vessel wall lesions and other MRI correlates of cerebrovascular disease, specifically CSVD markers.

In **Part II** we examine the smallest microvascular brain lesions observed on 7T brain MRI. Specifically, in **Chapter 6**, we focus on cortical microinfarcts and investigate their frequency, determinants and correlation with other cerebrovascular MRI markers, and their relation to cognitive functioning. In extension to this, in **Chapter 7**, we report on microinfarcts in the deep gray matter.

Part III focuses on WMH and cerebral atrophy. In **Chapter 8**, we explore the relation between WMH shape features, a novel metric of WMH, and cognitive functioning. Next, in **Chapter 9**, we examine the potential bidirectional relationship between cerebral blood flow and brain volume to elucidate the vascular contributions to brain atrophy.

To conclude, in **Chapter 10**, we will discuss the main findings of this thesis and propose directions for future research.

References

1. Sharma VK. Cerebrovascular Disease. In: Quah S, editor. *International Encyclopedia of Public Health*. 2nd ed. Oxford: Elsevier; 2016. 455–470 p.
2. Feigin VL, Stark BA, Johnson CO, Roth GA, Bisignano C, Abady GG, et al. Global, regional, and national burden of stroke and its risk factors, 1990–2019: A systematic analysis for the Global Burden of Disease Study 2019. *Lancet Neurol* 2021; 20: 1–26.
3. Bir SC, Khan MW, Javalkar V, Toledo EG, Kelley RE. Emerging Concepts in Vascular Dementia: A Review. *J Stroke Cerebrovasc Dis* 2021; 30: 105864.
4. Iadecola C, Duering M, Hachinski V, Joutel A, Pendlebury ST, Schneider JA, et al. Vascular Cognitive Impairment and Dementia: JACC Scientific Expert Panel. *J Am Coll Cardiol* 2019; 73: 3326–44.
5. Pendlebury ST, Rothwell PM. Prevalence, incidence, and factors associated with pre-stroke and post-stroke dementia: a systematic review and meta-analysis. *Lancet Neurol* 2009; 8: 1006–18.
6. Gutierrez J, Turan TN, Hoh BL, Chimowitz MI. Intracranial atherosclerotic stenosis: risk factors, diagnosis, and treatment. *Lancet Neurol* 2022; 21: 355–68.
7. Shi Y, Wardlaw JM. Update on cerebral small vessel disease: A dynamic whole-brain disease. *Stroke Vasc Neurol* 2016; 1: 83–92.
8. Leng X, Liebeskind DS, Qureshi AI, Caplan LR. Intracranial Atherosclerosis. In: Saba L, Raz E, editors. *Neurovascular Imaging*. New York: Springer New York; 2016. p. 205–32.
9. Wardlaw JM, Smith EE, Biessels GJ, Cordonnier C, Fazekas F, Frayne R, et al. Neuroimaging standards for research into small vessel disease and its contribution to ageing and neurodegeneration. *Lancet Neurol* 2013; 12: 822–38.
10. Grinberg LT, Thal DR. Vascular pathology in the aged human brain. *Acta Neuropathol* 2010; 119: 277–90.
11. Arenillas JF. Intracranial atherosclerosis: Current concepts. *Stroke*. 2011; 42(SUPPL. 1): s20–3.
12. Wardlaw JM, Smith C, Dichgans M. Mechanisms of sporadic cerebral small vessel disease: Insights from neuroimaging. *Lancet Neurol* 2013; 12: 483–97.
13. Cannistraro RJ, Badi M, Eidelman BH, Dickson DW, Middlebrooks EH, Meschia JF. CNS small vessel disease: A clinical review. *Neurology* 2019; 92: 1146.
14. van Veluw SJ, Shih AY, Smith EE, Chen C, Schneider JA, Wardlaw JM, et al. Detection, risk factors, and functional consequences of cerebral microinfarcts. *Lancet Neurol* 2017; 16: 730–40.
15. Wang Y, Meng R, Liu G, Cao C, Chen F, Jin K, et al. Intracranial atherosclerotic disease. *Neurobiol Dis* 2019; 124: 118.
16. Gorelick P, Wong KS, Liu L. Epidemiology. *Front Neurol Neurosci* 2016; 40: 34–46.
17. Wardlaw JM, Smith C, Dichgans M. Small vessel disease: mechanisms and clinical implications. *Lancet Neurol* 2019; 18: 684–96.
18. Degnan AJ. Underestimating the importance of middle cerebral artery atherosclerosis in lacunar stroke. *Cerebrovasc Dis* 2011; 32: 301.
19. Wardlaw JM. Response to the letter by A.J. Degnan titled “Underestimating the importance of middle cerebral artery atherosclerosis in lacunar stroke.” *Cerebrovasc Dis* 2011; 32: 302–303.
21. Kloppenborg RP, Nederkoorn PJ, Geerlings MI, Van Den Berg E. Presence and progression of white matter hyperintensities and cognition: A meta-analysis. *Neurology* 2014; 82: 2127–38.
22. Gouw AA, Seewann A, Van Der Flier WM, Barkhof F, Rozemuller AM, Scheltens P, et al. Heterogeneity of small vessel disease: A systematic review of MRI and histopathology correlations. *J Neurol Neurosurg Psychiatry* 2011; 82: 126–35.
23. Vemuri P, Decarli C, Duering M. Imaging Markers of Vascular Brain Health: Quantification, Clinical Implications, and Future Directions. *Stroke* 2022; 53: 416.
24. Frantellizzi V, Pani A, Ricci M, Locuratolo N, Fattapposta F, De Vincentis G. Neuroimaging in Vascular Cognitive Impairment and Dementia: A Systematic Review. *J Alzheimers Dis* 2020; 73: 1279–94.
25. Heiss WD, Rosenberg GA, Thiel A, Berlot R, de Reuck J. Neuroimaging in vascular cognitive impairment: A state-of-the-art review. *BMC Med* 2016; 14: 174.
26. Biessels GJ. Diagnosis and treatment of vascular damage in dementia. *Biochim Biophys Acta Mol Basis Dis* 2016; 1862: 869–77.
27. Suri MFK, Zhou J, Qiao Y, Chu H, Qureshi AI, Mosley T, et al. Cognitive impairment and intracranial atherosclerotic stenosis in general population. *Neurology* 2018; 90: e1240–47

28. Hilal S, Xu X, Ikram MK, Vrooman H, Venketasubramanian N, Chen C. Intracranial stenosis in cognitive impairment and dementia. *J Cereb Blood Flow Metab* 2017; 37: 2262–9.
29. De Cockler LJ, Lindenholz A, Zwanenburg JJ, van der Kolk AG, Zwartbol M, Luijten PR, et al. Clinical vascular imaging in the brain at 7T. *Neuroimage* 2018; 168: 452–58.
30. Hartevelde AA, Van Der Kolk AG, Van Der Worp HB, Dieleman N, Zwanenburg JJM, Luijten PR, et al. Detecting Intracranial Vessel Wall Lesions with 7T-Magnetic Resonance Imaging: Patients with Posterior Circulation Ischemia Versus Healthy Controls. *Stroke* 2017; 48: 2601–4.
31. van Veluw SJ, Zwanenburg JJM, Hendrikse J, van der Kolk AG, Luijten PR, Biessels GJ. High Resolution Imaging of Cerebral Small Vessel Disease with 7 T MRI. *Acta Neurochir Suppl* 2014; 119: 125–30.
32. van der Kolk AG, Zwanenburg JJM, Brundel M, Biessels GJ, Visser F, Luijten PR, et al. Intracranial vessel wall imaging at 7.0-T MRI. *Stroke* 2011; 42: 2478–84.
33. Alexander MD, Yuan C, Rutman A, Tirschwell DL, Palagallo G, Gandhi D, et al. High-resolution intracranial vessel wall imaging: imaging beyond the lumen. *J Neurol Neurosurg Psychiatry* 2016; 87: 589–97.
34. Dearborn JL, Zhang Y, Qiao Y, Suri MFK, Liu L, Gottesman RF, et al. Intracranial atherosclerosis and dementia. *Neurology* 2017; 88: 1556–63.
35. Smith EE, Schneider JA, Wardlaw JM, Greenberg SM. Cerebral microinfarcts: the invisible lesions. *Lancet Neurol* 2012; 11: 272–82.
36. Van Veluw SJ, Zwanenburg JJM, Engelen-Lee J, Spliet WGM, Hendrikse J, Luijten PR, et al. In vivo detection of cerebral cortical microinfarcts with high-resolution 7T MRI. *J Cereb Blood Flow Metab* 2013; 33: 322–9.
37. Van Veluw SJ, Hilal S, Kuijff HJ, Ikram MK, Xin X, Yeow TB, et al. Cortical microinfarcts on 3T MRI: Clinical correlates in memory-clinic patients. *Alzheimers Dement* 2015; 11: 1500–9.
38. Hilal S, Sikking E, Shaik MA, Chan QL, Van Veluw SJ, Vrooman H, et al. Cortical cerebral microinfarcts on 3T MRI: A novel marker of cerebrovascular disease. *Neurology* 2016; 87: 1583–90.
39. Ferro DA, van Veluw SJ, Koek HL, Exalto LG, Biessels GJ, Utrecht Vascular Cognitive Impairment (VCI) study group. Cortical cerebral microinfarcts on 3 Tesla MRI in patients with vascular cognitive impairment. *J Alzheimers Dis* 2017; 60: 1443–50.
40. Ghaznawi R, Geerlings MI, Jaarsma-Coes MG, Zwartbol MHT, Kuijff HJ, van der Graaf Y, et al. The association between lacunes and white matter hyperintensity features on MRI: The SMART-MR study. *J Cereb Blood Flow Metab* 2019; 39: 2486–96.
41. de Bresser J, Kuijff HJ, Zaanen K, Viergever MA, Hendrikse J, Biessels GJ, et al. White matter hyperintensity shape and location feature analysis on brain MRI; Proof of principle study in patients with diabetes. *Sci Rep* 2018; 8: 1–10.
42. Hartevelde AA, Denswil NP, Siero JCW, Zwanenburg JJM, Vink A, Pouran B, et al. Quantitative Intracranial Atherosclerotic Plaque Characterization at 7T MRI: An Ex Vivo Study with Histologic Validation. *AJNR Am J Neuroradiol* 2016; 37: 802–10.
43. De La Torre JC. Cardiovascular risk factors promote brain hypoperfusion leading to cognitive decline and dementia. *Cardiovasc Psychiatry Neurol* 2012; 2012: 367516.
44. Appelman APA, Van Der Graaf Y, Vincken KL, Tiehuis AM, Witkamp TD, Mali WPTMP, et al. Total cerebral blood flow, white matter lesions and brain atrophy: the SMART-MR study. *J Cereb Blood Flow Metab* 2008; 28: 633–9.
45. Zonneveld HI, Loehrer EA, Hofman A, Niessen WJ, Van Der Lugt A, Krestin GP, et al. The bidirectional association between reduced cerebral blood flow and brain atrophy in the general population. *J Cereb Blood Flow Metab* 2015; 35: 1882–7.

PART I

Vessel Wall Lesions and Intracranial Atherosclerosis on 7T MRI



2

Intracranial vessel wall lesions on 7T MRI

Maarten H.T. Zwartbol, Anja G. van der Kolk, Rashid Ghaznawi, Yolanda van der Graaf, Jeroen Hendrikse, Mirjam I. Geerlings, on behalf of the SMART Study Group

Published in *Stroke* 2019; 50: 88-94
doi: 10.1161/STROKEAHA.118.022509

Abstract

Intracranial vessel wall lesions are a novel imaging marker of intracranial atherosclerosis (ICAS), but data on their occurrence and risk factors are lacking. Our aim was to study the frequency, distribution and risk factors of intracranial vessel wall lesions on 7 tesla (7T) magnetic resonance imaging (MRI) in patients with a history of vascular disease.

Within the SMART-MR study cross-sectional analyses were performed in 130 patients (68±9 years) with assessable 7T intracranial vessel wall MRI data. Associations between vascular risk factors and ICAS burden, defined as the total number of vessel wall lesions, were estimated using linear regression analyses with ICAS burden as the dependent variable, adjusted for age and sex.

Ninety-six percent of patients had ≥1 vessel wall lesion. The mean±SD (range) ICAS burden was 8.5±5.7 (0-32) lesions. Significant associations were found between ICAS burden and age ($b = 2.0$ per +10 years; 95% CI 0.81 to 3.10), systolic blood pressure ($b = 0.9$ per +10 mmHg; 95% CI 0.27 to 1.42), diabetes ($b = 3.2$ for presence of diabetes; 95% CI 0.79 to 5.72), HbA1c level ($b = 1.2$ per +1%; 95% CI 0.19 to 2.26), apolipoprotein-B ($b = 4.7$ per +1 g/L; 95% CI 0.07 to 9.35), and CRP level ($b = 2.7$ for hs-CRP >3 mg/L; 95% CI 0.22 to 5.11). No significant associations were found with sex, smoking, and other lipid-factors.

Vessel wall lesions are a novel and direct MRI marker of ICAS. In this cohort, 96% of patients had at least one lesion on 7T vessel wall MRI. More lesions were found with older age, higher systolic blood pressure, diabetes and higher levels of HbA1c, apolipoprotein-B, and hs-CRP.

Introduction

Intracranial atherosclerosis (ICAS) is characterized by the development and progression of atherosclerotic plaques in the intracranial arteries. Symptomatic ICAS is one of the leading causes of ischemic stroke worldwide, and as such responsible for considerable morbidity and mortality.^{1,2} Other complications are an increased risk of recurrent stroke, transient ischemic attacks (TIA) and dementia.^{1,3} Studies report widely varying prevalence estimates of ICAS, ranging from 3% to 95%, depending on the specific population studied and imaging methods used.⁴

Intracranial arterial vessel wall lesions are a novel MRI marker of ICAS that can be visualized using high-resolution vessel wall MRI (VW-MRI). Vessel wall lesions have several potential advantages over conventional indirect markers such as stenosis and calcification.⁵ First, both stenotic and non-stenotic ICAS can be visualized, enabling a more complete assessment of ICAS burden.⁶ Furthermore, cerebral arteries do not calcify distal to the Circle of Willis (CoW) arteries, limiting assessment of this marker to the proximal arteries. Also, the etiology of calcification remains uncertain, and may in part be unrelated to atherosclerosis.

Vessel wall MRI studies have mainly been aimed at technical advancements, plaque characterization, and diagnostic efficacy.^{7,8} So far, only one study has reported on the risk factors and prevalence of vessel wall lesions.⁹ Assuming these to be identical to those of conventional ICAS markers may limit its utility. Also, risk factors and prevalence estimates differ between vessel wall lesions, calcification and stenosis.^{5,9,10} Age, diabetes, hypertension, and systolic blood pressure seem to show consistent associations with different ICAS markers. However, a definite risk factor model remains to be established.¹¹

This study had two main objectives. First, to study the frequency, distribution and burden of intracranial vessel wall lesions, assessed by means of intracranial VW-MRI at 7 tesla (7T), in a population of patients with a history of vascular disease; and second, to explore possible risk factors of this novel and direct marker of ICAS and relate these to known ICAS risk factors.

Methods

Study population

Data were used from the Second Manifestations of ARterial disease-Magnetic Resonance (SMART-MR) study, which is a prospective cohort study at our institution with the aim to investigate risk factors and clinical correlates of MRI neuroimaging markers in patients with vascular disease.¹² In brief, from 2001 through 2005, 1309 patients newly referred to our institution with coronary artery disease, cerebrovascular disease, peripheral arterial disease or abdominal aortic aneurysm, and without MRI contraindications were enrolled in the

SMART-MR study. On a one-day visit to our institution's hospital the participants received a 1.5T MRI of the brain, a physical examination, ankle-brachial index assessment, ultrasonography of the carotid arteries, blood and urine sampling, and questionnaires to assess risk factors, medical history, and daily functioning.¹³ All risk factors were assessed on the same day. Follow-up exams of the SMART-MR cohort were performed in 2006-2009 (first follow-up), and 2013-2017 (second follow-up).

A flowchart of the study sample is presented in Supplemental Figure 1. In brief, from June 2016 to October 2017, during the second follow-up period, a vessel wall MRI sequence was performed, as part of a standard 7T MRI of the brain. All patients who had received vessel wall imaging during this timeframe were included. A total of 147 patients were included, of which 17 were excluded due to artifacts inhibiting vessel wall assessment of ≥ 1 major segment of the Circle of Willis (CoW; major segments included the distal internal carotid artery and primary branches (M1, A1, P1) of the anterior, middle and posterior cerebral artery), leaving 130 patients for final analysis. Note, 7T MRI was performed one average 13 ± 1 years after baseline measurements. Risk factor assessment, including questionnaire data and blood and urine sampling, was performed median 2.3 (range, 0.6 to 8.6) years prior to the 7T MRI.

Comparison of age and sex between excluded and included patients showed that excluded patients were older, although this did not reach statistical significance (70 ± 7 vs. 68 ± 9 years; $p = 0.11$). Sex distribution did not differ (88% vs. 88% male; $p = 0.95$).

The SMART-MR study was approved by the institutional review board of our institution and written informed consent was obtained from all participants.

Vascular risk factors

Age, sex, smoking and alcohol usage were assessed using questionnaires. Weight and height measured without shoes and heavy clothing were used to calculate the body mass index (BMI; kg/m^2). Obesity was defined as a BMI $\geq 30 \text{ kg}/\text{m}^2$. Systolic blood pressure (SBP; mmHg) and diastolic blood pressure (DBP; mmHg) were measured by averaging three separate measurements with a sphygmomanometer. Hypertension was defined as a SBP of $>140 \text{ mmHg}$, a mean DBP of $>90 \text{ mmHg}$, or self-reported use of antihypertensive drugs. Fasted venous blood samples were taken to determine fasting glucose, hemoglobin A1c (HbA1c) levels, lipid levels, and high-sensitive C-reactive protein (hs-CRP). Diabetes mellitus was defined as fasting serum glucose levels of $\geq 7.0 \text{ mmol}/\text{L}$, and/or use of glucose-lowering medication, and/or a known history of diabetes. Patients not meeting these criteria, but with a fasting plasma glucose level $\geq 7.0 \text{ mmol}/\text{L}$ at baseline, were considered to have diabetes at baseline if they received treatment with glucose-lowering medication within 1 year after baseline.¹⁴ Hyperlipidemia was defined as a total cholesterol of $>5.0 \text{ mmol}/\text{L}$, a low-density lipoprotein cholesterol of $>3.2 \text{ mmol}/\text{L}$, or use of lipid-lowering medication. Metabolic syndrome was determined by the National Cholesterol Education Program Adult Treatment Panel III criteria.¹⁵ Serum hs-CRP was determined by immunonephelometry

(Nephelometer Analyzer BN II, Dade-Behring, Germany) with a lower detection limit of 0.1 mg/L. Hs-CRP measurements below the lower limit of the detection limit of 0.1 mg/L were set at 0.1 mg/L. Genotyping for APOE was performed on coded DNA specimens without knowledge of the diagnosis.¹⁶

MR Imaging

For MR imaging, a 7T whole-body system (Philips Healthcare, Cleveland, OH, USA) was used with a volume/transmit coil for transmission and a 32-channel receive head coil (Nova Medical, Wilmington, MA, USA). Intracranial vessel wall imaging was performed with a T₁-weighted Magnetization-Prepared Inversion Recovery Turbo Spin Echo (T₁-MPiR-TSE) sequence, with the following parameters: field-of-view (FOV) 250x250x190 mm³, acquired resolution 0.8x0.8x0.8 mm³ (reconstructed to 0.49x0.49x0.4 mm³), repetition time (TR) / inversion time (TI) / echo time (TE) 3952/1375/37 ms, acquisition time 10:40 minutes (min). A more detailed description of this MR sequence can be found elsewhere.¹⁷ A maximum intensity projection (maxIP) of the first echo of a dual echo susceptibility-weighted imaging (SWI) sequence was used as a faux MR angiography (MRA), with the following parameters: TR/TE1/TE2, 20/6.9/15.8 ms; FOV 200x200x120 mm³; acquired resolution 0.5x0.5x0.7 mm³ (reconstructed to 0.4x0.4x0.35 mm³); flip angle 12 degrees; acquisition time, 09:17 min.

Assessment of intracranial atherosclerosis

For image assessment, transverse multiplanar reconstructions (MPRs) were made from the T₁-MPiR-TSE sequence (slice thickness 0.8 mm; no slice gap), all angulated according to the nasion-foramen magnum line and using a standalone workstation (Philips Healthcare, Cleveland, OH, USA).

All images were assessed, blinded to patient characteristics, by one observer (MZ) who was trained by a senior observer with 8 years of experience in reading intracranial vessel wall images (AK). Training was based on a practice set of 15 patients from the Intracranial Vessel wall Imaging (IVI) study, a study population of patients with anterior circulation ischemic stroke and transient ischemic attack¹⁸, and a consensus set of 20 patients from the current study. An interobserver agreement was calculated between AK and MZ using the dice similarity coefficient (DSC) based on results from the consensus set. A coefficient of 0.75 was achieved and was regarded as good.

Vessel wall lesions were rated according to criteria described previously.¹⁹ In short, a vessel wall lesion was defined as either a clear focal or more diffuse thickening of the vessel wall, compared with the healthy contralateral or neighboring vessel wall. Inconspicuous lesions were evaluated in multiple planes for verification. Vessel wall lesions were rated per arterial segment, which included: the anterior cerebral arteries (ACA; A1, A2 segments), middle cerebral arteries (MCA; M1, M2 segments), distal internal carotid arteries (ICA; supraclinoid (C6) and communicating segment (C7)), posterior communicating

arteries (PCom), posterior cerebral arteries (PCA; P1, P2 segments, P1-P2 bifurcation), basilar artery and vertebral arteries. Arterial segments could contain multiple lesions. Lesions in bifurcations that stretched into multiple segments (e.g., from C7 segment into M1 segment) were counted as separate lesions for each affected segment. The maxIP of the SWI was used as a faux MRA to assess the course of the smaller arterial segments (M2, A1, P2, PCom). However, because of its sensitivity to artefacts (flow-related signal loss, susceptibility effects), we could not use it to reliably measure luminal stenosis.

Statistical analysis

First, characteristics of the study sample were calculated. Second, frequencies and distribution characteristics of vessel wall lesions were calculated per arterial segment, artery and circulatory region. Third, linear regression analysis was used to estimate associations between vascular risk factors and ICAS burden. Adjustments were made for age and sex. A sensitivity analysis was performed to control for the time interval (in days) between the date of risk factor measurements and date of the 7T MRI. Residual plots of all analyses were checked for regression assumptions. Alcohol use was entered into the model as a categorical variable (<1, 1-10, or ≥ 11 units per week). Smoking was entered into the model as a continuous (pack-years) or categorical (never, former, or current) variable. BMI was entered as a continuous variable and also dichotomized by clinical cut-off for obesity (cut-off ≥ 30 kg/m²). Hs-CRP was entered as a continuous variable and as a dichotomous variable (cut-off >3 mg/L).²⁰ APOE- $\epsilon 4$ allele status was entered into the model as a dichotomous variable: ≥ 1 $\epsilon 4$ allele versus no presence.

Statistical analyses were performed using IBM SPSS Statistics version 21 for Windows (IBM Corporation, Armonk, NY, USA).

Results

Characteristics of the 130 patients in our study sample (68 ± 9 years; 88% male) are presented in Table 1. Ninety-six percent of patients had evidence of ≥ 1 vessel wall lesion. A mean number of 8.5 ± 5.7 vessel wall lesions (median 7; range 0 - 32) were identified in the total cerebral circulation, with 5.3 ± 3.2 lesions (median 4; range 0 - 14) in the anterior, and 3.8 ± 3.0 (median 3; range 0-18) in the posterior circulation (table 2). A higher ICAS burden was found in patients with a history of cerebrovascular disease (10.9 ± 7.4 vs. 7.3 ± 4.9 lesions; $p = 0.01$). On the arterial level, lesions were most frequently identified in the distal ICAs (70% (left) - 62% (right) of patients) and basilar artery (59%). Figure 1 provides a schematic overview of the distribution and frequency of vessel wall lesions per segment. Examples of intracranial vessel wall lesions on MRI are provided in Figure 2. A more detailed overview of the number of vessel wall lesions per segment, artery and circulatory region is provided in Supplemental Table 1.

Table 1. Vascular risk factors in study population (n = 130).

| Conventional vascular risk factors | |
|--|-------------|
| Age (years) | 68 ± 9 |
| Male sex | 88% |
| Smoking status | |
| Current smoker | 15% |
| Former smoker | 71% |
| Pack-years | 21.7 ± 18.4 |
| Alcohol intake (units/week) | 2.0 ± 1.0 |
| Hypertension | 90% |
| Systolic blood pressure (mmHg) | 139 ± 17 |
| Diastolic blood pressure (mmHg) | 79 ± 9 |
| Metabolic vascular risk factors | |
| BMI (kg/m ²) | 27.3 ± 3.7 |
| Obesity* | 21% |
| Hyperlipidemia | 93% |
| Lipids, mmol/L | |
| Triglycerides | 1.5 ± 0.7 |
| LDL-C | 2.4 ± 0.8 |
| HDL-C | 1.3 ± 0.4 |
| Total | 4.4 ± 0.9 |
| Apo-B (g/L) | 0.8 ± 0.2 |
| Diabetes | 19% |
| HbA1c (%) | 5.9 ± 0.9 |
| Fasting glucose (mmol/L) | 6.3 ± 1.7 |
| Metabolic syndrome | 52% |
| Miscellaneous vascular risk factors | |
| hs-CRP (mg/L) | 2.6 ± 3.7 |
| hs-CRP > 3 mg/L | 20% |
| ≥1 APOE-ε4 allele | 30.8% |
| History of vascular disease† | |
| Cerebrovascular disease | 25% |
| Coronary artery disease | 79% |
| Abdominal aortic aneurysm | 2% |
| Peripheral artery disease | 19% |

Note: values are presented as mean ± SD for continuous variables and frequencies (%) for dichotomous variables.

* BMI ≥ 30 kg/m².

† Twenty-five percent of 130 patients had >1 vascular disease. Seven percent had cerebrovascular disease only. Abbreviations: BMI, body mass index; LDL, low-density lipoprotein; HDL, high-density lipoprotein; Apo-B, apolipoprotein B; HbA1c, hemoglobin A1c; APOE, apolipoprotein E; hs-CRP, high-sensitivity C-reactive protein.

Table 2. Overview of frequency and statistical dispersion of arterial wall lesions in circulatory regions in study population.

| Circulatory region | Frequency | Median (range) | Mean \pm SD |
|-----------------------|-----------|----------------|---------------|
| Total circulation | 96% | 7 (0-32) | 8.5 \pm 5.7 |
| Anterior circulation | 92% | 4 (0-14) | 5.3 \pm 3.2 |
| Posterior circulation | 88% | 3 (0-18) | 3.8 \pm 3.0 |

Note: a complete overview, including data of individual arteries and segments, is provided in Supplemental Table 1.

Abbreviations: SD, standard deviation.

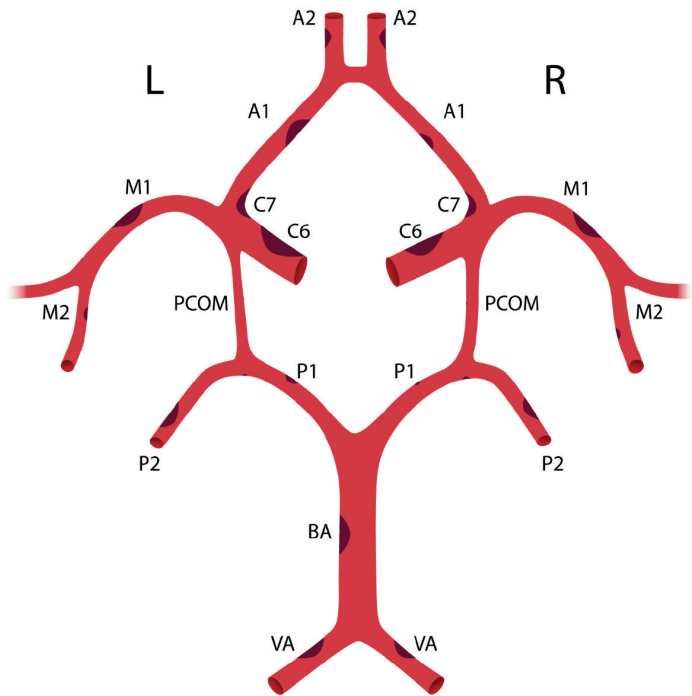


Figure 1. Schematic drawing of the Circle of Willis and its branches, with the frequency of intracranial vessel wall lesions in the current study population illustrated by means of ‘plaques’: a larger plaque indicates a higher frequency of lesions within the specific segment (see Supplemental Table 1).

Left: C6 = 63.1%; C7 = 42.3%; A1 = 35.4%; A2 = 30.0%; M1 = 49.2%; M2 = 20.0%; VA = 38.5%; P1 = 19.2%; P1-P2 bifurcation = 6.2%; P2 = 37.7%; PCom = 2.3%. Middle: BA = 58.5%. Right: C6 = 56.2%; C7 = 38.5%; A1 = 21.5%; A2 = 30.8%; M1 = 43.1%; M2 = 16.9%; VA = 30.0%; P1 = 9.2%; P1-P2 bifurcation = 12.3%; P2 = 31.5%; PCom = 5.4%.

Abbreviations: VA, vertebral artery; PCom, posterior communicating artery; BA, basilar artery.

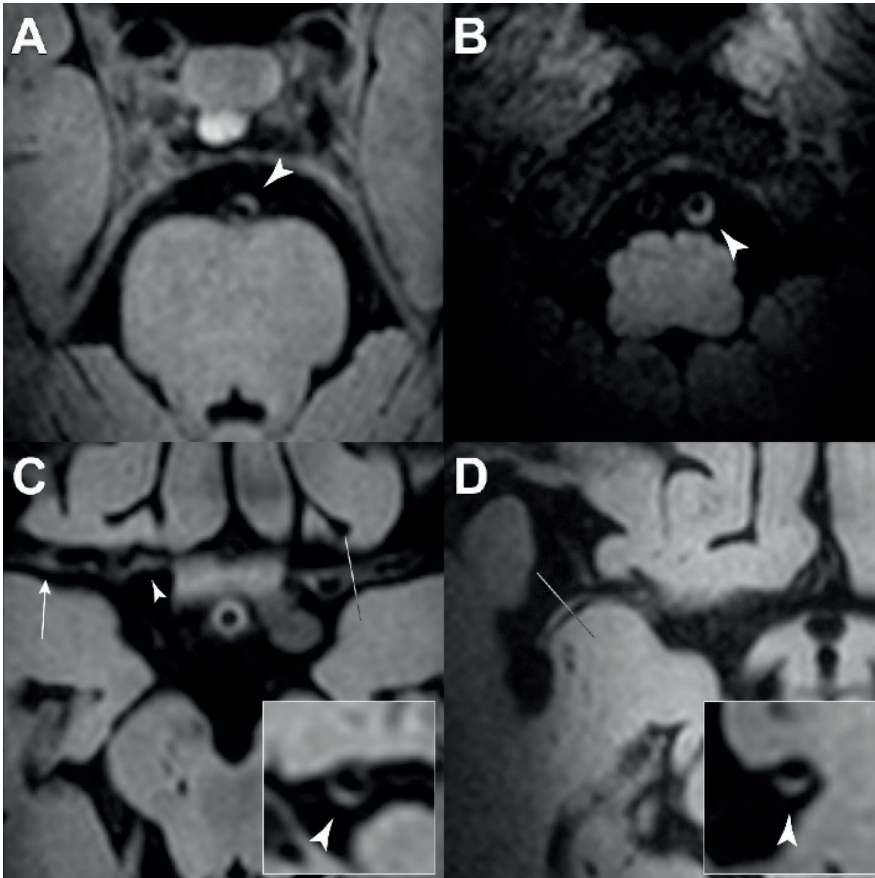


Figure 2. A 79-year-old male patient included with a history of coronary heart disease. On T₁-MPIR-TSE vessel wall MRI multiple lesions are identified (**A-D**). **A**) Vessel wall lesion of the basilar artery (arrowhead). **B**) Vessel wall lesion of the distal left vertebral artery (arrowhead) with normal right vertebral artery. **C**) Bilateral M1 vessel wall lesions (arrow, and arrowhead in sagittal MPR in enclosed panel). Also, note lesion in the proximal right A1 segment (small arrowhead). **D**) Vessel wall lesion in the proximal right M2 segment.

Table 3 reports the association between conventional vascular risk factors and ICAS burden. Increasing age was associated with a higher ICAS burden ($b = 2.0$ lesions per +10 years; 95% CI 0.84 to 3.14). Also, a significant association was observed between increasing SBP and ICAS burden ($b = 0.8$ lesions per +10 mmHg; 95% CI 0.27 to 1.42). No significant association was found between sex, smoking, alcohol intake, DBP or hypertension and ICAS burden.

Table 3. Association of conventional risk factors with ICAS burden.

| | ICAS burden, <i>b</i> (95% CI) | <i>p</i> value |
|------------------------------|--------------------------------|----------------|
| Male sex | 1.31 (-1.65 to 4.26) | 0.384 |
| Age, per +10 years | 1.96 (0.81 to 3.10) | 0.001 |
| Smoking status | | |
| Never smoker | 0 (reference) | |
| Former smoker | 0.21 (-2.68 to 3.09) | 0.887 |
| Current smoker | 0.24 (-3.40 to 3.89) | 0.895 |
| Pack-years, per +10 years | 0.33 (-0.20 to 0.86) | 0.224 |
| Alcohol intake | | |
| No or 1 < unit/week | 0 (reference) | |
| 1-10 units/week | -0.87 (-3.33 to 1.59) | 0.486 |
| ≥11 units/week | -1.36 (-4.08 to 1.37) | 0.326 |
| Hypertension, y/n | -0.83 (-4.12 to 2.47) | 0.620 |
| Blood pressure, per +10 mmHg | | |
| Systolic | 0.85 (0.27 to 1.42) | 0.004 |
| Diastolic | 0.51 (-0.59 to 1.61) | 0.361 |

Note: *b* values are unstandardized linear regression coefficients adjusted for age and sex.

Table 4 reports the association between metabolic and miscellaneous vascular risk factors with ICAS burden. Several metabolic risk factors were found to be significantly associated with a higher ICAS burden, namely: diabetes ($b = 3.3$ for presence of diabetes; 95% CI 0.81 to 5.73), Hba1c level ($b = 1.2$ lesions per +1%; 95% CI 0.20 to 2.27), and apolipoprotein-B ($b = 4.7$ per +1 g/L; 95% CI 0.03 to 9.29). Although positive trends were seen for obesity, metabolic syndrome, hyperlipidemia, total cholesterol levels and triglyceride levels, these did not reach statistical significance. In regard to miscellaneous risk factors, a significant association was found between increased hs-CRP and ICAS burden ($b = 2.8$ for hs-CRP >3.0 mg/L; 95% CI 0.30 to 5.24), when compared to normal hs-CRP (≤ 3.0 mg/L). No association was found between presence of ≥ 1 APOE- $\epsilon 4$ allele and ICAS burden.

As a sensitivity analysis, all models were additionally adjusted for the time interval between risk factors measurement and date of 7T MRI. Supplemental Table 2 and Supplemental Table 3 present the results of these analyses. As can be seen, although the estimates somewhat differed, this did not lead to different conclusions.

Eccentric versus concentric vessel wall lesions

An extensive overview of the number and ratio of eccentric and concentric vessel wall lesions is provided in Supplemental Table 4. Eccentric lesions were found in 95% of

Table 4. Association of metabolic and miscellaneous risk factors with ICAS burden.

| | ICAS burden, <i>b</i> (95% CI) | <i>p</i> value |
|-------------------------------|--------------------------------|----------------|
| BMI, per +1 kg/m ² | 0.10 (-0.18 to 0.38) | 0.463 |
| Obesity*, y/n | 2.31 (-0.22 to 4.83) | 0.073 |
| Hyperlipidemia, y/n | 3.37 (-0.49 to 7.22) | 0.087 |
| Lipids, per +1 mmol/L | | |
| Triglycerides | 1.28 (-0.16 to 2.72) | 0.082 |
| LDL-C | 1.00 (-0.23 to 2.23) | 0.110 |
| HDL-C | -0.23 (-3.04 to 2.58) | 0.815 |
| Total | 1.03 (-0.03 to 2.10) | 0.057 |
| Apo-B, per +1 g/L | 4.70 (0.07 to 9.35) | 0.047 |
| Diabetes, y/n | 3.24 (0.79 to 5.72) | 0.010 |
| HbA1c, per % increase | 1.22 (0.19 to 2.26) | 0.021 |
| Glucose, per +1 mmol/L | 0.39 (-0.18 to 0.97) | 0.180 |
| Metabolic syndrome, y/n | 1.85 (-0.10 to 3.80) | 0.062 |
| ≥1 APOE-ε4 allele, y/n | -1.48 (-3.63 to 0.67) | 0.175 |
| hs-CRP, per +1 mg/L | 0.02 (-0.26 to 0.30) | 0.882 |
| hs-CRP >3 mg/L, y/n | 2.67 (0.22 to 5.11) | 0.033 |

Note: *b* values are unstandardized linear regression coefficients adjusted for age and sex.

Abbreviations: BMI, body mass index; LDL-C, low-density lipoprotein; HDL-C, high-density lipoprotein; Apo-B, apolipoprotein B; HbA1c, hemoglobin A1c; APOE, apolipoprotein E; hs-CRP, high-sensitivity C-reactive protein.

* BMI ≥ 30 kg/m².

patients, whereas concentric lesions were found in 26% of patients. Furthermore, 75% of all lesions were eccentric, compared to 25% for concentric lesions. The age and sex-adjusted relative risk (RR) of concentric lesions increased significantly with increasing numbers of eccentric lesions, (RR = 1.03 per +1 eccentric lesion; 95% CI 1.01 to 1.04).

Discussion

In this cohort of 130 patients with a history of vascular disease, more than 95% of patients had at least one intracranial vessel wall lesion. Risk factors for these vessel wall lesions were older age, higher systolic blood pressure, diabetes, increased hemoglobin A1c and apolipoprotein-B and C-reactive protein levels. A trend was found for obesity, hyperlipidemia, metabolic syndrome and higher total cholesterol and triglyceride levels.

Recently, the Atherosclerosis Risk in Communities (ARIC) study was the first study to use high-resolution vessel wall MR imaging at 3T to assess vessel wall lesions, as a measure

of ICAS, in a large population-based cohort, and reported a prevalence of ≥ 1 vessel wall lesion in 36% of participants.⁹ This was higher than prevalence estimates from prior population-based studies based on detection of (hemodynamically-significant) stenosis, which reported estimates from 3% to 15%.¹ In cohorts with vascular risk this increases to 13-21%, and tops out at 40-67% in ischemic stroke patients.¹ Studies based on intracranial calcifications report estimates up to 80%, although the etiology of this marker is uncertain.⁵ Our reported high frequency of 96% is likely due to two factors. First, our cohort consisted of vascular disease patients and 88% were male. Hence, assuming ICAS has similar determinants as extracranial atherosclerosis, they are likely at risk of developing ICAS. Second, although our reconstructed spatial resolution is similar to the ARIC study, the increased MR signal at 7T was used to optimize the contrast-to-noise ratio (CNR), which may have enabled us to grade lesions with more certainty. All current vessel wall sequences are limited due to partial volume averaging. Increased CNR counteracts this limitation, and likely reduces both false-positives and false-negatives.²¹ Of note, 75% of our population had symptomatic atherosclerosis in extracranial arteries only. Although the mean ICAS burden in this group was lower than in patients with cerebrovascular disease, it was still considerable, and underlines that atherosclerosis is a generalized disease with varying symptomatic arteries.

A relatively regular distribution of vessel wall lesions was found, with the highest frequency in both distal ICAs and the basilar artery, which is in concordance with previous studies.^{18,22,23} Most lesions were of the eccentric type, although in the anterior cerebral arteries and vertebral arteries, concentric lesions occurred with a similar frequency. Furthermore, increasing numbers of eccentric lesions were associated with a higher risk of concentric lesions. This finding seems to suggest that concentricity is related to the overall severity of ICAS. Several factors may explain the higher frequency of lesions in the ICAs and basilar artery. First, it is thought that the proximal intracranial arteries – as opposed to the remaining intracranial vasculature – still possess vasa vasorum, which facilitates arterial wall functioning and plays a critical role in atherogenesis via initiation of an inflammatory cascade. Second, the distal ICA is a segment exposed to low shear stress, which is a hemodynamic risk factor for plaque formation.²⁴ Third, the distal ICA and the basilar artery have the largest radius of all intracranial arteries, which has been associated with the degree of atherosclerosis.²² Of course, lesions are harder to detect in smaller arteries. However, when grading lesions, the distal, proximal, and contralateral healthy segment was used as reference, as a way to mitigate this limitation which is inherent to current spatial resolutions. Last, it should be noted that artifacts hindered assessment of the vertebral arteries in 20-24% of cases and M2 segments in 6-9% of cases (see Supplemental Table 1). Therefore, the prevalence of vessel wall lesions at these locations may be higher than reported.

Older age, higher systolic blood pressure, diabetes, higher hemoglobin A1c and apolipoprotein-B levels, and hs-CRP >3 mg/L were associated with more vessel wall

lesions, which is largely in concordance with previous studies based on arterial stenosis detection.^{4,25,26} In the ARIC study, which tested associations between mid-life risk factors and late-life ICAS (stratified by race), presence of vessel wall lesions was associated with age, mid-life hypertension and hyperlipidemia in both blacks and whites. Sex, mid-life smoking and diabetes were exclusively associated with vessel wall lesions in blacks. Analysis with late-life risk factors, which more closely resembles our analysis, failed to show an association, which they note “could partly stem from reverse causation”.⁹ Our results are partly in concordance with their findings, although we did not find a significant association with hyperlipidemia. However, hyperlipidemia, obesity, metabolic syndrome, higher total cholesterol, and triglyceride levels all showed a statistical trend with more vessel wall lesions. No significant relationship was found with sex, hypertension, cigarette smoking, alcohol intake, other cholesterol levels (HDL-C, LDL-C), and APOE-ε4 allele status. Several factors may explain the absent or marginal associations between vessel wall lesions and these risk factors. First, the relationship of these factors with conventional markers such as arterial stenosis and calcification is also uncertain^{4,9–11,27–36}, and most were also not found in the ARIC study. In regard to lipid-related determinants, a reduced susceptibility of the intracranial arteries to cholesterol-induced atherogenesis might explain these inconsistencies.³⁷ Second, due to the follow-up design of the SMART study, changes in lifestyle and start of medical treatment due to risk factors detected at baseline is likely to weaken associations with those risk factors. Third, the modest size of our cohort, although large for a clinical 7T study, may have reduced statistical power to find significant associations, especially for dichotomous variables with highly skewed frequency distributions, such as sex and hypertension. Fourth, our use of a cumulative ‘burden’ score might favor certain risk factors and attenuate the relationship with others. For example, intima-media thickening is a more diffuse multifocal process and is linearly related to systolic blood pressure.³⁸ Stenosis is a more focal advanced lesion and closely associated with lipid disorders.³⁹ Following from this, our score would favor risk factors which are related to more lesions, and not so much the severity of a focal lesion. Lastly, due to a lack of radio-pathologic correlation studies it is uncertain if all lesions observed in our study are of atherosclerotic etiology.

So far, the ARIC study is the only other study that has investigated intracranial vessel wall lesions in non-stroke patients in vivo using vessel wall MRI. Although the associations between vessel wall lesions and common cardiovascular risk factors in both the ARIC and our study are similar, the novelty of our results lies in the fact that almost all included subjects showed vessel wall lesions, compared to 36% of patients in the ARIC study. Although this result indeed confirms previous reports of pathological studies, this confirmation also suggests that 7T vessel wall MRI can visualize the ‘real’ lesion burden, due to its high spatial resolution and contrast-to-noise ratio. One could argue that the additional, possibly smaller lesions that we see at 7T may not always be clinically relevant, and perhaps represent normal ageing; however, the observation that correlations with risk

factors remained even for this high percentage of subjects with vessel wall lesions suggests that the majority of these lesions are representative of the total vessel wall lesion burden. The impact of this study lies in that 7T vessel wall MRI seems to be able to visualize the total intracranial vessel wall lesion burden, compared to 3T MRI which only shows vessel wall lesions in a relatively small percentage of patients. This may also suggest that 7T MRI, not 3T MRI, should be used for e.g., screening of vessel wall lesions in patient populations with increased risks. Nonetheless, the clinical implications of these lesions are not yet clear, and long-term prospective studies are needed to investigate whether the observed total lesion burden will be clinically relevant, or whether other factors like enhancement and other lesion characteristics play a more prominent role.

Future studies on ultra-high field vessel wall imaging could focus on updating current MRI sequences, to keep up with advancements at lower field strengths, and more extensive histopathologic validation studies. In addition, more complex multiparametric scores, such as the Gensini-score for coronary heart disease, are an interesting direction of research which should be further explored. Current multisequence neurovascular MRI protocols can assess the number, location, stenosis, and biology of ICAS lesions. Hence, with the prevalence and functional impact of ICAS becoming more apparent, and the advent of therapeutic options, multiparametric scores like these will provide a more versatile way to study the relationship between treatment of risk factors, ICAS and outcomes. Furthermore, since ICAS phenotypes differ between ethnic populations, studies could investigate if tailoring multisequence MRI protocols to the patients' ethnicity improves effectiveness and efficiency of the study. Finally, and this is relevant both for 3T and 7T intracranial vessel wall imaging, there will be a need for longitudinal studies investigating the clinical relevance of the visualized vessel wall lesions.

Our study has several strengths. First, the increased MR signal at 7T field strength was used to optimize the contrast-to-noise ratio and enabled accurate visualization of wall pathology. Second, the large coverage area allowed assessment of the CoW branches over a great length. Hence, with regard to the assessment of ICAS in general, one could argue that it enabled a more complete assessment compared to studies based on calcification, which is limited to the large cerebral arteries, and stenosis, which ignores non-stenotic pathology. Further, completeness of data on a variety of determinants allowed us to perform an extensive exploratory analysis. Lastly, our ICAS burden metric is a basic uniparametric score, which makes it robust and easy to understand and implement. However, it is also limited, since it lacks information on luminal stenosis, which cannot accurately be measured. Also, we did not use any other sequences specifically aimed at characterization of the vessel wall; including this information might have additional value in the development of future multiparametric scores. Apart from the already mentioned limitations, the cross-sectional design is also a limitation, because it prohibits conclusions regarding causality. Furthermore, due to logistic reasons the risk factor assessment and the 7T MRI were not performed on the same day and in a number of participants the time

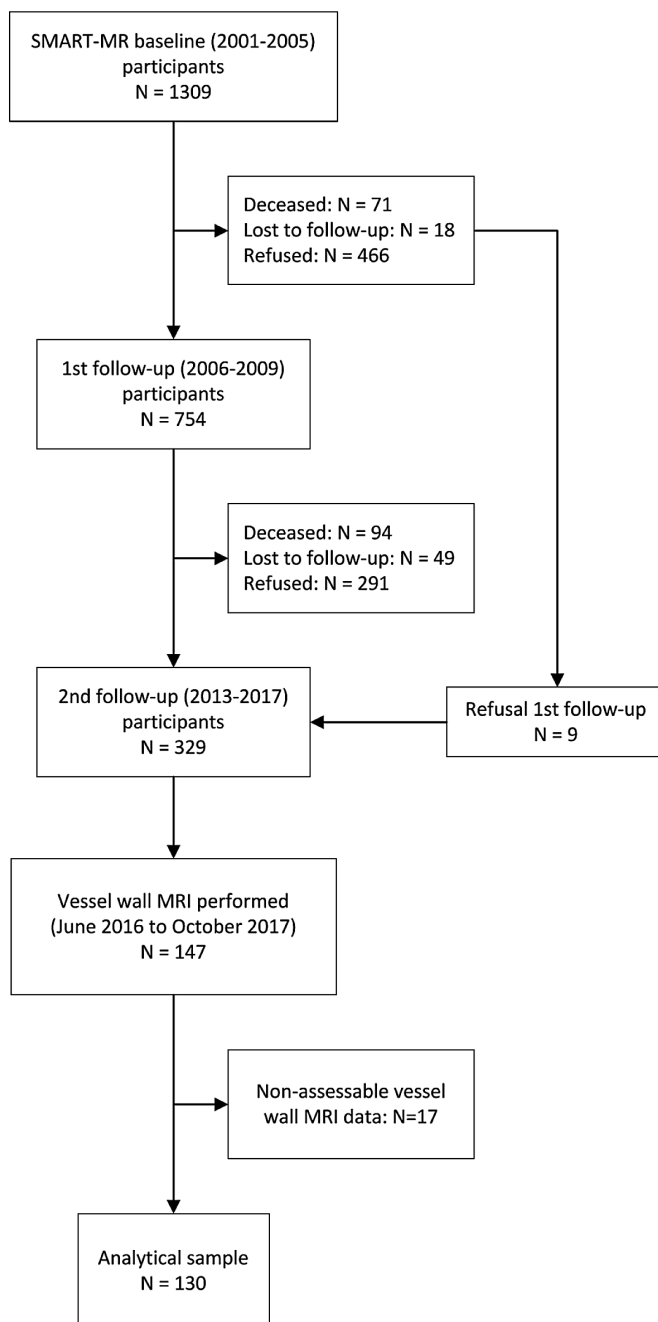
interval was quite large. As risk factor status could have changed during this interval this may have influenced the observed associations. However, when we adjusted for this interval, we did not find relevant differences in association estimates and confidence intervals. Lastly, we included participants who were part of a longitudinal study and who were willing and able to undergo a 7T MRI on average 13 ± 1 years after baseline. Most likely, the study sample consisted of the relatively healthy participants of the original SMART-MR cohort.

In conclusion, intracranial vessel wall lesions are a novel MRI marker of ICAS that offers a more direct approximation of disease burden than conventional indirect markers such as arterial stenosis and calcification. We have shown, using 7T vessel wall MR imaging, that these focal thickenings of the intracranial arterial walls are a highly common occurrence in middle-aged and older men and women with a history of vascular disease and that they have similar but not identical risk factors compared to conventional ICAS markers.

References

- Gorelick P, Wong KS, Liu L. Epidemiology. *Front Neurol Neurosci*. 2016; 40: 34–46.
- Bos D, Portegies MLP, van der Lugt A, Bos MJ, Koudstaal PJ, Hofman A, et al. Intracranial Carotid Artery Atherosclerosis and the Risk of Stroke in Whites. *JAMA Neurol* 2014; 71: 405–11.
- Dearborn JL, Zhang Y, Qiao Y, Suri MFK, Liu L, Gottesman RF, et al. Intracranial atherosclerosis and dementia: The Atherosclerosis Risk in Communities (ARIC) Study. *Neurology* 2017; 88: 1556–63.
- Qureshi AI, Caplan LR. Intracranial atherosclerosis. *Lancet* 2014; 383: 984–98.
- Bos D, Van Der Rijk MJM, Geeraedts TEA, Hofman A, Krestin GP, Witteman JCM, et al. Intracranial carotid artery atherosclerosis: Prevalence and risk factors in the general population. *Stroke*. 2012; 43: 1878–84.
- Qiao Y, Anwar Z, Intrapromkul J, Liu L, Zeiler SR, Leigh R, et al. Patterns and Implications of Intracranial Arterial Remodeling in Stroke Patients. *Stroke* 2016; 47: 434–40.
- Bhogal P, Navaei E, Makalanda HLD, Brouwer PA, Sjöstrand C, Mandell DM, et al. Intracranial vessel wall MRI. *Clin Radiol* 2016; 71: 293–303.
- Mandell DM, Mossa-Basha M, Qiao Y, Hess CP, Hui F, Matouk C, et al. Intracranial Vessel Wall MRI: Principles and Expert Consensus Recommendations of the American Society of Neuroradiology. *AJNR Am J Neuroradiol* 2017; 38: 218–29.
- Qiao Y, Suri FK, Zhang Y, Liu L, Gottesman R, Alonso A, et al. Racial differences in prevalence and risk for intracranial atherosclerosis in a US community-based population. *JAMA Cardiol* 2017; 2: 1341–8.
- López-Cancio E, Dorado L, Millán M, Reverté S, Suñol A, Massuet A, et al. The Barcelona-Asymptomatic Intracranial Atherosclerosis (AsIA) study: Prevalence and risk factors. *Atherosclerosis* 2012; 221: 221–5.
- Uehara T, Bang OY, Kim JS, Minematsu K, Sacco R. Risk Factors. *Front Neurol Neurosci* 2017; 40: 47–57.
- Geerlings MI, Appelman AP, Vincken KL, Algra A, Witkamp TD, Mali WP, et al. Brain volumes and cerebrovascular lesions on MRI in patients with atherosclerotic disease. The SMART-MR study. *Atherosclerosis* 2010; 210: 130–6.
- Appelman APA, Van Der Graaf Y, Vincken KL, Tiehuis AM, Witkamp TD, Mali WPTM, et al. Total cerebral blood flow, white matter lesions and brain atrophy: The SMART-MR study. *J Cereb Blood Flow Metab* 2008; 28: 633–9.
- Wassink AMJ, van der Graaf Y, van Haeften TW, Spiering W, Soedamah-Muthu SS, Visseren FLJ. Waist circumference and metabolic risk factors have separate and additive effects on the risk of future Type 2 diabetes in patients with vascular diseases. A cohort study. *Diabet Med* 2011; 28: 932–40.
- National Cholesterol Education Program (NCEP) Expert Panel on Detection, Evaluation, and Treatment of High Blood Cholesterol in Adults (Adult Treatment Panel III) (2002). Third Report of the National Cholesterol Education Program (NCEP) Expert Panel on Detection, Evaluation, and Treatment of High Blood Cholesterol in Adults (Adult Treatment Panel III) final report. *Circulation* 2002; 106: 3143–3421.
- Jochimsen HM, Geerlings MI, Visseren FL, Algra A, van der Graaf Y, Muller M, et al. Serum angiotensin-converting enzyme and recurrent vascular events. The SMART-MR study. *Atherosclerosis* 2012; 224: 486–91.
- Van Der Kolk AG, Hendrikse J, Brundel M, Biessels GJ, Smit EJ, Visser F, et al. Multi-sequence whole-brain intracranial vessel wall imaging at 7.0 tesla. *Eur Radiol* 2013; 23: 2996–3004.
- van der Kolk AG, Zwanenburg JJM, Brundel M, Biessels GJ, Visser F, Luijten PR, et al. Distribution and natural course of intracranial vessel wall lesions in patients with ischemic stroke or TIA at 7.0 tesla MRI. *Eur Radiol* 2015; 25: 1692–700.
- Lindenholz A, van der Kolk AG, Zwanenburg JJM, Hendrikse J. The Use and Pitfalls of Intracranial Vessel Wall Imaging: How We Do It. *Radiology* 2018; 286: 12–28.
- Pearson TA, Mensah GA, Alexander RW, Anderson JL, Cannon RO, Criqui M, et al. Markers of inflammation and cardiovascular disease: Application to clinical and public health practice: A statement for healthcare professionals from the centers for disease control and prevention and the American Heart Association. *Circulation* 2003; 107: 499–511.
- Hartevelde AA, van der Kolk AG, van der Worp HB, Dieleman N, Siero JCW, Kuijff HJ, et al. High-resolution intracranial vessel wall MRI in an elderly asymptomatic population: comparison of 3T and 7T. *Eur Radiol* 2017; 27: 1585–95.
- Resch J a, Loewenson RB, Baker a B. Physical factors in the pathogenesis of cerebral atherosclerosis. *Stroke* 1970; 1: 77–85.

23. Hartevelde AA, Van Der Kolk AG, Van Der Worp HB, Dieleman N, Zwanenburg JJM, Luijten PR, et al. Detecting Intracranial Vessel Wall Lesions with 7T-Magnetic Resonance Imaging: Patients with Posterior Circulation Ischemia Versus Healthy Controls. *Stroke* 2017; 48: 2601–4.
24. Cunningham KS, Gotlieb AI. The role of shear stress in the pathogenesis of atherosclerosis. *Laboratory Investigation* 2005; 85: 9–23.
25. Li MM, Lin YY, Huang YH, Zhuo ST, Yang ML, Lin HS, et al. Association of Apolipoprotein A1, B with Stenosis of Intracranial and Extracranial Arteries in Patients with Cerebral Infarction. *Clin Lab* 2015; 61: 1727–35.
26. Park JH, Hong KS, Lee EJ, Lee J, Kim DE. High levels of apolipoprotein B/AI ratio are associated with intracranial atherosclerotic stenosis. *Stroke* 2011; 42: 3040–6.
27. Wong KS, Huang YN, Yang HB, Gao S, Li H, Liu JY, et al. A door-to-door survey of intracranial atherosclerosis in Liangbei County, China. *Neurology* 2007; 68: 2031–4.
28. López-Cancio E, Dorado L, Millán M, Reverté S, Suñol A, Massuet A, et al. The population-based Barcelona-Asymptomatic Intracranial Atherosclerosis Study (ASIA): rationale and design. *BMC Neurol* 2011; 11: 22.
29. López-Cancio E, Galán A, Dorado L, Jiménez M, Hernández M, Millán M, et al. Biological signatures of asymptomatic extra- and intracranial atherosclerosis: The Barcelona-AsIA (Asymptomatic Intracranial Atherosclerosis) study. *Stroke* 2012; 43: 2712–9.
30. Kim DE, Kim JY, Jeong SW, Cho YJ, Park JM, Lee JH, et al. Association between changes in lipid profiles and progression of symptomatic intracranial atherosclerotic stenosis: A prospective multicenter study. *Stroke* 2012; 43: 1824–30.
31. Qian Y, Pu Y, Liu L, Wang DZ, Zhao X, Wang C, et al. Low HDL-C Level Is Associated with the Development of Intracranial Artery Stenosis: Analysis from the Chinese IntraCranial AtheroSclerosis (CICAS) Study. *PLoS One* 2013; 8: 1–6.
32. Lei C, Wu B, Liu M, Chen Y. Risk Factors and Clinical Outcomes Associated with Intracranial and Extracranial Atherosclerotic Stenosis Acute Ischemic Stroke. *J Stroke Cerebrovasc Dis* 2013; 23: 1–6.
33. Jin H, Peng Q, Nan D, Lv P, Liu R, Sun W, et al. Prevalence and risk factors of intracranial and extracranial artery stenosis in asymptomatic rural residents of 13 villages in China. *BMC Neurol* 2017; 17: 136.
34. Rincon F, Wright CB. Current pathophysiological concepts in cerebral small vessel disease. *Front Aging Neurosci* 2014; 6: 24.
35. Bos D, Ikram MA, Elias-Smale SE, Krestin GP, Hofman A, Witteman JCM, et al. Calcification in major vessel beds relates to vascular brain disease. *Arterioscler Thromb Vasc Biol* 2011; 31: 2331–7.
36. Huang HW, Guo MH, Lin RJ, Chen YL, Luo Q, Zhang Y, et al. Prevalence and risk factors of middle cerebral artery stenosis in asymptomatic residents in Rongqi County, Guangdong. *Cerebrovasc Dis* 2007; 24: 111–5.
37. D'Armiento FP, Bianchi A, de Nigris F, Capuzzi DM, D'Armiento MR, Crimi G, et al. Age-related effects on atherogenesis and scavenger enzymes of intracranial and extracranial arteries in men without classic risk factors for atherosclerosis. *Stroke* 2001; 32: 2472–9.
38. Ferreira JP, Girerd N, Bozec E, Machu JL, Boivin JM, London GM, et al. Intima-media thickness is linearly and continuously associated with systolic blood pressure in a population-based cohort (STANISLAS cohort study). *J Am Heart Assoc* 2016; 5: e003529.
39. Turan TN, Makki AA, Tsappidi S, Cotsonis G, Lynn MJ, Cloft HJ, et al. Risk factors associated with severity and location of intracranial arterial stenosis. *Stroke* 2010; 41: 1636–40.



Supplemental Figure 1. Flowchart of the study sample.

Supplemental Table 1. Overview of intracranial vessel wall lesions characteristics.

| | Frequency | Median (range) | Mean \pm SD |
|--|-----------|----------------|-----------------|
| Total circulation | 96.2% | 7 (0-32) | 8.51 \pm 5.69 |
| Anterior circulation | 91.5% | 4 (0-14) | 5.26 \pm 3.21 |
| Anterior cerebral artery (left) | 55.4% | 1 (0-4) | 1.26 \pm 0.63 |
| A1 segment | 35.4% | 0 (0-1) | 1.00 \pm 0.00 |
| A2 segment | 30.0% | 0 (0-3) | 1.15 \pm 0.43 |
| Anterior cerebral artery (right) | 41.5% | 0 (0-2) | 1.33 \pm 0.48 |
| A1 segment | 21.5% | 0 (0-2) | 1.04 \pm 0.19 |
| A2 segment | 30.8% | 0 (0-2) | 1.08 \pm 0.27 |
| Middle cerebral artery (left) | 49.2% | 0 (0-5) | 1.52 \pm 0.71 |
| M1 segment | 43.1% | 0 (0-2) | 1.18 \pm 0.39 |
| M2 segment | 20.0% | 0 (0-3) | 1.19 \pm 0.49 |
| Middle cerebral artery (right) | 46.9% | 0 (0-4) | 1.69 \pm 0.76 |
| M1 segment | 43.1% | 0 (0-3) | 1.34 \pm 0.51 |
| M2 segment | 16.9% | 0 (0-2) | 1.27 \pm 0.46 |
| Internal carotid artery (left) | 70.0% | 1 (0-3) | 1.53 \pm 0.52 |
| C6 segment | 63.1% | 1 (0-2) | 1.02 \pm 0.16 |
| C7 segment | 42.3% | 0 (0-2) | 1.00 \pm 0.00 |
| Internal carotid artery (right) | 62.3% | 1 (0-2) | 1.53 \pm 0.53 |
| C6 segment | 56.2% | 1 (0-2) | 1.01 \pm 0.12 |
| C7 segment | 38.5% | 0 (0-2) | 1.00 \pm 0.00 |
| Posterior circulation | 88.5% | 3 (0-18) | 3.81 \pm 2.96 |
| Posterior cerebral artery (left) | 48.5% | 0 (0-4) | 1.54 \pm 0.76 |
| P1 segment | 19.2% | 0 (0-1) | 1.08 \pm 0.40 |
| P2 segment | 37.7% | 0 (0-3) | 1.27 \pm 0.53 |
| P1-P2 bifurcation | 6.2% | 0 (0-1) | 1.00 \pm 0.00 |
| Posterior cerebral artery (right) | 47.7% | 0 (0-5) | 1.44 \pm 0.78 |
| P1 segment | 9.2% | 0 (0-1) | 1.00 \pm 0.00 |
| P2 segment | 31.5% | 0 (0-3) | 1.18 \pm 0.48 |
| P1-P2 bifurcation | 12.3% | 0 (0-2) | 1.06 \pm 0.25 |
| Posterior communicating artery (left) | 2.3% | 0 (0-1) | 1.00 \pm 0.00 |
| Posterior communicating artery (right) | 5.4% | 0 (0-2) | 1.29 \pm 0.49 |
| Basilar artery | 58.5% | 1 (0-4) | 1.57 \pm 0.79 |
| Vertebral artery (left) | 38.5% | 0 (0-4) | 1.48 \pm 0.76 |
| Vertebral artery (right) | 30.0% | 0 (0-3) | 1.21 \pm 0.47 |

Note: median and range values calculated in complete study sample. Mean and standard deviation calculated within subsample with lesions at location.

Percentage of non-assessable segments: left A2, 0.8%; right A2, 0.8%; left M2, 6.2%; right M2, 9.2%; basilar artery, 0.8%; left vertebral artery, 20.0%; right vertebral artery, 23.9%.

Abbreviations: SD, standard deviation.

Supplemental Table 2. Sensitivity analysis of association of conventional risk factors with ICAS burden.

| | ICAS burden, <i>b</i> (95% CI) | <i>p</i> value |
|------------------------------|--------------------------------|----------------|
| Male sex | 0.92 (-2.04 to 3.86) | 0.540 |
| Age, per +10 years | 1.86 (0.73 to 2.99) | 0.002 |
| Smoking status | | |
| Never smoker | 0 (reference) | |
| Former smoker | 0.70 (-2.19 to 3.59) | 0.632 |
| Current smoker | 0.73 (-2.91 to 4.36) | 0.693 |
| Pack-years, per +10 years | 0.32 (-0.20 to 0.85) | 0.227 |
| Alcohol intake | | |
| No or 1 < unit/week | 0 (reference) | |
| 1-10 units/week | -0.79 (-3.22 to 1.64) | 0.521 |
| ≥11 units/week | -1.48 (-4.17 to 1.21) | 0.279 |
| Hypertension, y/n | -0.96 (-4.22 to 2.30) | 0.560 |
| Blood pressure, per +10 mmHg | | |
| Systolic | 0.79 (0.21 to 1.36) | 0.008 |
| Diastolic | 0.45 (-0.65 to 1.54) | 0.420 |

Note: *b* values are unstandardized linear regression coefficients (95% CI) adjusted for age, sex, and time interval between risk factor measurement and 7T MRI.

Abbreviations: ICAS, intracranial atherosclerosis; CI, confidence interval.

Supplemental Table 3. Sensitivity analysis of association of metabolic and miscellaneous risk factors with ICAS burden.

| | ICAS burden, <i>b</i> (95% CI) | <i>p</i> value |
|-------------------------------|--------------------------------|----------------|
| BMI, per +1 kg/m ² | 0.08 (-0.20 to 0.36) | 0.580 |
| Obesity*, y/n | 2.12 (-0.39 to 4.63) | 0.097 |
| Hyperlipidemia, y/n | 3.71 (-0.11 to 7.52) | 0.057 |
| Lipids, per +1 mmol/L | | |
| Triglycerides | 1.10 (-0.35 to 2.54) | 0.135 |
| LDL-C | 0.96 (-0.26 to 2.18) | 0.123 |
| HDL-C | -0.33 (-3.11 to 2.45) | 0.812 |
| Total | 0.94 (-0.12 to 2.00) | 0.081 |
| Apo-B, per +1 g/L | 4.45 (-0.15 to 9.06) | 0.058 |
| Diabetes, y/n | 3.04 (0.59 to 5.50) | 0.016 |
| HbA1c, per +1% | 1.19 (0.16 to 2.21) | 0.024 |
| Glucose, per +1 mmol/L | 0.34 (-0.23 to 0.92) | 0.240 |
| Metabolic syndrome, y/n | 1.68 (-0.26 to 3.62) | 0.089 |
| APOE-ε4 allele, y/n | -1.22 (-3.37 to 0.94) | 0.265 |
| hs-CRP, per +1 mg/L | -0.02 (-0.29 to 0.26) | 0.900 |
| hs-CRP >3 mg/L, y/n | 2.47 (0.03 to 4.91) | 0.047 |

Note: *b* values are unstandardized linear regression coefficients (95% CI) adjusted for age, sex and time interval between risk factor measurement and 7T MRI.

Abbreviations: ICAS, intracranial atherosclerosis; CI, confidence interval; BMI, body mass index; LDL-C, low-density lipoprotein; HDL-C, high-density lipoprotein; Apo-B, apolipoprotein B; HbA1c, hemoglobin A1c; APOE, apolipoprotein E; hs-CRP, high-sensitivity C-reactive protein.

*BMI ≥ 30kg/m².

Supplemental Table 4. Overview of the ratio of concentric and eccentric vessel wall lesions.

| | Both types <i>n</i> | Concentric type <i>n</i> (%) | Eccentric type <i>n</i> (%) |
|--|--------------------------------|---|--|
| Total circulation | 1064 | 261 (25%) | 803 (75%) |
| Anterior circulation | 626 | 135 (22%) | 491 (78%) |
| Anterior cerebral artery (left) | 91 | 41 (45%) | 50 (55%) |
| A1 segment | 46 | 22 (48%) | 24 (52%) |
| A2 segment | 45 | 19 (42%) | 26 (58%) |
| Anterior cerebral artery (right) | 72 | 35 (49%) | 37 (51%) |
| A1 segment | 29 | 16 (55%) | 13 (45%) |
| A2 segment | 43 | 19 (44%) | 24 (56%) |
| Middle cerebral artery (left) | 97 | 12 (12%) | 85 (88%) |
| M1 segment | 66 | 5 (8%) | 61 (92%) |
| M2 segment | 31 | 7 (23%) | 24 (77%) |
| Middle cerebral artery (right) | 103 | 11 (11%) | 92 (89%) |
| M1 segment | 75 | 9 (12%) | 66 (88%) |
| M2 segment | 28 | 2 (7%) | 26 (93%) |
| Internal carotid artery (left) | 139 | 18 (13%) | 121 (87%) |
| C6 segment | 84 | 9 (11%) | 75 (89%) |
| C7 segment | 55 | 9 (16%) | 46 (84%) |
| Internal carotid artery (right) | 124 | 18 (15%) | 106 (85%) |
| C6 segment | 74 | 10 (14%) | 64 (86%) |
| C7 segment | 50 | 8 (16%) | 42 (84%) |
| Posterior circulation | 438 | 126 (29%) | 312 (71%) |
| Posterior cerebral artery (left) | 97 | 30 (31%) | 65 (69%) |
| P1 segment | 27 | 7 (26%) | 20 (74%) |
| P2 segment | 62 | 21 (34%) | 41 (66%) |
| P1-P2 bifurcation | 8 | 4 (50%) | 4 (50%) |
| Posterior cerebral artery (right) | 89 | 30 (34%) | 59 (6%) |
| P1 segment | 12 | 4 (33%) | 8 (67%) |
| P2 segment | 60 | 18 (30%) | 42 (70%) |
| P1-P2 bifurcation | 17 | 8 (47%) | 9 (53%) |
| Posterior communicating artery (left) | 3 | 0 (0%) | 3 (100%) |
| Posterior communicating artery (right) | 9 | 2 (22%) | 7 (78%) |
| Basilar artery | 119 | 15 (13%) | 104 (87%) |
| Vertebral artery (left) | 74 | 30 (41%) | 44 (59%) |
| Vertebral artery (right) | 47 | 17 (36%) | 30 (64%) |

Percentage of non-assessable segments: left A2, 0.8%; right A2, 0.8%; left M2, 6.2%; right M2, 9.2%; basilar artery, 0.8%; left vertebral artery, 20.0%; right vertebral artery, 23.9%.



3

Intracranial atherosclerotic burden on 7T MRI is associated with markers of extracranial atherosclerosis—the SMART-MR study

Maarten H.T. Zwartbol, Mirjam I. Geerlings, Rashid Ghaznawi, Jeroen Hendrikse, Anja G. van der Kolk, on behalf of the UCC-SMART Study Group

Published in *American Journal of Neuroradiology* 2019; 40: 2016-22
doi: 10.3174/ajnr.A6308

Abstract

Intracranial atherosclerosis (ICAS), a major risk factor for ischemic stroke, is thought to have different atherogenic mechanisms than extracranial atherosclerosis. Studies investigating their relationship *in vivo* are sparse and report inconsistent results. We studied the relationship between ICAS and extracranial atherosclerosis in a cohort of patients with a history of vascular disease.

Within the SMART-MR study cross-sectional analyses were performed in 130 patients (68 ± 9 years) with a history of vascular disease and with assessable 7T intracranial vessel wall-MRI data. ICAS burden was defined as the number of intracranial vessel wall lesions in the Circle of Willis and its major branches. Age- and sex-adjusted unstandardized regression coefficients (b) were calculated with ICAS burden as the dependent variable, and ECAS markers as independent variables.

Ninety-six percent of patients had one or more vessel wall lesions, with a mean ICAS burden of 8.5 ± 5.7 lesions. Significant associations were observed between higher ICAS burden and carotid intima-media thickness ($b = 5.3$ lesions per +1 mm; 95% CI 0.6 to 10.0), 50-100% carotid stenosis vs. no stenosis ($b = 6.6$ lesions; 95% CI 2.3 to 10.9), ankle-brachial index ≤ 0.9 vs. > 0.9 ($b = 4.9$ lesions; 95% CI 1.7 to 8.0) and estimated glomerular filtration rate ($b = -0.77$ lesions per +10 ml/min; 95% CI -1.50 to -0.03). No significant differences in ICAS burden were found between different categories of vascular disease.

ICAS was associated with various extracranial markers of atherosclerosis, not supporting a different etiology.

Introduction

Intracranial atherosclerosis (ICAS) is a major cause of adverse cerebrovascular events such as ischemic stroke.¹ Furthermore, it is associated with an increased risk of cognitive decline and dementia.² A wide range of prevalence estimates for ICAS have been reported, ranging from 4-51% in asymptomatic populations to 43-70% in ischemic stroke patients.^{3,4}

ICAS is currently seen as the intracranial phenotype of atherosclerosis, a generalized disease that can affect all large arteries. Nonetheless, correlations between intracranial and extracranial atherosclerotic disease in post-mortem studies are modest.⁵ Furthermore, ICAS has a later time of onset, slower rate of progression and different plaque morphology compared to other arterial territories.⁶⁻⁸ As a result, it has been suggested that ICAS might have a different etiology than extracranial disease. Studies investigating the relationship between intracranial and extracranial disease *in vivo* are sparse and often limited to one extracranial vessel bed. Furthermore, all of these studies have used lumenographic imaging methods, which can only assess atherosclerotic stenosis.^{9,10} Therefore, intracranial plaques without stenosis, i.e., due to arterial remodeling, will not be detected, leading to an underestimation of the actual ICAS burden.¹¹

Vessel wall lesions are a novel neuroimaging marker of ICAS which can be assessed using intracranial vessel wall-MRI.¹² Vessel wall-MRI enables visualization of the intracranial arterial walls, allowing a more direct evaluation of ICAS.¹³ Currently, 7 tesla (7T) is the highest field strength at which vessel wall-MRI has been performed in humans *in vivo*, and has been shown to be superior to lower field strengths in the detection of vessel wall anomalies.¹⁴

In the current study, we investigated in patients with atherosclerotic disease to what extent markers of extracranial atherosclerosis (ECAS) were associated with the burden of ICAS measured by 7T vessel wall-MRI, thereby providing insight into the etiology of ICAS and its relationship with ECAS.

Methods

Study sample

Data were used from the Second Manifestations of ARterial disease-Magnetic Resonance (SMART-MR) study, a prospective cohort study at our institution with the aim to investigate risk factors and clinical outcomes of MRI neuroimaging markers in patients with arterial disease.¹⁵ In brief, from 2001 through 2005, 1309 patients newly referred to our institution with cerebrovascular disease, peripheral arterial disease, coronary artery disease, or abdominal aortic aneurysm, and without MRI contraindications were enrolled in the SMART-MR study. On a one-day visit to our institution's hospital the participants received a 1.5T MRI of the brain, a physical examination, ankle-brachial index (ABI) assessment,

ultrasonography of the carotid arteries, blood and urine sampling, and questionnaires to assess risk factors, medical history, and daily functioning. Follow-up exams of the SMART-MR cohort were performed in 2006-2009, and 2013-2017.

From June 2016 to October 2017, we included 147 patients participating in the second follow-up examination of the SMART-MR study who had intracranial vessel wall-MRI performed as part of a 7T MRI of the brain.¹² A flowchart of the study sample is provided in Supplemental Figure 1. Seventeen patients were excluded from the current study because of artifacts hampering vessel wall-MRI assessment of ≥ 1 major segment of the Circle of Willis (CoW; major segments included the distal internal carotid artery and primary branches (M1, A1, P1) of the anterior, middle and posterior cerebral artery), leaving 130 patients for final analysis. For the current study, measurements of extracranial atherosclerosis, and risk factor assessment, including questionnaire data and blood and urine sampling, was performed median 2.3 (range, 0.6 to 8.6) years prior to the 7T MRI.

Comparison of ECAS markers between the excluded patients and the patients for final analysis showed a higher prevalence of 50-100% carotid stenosis in the excluded patients (7.0% vs. 23.5%; $p = 0.04$, χ^2 -test). Also, the excluded patients were older, although this was not statistically significant (70 ± 7 vs. 68 ± 9 years; $p = 0.11$, Student's t -test). Sex distribution did not differ between included and excluded patients (88% vs. 88% male; $p = 0.95$, χ^2 -test).

Vascular risk factors

Information on general vascular risk factors was obtained by questionnaires, physical examination and blood sampling. Height and weight were used to calculate the body mass index (BMI; kg/m²). Systolic blood pressure (SBP; mmHg) and diastolic blood pressure (DBP; mmHg) were measured by averaging three separate measurements with a sphygmomanometer. Hypertension was defined as a SBP of >140 mmHg, a mean DBP of >90 mmHg, or self-reported use of antihypertensive drugs. Diabetes mellitus was defined as fasting serum glucose levels of ≥ 7.0 mmol/L, and/or use of glucose-lowering medication, and/or a known history of diabetes. Patients who did not meet these criteria, but with a fasting plasma glucose level ≥ 7.0 mmol/L at baseline, were considered to have diabetes at baseline if they received treatment with glucose-lowering medication within 1 year after baseline. Hyperlipidemia was defined as a total cholesterol of >5.0 mmol/L, a low-density lipoprotein cholesterol of >3.2 mmol/L, or use of lipid-lowering medication. Metabolic syndrome was determined by the National Cholesterol Education Program Adult Treatment Panel III criteria.¹⁶

Markers of extracranial atherosclerosis

An experienced technician performed carotid ultrasonography with a 10MHz linear-array transducer. Mean carotid intima-media thickness (cIMT) was calculated from six measurements (anterolateral, posterolateral and mediolateral in both common carotid

arteries). Extracranial carotid stenosis was assessed ultrasonographically and defined according to standard criteria based on the peak systolic velocity.¹⁷ ABI measurements were conducted by experienced technicians and were calculated from the highest systolic blood pressure measured at the posterior tibial and dorsal pedal arteries by Doppler and at both brachial arteries by a semiautomatic oscillometric device in supine position. Renal function was assessed using the estimated glomerular filtration rate (eGFR) calculated by the Cockcroft-Gault equation adjusted for body weight and body mass index.¹⁸

Coronary artery disease was defined as a history of myocardial infarction, a history of coronary artery bypass graft surgery or percutaneous transluminal coronary angioplasty at inclusion or in the past. Cerebrovascular disease was defined as transient ischemic attack or stroke at inclusion or in the past. Peripheral artery disease was defined as intermittent claudication or rest pain at inclusion, or a history of surgery or angioplasty of the arteries supplying the lower extremities. Abdominal aortic aneurysm (AAA) was defined as presence of an AAA (distal aortic anteroposterior diameter ≥ 3 cm) or previous AAA surgery. Multivascular disease was defined of presence of ≥ 2 of the above defined vascular diseases.

7T MR imaging protocol

A 7T whole-body system (Philips Healthcare, USA) was used with a volume/transmit coil for transmission and a 32-channel receive head coil (Nova Medical, Wilmington, MA, USA). Vessel wall-MRI was performed using a T_1 -weighted Magnetization-Prepared Inversion Recovery Turbo Spin Echo (T_1 -MPIR-TSE) sequence, with the following parameters: FOV 250x250x190 mm³, acquired resolution 0.8x0.8x0.8 mm³ (reconstructed to 0.49x0.49x0.4 mm³), repetition time / inversion time / echo time 3952/1375/37 ms, acquisition time 10:40 minutes (min).¹⁹ In addition, an SWI sequence was performed, with the following parameters: FOV 200x200x120 mm³, acquired resolution 0.5x0.5x0.7 mm³ (reconstructed to 0.4x0.4x0.35 mm³), repetition time / echo time 1/ echo time 2, 20/6.9/15.8 ms, flip angle 12 degrees, acquisition time 09:17 min.

Assessment of intracranial atherosclerosis

For the assessment of vessel wall lesions, axial multiplanar reconstructions were calculated from the T_1 -MPIR-TSE sequence (slice thickness 0.8 mm; no slice gap); angulated to the nasion-foramen magnum line. One observer (MHTZ, 4.5 years of experience in neuroradiology) assessed all images, blinded to patient characteristics. MHTZ was trained by a senior observer with 8 years of experience in interpreting vessel wall-MRI images (AK), using a practice set of 15 patients from the IVI study²⁰; and a consensus set of 20 patients from the current study. An interobserver agreement of 0.75 (dice similarity coefficient) was obtained, which was regarded as good.

Vessel wall lesions were rated according to the methodology previously published by Lindenholz et al.²¹ A lesion was defined as either a focal or more diffuse thickening of

the arterial wall greater than 50%, assessed visually, using the normal contralateral or neighboring arterial wall as reference. Uncertain lesions were verified in multiple planes. After a lesion was identified, it was subsequently classified as eccentric ($\leq 50\%$ wall circumference) or concentric ($>50\%$ wall circumference) and by arterial segment location: internal carotid arteries (C6, C7), middle cerebral arteries (M1, M2), anterior cerebral arteries (A1, A2), posterior communicating arteries, posterior cerebral arteries (P1, P2 and P1-P2 bifurcation), basilar artery and vertebral arteries (V4). One single segment could contain multiple lesions, making the total lesion count theoretically unlimited. Lesions that extended into multiple segments were counted as separate lesions for each involved segment. Furthermore, lesions with eccentric and concentric components, were regarded as separate lesions.

A maximum intensity projection of the SWI was used to assess the course of smaller arteries (M2, A1, P2, PCom). We did not assess luminal stenosis because the SWI quality in our study did not permit accurate measurement, especially of small lesions. Of note, we did not perform a refined MRA because it was logistically not feasible, and at the time of study design, the diagnostic accuracy of MRA in the detection and grading of intracranial stenosis was still relatively low.²²

Statistical analysis

First, characteristics of the study sample were described. Next, the association of ECAS markers with ICAS burden was estimated using linear regression analyses, with the ECAS measure as the independent variable and ICAS burden as the dependent variable. ICAS burden was defined as the total number of intracranial vessel wall lesions. All analyses were adjusted for age and sex. ECAS measures were entered into the model as continuous and/or dichotomous variables. ABI was dichotomized by the clinical cut-off for peripheral artery disease (≤ 0.9).²³ For eGFR, the clinical threshold for chronic kidney disease (<60 ml/min) was used. cIMT was categorized into quartiles. Categorization of carotid stenosis was based on the most severe lesion in the bilateral extracranial common or internal carotid arteries. In the analyses of vascular disease, patients with ≥ 2 vascular diseases were categorized as multivascular, making categories mutually exclusive. Patient with only coronary artery disease were used as the reference category. A sensitivity analysis was performed to control for the time interval (in days) between the date of ECAS measurements and date of the 7T MRI.

Statistical analyses were performed using SPSS v. 25.0 for Windows (IBM Corporation, USA).

Results

Table 1 shows the characteristics of the 130 patients. Eighty-eight percent were men, and the mean age was 68 ± 9 years. Twenty-five percent had multivascular disease. Although 19% of the population had cerebrovascular disease, in just 9% it was the only disease. A large majority of 65% had a sole history of coronary artery disease. An overview of vascular risk factors can be found in Supplemental Table 1. Of the 130 patients, 96% had ≥ 1 intracranial vessel wall lesion, and a mean ICAS burden of 8.5 ± 5.7 lesions (median 7, range 0-32). Furthermore, in the anterior circulation a mean ICAS burden of 5.3 ± 3.2 lesions (median 4, range 0-14) was found, which was 3.8 ± 3.0 (median 3; range 0-18) for the

Table 1. Markers of extracranial atherosclerosis (n = 130).

| | |
|--|-----------|
| Age (years) | 68±9 |
| Male | 88% |
| Carotid IMT (mm) | 0.84±0.22 |
| Carotid stenosis ^a | |
| No stenosis | 23% |
| 1-49 stenosis% | 70% |
| 50-100% stenosis ^b | 7% |
| Ankle-brachial index | |
| ABI | 1.09±0.18 |
| ABI ≤ 0.9 | 11% |
| Renal function | |
| eGFR (ml/min) | 72.8±17.3 |
| eGFR < 60 ml/min | 21% |
| History of vascular disease ^c | |
| Cerebrovascular disease | 9% |
| Coronary artery disease | 65% |
| Peripheral artery disease | 9% |
| Multivascular disease | 17% |

Values are presented as mean±SD for continuous variables and percentages for dichotomous variable.

^a Categories are mutually exclusive. Patients were categorized according to most severe stenosis grade.

^b Includes 4 patients with ≥ 1 carotid artery occlusion(s).

^c Categories are mutually exclusive. Multivascular category consisted of 22 patients with a history of ≥ 2 vascular diseases: 95% had coronary artery disease, 60% cerebrovascular disease, 60% peripheral artery disease, and 14% abdominal aortic aneurysm.

Abbreviations: IMT, intima-media thickness; ICA, internal carotid artery; ABI, ankle-brachial index; eGFR, estimated glomerular filtration rate.

posterior circulation. More details regarding arterial or segmental distribution can be found in our prior publication.¹² Examples of vessel wall lesions in a 76-year-old male patient are shown in Figure 1.

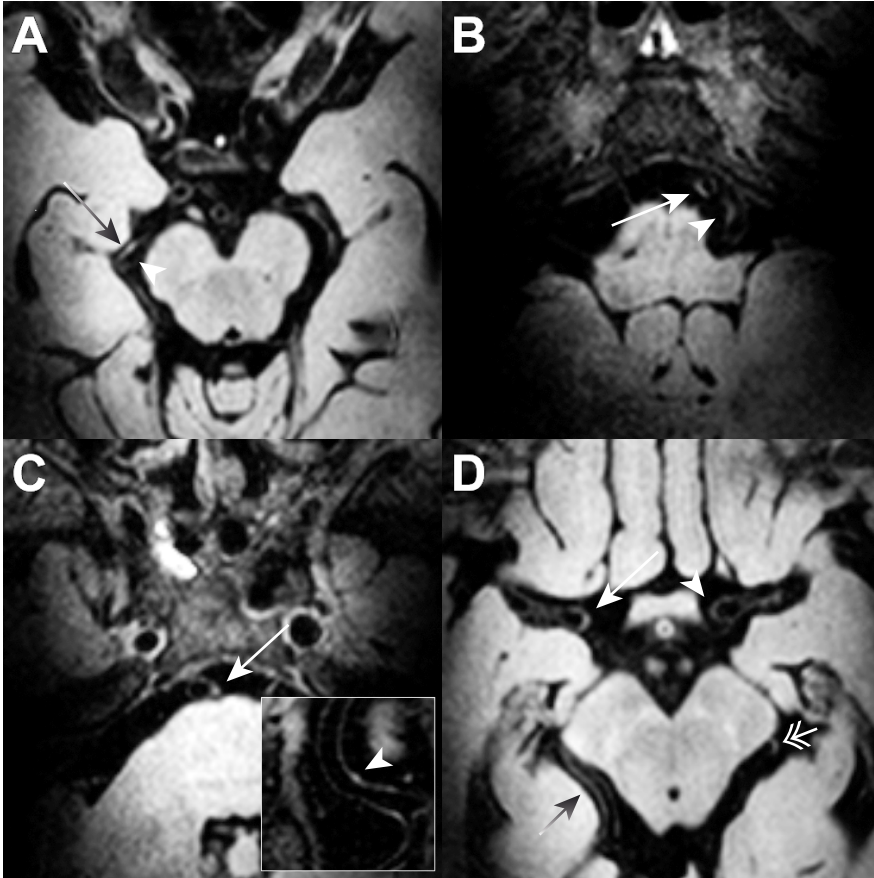


Figure 1. Examples of intracranial vessel wall lesions on vessel wall-MRI in a 76-year-old male patient with a history of coronary artery disease. A detailed description of rating criteria can be found in the methods section. A) Lesion in lateral wall of right P2 segment (arrow) versus non-discernable normal neighboring medial wall (arrowhead). B) Lesion in right vertebral (arrow) and left vertebral (arrowhead) artery. C) Lesion in proximal basilar artery (arrow), with coronal orientation shown in enclosed panel (arrowhead). D) Lesion in C7 segment of the right ICA (arrow), when compared to normal-appearing contralateral C7 segment (arrowhead) and proximal right M1 segment. Furthermore, note the long lesion in the distal half of the right P2 segment (grey arrow), and focal lesion in the left P2 segment (dual arrow).

Age and sex-adjusted linear regression analyses showed that cIMT was significantly associated with a higher ICAS burden ($b = 5.3$ lesions per +1 mm; 95% CI 0.55 to 9.97). Analysis of cIMT in quartiles indicated a threshold effect, with only Q4 suggesting an association with ICAS burden. However, since the 95% confidence interval contained 0.00, it was not statistically significant (Table 2).

Carotid stenosis of 1-49% was found to be associated with a higher ICAS burden, when compared to no carotid stenosis ($b = 2.5$ lesions for presence of 1-49% carotid stenosis; 95% CI 0.08 to 4.89). Carotid stenosis of 50-100% was also associated with a higher ICAS burden ($b = 6.6$ lesions for presence of 50-100% carotid stenosis; 95% CI 2.34 to 10.93) (Table 2).

Table 2. Association between carotid atherosclerosis and ICAS burden.

| | ICAS burden, b (95% CI) |
|-------------------|---------------------------|
| Carotid IMT | |
| (cIMT), per +1 mm | 5.26 (0.55 to 9.97) |
| cIMT quartiles | |
| Quartile 1 | 0 (reference) |
| Quartile 2 | 0.62 (-2.31 to 3.55) |
| Quartile 3 | 0.40 (-2.61 to 3.41) |
| Quartile 4 | 2.89 (-0.01 to 5.80) |
| Carotid stenosis | |
| No stenosis | 0 (reference) |
| 1-49% stenosis | 2.48 (0.08 to 4.89) |
| 50-100% stenosis | 6.62 (2.34 to 10.93) |

b values are unstandardized linear regression coefficients adjusted for age and sex.
Abbreviations: ICAS, intracranial atherosclerosis; cIMT, carotid intima-media thickness.

ABI did not show a significant association with ICAS burden when analyzed as a continuous variable. However, when dichotomized by 0.9, the clinical threshold for peripheral artery disease, a significant association with a higher ICAS burden was found, when compared to ABI > 0.9 ($b = 4.9$ lesions for presence of ABI ≤ 0.9; 95% CI 1.74 to 7.99) (Table 3).

eGFR was significantly associated with ICAS burden when analyzed as a continuous variable ($b = -0.77$ lesions per +10ml/min; 95% CI -1.50 to -0.03). Furthermore, renal dysfunction (eGFR < 60 ml/min) was also associated with a higher ICAS burden, when compared to eGFR ≥ 60 ml/min ($b = 3.2$ lesions; 95% CI 0.45 to 5.91) (Table 4).

Table 3. Association between ABI and ICAS burden.

| | ICAS burden, <i>b</i> (95% CI) |
|------------------------|--------------------------------|
| ABI, per +0.1 in ratio | -0.36 (-0.91 to 0.19) |
| ABI > 0.9 | 0 (reference) |
| ABI ≤ 0.9 | 4.86 (1.74 to 7.99) |

b values are unstandardized linear regression coefficients adjusted for age and sex.
Abbreviations: ICAS, intracranial atherosclerosis; ABI, ankle-brachial index.

Table 4. Association between renal function and ICAS burden.

| | ICAS burden, <i>b</i> (95% CI) |
|----------------------|--------------------------------|
| eGFR, per +10 ml/min | -0.77 (-1.50 to -0.03) |
| eGFR ≥ 60 ml/min | 0 (reference) |
| eGFR < 60 ml/min | 3.18 (0.45 to 5.91) |

b values are unstandardized linear regression coefficients adjusted for age and sex. Abbreviations: ICAS, intracranial atherosclerosis; eGFR, estimated glomerular filtration rate.

No significant differences in ICAS burden were observed between cerebrovascular, peripheral artery or multivascular disease groups, when compared to only coronary heart disease (Table 5).

As a sensitivity analysis, all models were additionally adjusted for the time interval between the date of ECAS measurement and date of 7T MRI. Supplemental Table 2 to 5 show the results of these analyses. Although the estimates slightly differed, this did not lead to a change in statistical significance.

Table 5. Association between history of vascular disease and ICAS burden.

| | ICAS burden, <i>b</i> (95% CI) |
|---------------------------|--------------------------------|
| Coronary artery disease | 0 (reference) |
| Peripheral artery disease | -0.22 (-3.99 to 3.55) |
| Cerebrovascular disease | 0.01 (-3.46 to 3.48) |
| Multivascular disease | 2.08 (-0.60 to 4.76) |

b values are unstandardized linear regression coefficients adjusted for age and sex.
Categories are mutually exclusive.
Abbreviations: ICAS, intracranial atherosclerosis.

Discussion

This study examined the association between ICAS, as measured by intracranial vessel wall-MRI at 7T, and several markers of ECAS, in a cohort of patients with a history of vascular disease. Our results show that increasing cIMT, presence of extracranial carotid stenosis, ABI ≤ 0.9 , and decreasing eGFR were all associated with a higher ICAS burden, defined as the number of intracranial vessel wall lesions. No differences in ICAS burden were observed between presence of peripheral, cerebrovascular or multivascular disease when compared to coronary heart disease, the main disease in our population.

Cerebral arteries are thought to have a different response to vascular risk factors than extracranial arteries, and the relationship between ECAS and ICAS may therefore be relatively weak or absent.^{8,24,25} However, studies investigating this hypothesis *in vivo* have been based on the detection of arterial calcification or hemodynamically-significant stenosis, both related to a more advanced stage of atherosclerotic disease. Furthermore, the heterogeneous etiology of arterial calcification and localization restricted to the proximal cerebral arteries might obscure detection of an association. Vessel wall-MRI directly visualizes the pathological vessel wall, enabling more accurate measurement of the ICAS burden.^{11,12,26}

A very high frequency of ICAS was found in the current population¹², especially when compared to other neuroimaging studies. This is in line with early post-mortem studies, which reported frequencies approaching 100% in older age.^{27,28} Furthermore, the distribution of vessel wall lesions, which we recently reported on¹², was also in line with the distribution of plaques in those post-mortem studies: particularly the increased involvement of the larger cerebral arteries compared to the smaller ones. These findings suggest that vessel wall-MRI at 7T allows for a more accurate approximation of the ICAS burden, compared to other neuroimaging methods. However, more studies in different populations, in regard to age, sex and disease status are needed to confirm this.

cIMT is an established marker of generalized atherosclerosis²⁹, although studies on its association with ICAS are limited. Our results are in line with a post-mortem study, which reported an association of cIMT with the intima-media ratio of the cerebral vasculature.³⁰ Furthermore, a longitudinal study in patients with intracranial stenosis found that patients with progressive stenosis on MRA had a larger cIMT compared to those without progression, although this difference was not statistically significant.³¹

Extracranial carotid disease and ICAS are often assessed separately, likely because their prevalence varies between different ethnic populations.³² Notably, ICAS is thought to be most prevalent in populations of African and Asian descent, where it is a major cause of ischemic stroke, whereas in whites it was thought to be less prevalent, and a minor cause of ischemic stroke. However, recent studies have shown that the prevalence and importance of ICAS in whites may have been underestimated.^{12,33,34} Our results show a strong association between extracranial carotid stenosis and ICAS, a finding which is in

concordance with a recent Asian study.³⁵ Hence, our findings question the current segregation, and suggest that they should not be assessed separately.

Low ABI has been associated with hemodynamically-significant intracranial stenosis in community-based and ischemic stroke cohorts.^{36–38} Our results are in line with these findings, and also show that low ABI is associated with the more continuous spectrum of disease measured by ICAS burden, and not just hemodynamically-significant stenosis.

Renal dysfunction is an independent risk factor for cardiovascular disease³⁹, and has been linked to ischemic stroke, cerebral small vessel disease, and medial arterial calcification.^{40,41} A recent scientific abstract reported an association between renal dysfunction and intracranial arterial wall thickening, which is in concordance with our results.⁴²

No significant differences in ICAS burden were observed in patients with a history of cerebrovascular, peripheral artery, or multivascular disease when compared to coronary heart disease. An association with cerebrovascular disease might have been expected, since ICAS is a major cause of ischemic stroke.¹ In our prior study, we did find an association between ICAS burden and presence of ischemic infarcts.¹² However, in the current analyses the outcome was clinical stroke and/or TIA, which is an overlapping but different entity. Furthermore, small sample sizes of all categories, except for coronary heart disease, may also have prevented observation of significant relationships. Notably, earlier studies from our group in acute ischemic stroke patients and controls also did not find an association between the number of vessel wall lesions and ischemic stroke.⁴³

A main strength is the use of vessel wall–MRI at 7T, one of the most accurate methods to assess intracranial atherosclerosis *in vivo*, which enabled visualization of atherosclerosis beyond stenosis. Furthermore, it provided a large coverage area which allowed assessment of CoW branches over a great length. Moreover, the increased contrast-to-noise ratio facilitated a more reliable identification of lesions than is possible at lower field strengths. A last strength is the various measures of ECAS which allowed for an integrated assessment of multiple arterial beds within the same patient.

Several limitations also need to be addressed. First, there is a paucity of radio-pathologic studies on vessel wall lesions, making it possible that not all lesions are atherosclerotic. Second, our sample size, although large compared to previous 7T studies, is still relatively small compared to other epidemiologic studies. Third, our cohort consisted of patients with a history of vascular disease with the majority being male, which may limit generalization of our results to other populations. Fourth, we used a basic uniparametric score to quantify ICAS burden, which does not account for other quantitative features, such as wall thickness. However, accurate quantitative assessment of lesions, especially the very small lesions visible at 7T, is limited at current spatial resolutions.⁴⁴ As a result, grading lesions is a qualitative process, and inherently less objective than quantitative grading. Nonetheless, increased objectiveness can be obtained by training, experience and attaining good reproducibility compared with senior observers, as was done in the

current study. Furthermore, we did not assess luminal stenosis, because we did not include a refined MRA in the protocol. As advancements to current vessel wall sequences are starting to enable more accurate measurements, development of multiparametric scoring systems (e.g. the Gensini score for coronary artery disease), taking into account lesion location, stenosis grade, different geometric characteristics (e.g. remodeling index), signal intensity on various weightings, and contrast-enhanced MRI, may enable a more versatile way to study the relation between ICAS, ECAS and clinical outcomes. Lastly, due to logistic reasons the ECAS assessment and the 7T MRI were not performed on the same day and in a number of participants the time interval was quite large. As ECAS markers could have changed during this interval this may have influenced the observed associations. However, most estimates differed only slightly, and did not lead to different conclusions.

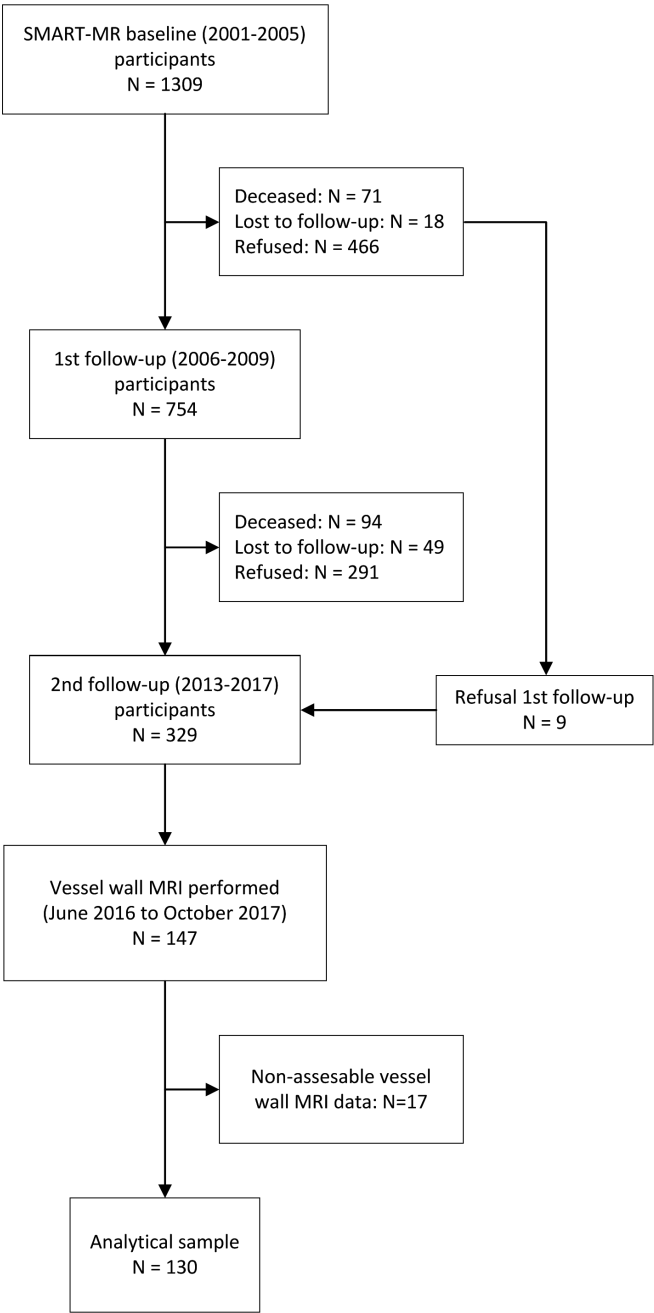
Conclusion

In summary, in patients with a history of various manifestations of vascular disease, ICAS burden, defined as number of intracranial vessel wall lesions, was associated with atherosclerotic disease in all extracranial arterial beds, not supporting a different etiology. Our results may be used to further elucidate the etiology of ICAS and may be of interest to clinical studies looking for effective ways to select patients at risk of ICAS.

References

1. Qureshi AI, Caplan LR. Intracranial atherosclerosis. *Lancet* 2014; 383: 984–98.
2. Dearborn JL, Zhang Y, Qiao Y, Suri MFK, Liu L, Gottesman RF, et al. Intracranial atherosclerosis and dementia: The Atherosclerosis Risk in Communities (ARIC) Study. *Neurology* 2017; 88: 1556–63.
3. Gorelick P, Wong KS, Liu L. Epidemiology. *Front Neurol Neurosci* 2016; 40: 34–46.
4. Qiao Y, Suri FK, Zhang Y, Liu L, Gottesman R, Alonso A, et al. Racial differences in prevalence and risk for intracranial atherosclerosis in a US community-based population. *JAMA Cardiol* 2017; 2: 1341–8.
5. Sternby NH. Atherosclerosis in a defined population. An autopsy survey in Malmö, Sweden. *Acta pathologica et microbiologica Scandinavica* 1968; Suppl 194:5+.
6. D'Armiento FP, Bianchi A, de Nigris F, Capuzzi DM, D'Armiento MR, Crimi G, et al. Age-related effects on atherogenesis and scavenger enzymes of intracranial and extracranial arteries in men without classic risk factors for atherosclerosis. *Stroke* 2001; 32: 2472–9.
7. Kiechl S, Willeit J, Group for the BS. The Natural Course of Atherosclerosis. Part I: incidence and progression. *Arterioscler Thromb Vasc Biol* 1999; 19: 1484–90.
8. Ritz K, Denswil NP, Stam OCG, Van Lieshout JJ, Daemen MJAPAP. Cause and mechanisms of intracranial atherosclerosis. *Circulation* 2014; 130: 1407–14.
9. Suri MFK, Qiao Y, Ma X, Guallar E, Zhou J, Zhang Y, et al. Prevalence of Intracranial Atherosclerotic Stenosis Using High-Resolution Magnetic Resonance Angiography in the General Population: The Atherosclerosis Risk in Communities Study. *Stroke* 2016; 47: 1187–93.
10. López-Cancio E, Dorado L, Millán M, Reverté S, Suñol A, Massuet A, et al. The Barcelona-Asymptomatic Intracranial Atherosclerosis (AsIA) study: Prevalence and risk factors. *Atherosclerosis* 2012; 221: 221–5.
11. Qiao Y, Anwar Z, Intrapiromkul J, Liu L, Zeiler SR, Leigh R, et al. Patterns and Implications of Intracranial Arterial Remodeling in Stroke Patients. *Stroke* 2016; 47: 434–40.
12. Zwartbol MHT, van der Kolk AG, Ghaznawi R, van der Graaf Y, Hendrikse J, Geerlings MI. Intracranial Vessel Wall Lesions on 7T MRI (Magnetic Resonance Imaging). *Stroke* 2019; 50: 88–94.
13. Bhogal P, Navaei E, Makalanda HLD, Brouwer PA, Sjöstrand C, Mandell DM, et al. Intracranial vessel wall MRI. *Clin Radiol* 2016; 71: 293–303.
14. Hartevelde AA, van der Kolk AG, van der Worp HB, Dieleman N, Siero JCW, Kuif HJ, et al. High-resolution intracranial vessel wall MRI in an elderly asymptomatic population: comparison of 3T and 7T. *Eur Radiol* 2017; 27: 1585–95.
15. Geerlings MI, Appelman AP, Vincken KL, Algra A, Witkamp TD, Mali WP, et al. Brain volumes and cerebrovascular lesions on MRI in patients with atherosclerotic disease. The SMART-MR study. *Atherosclerosis* 2010; 210: 130–6.
16. National Cholesterol Education Program (NCEP) Expert Panel on Detection, Evaluation, and Treatment of High Blood Cholesterol in Adults (Adult Treatment Panel III) (2002). Third Report of the National Cholesterol Education Program (NCEP) Expert Panel on Detection, Evaluation, and Treatment of High Blood Cholesterol in Adults (Adult Treatment Panel III) final report. *Circulation* 2002; 106: 3143–3421.
17. Simons PCG, Algra A, Van De Laak MF, Grobbee DE, Van Der Graaf Y. Second manifestations of ARTERial disease (SMART) study: Rationale and design. *Eur J Epidemiol* 1999; 15: 773–81.
18. Winter MA, Guhr KN, Berg GM. Impact of Various Body Weights and Serum Creatinine Concentrations on the Bias and Accuracy of the Cockcroft-Gault Equation. *Pharmacotherapy* 2012; 32: 604–12.
19. van der Kolk AG, Hendrikse J, Brundel M, Biessels GJ, Smit EJ, Visser F, et al. Multi-sequence whole-brain intracranial vessel wall imaging at 7.0 tesla. *Eur Radiol* 2013; 23: 2996–3004.
20. van der Kolk AG, Zwanenburg JJM, Brundel M, Biessels GJ, Visser F, Luijten PR, et al. Distribution and natural course of intracranial vessel wall lesions in patients with ischemic stroke or TIA at 7.0 tesla MRI. *Eur Radiol* 2015; 25: 1692–700.
21. Lindenholtz A, van der Kolk AG, Zwanenburg JJM, Hendrikse J. The Use and Pitfalls of Intracranial Vessel Wall Imaging: How We Do It. *Radiology* 2018; 286: 12–28.
22. Holmstedt CA, Turan TN, Chimowitz MI. Atherosclerotic intracranial arterial stenosis: Risk factors, diagnosis, and treatment. *Lancet Neurol* 2013; 12: 1106–14.
23. Aboyans V, Criqui MH, Abraham P, Allison MA, Creager MA, Diehm C, et al. Measurement and interpretation of the Ankle-Brachial Index: A scientific statement from the American Heart Association. *Circulation* 2012; 126: 2890–909.

24. López-Cancio E, Galán A, Dorado L, Jiménez M, Hernández M, Millán M, et al. Biological signatures of asymptomatic extra- and intracranial atherosclerosis: The Barcelona-AsIA (Asymptomatic Intracranial Atherosclerosis) study. *Stroke* 2012; 43: 2712–9.
25. Odink AE, van der Lugt A, Hofman A, Hunink MGM, Breteler MMB, Krestin GP, et al. Association between calcification in the coronary arteries, aortic arch and carotid arteries: The Rotterdam study. *Atherosclerosis* 2007; 193: 408–13.
26. Mandell DM, Mossa-Basha M, Qiao Y, Hess CP, Hui F, Matouk C, et al. Intracranial Vessel Wall MRI: Principles and Expert Consensus Recommendations of the American Society of Neuroradiology. *AJNR Am J Neuroradiol* 2016; 38: 218–29.
27. Resch JA, Baker AB. Etiologic Mechanisms in Cerebral Atherosclerosis: Preliminary Study of 3,839 Cases. *Arch Neurol* 1964; 10: 617–28.
28. Mathur KS, Kashyap SK, Kumar V. Correlation of the extent and severity of atherosclerosis in the coronary and cerebral arteries. *Circulation* 1963; 27: 929–34.
29. Bots ML, Sutton-Tyrrell K. Lessons from the past and promises for the future for carotid intima-media thickness. *J Am Coll Cardiol* 2012; 60: 1599–604.
30. Iwakiri T, Yano Y, Sato Y, Hatakeyama K, Marutsuka K, Fujimoto S, et al. Usefulness of carotid intima-media thickness measurement as an indicator of generalized atherosclerosis: Findings from autopsy analysis. *Atherosclerosis* 2012; 225: 359–62.
31. Mizukami H, Shimizu T, Maki F, Shiraishi M, Hasegawa Y. Progression of Intracranial Major Artery Stenosis is Associated with Baseline Carotid and Intracranial Atherosclerosis. *J Atheroscler Thromb* 2015; 22: 183–90.
32. Caplan LR, Gorelick PB, Hier DB. Race, sex and occlusive cerebrovascular disease: a review. *Stroke* 1986; 17: 648–55.
33. Bos D, Van Der Rijk MJM, Geeraedts TEA, Hofman A, Krestin GP, Wittteman JCM, et al. Intracranial carotid artery atherosclerosis: Prevalence and risk factors in the general population. *Stroke* 2012; 43: 1878–84.
34. Bos D, Portegies MLP, van der Lugt A, Bos MJ, Koudstaal PJ, Hofman A, et al. Intracranial Carotid Artery Atherosclerosis and the Risk of Stroke in Whites. *JAMA Neurology* 2014; 71: 405–11.
35. Man BL, Fu YP. Concurrent stenoses: A common etiology of stroke in Asians. *World J Clin Cases* 2014; 2: 201–5.
36. Manzano JJF, De Silva DA, Pascual JLR, Chang HM, Wong MC, Chen CPLH. Associations of ankle-brachial index (ABI) with cerebral arterial disease and vascular events following ischemic stroke. *Atherosclerosis* 2012; 223: 219–22.
37. Nakano T, Ohkuma H, Suzuki S. Measurement of ankle brachial index for assessment of atherosclerosis in patients with stroke. *Cerebrovasc Dis* 2004; 17: 212–7.
38. Jiménez M, Dorado L, Hernández-Pérez M, Alzamora MT, Pera G, Torán P, et al. Ankle-brachial index in screening for asymptomatic carotid and intracranial atherosclerosis. *Atherosclerosis* 2014; 233: 72–5.
39. Manjunath G, Tighiouart H, Ibrahim H, MacLeod B, Salem DN, Griffith JL, et al. Level of kidney function as a risk factor for atherosclerotic cardiovascular outcomes in the community. *J Am Coll Cardiol* 2003; 41: 47–55.
40. Makin SDJ, Cook FAB, Dennis MS, Wardlaw JM. Cerebral Small Vessel Disease and Renal Function: Systematic Review and Meta-Analysis. *Cerebrovasc Dis* 2015; 39: 39–52.
41. Power A, Chan K, Haydar A, Hamady M, Cairns T, Taube D, et al. Intracranial arterial calcification is highly prevalent in hemodialysis patients but does not associate with acute ischemic stroke. *Hemodial Int* 2011; 15: 256–63.
42. Hao Q, Gottesman R, Qiao Y, Sharma R, Liu L, Selvin E, et al. Association between kidney disease measures and intracranial atherosclerosis: The ARIC Study. *Stroke* 2018; 49(Suppl 1): ATP52.
43. Hartevelde AA, Van Der Kolk AG, Van Der Worp HB, Dieleman N, Zwanenburg JJM, Luijten PR, et al. Detecting Intracranial Vessel Wall Lesions with 7T-Magnetic Resonance Imaging: Patients with Posterior Circulation Ischemia Versus Healthy Controls. *Stroke* 2017; 48: 2601–4.
44. van Hespen KM, Zwanenburg JJM, Hartevelde AA, Luijten PR, Hendrikse J, Kuijff HJ. Intracranial Vessel Wall Magnetic Resonance Imaging Does Not Allow for Accurate and Precise Wall Thickness Measurements. *Stroke* 2019; 50: e283–84.



Supplemental Figure 1. Flowchart of the study sample.

Supplemental Table 1. Vascular risk factors in study sample (n = 130).

| | |
|--------------------------|----------|
| BMI (kg/m ²) | 27.3±3.7 |
| Current smoker | 15% |
| Hypertension | 90% |
| Hyperlipidemia | 93% |
| Diabetes | 19% |
| Metabolic syndrome | 52% |

Values are presented as mean±SD or %.

Abbreviations: BMI, body mass index; SD, standard deviation.

Supplemental Table 2. Sensitivity analysis of the association between carotid atherosclerosis and ICAS burden.

| | ICAS burden, <i>b</i> (95% CI) |
|-------------------|--------------------------------|
| cIMT, per +0.1 mm | 0.50 (0.04 to 0.97) |
| cIMT quartiles | |
| Quartile 1 | 0 (reference) |
| Quartile 2 | 0.93 (-1.98 to 3.83) |
| Quartile 3 | 0.35 (-2.62 to 3.33) |
| Quartile 4 | 2.85 (-0.02 to 5.72) |
| Carotid stenosis | |
| No stenosis | 0 (reference) |
| 1-49% stenosis | 2.06 (-0.37 to 4.50) |
| 50-100% stenosis | 6.23 (1.94 to 10.52) |

b values are unstandardized linear regression coefficients adjusted for age, sex, and time interval between carotid ultrasound and 7T MRI.

Abbreviations: ICAS, intracranial atherosclerosis; cIMT, carotid intima-media thickness.

Supplemental Table 3. Sensitivity analysis of the association between ABI and ICAS burden.

| | ICAS burden, <i>b</i> (95% CI) |
|------------------------|--------------------------------|
| ABI, per +0.1 in ratio | -0.34 (-0.89 to 0.2) |
| ABI > 0.9 | 0 (reference) |
| ABI ≤ 0.9 | 5.08 (2.00 to 8.16) |

b values are unstandardized linear regression coefficients adjusted for age, sex, and time interval between ABI measurement and 7T MRI.

Abbreviations: ICAS, intracranial atherosclerosis; ABI, ankle-brachial index.

Supplemental Table 4. Sensitivity analysis of the association between renal function and ICAS burden.

| | ICAS burden, <i>b</i> (95% CI) |
|----------------------|--------------------------------|
| eGFR, per +10 ml/min | -0.78 (-1.50 to -0.06) |
| eGFR ≥ 60 ml/min | 0 (reference) |
| eGFR < 60 ml/min | 3.02 (0.31 to 5.72) |

b values are unstandardized linear regression coefficients adjusted for age, sex, and time interval between eGFR measurement and 7T MRI.

Abbreviations: ICAS, intracranial atherosclerosis; eGFR, estimated glomerular filtration rate.

Supplemental Table 5. Sensitivity analysis of the association between history of vascular disease and ICAS burden.

| | ICAS burden, <i>b</i> (95% CI) |
|---------------------------|--------------------------------|
| Coronary artery disease | 0 (reference) |
| Peripheral artery disease | 0.09 (-3.66 to 3.84) |
| Cerebrovascular disease | 0.55 (-2.94 to 4.04) |
| Multivascular disease | 1.93 (-0.73 to 4.59) |

b values are unstandardized linear regression coefficients adjusted for age, sex, and time interval between ECAS and ICAS measurement.

Categories are mutually exclusive.

Abbreviations: ICAS, intracranial atherosclerosis.



4

Intracranial atherosclerosis on 7T MRI and cognitive functioning: The SMART-MR study

Maarten H.T. Zwartbol, Anja G. van der Kolk, Rashid Ghaznawi, Yolanda van der Graaf, Jeroen Hendrikse, Mirjam I. Geerlings, on behalf of the UCC-SMART Study Group

Published in *Neurology* 2020; 95: e1351-61
doi: 10.1212/WNL.00000000000010199

Abstract

Objective

To investigate the association between intracranial atherosclerosis (ICAS) and cognitive functioning in patients with a history of vascular disease.

Methods

Within the SMART-MR study cross-sectional analyses were performed in 130 patients (mean±SD age 68±9 years) with 7T vessel wall–magnetic resonance imaging data. Vessel wall lesions were rated according to established criteria and summed into a circulatory and artery-specific ICAS burden. Associations between ICAS burden and Z-scores of memory, executive functioning, working memory and processing speed, were estimated using linear regression analyses adjusted for age, sex, education, reading ability, and vascular risk factors.

Results

A total of 125 patients (96%) had ≥1 vessel wall lesions; the mean ICAS burden was 8.5±5.7. A statistically non-significant association was found between total ICAS burden and memory ($b = -0.03$ per +1 lesion; 95% CI -0.05 to 0.00). No associations were found for the other domains. A statistically significant association was found for ICAS burden of the posterior cerebral artery (PCA) and memory ($b = -0.12$ per +1 lesion; 95%CI -0.23 to -0.01) and executive functioning ($b = -0.10$ per +1 lesion; 95%CI -0.19 to -0.01). Statistically non-significant associations were found for the anterior cerebral artery (ACA) burden and memory ($b = -0.13$ per +1 lesion; 95%CI -0.26 to 0.01) and executive functioning ($b = -0.11$ per +1 lesion; 95%CI -0.22 to 0.01). Additional adjustments for large infarcts, white matter hyperintensities, lacunes and ≥50% carotid stenosis, produced similar results.

Conclusion

Our results suggest an artery-specific vulnerability of memory and executive functioning to ICAS, possibly due to strategic brain regions involved with these cognitive domains, which are located in the arterial territory of the PCA and ACA.

Introduction

Dementia is a debilitating condition with a large and increasing societal impact.¹ Dementia is the end-stage of cognitive decline: a multifactorial disorder in which multiple pathologies interact and accumulate over time.² Cerebrovascular pathologies, i.e. stroke and arteriole-sclerosis, are important contributors to cognitive decline and dementia.^{3,4} However, because of the interplay and co-occurrence of vascular pathologies, the exact mechanisms leading to cognitive decline are unclear.⁴

Intracranial atherosclerosis (ICAS) has been associated with cognitive impairment and dementia, including Alzheimer's disease, in post-mortem studies.^{5–7} A few studies, most based on detection of arterial stenosis or carotid calcification, have confirmed this association *in vivo*.^{8–11} However, data are lacking on this relationship in premorbid cognitive functioning, and on artery-specific relationships.^{10,11} Elucidating these uncertainties could help our understanding of how ICAS can lead to cognitive decline and dementia.

Vessel wall–magnetic resonance imaging (MRI) enables a more direct assessment of ICAS compared to conventional methods¹², which are limited to detection of stenotic plaques, or arterial calcification, which is restricted to the proximal intracranial arteries.^{13–16} Furthermore, 7 tesla (7T) vessel wall–MRI further improves assessment compared to 3T.^{17,18} As a result, a wider spectrum of ICAS can be assessed, which will aid in the detection of more subtle associations.

In this study, we used 7T vessel wall–MRI to examine the association between ICAS and cognitive functioning in a cohort of patients with a history of vascular disease: a population with an increased risk of ICAS and cognitive decline.

Methods

Study sample

The Second Manifestations of ARterial disease-Magnetic Resonance (SMART-MR) study is a prospective cohort study at our institution aimed at investigating changes on brain MRI in patient with symptomatic atherosclerotic disease.¹⁹ The SMART-MR is a sub-study of the SMART study, which runs parallel with different follow-up intervals.²⁰ Between May 2001 and December 2005, 1309 patients newly referred to our institution with coronary artery disease, cerebrovascular disease, peripheral artery disease or abdominal aortic aneurysm, and without MRI contraindications were invited to participate. On a one-day visit to our institution the patients underwent a 1.5T brain MRI, a physical examination, ankle-brachial index (ABI) assessment, ultrasonography of the carotid arteries, blood and urine sampling, and questionnaires to assess risk factors, medical history, and daily functioning.²¹ Follow-up exams of brain MRI, cognition, and depression assessment were performed in the first follow-up (2006 to 2009)²², and second follow-up period (2013 to 2017). A 7T brain MRI was added during the second follow-up period.

From June 2016 to October 2017, a vessel wall sequence was added to the 7T brain MRI protocol. We included all 147 patients who had 7T vessel wall–MRI performed. Seventeen patients were excluded from the current analysis due to artefacts inhibiting assessment of ≥ 1 major segment of the Circle of Willis. Excluded patients were older, although this did not reach statistical significance (70 ± 7 vs. 68 ± 9 years; $p = 0.11$). Sex distribution did not differ (88% vs. 88% male; $p = 0.95$). Of note, 7T MRI was performed median (range) 0.9 (0–2.7) years after neuropsychological assessment.

Data on vascular risk factors was obtained from the SMART study and was performed median (range) 0.0 (0.0 to 9.2) years prior to the neuropsychological assessment.

Comparison of characteristics between our current study sample and the rest of study population at baseline showed that our sample was younger (54 ± 8 vs. 59 ± 10 years; $p < 0.001$), had fewer women (12% vs. 22%; $p = 0.02$) and less often had cerebrovascular disease (16% vs. 24%; $p = 0.03$).

The SMART-MR study was approved by the ethics committee of our institution and written informed consent was obtained from all patients.

1.5T brain MRI protocol

A 1.5T whole-body system (Gyroscan ACS-NT, Philips Medical Systems, Best, the Netherlands) was used, with a standardized scan protocol. Axial T1-weighted [repetition time (TR) = 235 ms; echo time (TE) = 2 ms], T2-weighted [TR = 2200 ms; TE = 11 ms], fluid-attenuated inversion recovery (FLAIR) [TR = 6000 ms; TE = 100 ms; inversion time (TI) = 2000 ms] and T1-weighted inversion recovery images [TR = 2900 ms; TE = 22 ms; TI = 410 ms] were acquired with a voxel size of $1.0 \times 1.0 \times 4.0 \text{ mm}^3$ and contiguous slices.

7T brain MRI protocol

A 7T whole-body system (Philips Healthcare, Cleveland, OH, USA) was used with a volume transmit coil and a 32-channel receiver head coil (Nova Medical, Wilmington, MA, USA). Vessel wall–MRI was performed with an T₁-weighted MPR-TSE sequence, with parameters: field-of-view (FOV) $250 \times 250 \times 190 \text{ mm}^3$, acquired resolution $0.8 \times 0.8 \times 0.8 \text{ mm}^3$ (reconstructed to $0.49 \times 0.49 \times 0.4 \text{ mm}^3$), TR/TI/TE 3952/1375/37 ms, acquisition time 10:40 min.²³ Dual-echo susceptibility-weighted imaging (SWI) was performed, with parameters: TR/TE1/TE2, 20/6.9/15.8 ms; FOV $200 \times 200 \times 120 \text{ mm}^3$; acquired resolution $0.5 \times 0.5 \times 0.7 \text{ mm}^3$ (reconstructed to $0.4 \times 0.4 \times 0.35 \text{ mm}^3$); flip angle 12 degrees; acquisition time, 09:17 min.

Assessment of intracranial atherosclerosis

A trained observer (MHTZ) assessed all images blinded to patient characteristics. MHTZ was trained by a senior observer with 9 years of experience with intracranial vessel wall–MRI (AK). Training was based on 15 patients from the Intracranial Vessel wall Imaging (IVI) study²⁴, and a set of 20 randomly selected patients from the current study, which was also rated by AK. Interobserver agreement was regarded as good with a dice similarity coefficient of 0.75, calculated from the set of 20 patients.

Vessel wall lesions were rated according to criteria described previously.²⁵ In brief, a lesion was defined as a focal or a more diffuse thickening of the vessel wall, compared with the neighboring or contralateral wall. Inconspicuous lesions were evaluated in multiple planes for verification. Lesions were rated per arterial segment, which included: the anterior cerebral arteries (ACA; A1, A2 segments), middle cerebral arteries (MCA; M1, M2 segments), distal internal carotid arteries (ICA; supraclinoid (C6) and communicating segment (C7)), posterior communicating arteries (PCom), posterior cerebral arteries (PCA; P1, P2 segments, P1-P2 bifurcation), basilar artery and vertebral arteries. Multiple lesions could be present in a single segment.

A maximum intensity projection (maxIP) of the first echo of the SWI sequence was constructed for use as a *faux* MR angiography (MRA) to assess the course of arteries. However, because of its sensitivity to artefacts it could not be used to measure percentage stenosis.

Neuropsychological assessment

All patients underwent neuropsychological assessment for memory, executive functioning, working memory, and processing speed. Memory was assessed with the 15 Word Learning Test, a modification of the Rey Auditory Verbal Learning test, using a composite score of the immediate recall based on 5 trials, the delayed recall and the retention score; and the delayed recall of the Rey-Osterrieth Complex figure test.^{26,27} Executive functioning was assessed with the Visual Elevator test, the Brixton Spatial Anticipation test, and the Verbal Fluency test using the letter *n* and animals as categories.^{28–30} Working memory was assessed with the combined longest span scores of the Forward Digit Span and Backward Digit Span.³¹ Processing speed was assessed with the Digit Symbol Substitution Test (120 seconds).³² Composite Z-scores were calculated by converting raw scores to standardized Z-scores and averaging them across all subtests per domain. Prior to standardization, the Visual Elevator test scores were natural-log transformed. Also, scores of the Visual Elevator and Brixton Spatial Anticipation test were multiplied by -1 so that lower scores represented poorer performance.

Covariates

The Dutch version of the National Adult Reading Test (DART) was used to test reading ability.³³ Educational level was classified into seven categories, ranging from primary school to academic degree, according to the Dutch educational system. The Mini Mental State Examination (MMSE) was used to determine global cognitive functioning.³⁴

Blood sampling was performed after an overnight fast. Age, sex, alcohol use and cigarette smoking habits were determined by questionnaires. The body mass index (BMI; kg/m²) was calculated from the weight and height, measured without shoes and heavy clothing. Obesity was defined as a BMI ≥ 30 kg/m². Systolic blood pressure (SBP; mmHg) and diastolic blood pressure (DBP; mmHg) were measured by averaging three separate

measurements with a sphygmomanometer. Hypertension was defined as a SBP of >140 mmHg, a mean DBP of >90 mmHg, or self-reported use of antihypertensive drugs. Diabetes was defined as a history of diabetes, use of antidiabetic medication at baseline or follow-up or a fasting glucose level higher than 11.1 mmol/L. Additionally, if a patient had a glucose level between 7.0 and 11.1 at baseline and started antidiabetic medication within 1 year after inclusion, it was regarded as having diabetes at baseline. Hyperlipidemia was defined as a cholesterol ratio (total cholesterol divided by high-density cholesterol level) greater than or equal to 5, or use of lipid-lowering medication. Carotid ultrasonography was performed with a 10MHz linear-array transducer (ATL Ultramark 9). Carotid stenosis $\geq 50\%$ was based on blood flow velocity patterns and defined as peak systolic velocity >150 cm/s in the left and/or right common or internal carotid artery.

Large infarcts and lacunes of presumed vascular origin³⁵ were rated by a neuroradiologist in training, with 6 years of brain MRI experience (MHTZ), blinded to patient characteristics, on the T1-weighted, T2-weighted and FLAIR 1.5T MRI images. Large infarcts were defined as cortical infarcts or large subcortical infarcts (>1.5 cm in maximum diameter, to distinguish from lacunes). Uncertain lesions were re-evaluated in a consensus meeting with a senior neuroradiologist.

White matter hyperintensity (WMH) volume and intracranial volume were obtained using a *k*-nearest neighbor classification-based segmentation technique on the T1-weighted, FLAIR, and T1-weighted inversion recovery MRI images.³⁶ Cerebral infarcts and lacunes were segmented manually by an investigator (MHTZ) and WMH segmentations were visually checked by an investigator (RG), using an image processing application (MeVisLab 2.7.1., MeVis Medical Solutions AG, Bremen, Germany) to ensure that all infarcts and lacunes were correctly removed from the WMH segmentations. Voxels which were incorrectly segmented were added to the correct segmentation volumes automatically.

Statistical analysis

First, artery-specific ICAS burden was calculated by adding all lesions per artery. If arteries were paired, e.g., the left and right MCA, both ICAS burdens were summed to obtain one score. ICAS burdens for the anterior, posterior and total cerebral circulation were calculated. Second, associations between the artery-specific or circulatory ICAS burden and domain-specific cognitive functioning Z-scores were estimated with linear regression. Analyses were adjusted for age, sex, educational level, and reading ability in model 1, and additionally for systolic/diastolic blood pressure, ratio of cholesterol/HDL ≥ 5 , diabetes, cigarette smoking pack-years, alcohol use, and BMI (model 2). To gain more insight into the pathways through which ICAS could be associated with cognitive functioning, all analyses in which the ICAS burden estimate had an arbitrarily chosen *p*-value of less than 0.10 in model 2, were additionally adjusted for presence of large infarcts, markers of small vessel disease (WMH volume (natural-log of % intracranial volume) and presence of lacunes), and presence of $\geq 50\%$ carotid stenosis, each in separate models.

Statistical analyses were performed using IBM SPSS Statistics version 25 for Windows (IBM Corporation, Armonk, NY, USA).

Data Availability Statement

For use of anonymized data, a reasonable request has to be made in writing to the study group and the third party has to sign a confidentiality agreement.

Results

Table 1 presents the characteristics of the 130 patients. The mean age of the study sample was 68 ± 9 years, 88% was male, and the mean MMSE was 28.8 ± 1.4 . Of the total study sample, 96% had ≥ 1 vessel wall lesions present. The mean ICAS burden for the total

Table 1. Characteristics of study sample (n = 130).

| | |
|---|----------------|
| Age (years) | 68±9 |
| Male sex | 88% |
| Educational level (range 0-7) ^a | 5 (2, 6) |
| Reading ability (range 0-100) ^a | 85 (65, 96) |
| Mini-Mental State Examination | 28.8±1.4 |
| Alcohol use (% current) | 90% |
| Smoking (pack-years) | 21.7±18.4 |
| Hypertension | 90% |
| Diabetes | 19% |
| Hyperlipidemia | 93% |
| History of vascular disease ^b | |
| Coronary artery disease | 79% |
| Cerebrovascular disease | 19% |
| Peripheral artery disease | 19% |
| Abdominal aortic aneurysm | 2% |
| Carotid stenosis $\geq 50\%$ | 7% |
| Large infarcts | 9% |
| Lacunes of presumed vascular origin | 16% |
| White matter hyperintensities (ml) ^a | 1.5 (0.3, 9.0) |
| Total intracranial volume (ml) | 1456±116 |

Values are presented as mean±SD or %.

^a Median (10th, 90th percentile).

^b Multiple comorbidities are possible.

cerebral circulation ($ICAS_{TC}$) was 8.5 ± 5.7 lesions, for the anterior circulation ($ICAS_{AC}$) 5.3 ± 3.2 lesions, and for the posterior circulation ($ICAS_{PC}$) 3.8 ± 3.0 lesions. Figure 1 presents a schematic overview of the frequency and distribution of vessel wall lesions in the study sample. Figure 2 shows examples of vessel wall lesions on vessel wall-MRI.

A non-significant association was observed between $ICAS_{TC}$ and memory ($b = -0.02$ per +1 lesion; 95% CI -0.05 to 0.00) after adjusting for age, sex, educational level and reading ability (Table 2). Additional adjustment for vascular risk factors, and additionally for: large infarcts, WMH volume and lacunes and $\geq 50\%$ carotid stenosis, produced similar results. Figure 3 shows the cognitive functioning Z-scores per quartile of $ICAS_{TC}$, adjusted for age, sex, education level, reading ability and vascular risk factors. None of the models were statistically significant. Furthermore, no significant differences were observed between quartiles, using the lowest quartile as reference category.

A statistically significant association of $ICAS_{PC}$ with memory was observed ($b = -0.06$ per +1 lesion; 95% CI -0.10 to -0.01) after adjusting for age, sex, educational level and

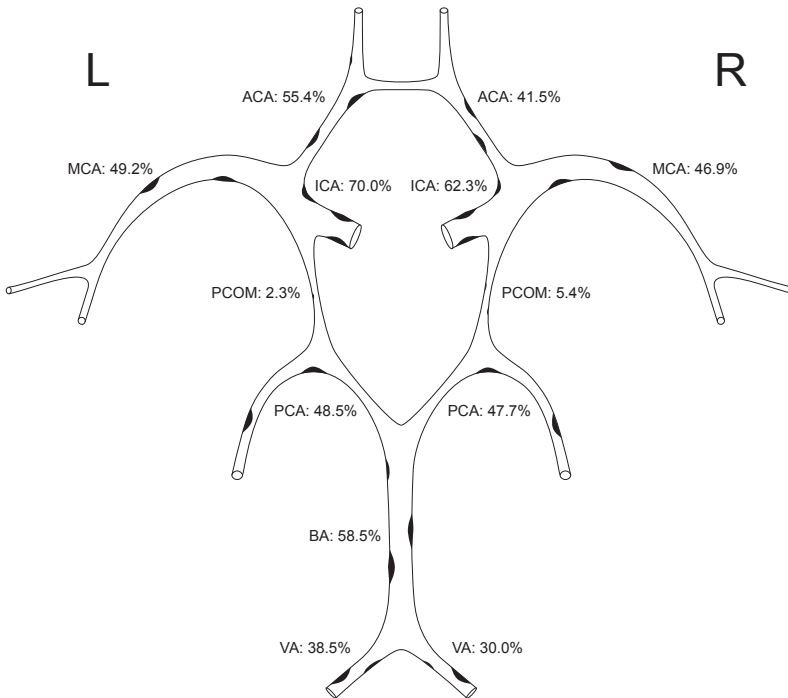


Figure 1. Frequency and distribution of intracranial vessel wall lesions. Schematic drawing of the Circle of Willis and its branches with the frequency of ≥ 1 vessel wall lesions illustrated by means of wall thickening. The number and size of thickenings indicates a higher frequency within the specific artery.

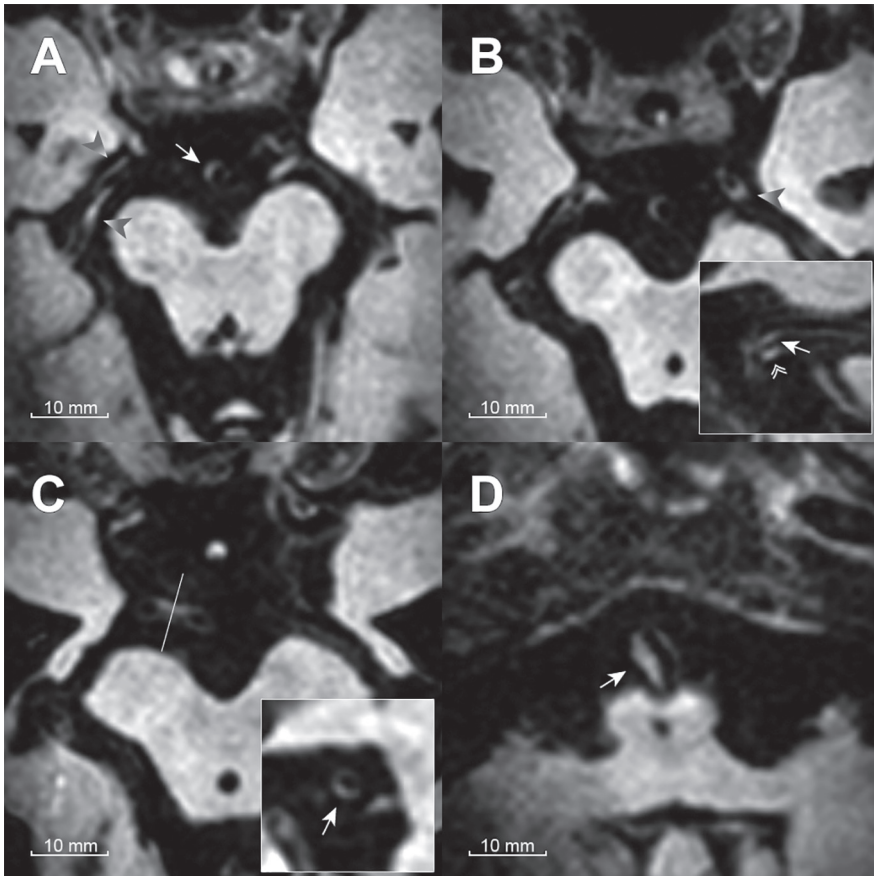


Figure 2. Vessel wall lesions on intracranial vessel wall–MRI at 7T. A) Two lesions (arrowheads) in the lateral and medial wall of the right P2 segment. Compare to normal, barely discernable, mirroring wall. A third lesion is visible in the distal basilar artery (arrow). B) Lesion in inferior wall of P2 segment left (arrowhead). On oblique multiplanar reconstruction angulated to the P2 segment (panel) a slight wall thickening (arrow) is appreciated. Note the passing oculomotor nerve (double arrowhead). C) Lesion in the inferior wall of the right P1 segment, best appreciated on oblique multiplanar reconstruction (arrow). D) Large lesion in the right wall of the proximal basilar artery.

reading ability (Table 2). After additional adjustment for vascular risk factors (model 2) the association remained. Additional adjustments of the latter model were made for: large infarcts ($b = -0.06$; 95% CI -0.11 to -0.00), WMH volume and lacunes ($b = -0.06$; 95% CI -0.12 to -0.01), and $\geq 50\%$ carotid stenosis ($b = -0.06$; 95% CI -0.11 to -0.00), causing no considerable change. No significant associations were observed for ICAS_{AC} (Table 2).

Table 2. Associations between ICAS burden of total, anterior, and posterior cerebral circulation and cognitive functioning Z-scores.

| ICAS burden | Model | Memory <i>b</i> (95% CI) | Executive functioning <i>b</i> (95% CI) | Working memory <i>b</i> (95% CI) | Processing speed <i>b</i> (95% CI) |
|--------------------|-------|-----------------------------|---|--|--|
| ICAS _{TC} | 1 | -0.02 (-0.05 to 0.00) | -0.02 (-0.04 to 0.00) | 0.01 (-0.01 to 0.04) | -0.01 (-0.03 to 0.01) |
| | 2 | -0.03 (-0.05 to 0.00) | -0.02 (-0.04 to 0.01) | 0.01 (-0.02 to 0.04) | -0.01 (-0.04 to 0.02) |
| ICAS _{AC} | 1 | -0.02 (-0.07 to 0.03) | -0.03 (-0.07 to 0.01) | 0.02 (-0.03 to 0.07) | -0.03 (-0.07 to 0.01) |
| | 2 | -0.02 (-0.07 to 0.03) | -0.02 (-0.07 to 0.02) | 0.02 (-0.03 to 0.08) | -0.03 (-0.07 to 0.02) |
| ICAS _{PC} | 1 | -0.06 (-0.10 to -0.01) | -0.03 (-0.07 to 0.01) | 0.02 (-0.03 to 0.07) | -0.00 (-0.05 to 0.04) |
| | 2 | -0.06 (-0.11 to -0.01) | -0.03 (-0.07 to 0.02) | 0.02 (-0.04 to 0.08) | -0.01 (-0.05 to 0.04) |

b values are unstandardized linear regression coefficients and represent the difference in cognitive functioning (Z-score) per 1 lesion increase in ICAS burden.

Model 1: adjusted for age, sex, educational level and reading ability.

Model 2: model 1 with additional adjustment for vascular risk factors (blood pressure, cholesterol/HDL ≥ 5 , diabetes, cigarette smoking (pack-years), alcohol use (units per week) and body mass index).

Abbreviations: ICAS, intracranial atherosclerosis. ICAS_{TC}, total circulation. ICAS_{AC}, anterior circulation. ICAS_{PC}, posterior circulation.

Table 3 presents the results of the linear regression analyses of the association between the artery-specific ICAS burden and domain-specific cognitive functioning Z-scores. A significant association was found between the posterior cerebral artery (ICAS_{PCA}) and memory ($b = -0.13$ per +1 lesion; 95% CI -0.24 to -0.02), after adjustment for age, sex, educational level and reading ability. Additional adjustment for vascular risk factors did not considerably change the association. Furthermore, additional adjustments of model 2 for: large infarcts ($b = -0.12$ per +1 lesion; 95% CI -0.23 to -0.01), WMH volume and lacunes ($b = -0.14$ per +1 lesion; 95% CI -0.25 to -0.03), and $\geq 50\%$ carotid stenosis ($b = -0.12$ per +1 lesion; 95% CI -0.23 to -0.02) also did not considerably change the results. Moreover, a significant association was found between ICAS_{PCA} and executive functioning ($b = -0.09$ per +1 lesion; 95% CI -0.17 to -0.01) after adjustment for age, sex, educational level and reading ability; and remained associated after vascular risk factors were added to the model. Additional adjustments of model 2 were made for: large infarcts ($b = -0.09$ per +1 lesion; 95% CI -0.18 to 0.01), WMH volume and lacunes ($b = -0.10$ per +1 lesion; 95% CI -0.19 to -0.00), and $\geq 50\%$ carotid stenosis ($b = -0.10$ per +1 lesion; 95% CI -0.19 to -0.01), respectively. A non-significant association was observed between the anterior cerebral

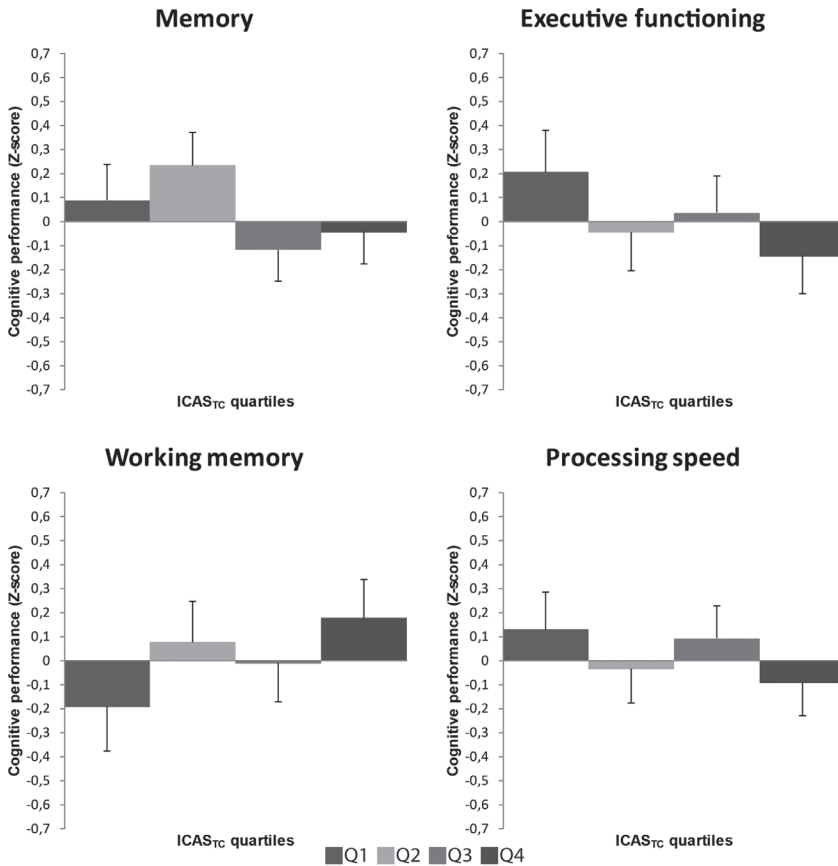


Figure 3. Adjusted mean cognitive functioning Z-scores per approximate quartile of ICAS_{TC}. Values are presented as adjusted mean ± SE Z-scores adjusted for age, sex, educational level, reading ability, and vascular risk factors. ANCOVA was used to test for differences in cognitive performance with the lowest quartile as reference. Adjusted mean ± SE Z-score with *p*-value for estimated marginal means pairwise comparisons for memory (*p* = 0.57): Q1, 0.09 ± 0.15; Q2, 0.23 ± 0.14; Q3, -0.12 ± 0.13; Q4, -0.05 ± 0.13; executive functioning (*p* = 0.29): Q1, 0.20 ± 0.18; Q2, -0.05 ± 0.16; Q3, 0.04 ± 0.15; Q4, -0.15 ± 0.16; working memory (*p* = 0.55): Q1, -0.19 ± 0.18; Q2, 0.08 ± 0.16; Q3, -0.01 ± 0.16; Q4, 0.18 ± 0.16; processing speed (*p* = 0.69): Q1, 0.13 ± 0.16; Q2, -0.04 ± 0.14; Q3, 0.09 ± 0.13; Q4, -0.09 ± 0.14.

artery (ICAS_{ACA}) and memory (*b* = -0.11 per +1 lesion; 95% CI -0.23 to 0.02), after adjustment for age, sex, educational level and reading ability, with similar results after vascular risk factor adjustment in model 2. Additional adjustment for large infarcts, WMH volume and lacunes, and ≥50% carotid stenosis, produced similar results. Moreover, ICAS_{ACA} showed a non-significant association with executive functioning (*b* = -0.10 per +1 lesion; 95% CI

Table 3. Associations between artery-specific ICAS burden and cognitive functioning Z-scores.

| ICAS burden | Model | Memory <i>b</i> (95% CI) | Executive functioning <i>b</i> (95% CI) | Working memory <i>b</i> (95% CI) | Processing speed <i>b</i> (95% CI) |
|---------------------------------|-------|---------------------------|---|----------------------------------|------------------------------------|
| ICAS _{ICA} | 1 | -0.03 (-0.13 to 0.07) | -0.06 (-0.15 to 0.03) | 0.04 (-0.07 to 0.15) | -0.08 (-0.17 to 0.02) |
| | 2 | -0.02 (-0.14 to 0.09) | 0.04 (-0.14 to 0.06) | 0.05 (-0.07 to 0.17) | -0.07 (-0.17 to 0.03) |
| ICAS _{MCA} | 1 | 0.00 (-0.09 to 0.09) | -0.02 (-0.10 to 0.06) | 0.04 (-0.05 to 0.13) | -0.02 (-0.10 to 0.06) |
| | 2 | -0.00 (-0.10 to 0.09) | 0.00 (-0.08 to 0.08) | 0.04 (-0.06 to 0.14) | -0.02 (-0.10 to 0.07) |
| ICAS _{ACA} | 1 | -0.11 (-0.23 to 0.02) | -0.10 (-0.21 to 0.01) | 0.03 (-0.10 to 0.16) | -0.05 (-0.16 to 0.06) |
| | 2 | -0.13 (-0.26 to 0.01) | -0.11 (-0.22 to 0.01) | 0.02 (-0.12 to 0.16) | -0.07 (-0.18 to 0.05) |
| ICAS _{BA} | 1 | -0.08 (-0.23 to 0.08) | -0.08 (-0.21 to 0.05) | 0.07 (-0.09 to 0.23) | -0.05 (-0.19 to 0.08) |
| | 2 | -0.07 (-0.23 to 0.09) | -0.08 (-0.21 to 0.05) | 0.07 (-0.10 to 0.23) | -0.07 (-0.21 to 0.07) |
| ICAS _{VA} ^a | 1 | -0.10 (-0.23 to 0.03) | 0.00 (-0.11 to 0.11) | 0.05 (-0.07 to 0.17) | 0.10 (-0.01 to 0.21) |
| | 2 | -0.08 (-0.22 to 0.06) | 0.03 (-0.10 to 0.15) | 0.05 (-0.09 to 0.19) | 0.11 (-0.01 to 0.23) |
| ICAS _{PCA} | 1 | -0.13 (-0.24 to -0.02) | -0.09 (-0.17 to -0.01) | 0.04 (-0.06 to 0.14) | -0.08 (-0.16 to 0.01) |
| | 2 | -0.12 (-0.23 to -0.01) | -0.10 (-0.19 to -0.01) | 0.05 (-0.07 to 0.16) | -0.08 (-0.18 to 0.01) |

b values are unstandardized linear regression coefficients and represent the difference in cognitive functioning (Z-score) per 1 lesion increase in ICAS burden.

Model 1: adjusted for age, sex, educational level and reading ability.

Model 2: model 1 with additional adjustment for vascular risk factors (blood pressure, cholesterol/HDL ≥ 5 , diabetes, cigarette smoking (pack-years), alcohol use (units per week) and body mass index).

Abbreviations: ICAS, intracranial atherosclerosis. ICAS_{ICA}, internal carotid artery. ICAS_{MCA}, middle cerebral artery. ICAS_{ACA}, anterior cerebral artery. ICAS_{BA}, basilar artery.

ICAS_{VA}, vertebral artery. ICAS_{PCA}, posterior cerebral artery.

^a Analysis in 95 patients because one or both vertebral arteries were not assessed due to imaging artifacts.

-0.21 to 0.01), after adjustment for age, sex, educational level and reading ability, with similar results after vascular risk factor adjustment in model 2, and after additional adjustment for large infarcts, WMH volume and lacunes, and $\geq 50\%$ carotid stenosis. No significant associations were found for the middle cerebral artery, internal carotid artery, vertebral artery and basilar artery.

Figure 4 presents the mean cognitive performance Z-scores for memory and executive functioning per approximate quartile of ICAS_{ACA} and ICAS_{PCA}. Means were adjusted for

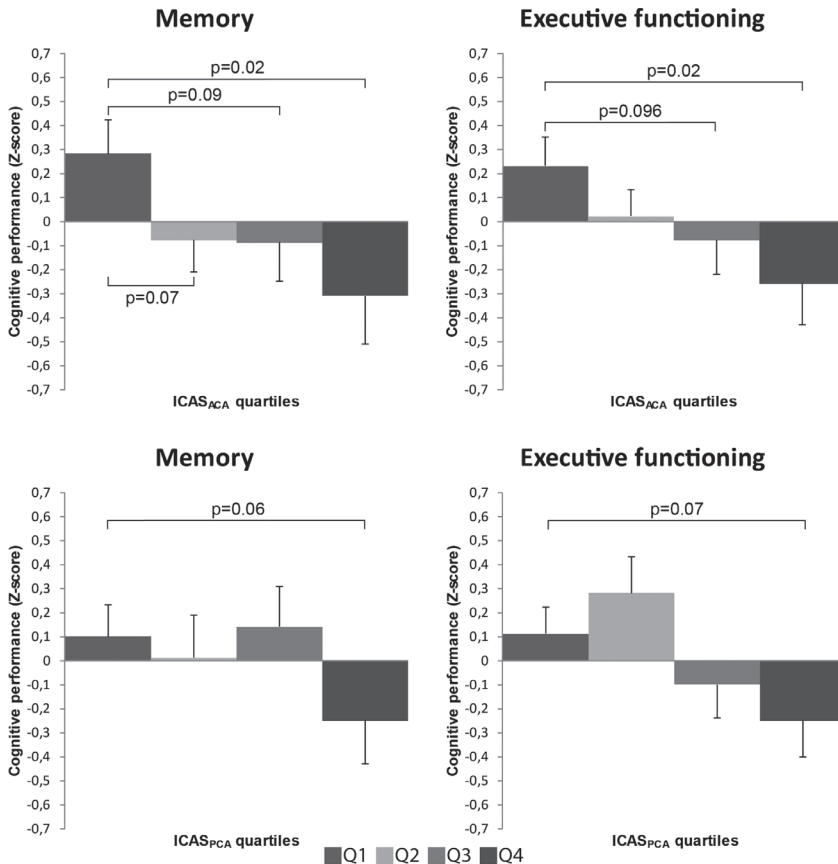


Figure 4. Adjusted mean executive functioning and memory Z-scores per approximate quartile of ICAS_{ACA} and ICAS_{PCA}. Values are presented as adjusted mean ± SE Z-scores adjusted for age, sex, educational level, reading ability, and vascular risk factors. ANCOVA was used to test for differences in cognitive performance with the lowest quartile as reference. Adjusted mean ± SE Z-score per ICAS_{ACA} quartile with *p*-value for estimated marginal means pairwise comparisons for memory (*p* = 0.09): Q1, 0.28 ± 0.14; Q2, -0.08 ± 0.13; Q3, -0.09 ± 0.16; Q4, -0.31 ± 0.20; executive functioning (*p* = 0.12): Q1, 0.23 ± 0.12; Q2, 0.02 ± 0.11; Q3, -0.08 ± 0.14; Q4, -0.26 ± 0.17. Adjusted mean ± SE Z-score per ICAS_{PCA} quartile with *p*-value for estimated marginal means pairwise comparisons for memory (*p* = 0.18): Q1, 0.10 ± 0.13; Q2, 0.01 ± 0.18; Q3, 0.14 ± 0.17; Q4, -0.25 ± 0.18; executive functioning (*p* = 0.07): Q1, 0.11 ± 0.11; Q2, 0.28 ± 0.15; Q3, -0.10 ± 0.14; Q4, -0.25 ± 0.15.

age, sex, level of education, reading ability, and vascular risk factors. As can be seen, for both arteries there was a negative direction of association, with cognitive performance estimates being lowest in the upper quartile of ICAS burden. For the ACA, a significant mean

difference in Z-score was observed between Q1 and Q4 for memory (mean difference: -0.59; 95% CI -1.08 to -0.09) and executive functioning (mean difference: -0.49; 95% CI -0.91 to -0.07). For the PCA, a considerable mean difference in Z-score was observed between Q1 and Q4 for memory (mean difference: -0.45; 95% CI -0.91 to 0.01), and executive functioning (mean difference -0.36; 95% CI -0.75 to 0.03), however, the confidence interval contained 0.00.

Charts for the other arteries are presented in Supplemental Figure 1. As can be seen, although sporadic differences can be observed, they are less clear than for the PCA and ACA, and largely non-significant.

Discussion

In patients with a history of vascular disease, we observed that a higher ICAS burden in the PCA was associated with poorer memory and executive functioning. Similar effect estimates, although not statistically significant, were found for the ACA. No significant relationship was found between total ICAS burden and cognitive functioning.

Atherosclerosis of the circle of Willis and major cerebral arteries has been associated with an increased risk of dementia in post-mortem studies.^{5,7,37} Several studies have reported on the association between ICAS and cognitive impairment and dementia *in vivo*.^{8–11} In the Rotterdam Study, intracranial carotid artery calcification was associated with an increased risk of cognitive decline and dementia, although this association lost significance after adjustment for vascular risk factors.¹⁰ A recent cross-sectional study reported that presence of $\geq 50\%$ stenosis of any intracranial artery, detected on 3T MR angiography, was associated with AD and vascular dementia.⁹ No artery-specific analyses were performed. The Atherosclerosis Risk in Communities (ARIC) study, a population-based 3T vessel wall-MRI study, found that ACA plaque, >2 intracranial arteries with plaque, or $>50\%$ intracranial stenosis were associated with an increased prevalence of dementia but not MCI.¹¹ Conversely, PCA plaque was associated with increased risk of MCI but not dementia. No associations were found for the other cerebral arteries.

Our findings have significance because they replicate and extend the results of the ARIC study. We also found associations for the ACA and PCA, and not for the other cerebral arteries; and also, did not observe an association between total ICAS burden and cognitive functioning. Extending the findings of the ARIC study for MCI or AD, we observed a relation with decline of executive functioning and memory, both early features of dementia and MCI, suggesting that this relationship is already present in very early stages of cognitive decline.^{38,39} Notably, a post-mortem study also found the PCA to be the most frequent severely affected artery in patients with AD compared to age and sex-matched non-demented controls.³⁷

We did not observe a significant association between total ICAS burden and cognitive functioning. A possible explanation is that on this global level the effect estimates of the more specifically associated arteries, e.g., the PCA and ACA, are attenuated by the arteries with an effect size closer to 0.00.

Although our study design only allows for detection of associations, we can hypothesize about possible explanations for these associations. Mechanistically, an explanation could be the role of the ACA and PCA as main arterial blood supply of brain regions involved with memory, such as the nucleus basalis of Meynert (ACA), hippocampus (PCA), thalamus (PCA), and cingulate cortex (ACA/PCA), and with executive functioning, such as the medial prefrontal cortex (ACA) and subcortical nuclei (including thalamus) (ACA/PCA/MCA).^{37,40–42} Atherosclerosis can lead to luminal stenosis and obstruction of the ostia of small perforating arteries, causing progressive decrease of regional blood flow and a chronic hypoxic/ischemic state, ultimately leading to failure of metabolic and electrophysiological functions.^{37,43} Moreover, it can also lead to infarction: thromboembolic lesions of the hippocampus have been linked to memory deficits.⁴⁴ A second hypothesis to explain the association between ACA/PCA burden and cognitive functioning is that they are markers of the underlying arterial and arteriolar disease processes, including cerebral small vessel disease (CSVD), with effects on cognitive functioning through parallel pathways. However, we performed extensive adjustments, with little to no change of the effect estimates.

We failed to find an association between ICAS and processing speed and working memory. Cognitive processing speed has been associated with disruption of white matter pathways.⁴⁵ ICAS could hypothetically cause disruption of white matter pathways through its association with WMH and stroke.^{46,47} Apart from general limitations regarding our study, we have no specific explanation why these association would be absent, in correlation with the other detected associations.

Our study has several strengths. First, 7T vessel wall-MRI is one of the most accurate methods to measure ICAS *in vivo*, enabling detection of stenotic and non-stenotic disease.^{12,14,18} Second, extensive cognitive function assessments over several cognitive domains allowed an artery-specific and domain-specific analysis. Third, extensive data on vascular risk factors and MRI markers of cerebrovascular disease allowed us to gain more insight into potential confounding or mediating variables.

Several limitations also need to be addressed. First, because of the cross-sectional design we do not know who will develop MCI and dementia. Also, potential unknown shared risk factors may lead to ICAS and cognitive impairment. Second, the sample size, although large for a 7T MRI study, is still relatively small and may have limited the ability to observe small associations. Third, due to logistic reasons the 7T MRI was performed on average 1 year after the neuropsychological assessment, and it is possible that in some patient's vessel wall lesions appeared after the neuropsychological assessment. However, because the ratio of ICAS burden increase per year to the standard deviation of ICAS

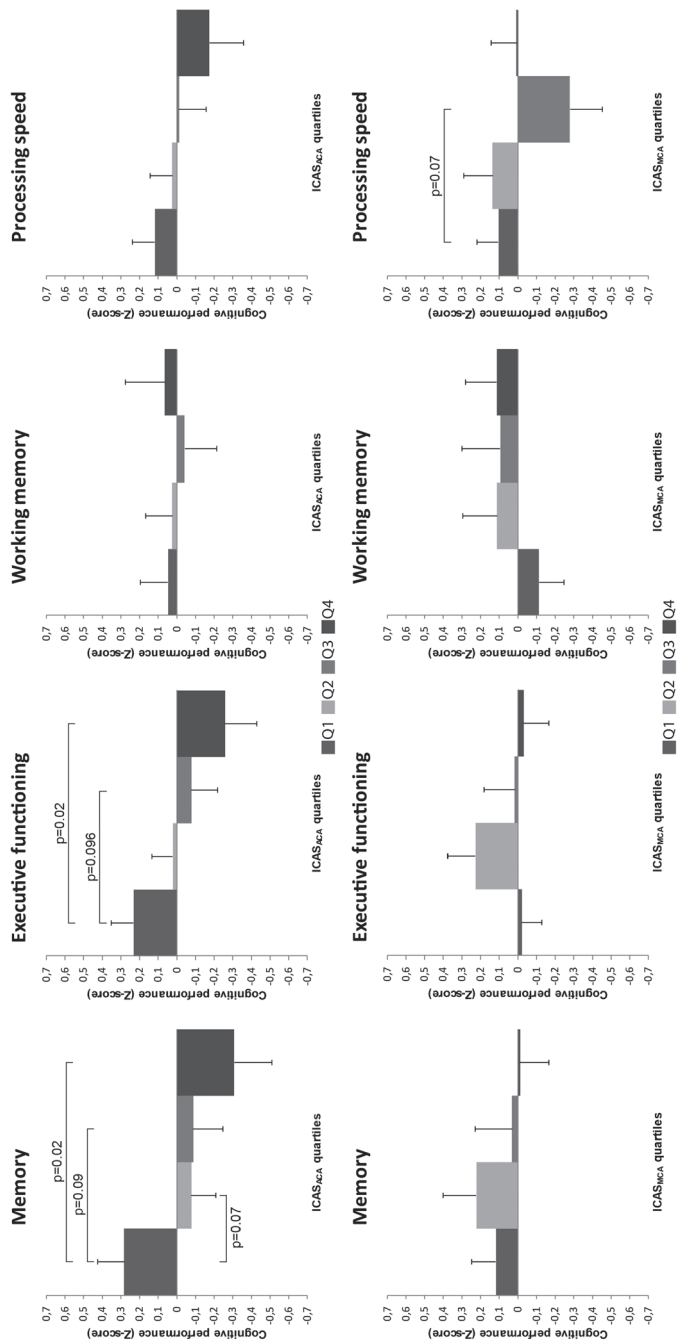
burden in our study sample was so small, we hypothesized the effect on the outcome would be small to negligible. Fourth, patients who dropped out during follow-up cannot be weighted back to the cohort that was included at baseline, because we do not have baseline data on vessel wall lesions and cognition. Thus, our findings are generalizable to patients with a history of vascular disease who survived until the second follow-up after on average 12 years and were able to undergo 7T imaging. Lastly, we did not assess arterial stenosis and, as a result, cannot differentiate which lesions are hemodynamically significant. Future studies could include this to construct a multiparametric 'ICAS burden' score and examine if this better models the association between ICAS and cognitive functioning.

In summary, in patients with a history of vascular disease, a higher ICAS burden in the PCA was associated with poorer memory and executive functioning. Furthermore, the ACA showed a similar association, although not statistically significant, with the same domains. Within a paucity of *in vivo* studies regarding ICAS and cognitive functioning, to the best of our knowledge this is the second study to find this association. Our results suggest an artery-specific vulnerability of memory and executive functioning to ICAS, possibly due to strategic brain regions involved with these cognitive domains, located in the arterial territory of the PCA and ACA.

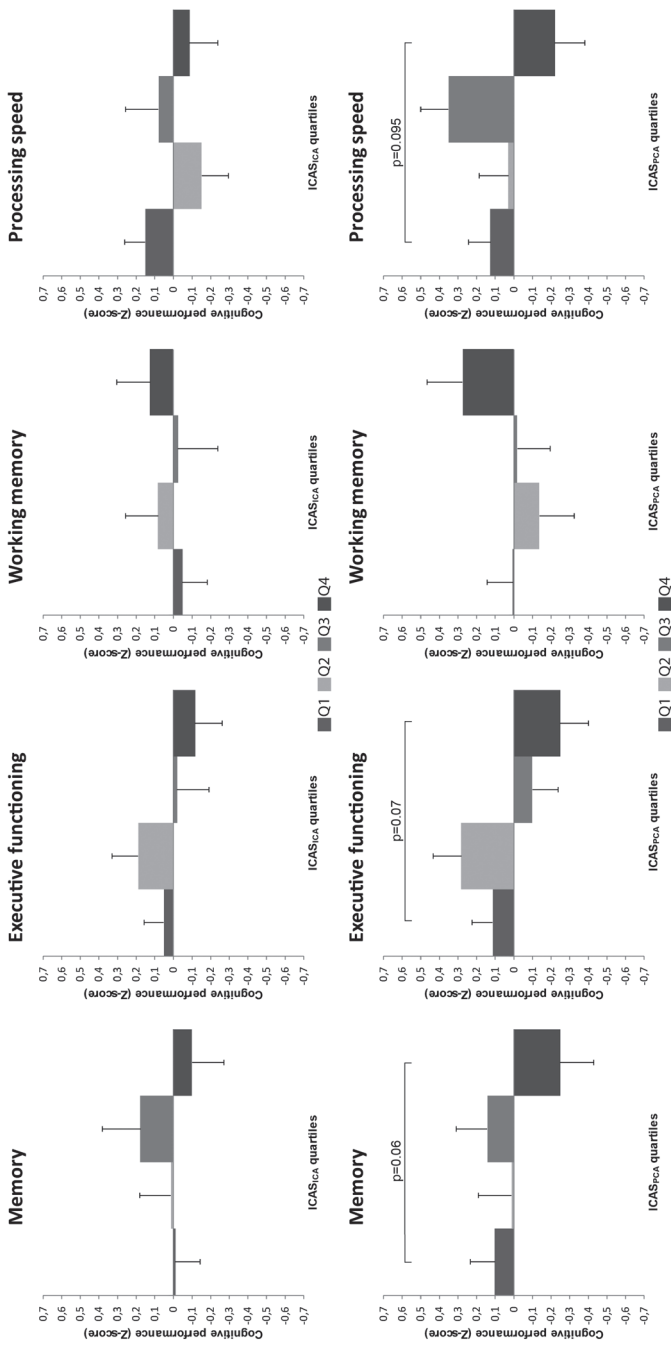
References

1. Wimo A, Jönsson L, Bond J, Prince M, Winblad B. The worldwide economic impact of dementia 2010. *Alzheimers Dement* 2013; 9: 1–11.
2. Schneider JA, Arvanitakis Z, Bang W, Bennett DA. Mixed brain pathologies account for most dementia cases in community-dwelling older persons. *Neurology* 2007; 69: 2197–204.
3. Knopman DS. Cerebrovascular disease and dementia. *Br J Radiol* 2007; 80(Spec No 2): S121–7.
4. Gorelick P, Scuteri A, Black S. Vascular Contributions to Cognitive Impairment and Dementia: A Statement for Healthcare Professionals From the American Heart Association/American Stroke Association. *Stroke* 2011; 42: 2672–713.
5. Qureshi AI, Caplan LR. Intracranial atherosclerosis. *Lancet* 2014; 383: 984–98.
6. Roher AE, Esh C, Kokjohn TA, Kalback W, Luehrs DC, Seward JD, et al. Circle of Willis Atherosclerosis Is a Risk Factor for Sporadic Alzheimer's Disease. *Arterioscler Thromb Vasc Biol* 2003; 23: 2055–62.
7. Beach TG, Wilson JR, Sue LI, Newell A, Poston M, Cisneros R, et al. Circle of Willis atherosclerosis: association with Alzheimer's disease, neuritic plaques and neurofibrillary tangles. *Acta Neuropathol* 2006; 113: 13–21.
8. Zhu J, Wang Y, Li J, Deng J, Zhou H. Intracranial artery stenosis and progression from mild cognitive impairment to Alzheimer disease. *Neurology* 2014; 82: 842–9.
9. Hilal S, Xu X, Ikram MK, Vrooman H, Venketasubramanian N, Chen C. Intracranial stenosis in cognitive impairment and dementia. *J Cereb Blood Flow Metab* 2017; 37: 2262–9.
10. Bos D, Vernooij MW, De Bruijn RFAG, Koudstaal PJ, Hofman A, Franco OH, et al. Atherosclerotic calcification is related to a higher risk of dementia and cognitive decline. *Alzheimers Dement* 2015; 11: 639–647.e1.
11. Dearborn JL, Zhang Y, Qiao Y, Suri MFK, Liu L, Gottesman RF, et al. Intracranial atherosclerosis and dementia. *Neurology* 2017; 88: 1556–63.
12. Qiao Y, Anwar Z, Intrapiromkul J, Liu L, Zeiler SR, Leigh R, et al. Patterns and Implications of Intracranial Arterial Remodeling in Stroke Patients. *Stroke* 2016; 47: 434–40.
13. Suri MFK, Qiao Y, Ma X, Guallar E, Zhou J, Zhang Y, et al. Prevalence of Intracranial Atherosclerotic Stenosis Using High-Resolution Magnetic Resonance Angiography in the General Population: The Atherosclerosis Risk in Communities Study. *Stroke* 2016; 47: 1187–93.
14. Mandell DM, Mossa-Basha M, Qiao Y, Hess CP, Hui F, Matouk C, et al. Intracranial Vessel Wall MRI: Principles and Expert Consensus Recommendations of the American Society of Neuroradiology. *AJNR Am J Neuroradiol* 2016; 38: 218–29.
15. Zwartbol MHT, van der Kolk AG, Ghaznavi R, van der Graaf Y, Hendrikse J, Geerlings MI. Intracranial Vessel Wall Lesions on 7T MRI (Magnetic Resonance Imaging). *Stroke* 2019; 50: 88–94.
16. Jung SC, Kang DWW, Turan TN. Vessel and Vessel Wall Imaging. *Front Neurol Neurosci* 2016; 40: 109–23.
17. Zhu C, Haraldsson H, Tian B, Meisel K, Ko N, Lawton M, et al. High resolution imaging of the intracranial vessel wall at 3 and 7 T using 3D fast spin echo MRI. *MAGMA* 2016; 29: 1–12.
18. Hartevelde AA, van der Kolk AG, van der Worp HB, Dieleman N, Siero JCW, Kuijff HJ, et al. High-resolution intracranial vessel wall MRI in an elderly asymptomatic population: comparison of 3T and 7T. *Eur Radiol* 2017; 27: 1585–95.
19. Geerlings MI, Appelman AP, Vincken KL, Algra A, Witkamp TD, Mali WP, et al. Brain volumes and cerebrovascular lesions on MRI in patients with atherosclerotic disease. The SMART-MR study. *Atherosclerosis* 2010; 210: 130–6.
20. Simons PCG, Algra A, Van De Laak MF, Grobbee DE, Van Der Graaf Y. Second manifestations of ARterial disease (SMART) study: Rationale and design. *Eur J Epidemiol* 1999; 15: 773–81.
21. Appelman APA, Van Der Graaf Y, Vincken KL, Tiehuis AM, Witkamp TD, Mali WPTMP, et al. Total cerebral blood flow, white matter lesions and brain atrophy: the SMART-MR study. *J Cereb Blood Flow Metab* 2008; 28: 633–9.
22. Knoop AJ, Gerritsen L, van der Graaf Y, Mali WP, Geerlings MI. Basal hypothalamic pituitary adrenal axis activity and hippocampal volumes: the SMART-Medea study. *Biol Psychiatry* 2010; 67: 1191–8.
23. van der Kolk AG, Hendrikse J, Brundel M, Biessels GJ, Smit EJ, Visser F, et al. Multi-sequence whole-brain intracranial vessel wall imaging at 7.0 tesla. *Eur Radiol* 2013; 23: 2996–3004.
24. van der Kolk AG, Zwanenburg JJM, Brundel M, Biessels GJ, Visser F, Luijten PR, et al. Distribution and natural course of intracranial vessel wall lesions in patients with ischemic stroke or TIA at 7.0 tesla MRI. *Eur Radiol* 2015; 25: 1692–700.

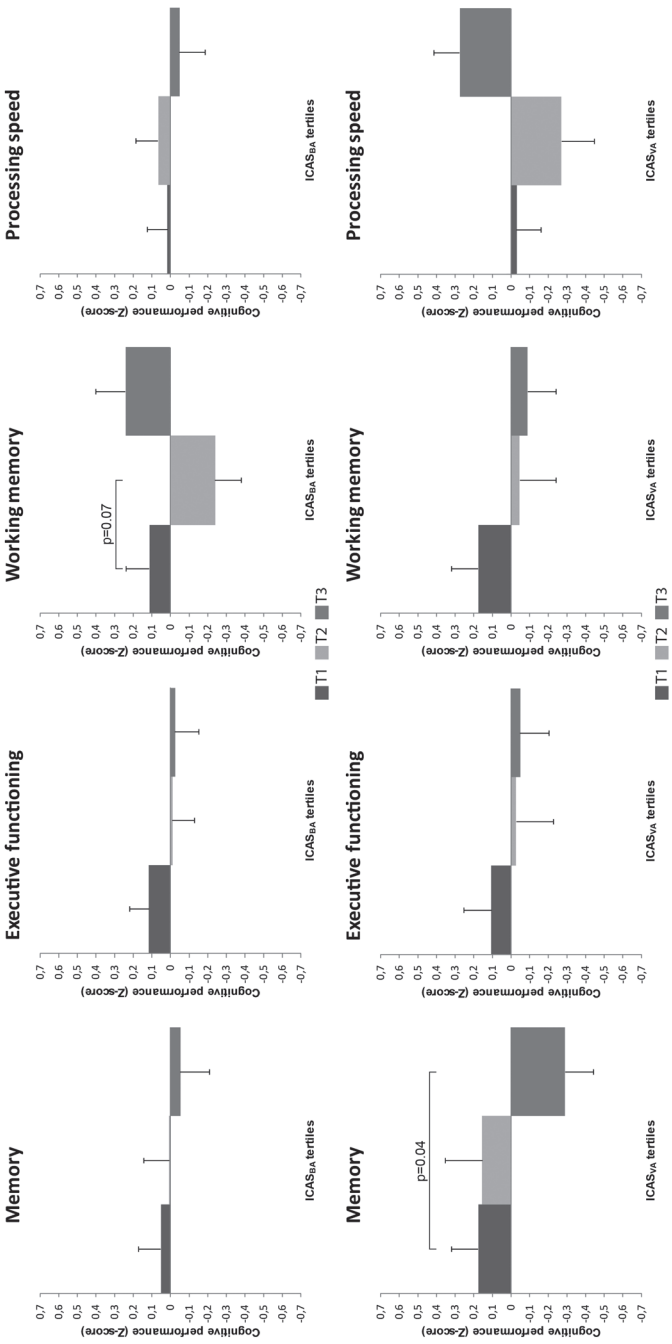
25. Hartevelde AA, Van Der Kolk AG, Van Der Worp HB, Dieleman N, Zwanenburg JJM, Luijten PR, et al. Detecting Intracranial Vessel Wall Lesions with 7T-Magnetic Resonance Imaging: Patients with Posterior Circulation Ischemia Versus Healthy Controls. *Stroke* 2017; 48: 2601–4.
26. Brand N, Jolles J. Learning and retrieval rate of words presented auditorily and visually. *J Gen Psychol* 1985; 112: 201–10.
27. Osterrieth P. Filetest de copie d'une figure complex: contribution a l'étude de la perception et de la memoire [The test of copying a complex figure: a contribution to the study of perception and memory]. *Arch Psychol* 1944; 30: 286–356.
28. Robertson IH, Ward T, Ridgeway V, Nimmo-Smith I. The structure of normal human attention: The Test of Everyday Attention. *J Int Neuropsychol Soc* 1996; 2 : 525–34.
29. Burgess PW, Shallice T. Bizarre responses, rule detection and frontal lobe lesions. *Cortex* 1996; 32: 241–59.
30. Wilkins AJ, Shallice T, McCarthy R. Frontal lesions and sustained attention. *Neuropsychologia* 1987; 25: 359–65.
31. Wechsler D. *Wechsler Adult Intelligence Scale—Fourth Edition*. 4th ed. San Antonio, TX: Pearson; 2008.
32. Lezak M, Howieson D, Loring D. *Neuropsychological Assessment*. 4th ed. New York: Oxford University Press; 2004.
33. Schmand B, Geerlings MI, Jonker C, Lindeboom J. Reading ability as an estimator of premorbid intelligence: does it remain stable in emergent dementia? *J Clin Exp Neuropsychol* 1998; 20: 42–51.
34. Folstein MF, Folstein SE, McHugh PR. "Mini-mental state". A practical method for grading the cognitive state of patients for the clinician. *J Psychiatr Res* 1975; 12:189–98.
35. Wardlaw JM, Smith EE, Biessels GJ, Cordonnier C, Fazekas F, Frayne R, et al. Neuroimaging standards for research into small vessel disease and its contribution to ageing and neurodegeneration. *Lancet Neurol* 2013; 12: 822–38.
36. Anbeek P, Vincken KL, van Osch MJ, Bisschops RH, van der Grond J. Probabilistic segmentation of white matter lesions in MR imaging. *Neuroimage* 2004; 21: 1037–44.
37. Roher AE, Tyas SL, Maarouf CL, Dausgs ID, Kokjohn TA, Emmerling MR, et al. Intracranial atherosclerosis as a contributing factor to Alzheimer's disease dementia. *Alzheimers Dement* 2011; 7: 436–44.
38. Baudic S, Barba GD, Thibaudet MC, Smagghe A, Remy P, Traykov L. Executive function deficits in early Alzheimer's disease and their relations with episodic memory. *Arch Clin Neuropsychol* 2006; 21: 15–21.
39. Knopman DS, Petersen RC. Mild Cognitive Impairment and Mild Dementia: A Clinical Perspective. *Mayo Clin Proc* 2014; 89: 1452–9.
40. Jurado MB, Rosselli M. The elusive nature of executive functions: A review of our current understanding. *Neuropsychol Rev* 2007; 17: 213–33.
41. Liu AKL, Chang RCC, Pearce RKB, Gentleman SM. Nucleus basalis of Meynert revisited: anatomy, history and differential involvement in Alzheimer's and Parkinson's disease. *Acta Neuropathol* 2015; 129: 527–40.
42. Zijlmans M, Huibers CJA, Huiskamp GJ, De Kort GAP, Alpherts WCJ, Leijten FSS, et al. The contribution of posterior circulation to memory function during the intracarotid amobarbital procedure. *J Neurol* 2012; 259: 1632–8.
43. Hossmann KA. The hypoxic brain. Insights from ischemia research. *Adv Exp Med Biol* 1999; 474: 155–69.
44. Szabo K, Förster A, Jäger T, Kern R, Griebel M, Hennerici MG, et al. Hippocampal lesion patterns in acute posterior cerebral artery stroke: Clinical and MRI findings. *Stroke* 2009; 40: 2042–5.
45. Turken AU, Whitfield-Gabrieli S, Bammer R, Baldo J, Dronkers NF, Gabrieli JDE. Cognitive Processing Speed and the Structure of White Matter Pathways: Convergent Evidence From Normal Variation and Lesion Studies. *NeuroImage* 2008; 42: 1032–44.
46. Lee SJ, Kim JS, Chung SW, Kim BS, Ahn KJ, Lee KS. White matter hyperintensities (WMH) are associated with intracranial atherosclerosis rather than extracranial atherosclerosis. *Arch Gerontol Geriatr* 2011; 53: e129–32.
47. Nam KWW, Kwon HMM, Jeong HYY, Park JHH, Kim SSHS, Jeong SMM, et al. Cerebral white matter hyperintensity is associated with intracranial atherosclerosis in a healthy population. *Atherosclerosis* 2017; 265: 179–83.



Supplemental Figure 1. Adjusted mean domain-specific cognitive functioning Z-scores per approximate quartile (or tertile) of artery-specific ICAS burden.



Supplemental Figure 1. Continued.



Supplemental Figure 1. Continued.

Supplemental Figure 1. Continued.

Values are presented as adjusted mean \pm SE Z-scores adjusted for age, sex, educational level, reading ability, and vascular risk factors. ANCOVA was used to test for differences in cognitive performance with the lowest quartile (or tertile) as reference.

Adjusted mean \pm SE Z-score per ICAS_{NCA} quartile with *p*-value for estimated marginal means pairwise comparisons for memory (*p* = 0.09): Q1, 0.28 \pm 0.14; Q2, -0.08 \pm 0.13; Q3, -0.09 \pm 0.16; Q4, -0.31 \pm 0.20; executive functioning (*p* = 0.12): Q1, 0.23 \pm 0.12; Q2, 0.02 \pm 0.11; Q3, -0.08 \pm 0.14; Q4, -0.26 \pm 0.17; working memory (*p* = 0.98): Q1, 0.05 \pm 0.15; Q2, 0.02 \pm 0.14; Q3, -0.04 \pm 0.18; Q4, 0.06 \pm 0.22; processing speed (*p* = 0.62): Q1, 0.12 \pm 0.12; Q2, 0.02 \pm 0.12; Q3, -0.01 \pm 0.15; Q4, -0.18 \pm 0.18.

Adjusted mean \pm SE Z-score per ICAS_{MCA} quartile with *p*-value for estimated marginal means pairwise comparisons for memory (*p* = 0.51): Q1, 0.12 \pm 0.13; Q2, 0.22 \pm 0.18; Q3, 0.03 \pm 0.20; Q4, -0.01 \pm 0.16; executive functioning (*p* = 0.55): Q1, -0.02 \pm 0.11; Q2, 0.23 \pm 0.15; Q3, 0.01 \pm 0.17; Q4, -0.03 \pm 0.14; working memory (*p* = 0.67): Q1, -0.12 \pm 0.14; Q2, 0.11 \pm 0.19; Q3, 0.09 \pm 0.21; Q4, 0.11 \pm 0.17; processing speed (*p* = 0.28): Q1, 0.10 \pm 0.11; Q2, 0.13 \pm 0.15; Q3, -0.28 \pm 0.17; Q4, 0.00 \pm 0.14.

Adjusted mean \pm SE Z-score per ICAS_{ICA} quartile with *p*-value for estimated marginal means pairwise comparisons for memory (*p* = 0.78): Q1, -0.01 \pm 0.13; Q2, 0.01 \pm 0.17; Q3, 0.18 \pm 0.20; Q4, -0.10 \pm 0.17; executive functioning (*p* = 0.50): Q1, 0.05 \pm 0.11; Q2, 0.19 \pm 0.14; Q3, -0.02 \pm 0.17; Q4, -0.12 \pm 0.14; working memory (*p* = 0.87): Q1, -0.05 \pm 0.14; Q2, 0.08 \pm 0.17; Q3, -0.03 \pm 0.21; Q4, 0.12 \pm 0.18; processing speed (*p* = 0.36): Q1, 0.15 \pm 0.11; Q2, -0.15 \pm 0.15; Q3, -0.08 \pm 0.18; Q4, -0.09 \pm 0.15.

Adjusted mean \pm SE Z-score per ICAS_{PCA} quartile with *p*-value for estimated marginal means pairwise comparisons for memory (*p* = 0.18): Q1, 0.10 \pm 0.13; Q2, 0.01 \pm 0.18; Q3, 0.14 \pm 0.17; Q4, -0.25 \pm 0.18; executive functioning (*p* = 0.07): Q1, 0.11 \pm 0.11; Q2, 0.28 \pm 0.15; Q3, -0.10 \pm 0.14; Q4, -0.25 \pm 0.15; working memory (*p* = 0.49): Q1, 0.00 \pm 0.14; Q2, -0.14 \pm 0.19; Q3, -0.02 \pm 0.18; Q4, 0.27 \pm 0.19; processing speed (*p* = 0.41): Q1, 0.12 \pm 0.12; Q2, 0.03 \pm 0.16; Q3, 0.35 \pm 0.15; Q4, -0.22 \pm 0.16.

Adjusted mean \pm SE Z-score per ICAS_{BA} tertile with *p*-value for estimated marginal means pairwise comparisons for memory (*p* = 0.87): T1, 0.05 \pm 0.12; T2, 0.00 \pm 0.14; T3, -0.06 \pm 0.16; executive functioning (*p* = 0.62): T1, 0.11 \pm 0.10; T2, -0.01 \pm 0.12; T3, -0.03 \pm 0.13; working memory (*p* = 0.07): T1, 0.11 \pm 0.13; T2, -0.24 \pm 0.14; T3, 0.24 \pm 0.16; processing speed (*p* = 0.83): T1, 0.01 \pm 0.11; T2, 0.06 \pm 0.12; T3, -0.05 \pm 0.14.

Adjusted mean \pm SE Z-score per ICAS_{VA} tertile with *p*-value for estimated marginal means pairwise comparisons for memory (*p* = 0.08): T1, 0.17 \pm 0.15; T2, 0.15 \pm 0.20; T3, -0.29 \pm 0.16; executive functioning (*p* = 0.78): T1, 0.10 \pm 0.16; T2, -0.03 \pm 0.20; T3, -0.05 \pm 0.16; working memory (*p* = 0.47): T1, 0.17 \pm 0.15; T2, -0.05 \pm 0.20; T3, -0.09 \pm 0.16; processing speed (*p* = 0.05): T1, -0.03 \pm 0.13; T2, -0.27 \pm 0.18; T3, 0.27 \pm 0.14.



5

Intracranial vessel wall lesions on 7T MRI and MRI features of cerebral small vessel disease – the SMART-MR study

Maarten H.T. Zwartbol, Anja G. van der Kolk, Hugo J. Kuijf, Theo D. Witkamp, Rashid Ghaznawi, Jeroen Hendrikse, Mirjam I. Geerlings, on behalf of the UCC-SMART Study Group

Published in *Journal of Cerebral Blood Flow and Metabolism* 2021; 41: 1219-28
doi: 10.1177/0271678X20958517

Abstract

The etiology of cerebral small vessel disease (CSVD) is the subject of ongoing research. Although intracranial atherosclerosis (ICAS) has been proposed as a possible cause, studies on their relationship remain sparse. We used 7T vessel wall-MRI to study the association between intracranial vessel wall lesions—a neuroimaging marker of ICAS—and MRI features of CSVD.

Within the SMART-MR study, cross-sectional analyses were performed in 130 patients (68 ± 9 y; 88% male). ICAS burden—defined as the number of vessel wall lesions—was determined on 7T vessel wall-MRI. CSVD features were determined on 1.5T and 7T MRI. Associations between ICAS burden and CSVD features were estimated with linear or modified-Poisson regression, adjusted for age, sex, vascular risk factors and medication use.

In 125 patients, ≥ 1 vessel wall lesions were found (mean 8.5 ± 5.7 lesions). ICAS burden (per +1 SD) was associated with presence of large subcortical and/or cortical infarcts (RR = 1.65; 95% CI 1.12-2.43), lacunes (RR = 1.45; 95% CI 1.14-1.86), cortical microinfarcts (RR = 1.48; 95% CI 1.13-1.94) and total white matter hyperintensity volume ($b = 0.24$; 95% CI 0.02-0.46).

Concluding, patients with a higher ICAS burden had more CSVD features, although no evidence of co-location was observed. Further longitudinal studies are required to determine if ICAS precedes development of CSVD.

Introduction

Cerebral small vessel disease (CSVD), a common finding in the ageing brain, is used to describe a group of pathological changes affecting the small arteries, arterioles, capillaries, and venules of the brain.¹ It is thought to be one of the major causes of ischemic stroke.¹ Furthermore, it is one of the leading causes of vascular dementia and is a key contributor to the incidence of Alzheimer's disease.¹ Magnetic resonance imaging (MRI) features of CSVD include: recent small subcortical infarcts, white matter hyperintensities, microbleeds, lacunes of presumed vascular origin, prominent perivascular spaces and brain atrophy.²

Although the MRI features are generally considered to be caused by ischemia, the etiological mechanisms leading up to this stage remain to be elucidated.³ A wide range of potential mechanisms has been proposed, going from intrinsic disease of the smaller vessels (i.e. lipohyalinosis) to more extrinsic causes, i.e. emboli, atheroma of parent artery or perforating arteriole, impaired cerebral blood flow, to non-ischemic causes, e.g. capillary endothelial failure.^{3,4}

The current view is that intrinsic changes of the small vessels are likely the dominant etiology.⁴ Intracranial atherosclerosis (ICAS)—which can cause atheroma, emboli, and impaired cerebral blood flow—has largely been dismissed as a major CSVD etiology.^{4–6} However, in the well-known (clinico)pathological study on lacunes by Fisher et al., ICAS and emboli accounted for the majority of lacunes.⁷ Several studies in Asian populations have observed this association in vivo as well.^{8,9} In our view, this warrants further study, because a better understanding of the cause of MRI features of CSVD might help explain the heterogeneous results regarding risk factors and clinical symptoms.¹⁰

A limitation of prior neuroimaging studies into ICAS is that most are based on angiography or transcranial Doppler, which can only assess luminal stenosis in the larger proximal cerebral arteries. Hence, plaques without stenosis, i.e., because of arterial remodeling, cannot be assessed. This is of importance, because most CSVD lesions are chronic, which means that arterial remodeling—leading to a normalization of the arterial lumen—could have taken place in the meantime, hindering the ability to find a potential association between ICAS and CSVD lesions.¹¹ Furthermore, non-stenotic plaques can still cause emboli or stenosis of the ostia of subcortical perforators.

Vessel wall–MRI can be used to image the actual vessel wall, making it possible to detect arterial vessel wall thickening independently from stenosis, leading to a significant improvement in plaque detection^{12,13}, with 7T MRI adding further improvement.^{14,15} Of note, intracranial vessel wall lesions have been associated with vascular risk factors¹⁶ and markers of extracranial atherosclerosis¹⁷, supporting its use as a neuroimaging marker of ICAS burden.

In the current study, we set out to determine the association between the number of vessel wall lesions and MRI features of CSVD in a population of older adults with a history of vascular disease.

Methods

Study sample

The Second Manifestations of ARterial disease-Magnetic Resonance (SMART-MR) study, an ongoing prospective cohort study at our institution, focuses on neuroimaging MRI markers in patient with symptomatic atherosclerotic disease.¹⁸ From May 2001 to December 2005, patients newly referred to our institution with coronary artery disease, cerebrovascular disease, peripheral artery disease or an abdominal aortic aneurysm, and without contraindications for MRI, were included. On a one-day visit, patients underwent extensive examinations, including a 1.5T brain MRI, physical examination, ultrasonography of the carotid arteries, blood and urine sampling, and questionnaires to assess risk factors, medical history, and daily functioning.¹⁹ Follow-up of 1.5T brain MRI, cognitive functioning, and depression assessment were performed from 2006 to 2009²⁰, and from 2013 to 2017.¹⁶ During the most recent follow-up, a 7T brain MRI was included in the standard research protocol. Within this period, from June 2016 to October 2017, a vessel wall-MRI sequence was added to the 7T brain MRI protocol.

In this study, we included all patients whom had 7T vessel wall-MRI performed during this period, which led to a total of 147 patients.¹⁶ We excluded 17 patients from the final analysis, leaving 130 patients, because of artifacts inhibiting vessel wall assessment of ≥ 1 major segment of the Circle of Willis (CoW; major segments included the distal internal carotid artery and primary branches (M1, A1, P1) of the anterior, middle and posterior cerebral artery). Excluded patients did not differ in sex (88% vs. 88% male; $p = 0.95$, χ^2 -test), and were not significantly older (70 ± 7 vs. 68 ± 9 years; $p = 0.11$, Student's t -test). Vascular risk factor assessment, including questionnaire data and blood and urine sampling, was available from median (range) 2.3 (0.6 to 8.6) years prior to the 7T brain MRI.

The SMART-MR study was approved by the medical ethics committee of the University Medical Center Utrecht according to the guidelines of the Declaration of Helsinki of 1975 and written informed consent was obtained from all participants.

Covariates

Questionnaires were used to assess age, sex, educational level, alcohol use, smoking habits, and medication use. Weight and height measurements were taken for calculation of the body mass index (BMI; kg/m^2). Educational level was classified into seven categories, ranging from primary school to academic degree, according to the Dutch educational system. Systolic blood pressure (SBP; mmHg) and diastolic blood pressure (DBP; mmHg) were measured with a sphygmomanometer and defined as the average of three separate measurements. Venous blood samples were taken after an overnight fast. Diabetes was defined as a fasting serum glucose level of >11.1 mmol/L, a history of diabetes or use of antidiabetic medication at baseline or follow-up. Cholesterol levels were determined. An experienced technician performed carotid ultrasonography with a 10MHz linear-array

transducer. Carotid stenosis was defined according to standard criteria based on the peak systolic velocity.²¹ Mean carotid intima-media thickness was calculated from six measurements (anterolateral, posterolateral and mediolateral in both common carotid arteries). Ankle-brachial index measurement was performed by experienced technicians and was calculated from the highest systolic blood pressure measured in both brachial arteries (using a semiautomatic oscillometric device in supine position), and the posterior tibial and dorsal pedal arteries (using Doppler ultrasound).

1.5T MRI protocol

A 1.5T whole-body system (Gyrosan ACS-NT, Philips Medical Systems, Best, the Netherlands) was used performing a standard protocol: a T1-weighted sequence (3D acquisition; repetition time (TR)/echo time (TE): 7.0/3.2 ms; voxel size = 0.94x0.94x1.0 mm³ isotropic), a T1-weighted inversion recovery sequence (2D acquisition; TR/TE: 2900/22 ms; TI = 410 ms), a T2-weighted sequence (2D acquisition; TR/TE: 2200/10.5 ms) and a FLAIR sequence (2D acquisition; TI/TR/TE: 2000/6000/100 ms). All 2-dimensional sequences were acquired with a voxel size of 1.0x1.0x4.0 mm³ and contiguous slices. A phase-contrast MR angiography sequence (2D slice acquisition; TR/TE: 16/9 ms; voxel size = 0.98 x 0.98 x 5.00 mm³; velocity sensitivity 100 cm/s; acquisition at the level of the proximal cavernous segment of the ICA and prepontine basilar artery) was also performed.

7T MRI protocol

A 7.0 T whole-body MRI system (Philips Healthcare, Cleveland, OH, USA) with a 32-channel receiver head coil (Nova Medical, Wilmington, MA, USA) was used. The standard MRI protocol consisted of: a T1-weighted (3D acquisition; TI/TR/TE = 1225/4.8/2.2 ms; acquired voxel size = 1.00 x 1.00 x 1.00 mm³; reconstructed = 0.66 x 0.66 x 0.50 mm³), T2-weighted Turbo-Spin Echo (3D acquisition; TR/TE = 3158/301 ms; acquired voxel size = 0.70 x 0.70 x 0.70 mm³; reconstructed = 0.35 x 0.35 x 0.35 mm³), magnetization-prepared FLAIR (3D acquisition, TR/TE = 8000/300 ms, acquired voxel size = 0.80 x 0.80 x 0.80 mm³, reconstructed = 0.49 x 0.49 x 0.49 mm³), and a dual echo susceptibility-weighted imaging (SWI) (TR/TE1/TE2 = 20/6.9/15.8 ms, acquired voxel size = 0.50 x 0.50 x 0.70 mm³, reconstructed = 0.40 x 0.40 x 0.35 mm³) sequence. Vessel wall MRI was performed with a T1-weighted Magnetization-Prepared Inversion Recovery Turbo Spin Echo sequence with the following settings: field-of-view (FOV) 250x250x190 mm³, acquired resolution 0.8 x 0.8 x 0.8 mm³ (reconstructed to 0.49 x 0.49 x 0.4 mm³), TR/TI/TE = 3952/1375/37 ms.²²

Assessment of intracranial atherosclerosis

All patients were assessed by a trained observer (M.H.T.Z.) blinded to patient characteristics.¹⁶ MHTZ was trained by an experienced observer with 8 years of experience with 7T vessel wall-MRI 7T assessment (A.G.vd.K.). Of note, 7T vessel wall assessment was not blinded to the brain parenchyma, the latter of which is also visible on the vessel wall sequence,

although with low tissue contrast. Therefore, assessments were performed zooming in on the vessel wall of interest. Lesions were rated according to recently published criteria.^{16,23} A lesion was defined as a diffuse or focal thickening of $\geq 50\%$ of the arterial wall, compared to the expected normal thickness, using the contralateral artery or neighboring arterial segment as reference. Assessment was performed visually; we did not measure lesion thickness. Lesions which were uncertain were assessed in multiple planes for verification. Lesions were rated per arterial segment, with each segment being able to contain multiple lesions, making the maximum lesion count theoretically unlimited. We rated the following segments: the anterior cerebral arteries (ACA; A1, A2 segments), middle cerebral arteries (MCA; M1, M2 segments), distal internal carotid arteries (ICA; supraclinoid (C6) and communicating segment (C7)), posterior communicating arteries (PCom), posterior cerebral arteries (PCA; P1, P2 segments, P1-P2 bifurcation), basilar artery and vertebral arteries. A lesion which stretched into multiple segments was counted as a separate lesion for each segment. Lesions with eccentric and concentric components were regarded as separate lesions for each segment. An MR angiography sequence was not included in the 7T brain MRI protocol because of logistical reasons. As a result, we were not able to assess luminal stenosis.

Assessment of MRI markers of cerebrovascular disease

All assessments were performed by an experienced observer (M.H.T.Z.) blinded to patient characteristics. Assessment of 1.5T MRI was performed blinded to 7T MRI assessment, and vice versa. Cortical infarcts, large subcortical infarcts, cerebellar infarcts and lacunes of presumed vascular origin were visually rated on 1.5T MRI images, on the T1-weighted, T2-weighted and FLAIR images. Cortical infarcts were defined as a cortical or cortico-subcortical area of tissue necrosis with a minimum diameter of 4 mm, to distinguish from cortical microinfarcts. Large subcortical infarcts were defined as a subcortical area of cavitated tissue necrosis >15 mm in minimum diameter, to distinguish from lacunes. Cortical and subcortical infarcts were combined into 'large subcortical and/or cortical infarcts' for further analyses, because both are thought to be primarily caused by large artery disease. Cerebellar cortical infarcts were defined as areas of tissue necrosis with involvement of the cerebellar cortex. Lacunes of presumed vascular origin were defined according to the STRIVE criteria.² In brief, a lacune was defined as round or ovoid cerebrospinal-fluid filled subcortical lesion, 3 to 15 mm in size, with a variable FLAIR rim, and not being a perivascular space. A consensus was performed with an experienced neuroradiologist (T.D.W.) for uncertain lesions. Cerebral cortical microinfarcts were rated on 7T MRI, using the T1-weighted, T2-weighted, FLAIR and SWI images, using standard rating criteria.²⁴ In short, a microinfarct was defined as a strictly intracortical lesion, visible in two or more directions, with a maximum diameter of 4 mm, which had to be hyperintense to cortex on T2-weighted imaging and hypointense on T1-weighted imaging, without an accompanying microbleed on susceptibility-weighted imaging. Cerebral microbleeds

were rated on the 7T SWI source data and a reconstructed minimum intensity projection (slice thickness 4 mm, overlap 2 mm).²⁵ We distinguished lobar and deep microbleeds according to the Microbleed Anatomical Rating Scale.²⁶

White matter hyperintensity, gray matter, white matter and CSF volumes were obtained with a previously validated probabilistic segmentation technique using *k*-nearest neighbor classification, on the 1.5T T1-weighted, FLAIR, and T2-weighted inversion recovery sequences of the MR scans.²⁷ An investigator (R.G.) checked all white matter hyperintensity segmentations using an image processing framework (MeVisLab 2.7.1., MeVis Medical Solutions AG, Bremen, Germany), and manually adjusted incorrect segmentations. Infarcts were manually segmented (M.H.T.Z.) and subtracted from the other segmentation volumes in three-dimensional space. Volumes of gray matter, white matter, total white matter hyperintensity, and brain infarcts were summed to obtain total brain volume. Total intracranial volume was calculated by summing the total brain volume and the volume of the cerebrospinal fluid. Deep white matter hyperintensity was defined as >1 cm from the lateral ventricles, while periventricular white matter hyperintensity was defined as ≤1 cm of the lateral ventricles.

Statistical analysis

All analyses were performed using IBM SPSS Statistics version 25 for Windows (IBM Corporation, Armonk, NY, USA). We performed multiple imputation with 10 datasets to address missing values. Analyses were performed by pooling the 10 imputed datasets.

ICAS burden, defined as the total number of vessel wall lesions per patient, was standardized into a Z-score and was used as the independent variable in all analyses. Modified-Poisson regression with robust standard errors was used to calculate relative risks (RRs) for binary dependent variables. Standard linear regression was used to calculate unstandardized regression coefficients (*b*) for continuous dependent variables. Analyses were adjusted for age and sex in model 1, and additionally for educational level, BMI, smoking pack-years, alcohol use, diabetes, systolic and diastolic blood pressure, total cholesterol level, total high-density lipoprotein level, use of antihypertensive, lipid-lowering, antiplatelet, or oral anticoagulant medication (model 2). In model 3, additional adjustments were made for carotid stenosis ≥50%, carotid intima-media thickness and ankle-brachial index. All models of cerebral blood flow were additionally adjusted for total brain volume. All models of total brain volume and white matter hyperintensity volume were additionally adjusted for intracranial volume. White matter hyperintensity volumes were natural-log transformed before being entered into the model, to obtain a normal distribution. Residual plots of all linear regression analyses were checked for regression assumptions (e.g., normal distribution).

Finally, we stratified the study sample into a right-, left-dominant or symmetric ICAS distribution and calculated descriptives of ICAS distribution and CSVD lesion distribution per hemisphere to explore co-localization between ICAS burden and CSVD. ICAS

hemispheric dominance was defined as an interhemispherical difference of one or more vessel wall lesions. An interhemispherical difference of zero was defined as symmetric.

Data availability statement

For use of anonymized data, a reasonable request has to be made in writing to the study group, and the third party has to sign a confidentiality agreement.

Results

Table 1 shows the characteristics of the study sample ($n = 130$; 88% male; 68 ± 9 years). Table 2 gives an overview of the MRI neuroimaging markers in the study sample. Brain infarcts were commonly found, lacunes of presumed vascular origin being most common with a frequency of 16%. In addition, there was a high prevalence of microbleeds, with 57% of participants having ≥ 1 microscopic hemorrhage. Vessel wall lesions were found in 96% of patients, with a mean ICAS burden was 8.5 ± 5.7 lesions (median 7, range 0-32). A mean ICAS burden of 5.3 ± 3.2 lesions (median 4, range 0-14) was found in the anterior circulation, and a mean ICAS burden of 3.8 ± 3.0 lesions (median 3; range 0-18) in the posterior circulation. A detailed overview of the vessel wall lesion distribution can be found in our prior publication.¹⁶ Figure 1 presents an example of vessel wall lesions on 7T vessel wall-MRI and the parenchymal lesions associated with a higher number of vessel wall lesions (i.e., higher ICAS burden).

Table 3 presents the relative risk of brain infarcts per +1 SD in ICAS burden, calculated using modified-Poisson regression analysis. ICAS burden was associated with presence of large subcortical and/or cortical infarcts ($RR = 1.65$; 95% CI 1.12 to 2.43), lacunes of presumed vascular origin ($RR = 1.45$; 95% CI 1.14 to 1.86), and cortical microinfarcts ($RR = 1.48$; 95% CI 1.13 to 1.94), after adjustment for age, sex, vascular risk factors and medication use. Additional adjustment for carotid stenosis $\geq 50\%$, carotid intima-media thickness and ankle-brachial index caused no considerable change. No significant association was found with cerebellar infarcts ($RR = 1.15$; 95% CI 0.78 to 1.70), after adjustment for age, sex, vascular risk factors and medication use.

Table 4 presents the relative risk of microbleeds per +1 SD in ICAS burden, calculated using modified-Poisson regression analysis. As can be seen, no association was found with presence of microbleeds at any, lobar, or deep location.

Table 5 presents the unstandardized regression coefficient estimates for total brain volume, white matter hyperintensity volumes, and cerebral blood flow, per +1 SD in ICAS burden. ICAS burden was associated with natural-log transformed total white matter hyperintensity volume ($b = 0.24$; 95% CI 0.02 to 0.46) and natural-log transformed periventricular white matter hyperintensity volume ($b = 0.32$; 95% CI 0.08 to 0.56), but not deep white matter hyperintensity volume, after adjustment for age, sex, intracranial volume, vascular

Table 1. Characteristics of study sample (n = 130).

| | |
|--|------------------|
| Age (years) | 68 ± 9 |
| Men (%) | 88% |
| Body mass index (kg/m ²) | 27.3 ± 3.7 |
| Educational level (range 1-7) ^a | 5 (2, 6) |
| Smoking pack-years ^a | 19.8 (0.0, 43.4) |
| Alcohol use (%) | |
| 1-10 units/week | 43% |
| >11 units/week | 29% |
| Systolic blood pressure (mmHg) | 139 ± 17 |
| Diastolic blood pressure (mmHg) | 79 ± 9 |
| Cholesterol, mmol/L | |
| LDL-C | 2.4 ± 0.8 |
| HDL-C | 1.3 ± 0.4 |
| Total | 4.4 ± 0.9 |
| Diabetes (%) | 19% |
| Carotid stenosis ≥50% | 10% |
| Carotid intima-media thickness (mm) | 0.85 ± 0.23 |
| Ankle-brachial index | 1.09 ± 0.18 |
| History of vascular disease (%) ^b | |
| Coronary heart disease | 82% |
| Cerebrovascular disease | 19% |
| Peripheral arterial disease | 19% |
| Abdominal aortic aneurysm | 2% |
| Medication use (%) | |
| Antihypertensive medication | 83% |
| Lipid-lowering medication | 90% |
| Antiplatelet medication | 89% |
| Oral anticoagulants | 10% |

Values are presented as mean ± SD or frequencies (as %).

^a Median (10th, 90th percentile).

^b Comorbid disease is possible.

risk factors and medication use. Additional adjustment for carotid stenosis ≥50%, carotid intima-media thickness and ankle-brachial index caused no considerable change. A non-significant association between higher ICAS burden and lower cerebral blood flow

Table 2. MRI markers of cerebrovascular disease in study sample (n = 130).

| | |
|--|-----------------|
| Brain infarcts | |
| Cortical infarcts | 6.2% |
| Large subcortical infarcts | 3.1% |
| Lacunes of presumed vascular origin | 16.2% |
| Cerebellar infarcts | 11.5% |
| Cortical microinfarcts | 13.1% |
| Microbleeds | |
| Any microbleeds | 57% |
| Lobar microbleeds | 53% |
| Deep microbleeds | 32% |
| Brain volumes | |
| Brain volume (ml) | 1128 ± 98 |
| Total WMH volume (ml) ^a | 1.5 (0.3, 9.04) |
| Periventricular WMH volume (ml) ^a | 1.2 (0.2, 8.5) |
| Deep WMH volume (ml) ^a | 0.2 (0.0, 1.0) |
| Cerebral blood flow (ml/min) | 526 ± 105 |

Note: values are presented as mean ± SD or frequencies (%).

^a Median (10th, 90th percentile).

Abbreviations: SD, standard deviation; WMH: white matter hyperintensities.

was found ($b = -15.24$ ml/min; 95% CI -34.85 to 4.38). No association was found between ICAS burden and total brain volume.

Table 6 shows the descriptives of the ICAS and CSVD lesion distribution between the right and left hemispheres stratified by ICAS distribution dominance. As expected, the mean number of vessel wall lesions were similar in the symmetric group, higher in the left circulation in the left-dominant group and higher in the right circulation in the right-dominant group. In the group with a right hemispheric dominance of vessel wall lesions, the white matter hyperintensity volume was quite symmetric. If anything, lacunes and microinfarcts were more present in the left hemisphere. In the group with a left hemispheric dominance of vessel wall lesions, white matter hyperintensity volume and lacune presence was quite symmetric and lacunes were more present on the right.

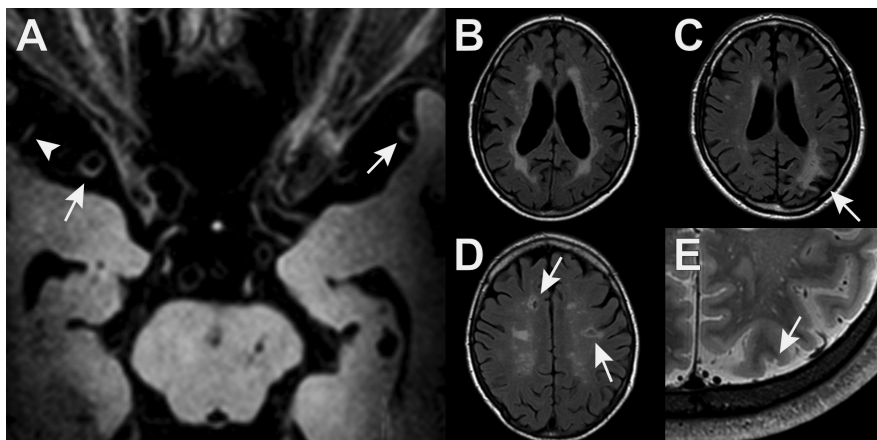


Figure 1. Examples of intracranial vessel wall lesions on 7T vessel wall-MRI (A) and associated parenchymal lesions (B-E). A) Vessel wall lesions in the M1 segment on both sides (arrows) and M2 lesion on the right (arrowhead). B) periventricular white matter hyperintensities. C) cortical infarct (arrow). D) lacunes of presumed vascular origin (arrows). E) cortical microinfarct (arrow).

Table 3. Association between ICAS burden and presence of brain infarcts (yes vs. no).

| | Model | Large (sub)cortical infarcts ^b RR (95% CI) | Lacunes RR (95% CI) | Cerebellar infarcts RR (95% CI) | Cortical microinfarcts RR (95% CI) |
|--------------------------|-------|--|------------------------|------------------------------------|---------------------------------------|
| ICAS burden ^a | 1 | 1.71 (1.34 to 2.19) | 1.50 (1.19 to 1.89) | 1.28 (0.87 to 1.86) | 1.62 (1.29 to 2.03) |
| | 2 | 1.65 (1.12 to 2.43) | 1.45 (1.14 to 1.86) | 1.15 (0.78 to 1.70) | 1.48 (1.13 to 1.94) |
| | 3 | 1.56 (1.12 to 2.27) | 1.41 (1.10 to 1.82) | 1.10 (0.72 to 1.70) | 1.43 (1.07 to 1.94) |

Values are relative risks (RR) with 95% confidence intervals calculated with modified-Poisson regression analysis with robust error variance.

Model 1: adjusted for age and sex. Model 2: model 1 + adjustment for educational level, body mass index, smoking pack-years, alcohol use, diabetes, systolic/diastolic blood pressure, total cholesterol level, total high-density lipoprotein level, use of antihypertensive, lipid-lowering, antiplatelet or oral anticoagulant medication. Model 3: model 2 + adjustment for carotid stenosis $\geq 50\%$, carotid intima-media thickness or ankle-brachial index.

^a Standardized into Z-score.

^b Defined as presence of large subcortical infarcts and/or cortical infarcts.

Table 4. Association between ICAS burden and presence of cerebral microbleeds (yes vs. no).

| | Model | Any microbleed RR (95% CI) | Lobar microbleeds RR (95% CI) | Deep microbleeds RR (95% CI) |
|--------------------------|-------|-------------------------------|----------------------------------|---------------------------------|
| ICAS burden ^a | 1 | 1.04 (0.89 to 1.21) | 1.03 (0.86 to 1.23) | 1.14 (0.91 to 1.42) |
| | 2 | 1.09 (0.92 to 1.29) | 1.10 (0.90 to 1.34) | 1.18 (0.92 to 1.51) |
| | 3 | 1.10 (0.93 to 1.30) | 1.11 (0.91 to 1.35) | 1.19 (0.92 to 1.54) |

Values are relative risks (RR) with 95% confidence intervals calculated with modified-Poisson regression analysis with robust error variance.

Model 1: adjusted for age and sex. Model 2: model 1 + adjustment for educational level, body mass index, smoking pack-years, alcohol use, diabetes, systolic/diastolic blood pressure, total cholesterol level, total high-density lipoprotein level, use of antihypertensive, lipid-lowering, antiplatelet or oral anticoagulant medication. Model 3: model 2 + adjustment for carotid stenosis $\geq 50\%$, carotid intima-media thickness or ankle-brachial index.

^a Standardized into Z-score.

Table 5. Association between ICAS burden and brain volumes and cerebral blood flow.

| | Model | Total brain volume (ml) <i>b</i> (95% CI) | Total WMH volume (ml) ^b <i>b</i> (95% CI) | Periventricular WMH volume (ml) ^b <i>b</i> (95% CI) | Deep WMH volume (ml) ^b <i>b</i> (95% CI) | Cerebral blood flow (ml/min) <i>b</i> (95% CI) |
|-----------------------------|-------|---|--|--|---|--|
| ICAS burden ^a | 1 | 0.34 (-5.05 to 5.73) | 0.24 (0.04 to 0.43) | 0.31 (0.1 to 0.52) | 0.02 (-0.21 to 0.25) | -15.62 (-32.97 to 1.72) |
| | 2 | 1.99 (-4.01 to 7.98) | 0.24 (0.02 to 0.46) | 0.32 (0.08 to 0.56) | 0.01 (-0.26 to 0.26) | -15.24 (-34.85 to 4.38) |
| | 3 | 2.14 (-3.92 to 8.2) | 0.25 (0.03 to 0.48) | 0.33 (0.10 to 0.57) | 0.01 (-0.26 to 0.27) | -12.39 (-31.87 to 7.09) |

Values are unstandardized linear regression coefficients (*b*) with 95% confidence intervals calculated with standard linear regression analysis.

Model 1: adjusted for age and sex. Model 2: model 1 + adjustment for educational level, body mass index, smoking pack-years, alcohol use, diabetes, systolic/diastolic blood pressure, total cholesterol level, total high-density lipoprotein level, use of antihypertensive, lipid-lowering, antiplatelet or oral anticoagulant medication. Model 3: model 2 + adjustment for carotid stenosis $\geq 50\%$, carotid intima-media thickness or ankle-brachial index.

^a Standardized into Z-score.

^b Natural-log transformed.

Table 6. Descriptives of CSVD lesion–distribution stratified by left vs. right dominant or symmetric ICAS distribution.

| ICAS dominance | ICAS burden (no. lesions) | | WMH volume (% ICV) ^a | | Lacunes present (%) | | CMIs present (%) | |
|--------------------|---------------------------|------|---------------------------------|----------------------|---------------------|------|------------------|------|
| | Right | Left | Right | Left | Right | Left | Right | Left |
| Symmetric (n = 29) | 4.1 | 4.1 | 0.10 (0.02, 0.68) | 0.10 (0.03, 0.64) | 10% | 3% | 10% | 10% |
| Right (n = 45) | 5.1 | 3.6 | 0.11 (0.02, 0.49) | 0.09 (0.01, 0.56) | 9% | 16% | 7% | 13% |
| Left (n = 56) | 3.0 | 4.8 | 0.10 (0.02, 0.56) | 0.09 (0.02, 0.57) | 11% | 11% | 9% | 5% |

Note: right indicates right hemisphere and left indicates left hemisphere.

^a Median (10th, 90th percentile).

Discussion

In this cohort of 130 patients with a history of vascular disease, vessel wall lesions on 7T MRI were very common and a higher number of lesions was associated with large subcortical and/or cortical infarcts as well as MRI features of CSVD, including lacunes of presumed vascular origin, periventricular and total white matter hyperintensity volume, and cortical microinfarcts.

Our findings regarding lacunes are in concordance with early post-mortem studies^{7,28} and a few neuroimaging studies in Asian populations^{8,9}, but contradict the conclusion of a study in whites with lacunar stroke.⁵ A possible explanation for the latter discrepancy could be the difference in ICAS imaging: ultra-high field vessel wall MRI versus transcranial Doppler ultrasound. Furthermore, we found an association between vessel wall lesions and white matter hyperintensities. Although a relation between ICAS and white matter lesions is a matter of ongoing dispute²⁹, several studies have found associations with ICAS^{30–32}, and with carotid stenosis.^{33–35} Our findings add to the growing body of evidence that ICAS is related to white matter hyperintensities. Moreover, we found an association between vessel wall lesions and cortical microinfarcts, which is in line with the few small in vivo studies published on this subject.^{36–38} A possible pathway linking vessel wall lesions to these CSVD features could be steno-occlusive disease or (micro)embolisms; both can lead to downstream ischemic lesions.²⁴

We did not find an association between vessel wall lesions and microbleeds. However, this seems in concordance with the view that incidental microbleeds are generally caused by intrinsic small vessel disease, e.g., hypertensive vasculopathy and cerebral amyloid angiopathy.³⁹ Although we observed an association between higher numbers of vessel

wall lesions and lower cerebral blood flow, it did not reach statistical significance. Vessel wall thickening can cause a reduction of downstream cerebral blood flow by means of luminal stenosis.⁴⁰ Unfortunately, we don't have data on stenosis grade, because we did not include an MR angiography sequence in our protocol. A possible explanation for the absent association is that the effect of the hemodynamically-significant stenotic lesions is attenuated by a bulk of non-stenotic lesions. However, we have no way to examine this. Lastly, no association was found between ICAS and total brain volume. As far as we know, no prior studies have observed this association, although associations between carotid stenosis and cerebral atrophy have been observed.^{34,41}

Our study has several strengths. First, 7T vessel wall-MRI enabled visualization of the actual pathology which is located in the vessel wall, enabling identification of ICAS independent of luminal stenosis. In addition, the large coverage area and increased contrast-to-noise ratio compared to lower field strengths facilitated a more complete and accurate assessment of ICAS than is possible at lower field strengths. Further, we were able to examine various MRI markers of large vessel and small vessel disease within one study and data on vascular risk factors and medication use allowed to adjust for possible confounding factors. Lastly, microinfarcts and microbleeds were assessed on 7T field strength, which is the most sensitive field strength for these lesions *in vivo*.

Several limitations also need to be addressed. First, because the data were analyzed cross-sectionally, we cannot draw any conclusions regarding causality. Second, there is a lack of radiopathologic correlation studies on intracranial vessel wall lesions, which leaves the possibility that not all lesions are of atherosclerotic pathology. However, this is a limitation of all current vessel wall imaging studies. Furthermore, we think the a priori probability of a lesion being non-atherosclerotic (e.g., dissection, vasculitis), especially in our population and study setting, is very low. Additionally, their correlation with vascular risk factors¹⁶ and extracranial atherosclerosis¹⁷, further supports its use as a marker of ICAS. Third, our study sample has a high burden of manifest arterial disease and high frequency of vascular risk factors, which may have limited power to adjust for these factors. We tried to carefully adjust for these vascular risk factors by adding continuous (e.g., pack-years of smoking, blood pressure) instead of dichotomous measures (e.g., smoking, hypertension) to the models, which resulted in higher variability in risk factor exposure. Studies in different settings are needed to see if the observed relationships can be generalized to the other populations. Fourth, although vessel assessment was blinded to 1.5T and 7T brain MRI assessment, it was not blinded to the brain parenchyma, the latter of which is also visible on the vessel wall sequence. However, the intraparenchymal contrast is very low and assessment was performed zoomed in on the vessel of interest. Nonetheless, a large cortical infarct is difficult to overlook and could have involuntarily led to more thorough assessment of the vessel walls. Of note, white matter hyperintensities and microinfarcts are not easily visible on this sequence and were also associated with ICAS. Lastly, a large majority of our study sample were taking one or more vascular medications,

which might have modified the association between ICAS and MRI features of CSVD. Due to the sample size, we were not able to stratify analyses on medication use.

Our findings have importance, because the association between vessel wall lesions and MRI features of CSVD suggests that ICAS might have a role in the etiology of MRI features CSVD. However, ICAS burden could also be a marker of intracranial large and small vessel disease. Meaning, the severity of large and small vessel disease is correlated, e.g., due to shared risk, but it is the small artery disease that causes the brain lesions. As we did not image the actual small vessels—but only the parenchymal sequelae on MRI, we cannot reliably untangle this. Further, we did not find evidence of co-location of ICAS and CSVD lesions, which could have strengthened the case for causality. Future studies should try to functionally and structurally visualize the small(est) vessels and large vessels and test if they are differentially associated with MRI markers of CSVD, preferably in a longitudinal study design. Apart from this, the co-occurrence could still help explain part of the heterogeneity of CSVD¹⁰ (e.g., in regard to clinical functioning).

In conclusion, a higher ICAS burden was associated with more MRI features of CSVD, although no evidence of co-location was observed. Further longitudinal studies, preferably employing high-resolution vascular imaging^{42,43}, are required to determine if ICAS precedes development of CSVD.

References

1. Pantoni L. Cerebral small vessel disease: from pathogenesis and clinical characteristics to therapeutic challenges. *Lancet Neurol* 2010; 9: 689–701.
2. Wardlaw JM, Smith EE, Biessels GJ, Cordonnier C, Fazekas F, Frayne R, et al. Neuroimaging standards for research into small vessel disease and its contribution to ageing and neurodegeneration. *Lancet Neurol* 2013; 12: 822–38.
3. Wardlaw JM, Smith C, Dichgans M. Mechanisms of sporadic cerebral small vessel disease: Insights from neuroimaging. *Lancet Neurol* 2013; 12: 483–97.
4. Wardlaw JM, Smith C, Dichgans M. Small vessel disease: mechanisms and clinical implications. *Lancet Neurol* 2019; 18: 684–96.
5. Wardlaw JM, Doubal FN, Eadie E, Chappell F, Shuler K, Cvorovic V. Little association between intracranial arterial stenosis and lacunar stroke. *Cerebrovasc Dis* 2010; 31: 12–8.
6. Arenillas JF, Lopez-Cancio E, Wong KS. Biomarkers, Natural Course and Prognosis. *Front Neurol Neurosci* 2016; 40: 93–108.
7. Fisher C. Lacunar Infarcts - A Review. *Cerebrovasc Dis* 1991; 1:311–20.
8. Chung JW, Kim BJ, Sohn CH, Yoon BW, Lee SH. Branch Atheromatous Plaque: A Major Cause of Lacunar Infarction (High-Resolution MRI Study). *Cerebrovasc Dis Extra* 2012; 2: 36–44.
9. Miyaji Y, Kawabata Y, Joki H, Seki S, Mori K, Kamide T, et al. High-resolution magnetic resonance imaging findings of basilar artery plaque in a patient with branch atheromatous disease: A case report. *J Med Case Rep* 2014; 8:1–3.
10. ter Telgte A, van Leijssen EMC, Wiegertjes K, Klijn CJM, Tuladhar AM, de Leeuw FE. Cerebral small vessel disease: from a focal to a global perspective. *Nat Rev Neurol* 2018; 14: 387–98.
11. Degnan AJ. Underestimating the importance of middle cerebral artery atherosclerosis in lacunar stroke. *Cerebrovasc Dis* 2011; 32: 301.
12. Mandell DM, Mossa-Basha M, Qiao Y, Hess CP, Hui F, Matouk C, et al. Intracranial Vessel Wall MRI: Principles and Expert Consensus Recommendations of the American Society of Neuroradiology. *AJNR Am J Neuroradiol* 2016; 38: 218–29.
13. Qiao Y, Anwar Z, Intrapirumkul J, Liu L, Zeiler SR, Leigh R, et al. Patterns and Implications of Intracranial Arterial Remodeling in Stroke Patients. *Stroke* 2016; 47: 434–40.
14. Zhu C, Haraldsson H, Tian B, Meisel K, Ko N, Lawton M, et al. High resolution imaging of the intracranial vessel wall at 3 and 7 T using 3D fast spin echo MRI. *MAGMA* 2016; 29: 1–12.
15. Hartevelde AA, van der Kolk AG, van der Worp HB, Dieleman N, Siero JCW, Kuijff HJ, et al. High-resolution intracranial vessel wall MRI in an elderly asymptomatic population: comparison of 3T and 7T. *Eur Radiol* 2017; 27: 1585–95.
16. Zwartbol MHT, van der Kolk AG, Ghaznawi R, van der Graaf Y, Hendrikse J, Geerlings MI. Intracranial Vessel Wall Lesions on 7T MRI (Magnetic Resonance Imaging). *Stroke* 2019; 50: 88–94.
17. Zwartbol MHT, Geerlings MI, Ghaznawi R, Hendrikse J, Van Der Kolk AG, Asselbergs FW, et al. Intracranial atherosclerotic burden on 7T MRI is associated with markers of extracranial atherosclerosis: The SMART-MR study. *AJNR Am J Neuroradiol* 2019; 40: 2016–22.
18. Geerlings MI, Appelman AP, Vincken KL, Algra A, Witkamp TD, Mali WP, et al. Brain volumes and cerebrovascular lesions on MRI in patients with atherosclerotic disease. The SMART-MR study. *Atherosclerosis* 2010; 210: 130–6.
19. Appelman APA, Van Der Graaf Y, Vincken KL, Tiehuis AM, Witkamp TD, Mali WPTMP, et al. Total cerebral blood flow, white matter lesions and brain atrophy: the SMART-MR study. *J Cereb Blood Flow Metab* 2008; 28: 633–9.
20. Knoops AJ, Gerritsen L, van der Graaf Y, Mali WP, Geerlings MI. Basal hypothalamic pituitary adrenal axis activity and hippocampal volumes: the SMART-Medea study. *Biol Psychiatry* 2010; 67: 1191–8.
21. Simons PCG, Algra A, Van De Laak MF, Grobbee DE, Van Der Graaf Y. Second manifestations of ARterial disease (SMART) study: Rationale and design. *Eur J Epidemiol* 1999; 15: 773–81.
22. van der Kolk AG, Hendrikse J, Brundel M, Biessels GJ, Smit EJ, Visser F, et al. Multi-sequence whole-brain intracranial vessel wall imaging at 7.0 tesla. *Eur Radiol* 2013; 23: 2996–3004.

23. Lindenholz A, van der Kolk AG, Zwanenburg JJM, Hendrikse J. The Use and Pitfalls of Intracranial Vessel Wall Imaging: How We Do It. *Radiology* 2018; 286: 12–28.
24. van Veluw SJ, Shih AY, Smith EE, Chen C, Schneider JA, Wardlaw JM, et al. Detection, risk factors, and functional consequences of cerebral microinfarcts. *Lancet Neurol* 2017; 16: 730–40.
25. De Bresser J, Brundel M, Conijn MM, Van Dillen JJ, Geerlings MI, Viergever MA, et al. Visual cerebral microbleed detection on 7T MR imaging: Reliability and effects of image processing. *AJNR Am J Neuroradiol* 2013; 34: e61–4.
26. Gregoire SM, Chaudhary UJ, Brown MM, Yousry TA, Kallis C, Jäger HR, et al. The Microbleed Anatomical Rating Scale (MARS): Reliability of a tool to map brain microbleeds. *Neurology* 2009; 73: 1759–66.
27. Anbeek P, Vincken KL, van Osch MJ, Bisschops RH, van der Grond J. Probabilistic segmentation of white matter lesions in MR imaging. *Neuroimage* 2004; 21: 1037–44.
28. Fisher CM. The arterial lesions underlying lacunes. *Acta Neuropathol* 1969; 12: 1–15.
29. Topakian R. Conflicting evidence on the association of white matter hyperintensities with large-artery disease. *Eur J Neurol* 2015; 22: 4–5.
30. Nam KWW, Kwon HMM, Jeong HYY, Park JHH, Kim SSHS, Jeong SMM, et al. Cerebral white matter hyperintensity is associated with intracranial atherosclerosis in a healthy population. *Atherosclerosis* 2017; 265: 179–83.
31. Park JHH, Kwon HMM, Lee J, Kim DSS, Ovbiagele B. Association of intracranial atherosclerotic stenosis with severity of white matter hyperintensities. *Eur J Neurol* 2015; 22: 44–52.
32. Lee SJ, Kim JS, Chung SW, Kim BS, Ahn KJ, Lee KS. White matter hyperintensities (WMH) are associated with intracranial atherosclerosis rather than extracranial atherosclerosis. *Arch Gerontol Geriatr* 2011; 53: 129–32.
33. Romero JR, Beiser A, Seshadri S, Benjamin EJ, Polak JF, Vasan RS, et al. Carotid artery atherosclerosis, MRI indices of brain ischemia, aging, and cognitive impairment: The framingham study. *Stroke* 2009; 40: 1590–6.
34. Manolio TA, Burke GL, O'Leary DH, Evans G, Beauchamp N, Knepper L, et al. Relationships of cerebral MRI findings to ultrasonographic carotid atherosclerosis in older adults: The cardiovascular health study. *Arterioscler Thromb Vasc Biol* 1999; 19: 356–65.
35. Bos D, Ikram MA, Elias-Smale SE, Krestin GP, Hofman A, Witteman JCMM, et al. Calcification in major vessel beds relates to vascular brain disease. *Arterioscler Thromb Vasc Biol*. 2011; 31: 2331–7.
36. Hilal S, Sikking E, Shaik MA, Chan QL, Van Veluw SJ, Vrooman H, et al. Cortical cerebral microinfarcts on 3T MRI: A novel marker of cerebrovascular disease. *Neurology* 2016; 87: 1583–90.
37. Dieleman N, van der Kolk AG, Zwanenburg JJ, Brundel M, Hartevelde AA, Biessels GJ, et al. Relations between location and type of intracranial atherosclerosis and parenchymal damage. *J Cereb Blood Flow Metab* 2016; 36: 1271–80.
38. Van Veluw SJ, Hilal S, Kuijff HJ, Ikram MK, Xin X, Yeow TB, et al. Cortical microinfarcts on 3T MRI: Clinical correlates in memory-clinic patients. *Alzheimers Dement* 2015; 11: 1500–9.
39. Greenberg SM, Vernooij MW, Cordonnier C, Salman RA shahi, Edin F, Warach S, et al. Cerebral Microbleeds: A Field Guide to their Detection and Interpretation. *Lancet Neurol* 2009; 8: 165–74.
40. Pu Y, Lan L, Leng X, Wong LK, Liu L. Intracranial atherosclerosis: From anatomy to pathophysiology. *Int J Stroke* 2017; 12: 236–45.
41. Muller M, van der Graaf Y, Algra A, Hendrikse J, Mali WP, Geerlings MI, et al. Carotid atherosclerosis and progression of brain atrophy: the SMART-MR study. *Ann Neurol* 2011; 70: 237–44.
42. De Cockler LJ, Lindenholz A, Zwanenburg JJ, van der Kolk AG, Zwartbol M, Luijten PR, et al. Clinical vascular imaging in the brain at 7T. *Neuroimage* 2018; 168: 452–58.
43. Geurts LJ, Zwanenburg JJM, Klijn CJM, Luijten PR, Biessels GJ. Higher Pulsatility in Cerebral Perforating Arteries in Patients With Small Vessel Disease Related Stroke, a 7T MRI Study. *Stroke* 2019; 50: 62–8.

PART II

Cerebral Microinfarcts on 7T MRI



6

Cortical cerebral microinfarcts on 7T MRI: risk factors, neuroimaging correlates and cognitive functioning – The Medea-7T study

Maarten H.T. Zwartbol, Ina Rissanen, Rashid Ghaznawi, Jeroen de Bresser, Hugo J. Kuijf, Kim Blom, Theo D. Witkamp, Huiberdina L. Koek, Geert Jan Biessels, Jeroen Hendrikse, Mirjam I. Geerlings, on behalf of the UCC-SMART Study Group

Published in *Journal of Cerebral Blood Flow and Metabolism* 2021; 41: 3127-38
doi: 0.1177/0271678X211025447

Abstract

We determined the occurrence and association of cortical cerebral microinfarcts (CMIs) at 7T MRI with risk factors, neuroimaging markers of small and large vessel disease, and cognitive functioning.

Within the Medea-7T study, a diverse cohort of older persons with normal cognition, patients with vascular disease, and memory clinic patients, we included 386 participants (68 ± 9 years) with available 7T and 1.5T/3T brain MRI, and risk factor and neuropsychological data.

CMIs were found in 10% of participants and were associated with older age (RR = 1.79 per +10 years, 95% CI 1.28–2.50), history of stroke and/or TIA (RR = 4.03, 95% CI 2.18–7.43), cortical infarcts (RR = 5.28, 95% CI 2.91–9.55), lacunes (RR = 5.66, 95% CI 2.85–11.27), cerebellar infarcts (RR = 2.73, 95% CI 1.27–5.84) and decreased cerebral blood flow (RR = 1.35 per -100 ml/min, 95% CI 1.00–1.83), after adjustment for age and sex. Furthermore, participants with >2 CMIs had 0.5 SD (95% CI 0.05–0.91) lower global cognitive performance, compared to participants without CMIs.

Our results indicate that CMIs on 7T MRI are observed in vascular and memory clinic patients with similar frequency, and are associated with older age, other brain infarcts, and poorer global cognitive functioning.

Introduction

Cortical cerebral microinfarcts (CMLs), defined as microscopic regions of ischemic infarction in the brain, have gained increasing attention because of their discovery on 7 tesla (7T) magnetic resonance imaging (MRI).^{1,2} Previous studies have suggested that they are the most widespread type of brain infarction, often occurring in large numbers, and are correlated with measurable disruption of brain function.³ Furthermore, they may be a key part of the “silent” cerebrovascular burden, and have been associated with both small and large vessel disease.^{2,3}

Frequency estimates of CMLs vary widely, likely depending on the study population, MRI field strength and rating criteria.^{1–8} Studies using 3T MRI report estimates ranging from 6% in the general population, 20–29% in memory-clinic patients, to 57% in patients with cerebral amyloid angiopathy.^{6–9} At 7T MRI, frequencies have been reported ranging from 27% to 72% in brains of non-demented persons, and from 55% to 86% in mild cognitive impairment (MCI) and Alzheimer’s disease patients.^{1,4,5}

The current view regarding the etiology of CMLs is one of multiple causes. The main etiologies of CMLs are thought to be both cerebral small vessel disease (CSVD) and large vessel disease, the latter by means of hypoperfusion and microemboli.² However, evidence to support these hypotheses is inconsistent, or scarce. Apart from studies in patients with cerebral amyloid angiopathy, associations with MRI features of CSVD are inconsistent.^{6–8,10–15} Studies regarding cerebral perfusion and CMLs are few.¹⁶ Only the microembolic etiology has substantial supporting evidence, by means of the association between carotid endarterectomy and acute CMLs.¹⁷ Furthermore, CMLs’ associations with risk factors such as age, sex, smoking, alcohol use, hypertension, hyperlipidemia, and diabetes, are similarly inconsistent.^{6–8,11–14} In addition, CMLs have been associated with ante mortem cognitive decline and dementia in autopsy studies.² A few neuroimaging studies have found similar associations in vivo.^{11,12,14}

We think that more comprehensive studies in larger study populations are needed to elucidate risk factors, potential etiologies, associations with cognitive functioning, and clarify the importance of CMLs. Furthermore, studies at 7T field strength are needed to get a more accurate prevalence of CMLs in vivo, since it detects almost four times the number of CMLs compared to 3T.¹¹

We utilized 7T MRI to determine the frequency of CMLs in a diverse and large cohort of older persons with normal cognition, a history of vascular disease, or MCI or early Alzheimer’s disease. Furthermore, we examined associations between CMLs and vascular risk factors, neuroimaging markers of small and large vessel disease, and cognitive functioning.

Methods

Study population

Data were used from the Memory Depression and Aging (Medea)-7T study, a cohort study at the University Medical Center (UMC) Utrecht, the Netherlands, with the objective to investigate risk factors and outcomes of brain changes defined on 7T MRI.

We recruited participants from four settings: 1) persons registered in one general practice in Utrecht, 2) participants of the PREDICT-MR study¹⁸, 3) patients of the SMART-MR study¹⁹, and 4) patients from the memory clinics of two hospitals in Utrecht. A detailed description of the recruitment settings is published elsewhere.²⁰ 1) Recruited general practice patients were ≥ 60 years; had no clinical diagnosis of mild cognitive impairment (MCI), dementia or other neurological conditions affecting cognition; had no terminal illness; had no previous medical evaluations for cognitive complaints; and had a Clinical Dementia Rating Scale (CDR) 0. 2) The PREDICT-MR study originated from a multicenter prospective cohort investigating major depressive disorder in adult primary care patients. Adult persons were recruited in waiting rooms of general practices, irrespective of the reason for consulting. 3) The SMART-MR study is a prospective cohort at the UMC Utrecht with the goal to investigate risk factors and clinical outcomes of MRI neuroimaging markers in patients with arterial disease. Adult persons newly referred to the UMC Utrecht for treatment of symptomatic atherosclerotic disease (coronary artery disease, cerebrovascular disease, peripheral arterial disease or abdominal aortic aneurysm) and without MRI contraindications were enrolled in the SMART-MR study. 4) Outpatient memory clinic patients were recruited from the UMC Utrecht and a general hospital in Utrecht if they had MCI or early Alzheimer's disease (AD). Patients with moderate or severe AD were not included in the study. Inclusion criteria were age ≥ 60 years, a diagnosis of possible or probable AD according to the NINCDS-ADRDA workgroup criteria²¹, or MCI according to Petersen criteria²²; a CDR 0.5 or 1; and a Mini Mental State Examination score of ≥ 20 .

A total of 368 participants were included in the Medea-7T study between January 2010 and October 2017: 70 from the general practice, 50 from the PREDICT-MR study, 213 from the SMART-MR study, and 35 from the memory clinics. All participants underwent a 7T brain MRI using the same MRI sequences, and similar assessment of risk factors and outcomes and clinical examinations, all performed at the UMC Utrecht. Approval of the medical ethics committee of the UMC Utrecht was obtained according to the guidelines of the Declaration of Helsinki of 1975, and all participants provided written informed consent.

7T MRI protocol

A 7T MRI scan of the brain was performed using a 7.0 T MRI system (Philips Healthcare, Cleveland, OH, USA) with a 16 or 32-channel receiver head coil (Nova Medical, Wilmington, MA, USA). The standard MRI protocol consisted of: a T1-weighted (3D acquisition; TI/TR/TE

= 1225/4.8/2.2 ms; acquired voxel size = $1.00 \times 1.00 \times 1.00 \text{ mm}^3$; reconstructed = $0.66 \times 0.66 \times 0.50 \text{ mm}^3$), T2-weighted Turbo-Spin Echo (3D acquisition; TR/TE = 3158/301 ms; acquired voxel size = $0.70 \times 0.70 \times 0.70 \text{ mm}^3$; reconstructed = $0.35 \times 0.35 \times 0.35 \text{ mm}^3$), magnetization-prepared FLAIR (3D acquisition, TR/TE = 8000/300 ms, acquired voxel size = $0.80 \times 0.80 \times 0.80 \text{ mm}^3$, reconstructed = $0.49 \times 0.49 \times 0.49 \text{ mm}^3$), and a dual echo susceptibility-weighted imaging (SWI) (TR/TE1/TE2 = 20/6.9/15.8 ms, acquired voxel size = $0.50 \times 0.50 \times 0.70 \text{ mm}^3$, reconstructed = $0.40 \times 0.40 \times 0.35 \text{ mm}^3$) sequence.

Assessment of cortical microinfarcts on 7T MRI

Cortical CMIs were visually rated on 7T MRI by one rater (MHTZ, 6 years of experience in neuroradiology), blinded to patient characteristics, on the T1-weighted, T2-weighted and FLAIR images according to proposed neuroimaging criteria.² In brief, a CMI had to be a strictly intracortical lesion, visible in at least two directions, less than 4 mm in greatest dimension, hyperintense (to cortex) on T2-weighted imaging and hypointense on T1-weighted imaging. We did not use a FLAIR criterion since the FLAIR signal of a CMI ranges from hypo-, iso-, to hyperintense based on size and cavitation. Hence, we did not distinguish cavitated from non-cavitated lesions. A lesion was disregarded as a CMI if there was an accompanying susceptibility artefact on SWI, or if it was within 1 cm from a large cortical infarct. Size of a CMI was defined as the maximum diameter in any direction on T2-weighted imaging.

Intra-rater agreement was good with an intraclass correlation coefficient (20 cases, 2-way mixed-effects model, absolute agreement) of 0.85.

Vascular risk factors

Questionnaires were used to assess age, sex, educational level, smoking, and alcohol use. Educational level, as a proxy of socioeconomic status, consisted of 8 levels, ranging from (un)completed primary school to academic degree, and was categorized into 4 categories in the analyses. Smoking was categorized as never, current, or former smoker. Alcohol use was expressed in units per week and categorized as none or <1 unit per week, 1-10 units per week, and >10 units per week. Systolic and diastolic blood pressures were both defined as an average of three measurements in supine position. Hypertension was defined as a mean systolic blood pressure of >140 mmHg or a mean diastolic blood pressure of >90 mmHg or use of antihypertensive drugs. Hypercholesterolemia was defined as a total cholesterol/high-density lipoprotein ratio ≥ 5.0 or use of lipid-lowering drugs. Weight (kg) and height (m) measurements without shoes and heavy clothing were used to calculate body mass index (BMI). Diabetes mellitus was defined as the use of antidiabetic medication, a known history of diabetes, a fasting glucose of $\geq 7.0 \text{ mmol/L}$ or—in participants from PREDICT-MR—a non-fasting blood glucose $\geq 11.1 \text{ mmol/L}$.

1.5T and 3T MRI protocol

In the PREDICT-MR and SMART-MR cohorts a 1.5 T whole-body system (Gyrosan ACS-NT, Philips Medical Systems, Best, the Netherlands) was performed in addition to the 7T MRI. The standard MRI protocol consisted of a T1-weighted sequence (SMART-MR: 3D acquisition; repetition time (TR)/echo time (TE): 7.0/3.2 ms; voxel size = $0.94 \times 0.94 \times 1.00 \text{ mm}^3$ isotropic; PREDICT-MR: 3D acquisition; TR/TE: 6.9/3.1 ms; voxel size = $0.98 \times 0.98 \times 1.10 \text{ mm}^3$ isotropic), a T2-weighted sequence (SMART-MR and PREDICT-MR: 2D acquisition; TR/TE 2200/10.5 ms; voxel size = $0.90 \times 0.90 \times 4.00 \text{ mm}^3$), a FLAIR sequence (SMART-MR: 2D acquisition; TI/TR/TE 2000/6000/100 ms; $0.90 \times 0.90 \times 4.00 \text{ mm}^3$; PREDICT-MR: 3D acquisition; TI/TR/TE 1600/4800/329.7 ms; voxel size = $0.98 \times 0.98 \times 1.10 \text{ mm}^3$ isotropic), and a phase-contrast MR angiography sequence (SMART-MR and PREDICT-MR: 2D slice acquisition; TR/TE, 16/9 ms; voxel size = $0.98 \times 0.98 \times 5.00 \text{ mm}^3$; velocity sensitivity 100 cm/s; acquisition at the level of the proximal cavernous segment of the ICA and prepontine basilar artery).

In the participants recruited from the general practice and the memory clinic patients, a 3.0 T MRI whole-body system (Philips Medical Systems, Best, the Netherlands) was used for brain imaging. The standard MRI protocol consisted of a T1-weighted sequence (3D acquisition; TR/TE=8.0/4.5 ms; voxel size = $1.00 \times 1.00 \times 1.00 \text{ mm}^3$ isotropic), a T2-weighted sequence (2D acquisition; TR/TE 3197.5/140 ms; $0.96 \times 0.96 \times 3.00 \text{ mm}^3$), a FLAIR sequence (2D acquisition; TI/TR/TE 2800/11000/125 ms; voxel size = $0.96 \times 0.96 \times 3.00 \text{ mm}^3$), and a phase-contrast MR angiography sequence (2D slice acquisition; TR/TE 14/8.8 ms; voxel size = $0.59 \times 0.59 \times 5.00 \text{ mm}^3$; velocity sensitivity 100 cm/s; acquisition at the level of the proximal cavernous segment of the ICA and prepontine basilar artery).

Assessment of neuroimaging markers of cerebrovascular disease

All assessments of cerebrovascular disease markers were performed blinded to patient characteristics. Cerebral infarcts and lacunes of presumed vascular origin²³ were visually rated on 1.5T or 3T MRI by one rater (MHTZ), on the T1-weighted, T2-weighted and FLAIR images. Uncertain lesions were discussed during a consensus meeting between MHTZ and an experienced neuroradiologist (TDW) to reach agreement. Cerebral microbleeds were rated by one rater (MHTZ) on the 7T MRI dual echo SWI images using a minimum intensity projection reconstruction and source data. Microbleeds were labeled as lobar or deep using the Microbleed Anatomical Rating Scale.²⁴

Segmentation of gray matter, white matter, cerebrospinal fluid (CSF), and cortical thickness on 1.5T or 3T was performed using the Computational Anatomy Toolbox (Cat12; version 1155) using T1-weighted and FLAIR images.²⁵ Segmentation of white matter hyperintensities (WMH) was performed using the lesion growth algorithm from the Lesion Segmentation Tool (LST; version 2.0.15; www.statistical-modeling.de/lst.html) using T1-weighted and FLAIR images, with a threshold of 0.1.²⁶ Cat12 and LST are toolboxes implemented in the Statistical Parametric Mapping 12 (SPM12; version 6906; Wellcome

Institute of Neurology, University College London, UK, <http://www.fil.ion.ucl.ac.uk/spm/doc/>) for Matlab (version 8.6; The MathWorks, Inc., Natick, Massachusetts, United States). Of note, we used lesion-filling on the T1-weighted sequence before segmenting it in Cat12, using the WMH segmentation from LST. Lesion-filling increases the T1-weighted signal of WMH and prevents incorrect labeling as gray matter. Furthermore, brain lesions were manually segmented on FLAIR images by a single rater (MHTZ) and used to correct the final (white/gray matter, CSF) Cat12 segmentations. Total brain volume (TBV; ml) was calculated by summing gray matter, white matter and total infarct volume. Intracranial volume (ICV; ml) was calculated by summing TBV and CSF.

Cerebral blood flow was calculated from the 1.5T and 3T phase-contrast MR angiography data using native Q-flow post-processing software on a stand-alone workstation (Philips, Best, the Netherlands). Blood flow through the prepontine basilar artery and the left and right cavernous internal carotid arteries was summed to calculate the total cerebral blood flow (ml/min). Of note, because flow was measured in the prepontine basilar artery, flow from proximal vertebrobasilar branches was not included in the measure of total CBF (e.g., posterior inferior cerebellar artery and pontomedullary perforators). Hence, the total CBF is a slight underestimation of actual CBF.

Assessment of extracranial atherosclerosis

Markers of extracranial atherosclerosis were measured in the 213 participants of the SMART-MR cohort and included common carotid intima-media thickness (cIMT), carotid stenosis, and ankle-brachial index (ABI). An experienced technician performed carotid ultrasonography with a 10MHz linear-array transducer. Mean cIMT was calculated from six measurements (anterolateral, posterolateral and mediolateral in both common carotid arteries). Carotid stenosis was assessed in the bilateral common and internal carotid arteries, and defined as the most severe stenosis, according to standard criteria based on the peak systolic velocity.²⁷ ABI was calculated from the highest systolic blood pressure, measured by experienced technicians, at the posterior tibial and dorsal pedal arteries by Doppler and at both brachial arteries by a semiautomatic oscillometric device in supine position. We categorized carotid stenosis by presence of $\geq 50\%$ stenosis, and ABI by ≤ 0.8 , the clinical cutoff for peripheral artery disease.

Neuropsychological assessment

The Mini Mental-State Examination was performed for all participants to compare the cognitive functioning characteristics of sub-cohorts. In addition, all patients underwent neuropsychological assessment for memory, executive functioning and working memory. Information processing speed was also assessed in the PREDICT-MR and SMART-MR cohorts. Memory was assessed with the 15 Word Learning Test, using a composite score of the immediate recall based on 5 trials, the delayed recall and the retention score; and the delayed recall of the Rey-Osterrieth Complex figure test.^{28,29} Executive functioning

was assessed with the Verbal Fluency test using animals as categories (2 minutes).^{30–32} Working memory was assessed with the combined longest span scores of the Forward Digit Span and Backward Digit Span.³³ Processing speed was assessed with the Digit Symbol Substitution Test (120 seconds).³⁴ Composite Z-scores were calculated by converting raw scores to standardized Z-scores and averaging them across all subtests per domain. A global cognitive functioning composite Z-score was calculated by standardizing the cumulative of all averaged domain-specific Z-scores.

Statistical analysis

We performed multiple imputation with 20 datasets to address missing values of studied risk factors, imaging markers of cerebrovascular disease, and cognitive functioning. Data were analyzed by pooling the 20 imputed datasets. Multiple imputation and statistical analysis were performed using SPSS Statistics for Windows, Version 25.0 (IBM, Armonk, NY, USA). Missing data ranged from 0.3% to 20%: level of education 0.5%; Mini-Mental State Examination 1.4%; BMI 0.3%; diabetes 0.8%; alcohol use 14.1%; infarcts 0.5%; cortical microinfarcts 3.0%; cerebral microbleeds 20%; intracranial volume 3.8%; total brain volume 3.8%; cortical thickness 3.8%; WMH volume 2.9%; and cerebral blood flow 2.7%.

Characteristics of vascular risk factors and MRI markers of cerebrovascular disease were calculated in the total study population and separate cohorts.

Modified Poisson regression with robust error variance was used to estimate relative risks (RR) for presence of CMIs, with vascular risk factors and MRI markers of cerebrovascular disease as independent variables, adjusted for age and sex (model 1). We used modified Poisson regression because it has similar flexibility and robustness as log-binomial regression but does not suffer from convergence errors. Furthermore, compared to log-binomial regression, it is less sensitive to omitted covariates.³⁵ Analyses of MRI markers were additionally adjusted for educational level, history of stroke or TIA, BMI, smoking status, alcohol intake, hypertension, diabetes, and hypercholesterolemia (model 2). Analyses of TBV and WMH volume were also adjusted for ICV, and the analysis of CBF for TBV, in model 2. Moreover, the association with $\geq 50\%$ carotid stenosis, cMNT and ABI was analyzed within the SMART-MR cohort ($n = 213$), using the same models used for the analyses of MRI markers.

ANCOVA was used to estimate age, sex and education level-adjusted mean cognitive functioning Z-scores, categorized by presence of no CMIs, 1–2 CMIs, and >2 CMIs. We used ANCOVA because of the low frequency and high skewed distribution of CMIs. Furthermore, linear regression analysis was used to estimate the association between >2 CMIs and cognitive functioning (using no CMIs as reference category) and total number of CMIs and cognitive functioning and, with identical adjustments, in the total study population and separate cohorts. Residual plots of all linear regression analyses were checked for regression assumptions.

Results

Characteristics of the vascular risk factors and MRI markers of cerebrovascular disease in the 368 participants (68.3 ± 9.0 years; 30.4% women) are presented in Table 1 and Table 2, respectively. A total of 129 CMLs were found in 10% ($n = 35$) of the study population, with a mean (min, max) number of 3.4 (1.0, 15.0) CMLs in affected brains. CML frequencies per cohort ranged from 0.6% to 13.2% (Fig 1). Of the 58 participants with a history of stroke or TIA, 25.8% ($n = 15$) had CMLs. Within the SMART-MR cohort, 21% of the 62 participants with brain infarcts had CMLs. Within the memory clinic patients, 33% of the 6 participants with brain infarcts had CMLs.

Risk factors of CMLs

An increased RR of CMLs was found for older age ($RR = 1.79$ per +10 years, 95% CI 1.28 to 2.50) adjusted for sex; and for history of stroke or TIA ($RR = 4.03$, 95% CI 2.18 to 7.43) adjusted for age and sex (model 1, Table 3). These associations remained after further adjustments in model 2. Male sex was associated with increased RR of 3.08 (95% CI 1.07 to 8.83) for CMLs when adjusting for age and vascular risk factors in model 2. No association was found with educational level, BMI, smoking status, alcohol use, hypertension, diabetes or hypercholesterolemia and CMLs in our sample.

Cerebrovascular disease on brain MRI and CMLs

An increased RR of CMLs was found for presence of all types of infarcts (Table 4). After adjusting for age and sex in model 1, the highest RR was observed for lacunes of presumed vascular origin ($RR = 5.66$, 95% CI 2.85 to 11.27) and cortical infarcts ($RR = 5.28$, 95% CI 2.91 to 9.55). The RR estimates decreased after adjustment for vascular risk factors in model 2, however, apart from cerebellar infarcts, confidence intervals did not cross 1. Decreased cerebral blood flow associated with an increased RR of 1.35 (95% CI 1.00 to 1.83) per -100 ml/min for CMLs in model 1. No associations with CMLs were found for microbleeds, total brain volume, WMH volume, or cortical thickness.

Extracranial atherosclerosis and CMLs

Within the 213 participants (68.4 ± 8.2 years; 17.4% women) of the SMART-MR sub-cohort, increased RRs for presence of CMLs were found for higher cIMT ($RR = 5.81$ per +1 mm, 95% CI 2.55 to 13.21), $\geq 50\%$ carotid stenosis ($RR = 6.18$, 95% CI 2.87 to 13.33), and $ABI \leq 0.8$ ($RR = 3.80$, 95% CI 1.72 to 8.37). Additional adjustment for vascular risk factors in Model 2 did not materially change these associations (Table 5). Of the 19 persons with $\geq 50\%$ carotid stenosis (ranging from ≥ 50 -69% stenosis to occlusion), around 53% had presence of CMLs. Of the 149 persons with stenosis $< 50\%$, 10% were found to have CMLs. No CMLs were found in persons without carotid plaque or stenosis.

Table 1. Characteristics of total study population and each included cohort in the Medea-7T study (n = 368).

| | Total population (n = 368) | General practice (n = 70) | PREDICT-MR (n = 50) | SMART-MR (n = 213) | Memory clinics (n = 35) |
|--------------------------------------|-------------------------------|------------------------------|------------------------|-----------------------|----------------------------|
| Age (years) | 68.3 ± 9.0 | 71 ± 7 | 60 ± 11 | 68 ± 8 | 75 ± 7 |
| Women | 30.4% | 47% | 62% | 17% | 31% |
| High educational level ^a | 38.4% | 66% | 28% | 33% | 34% |
| Mini-Mental State Examination | 28.6 ± 1.7 | 29.2 ± 1.2 | 28.9 ± 1.1 | 28.7 ± 1.5 | 26.4 ± 2.4 |
| Body mass index (kg/m ²) | 26.6 ± 3.8 | 26 ± 4 | 26 ± 4 | 27 ± 4 | 25 ± 3 |
| Smoking | | | | | |
| Never | 23.6% | 29% | 48% | 14% | 37% |
| Former | 63.0% | 64% | 40% | 69% | 60% |
| Current | 13.3% | 7% | 12% | 17% | 3% |
| Alcohol | | | | | |
| No alcohol | 13.4% | 17% | 18% | 10% | 23% |
| 1-10 units p/week | 60.1% | 53% | 72% | 60% | 57% |
| > 10 units p/week | 26.5% | 30% | 10% | 30% | 20% |
| History of stroke or TIA | 15.8% | 0% | 0% | 27% | 3% |
| Hypertension | 81.8% | 73% | 58% | 90% | 86% |
| Systolic BP | 142 ± 18 | 148 ± 20 | 135 ± 16 | 140 ± 17 | 148 ± 18 |
| Diastolic BP | 80 ± 10 | 81 ± 10 | 80 ± 9 | 79 ± 10 | 79 ± 10 |
| Diabetes | 13.6% | 3% | 10% | 17% | 17% |
| Hypercholesterolemia | 67.1% | 23% | 30% | 92% | 57% |

Values are presented as mean ± SD or percentages after imputation.

^a Defined as higher vocational or academic degree.

BP: blood pressure.

Table 2. Cerebrovascular MRI markers in total study population and each included cohort in the Medea-7T study (n = 368).

| | Total population (n = 368) | General practice (n = 70) | PREDICT-MR (n = 50) | SMART-MR (n = 213) | Memory clinics (n = 35) |
|------------------------------|-------------------------------|------------------------------|------------------------|-----------------------|----------------------------|
| Any infarct | 20.7% | 4% | 6% | 31% | 17% |
| Cortical infarcts | 6.3% | 0% | 4% | 10% | 3% |
| Lacunar infarcts | 11.4% | 1% | 2% | 18% | 6% |
| Cerebellar infarcts | 8.2% | 1% | 2% | 12% | 11% |
| Other infarcts | 3.8% | 1% | 4% | 4% | 6% |
| Cortical microinfarcts | 9.5% | 3% | 1% | 13% | 13% |
| Any microbleeds | 61% | 60% | 49% | 66% | 45% |
| Lobar microbleeds | 56% | 51% | 47% | 62% | 37% |
| Deep microbleeds | 30% | 26% | 13% | 37% | 25% |
| Intracranial volume (ml) | 1511 ± 142 | 1519 ± 151 | 1459 ± 154 | 1522 ± 135 | 1495 ± 139 |
| Total brain volume (ml) | 1111 ± 115 | 1103 ± 113 | 1099 ± 125 | 1128 ± 108 | 1040 ± 118 |
| WMH volume (ml) ^a | 3.4 (0.8, 15.2) | 3.2 (0.9, 11.0) | 2.5 (0.4, 11.2) | 3.1 (0.7, 14.8) | 6.8 (3.2, 27.3) |
| Cerebral blood flow (ml/min) | 545 ± 136 | 580 ± 171 | 586 ± 140 | 527 ± 118 | 530 ± 139 |
| Cortical thickness (mm) | 2.54 ± 0.19 | 2.59 ± 0.08 | 2.55 ± 0.14 | 2.54 ± 0.15 | 2.49 ± 0.12 |

Values are presented as mean ± SD or frequencies after imputation.
^a Median (10th, 90th percentile).
WMH: white matter hyperintensities.

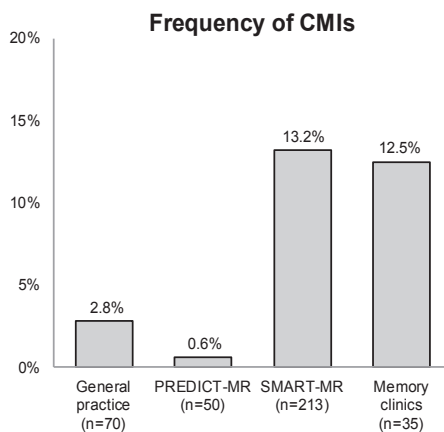


Figure 1. Presence of 1 or more cortical microinfarcts in each cohort.

Table 3. Association between risk factors and presence of cortical microinfarcts.

| | Cortical microinfarcts (yes vs. no) RR (95% CI) | |
|---|--|----------------------|
| | Model 1 | Model 2 |
| Age, per +10 years | 1.79 (1.28 to 2.50) | 1.65 (1.04 to 2.61) |
| Male sex | 2.66 (0.98 to 7.24) | 3.08 (1.07 to 8.83) |
| Education, high vs. low-medium ^a | 0.53 (0.16 to 1.77) | 0.55 (0.14 to 2.25) |
| Body mass index, per +1 kg/m ² | 1.03 (0.94 to 1.12) | 1.00 (0.91 to 1.09) |
| Smoking, current vs. never | 1.34 (0.33 to 5.48) | 1.28 (0.33 to 5.03) |
| Alcohol use | | |
| No, or <1 unit/week | Reference | Reference |
| 1 – 10 units/week | 1.39 (0.45 to 4.36) | 1.64 (0.00 to 4.62) |
| >10 units/week | 1.42 (0.41 to 4.89) | 1.28 (0.33 to 5.03) |
| History of stroke or TIA | 4.03 (2.18 to 7.43) | 4.15 (2.22 to 7.75) |
| Hypertension | 2.36 (0.56 to 10.01) | 2.54 (0.60 to 10.75) |
| Systolic BP, per +10 mmHg ^b | 1.06 (0.87 to 1.28) | 1.07 (0.90 to 1.27) |
| Diastolic BP, per +10 mmHg ^b | 0.93 (0.65 to 1.33) | 0.93 (0.67 to 1.29) |
| Diabetes | 1.55 (0.68 to 3.50) | 1.53 (0.65 to 3.61) |
| Hypercholesterolemia | 1.31 (0.55 to 3.15) | 0.83 (0.14 to 2.02) |

Values are relative risks (RR) with 95% confidence intervals calculated with modified-Poisson regression analysis with robust error variance.

Model 1: adjusted for age and sex. Model 2: model 1 with additional adjustment for educational level, history of stroke or TIA, body mass index, smoking status, alcohol use, hypertension, diabetes, hypercholesterolemia.

^a High educational level indicates a higher vocational or academic degree (n = 142). Low-medium educational level indicates a lower vocational degree or lower (n = 122).

^b In model 2 hypertension was replaced by systolic and diastolic blood pressure.
BP: blood pressure.

Table 4. Association between MRI markers of cerebrovascular disease and presence of cortical microinfarcts.

| | Cortical microinfarcts (yes vs. no) RR (95% CI) ^a | |
|--|---|---------------------|
| | Model 1 | Model 2 |
| Any infarct, yes vs. no | 5.34 (2.53 to 11.27) | 3.96 (1.65 to 9.52) |
| Cortical infarct, yes vs. no | 5.28 (2.91 to 9.55) | 2.88 (1.23 to 6.73) |
| Lacunar infarct, yes vs. no | 5.66 (2.85 to 11.27) | 4.52 (2.17 to 9.38) |
| Cerebellar infarct, yes vs. no | 2.73 (1.27 to 5.84) | 1.73 (0.88 to 3.40) |
| Lobar microbleed, yes vs. no | 1.22 (0.61 to 2.46) | 1.15 (0.58 to 2.30) |
| Deep microbleed, yes vs. no | 1.27 (0.57 to 2.81) | 1.15 (0.52 to 2.55) |
| Total brain volume, per -10 ml ^a | 1.02 (0.94 to 1.1) | 0.99 (0.93 to 1.07) |
| Total WMH volume, per +1 natural-log (ml) ^a | 1.00 (0.67 to 1.50) | 0.91 (0.62 to 1.32) |
| Cortical thickness, per -0.01 mm | 1.02 (0.99 to 1.05) | 1.01 (0.98 to 1.04) |
| Cerebral blood flow, per -100 ml/min ^b | 1.35 (1.00 to 1.83) | 1.19 (0.92 to 1.55) |

Values are relative risks (RR) with 95% confidence intervals calculated with modified-Poisson regression analysis with robust error variance.

Model 1: adjusted for age and sex. Model 2: model 1 with additional adjustment for educational level, history of stroke or TIA, body mass index, smoking status, alcohol use, hypertension, diabetes, hypercholesterolemia.

^a Model 1 and 2 additionally adjusted for intracranial volume.

^b Model 1 and 2 additionally adjusted for total brain volume.

WMH: white matter hyperintensities.

Table 5. Association between markers of extracranial atherosclerosis and presence of cortical microinfarcts in the SMART-MR cohort (n = 213).

| | Cortical microinfarcts (yes vs. no) RR (95% CI) ^a | |
|-------------------------------------|---|----------------------|
| | Model 1 | Model 2 |
| Intima-media thickness, per +0.1 mm | 5.81 (2.55 to 13.21) | 4.66 (1.04 to 1.31) |
| Carotid stenosis ≥50% vs. <50% | 6.18 (2.87 to 13.33) | 6.33 (2.69 to 14.91) |
| Ankle-brachial index ≤0.8 vs. >0.8 | 3.80 (1.72 to 8.37) | 4.24 (1.54 to 11.62) |

Values are relative risks (RR) with 95% confidence intervals calculated with modified-Poisson regression analysis with robust standard errors.

Model 1: adjusted for age and sex. Model 2: model 1 with additional adjustment for educational level, history of stroke or TIA, body mass index, smoking status, alcohol use, hypertension, diabetes, hypercholesterolemia.

CMLs and cognitive functioning

Figure 2 shows domain-specific and global cognitive functioning Z-scores adjusted for age, sex and educational level, according to presence of no CMLs (n = 333), 1 or 2 CMLs

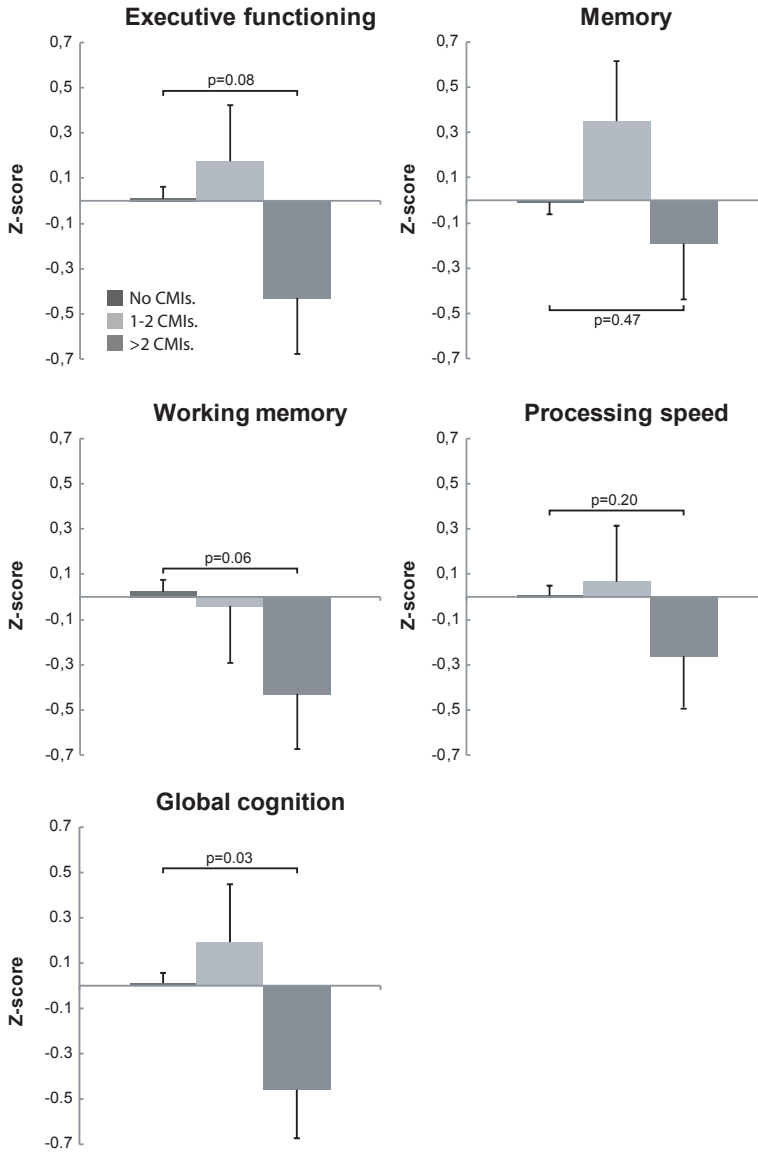


Figure 2. Cognitive functioning by presence of cortical microinfarcts. Values are estimated mean (95% CI) Z-scores, adjusted for age, sex and educational level. Executive functioning: no CMIs, 0.01 (-0.08 to 0.11); 1-2 CMIs, 0.18 (-0.26 to 0.61); >2 CMIs, -0.43 (-0.91 to 0.05). Memory: no CMIs, -0.01 (-0.11 to 0.09); 1-2 CMIs, 0.35 (-0.18 to 0.88); >2 CMIs, -0.19 (-0.68 to 0.29). Working memory: no CMIs, 0.02 (-0.08 to 0.13); 1-2 CMIs, -0.04 (-0.53 to 0.45); >2 CMIs, -0.43 (-0.90 to 0.04). Processing speed: no CMIs, 0.01 (-0.08 to 0.10); 1-2 CMIs, 0.07 (-0.41 to 0.55); >2 CMIs, -0.26 (-0.71 to 0.18). Global cognition: no CMIs, 0.01 (-0.08 to 0.10); 1-2 CMIs, 0.19 (-0.25 to 0.64); >2 CMIs, -0.46 (-0.88 to -0.04).

($n = 18$) and more than 2 CMIs ($n = 17$). Participants with more than 2 CMIs had lower global cognitive functioning, compared to participants with no CMIs (mean difference = -0.48 standard deviations, 95% CI -0.91 to -0.05). Of all cognitive functions, presence of >2 CMIs seemed to be associated most with lower executive functioning (mean difference = -0.45 standard deviations, 95% CI -0.94 to 0.05) and working memory (mean difference = -0.46 standard deviations, 95% CI -0.95 to 0.02). Additional linear regression analyses showed a similar image. We found associations between CMIs and executive functioning ($b = -0.08$ per +1 CMI; 95% CI -0.16 to 0.00), working memory ($b = -0.08$ per +1 CMI; 95% CI -0.15 to -0.01), and global cognitive functioning ($b = -0.08$ per +1 CMI; 95% CI -0.15 to -0.02), with the latter being the strongest association. We did not observe an association with memory ($b = -0.02$ per +1 CMI; 95% CI -0.09 to 0.05) and processing speed ($b = -0.05$ per +1 CMI; 95% CI -0.13 to 0.03). The association between CMIs and cognitive functioning was similar in the SMART-MR and memory clinic cohorts as in the total sample (Supplemental Table 1).

Discussion

In this diverse cohort of 368 older adults with 7T brain MRI we observed an overall CMI frequency of 10%, ranging from 1-3% in older persons with normal cognition, to 13% in patients with MCI or early AD, and 13% in patients with a history of vascular disease. Presence of CMIs was associated with older age, male sex, history of stroke or TIA, ischemic lesions on brain MRI and decreased cerebral blood flow. In a subcohort of persons with manifest arterial disease, presence of CMIs associated with extracranial atherosclerosis. Furthermore, presence of more than two CMIs was associated with lower global cognitive performance, in particular lower executive functioning and working memory.

Our study presents data on the largest 7T brain MRI cohort to date and is one of the larger *in vivo* studies on CMIs currently published. Strengths of this study include 7T MR imaging that is superior to lower field strength MRI for CMI detection¹¹, which should improve measures of CMI frequency and aid in the study of determinants. Furthermore, the inclusion of participants from various cohorts increased the variability in exposure and outcome status, allowed us to describe the occurrence of CMIs across these cohorts, and increases the generalizability of our results to other populations. Although it could be argued that combining different cohorts leads to incorrect estimates if effect modification by cohort was present, we have no *a priori* reason to assume that the relationships studied were different across cohorts. For instance, when we repeated the analyses with cognition within strata of cohorts, we found very similar effect estimates. A last strength is the extensive data on risk factors, neuroimaging markers and cognitive functioning.

Our study has several limitations. First, the cross-sectional design, which does not allow interpretation of causality. In particular, we cannot conclude which came first in the associations with brain MRI markers of small and large vessel disease and they may be

explained by shared risk factors. Second, treatment of vascular risk factors before the 7T MRI may have influenced associations with risk factors.³⁶ Third, pooling cohorts with different in- and exclusion criteria can cause under- or overestimation of the examined associations. Fourth, CMLs and CMBs were rated on 7T MRI data whereas the other MRI markers were evaluated on 1.5T or 3T MRI data. Ideally, all MRI markers should have been evaluated on 7T MRI data because it provides a higher spatial resolution and contrast-to-noise ratio. However, it is currently unclear if STRIVE criteria are valid on 7T MRI. Furthermore, as far as we know, there is no robust and validated brain segmentation software for 7T MRI data. A related limitation are the differences in MR image quality between the various cohorts which may have caused variations in the accuracy of lesion rating and segmentation. However, apart from the PREDICT cohort, variations in image quality were visually minimal. In the PREDICT cohort the higher spatial resolution of the FLAIR sequence may have resulted in more accurate rating and segmentation of brain lesions, compared to the other cohorts. We tested for this excluding the PREDICT cohort from the analyses, which caused no considerable change in associations (data not shown). Fifth, although the size of our population is large for a 7T cohort, it may have had limited statistical power to detect small associations.

Previous neuroimaging studies with 3T MRI have reported frequencies of CMLs ranging from 6% in non-demented older adults with hypertension⁶, and a population-based cohort¹², 15% in acute stroke/TIA patients (also including acute CMLs)⁷ to 20-32% in memory clinic patients.^{11,14,37} Earlier 7T studies reported much higher frequencies ranging from 27-72% in non-demented elders^{1,38} to 55-86% in MCI/AD patients.^{4,5} The frequencies observed in this 7T study are much lower, which might be explained by the evolving insight regarding neuroimaging characteristics of CMLs and changes in imaging criteria², which may have increased the diagnostic accuracy leading to a decreased number of detections. Furthermore, the relatively low CML frequency in our memory clinic population, compared to prior studies, might be explained by the comparatively lower overall cerebrovascular disease burden compared to previous studies.

With regard to vascular risk factors, older age, male sex, and prior stroke or TIA were associated with presence of CMLs in this study. An association with prior stroke or TIA is the most consistently reported association in previous literature.^{7,11,12,14} Associations with vascular risk factors in prior reports are conflicting, with not one conventional risk factor showing a consistent relationship. Age has been associated with CMLs in some studies^{6,12}, but not in others.^{7,8,14,37} Male sex shows a similar picture, being associated with CMLs in some studies^{7,11,14} and absent in others.^{6,8,12,37} All other risk factors show equivocal associations across neuroimaging and neuropathology studies, which was noted in a recent review article on CMLs.²

In regard to imaging markers of cerebrovascular disease, we found that all types of brain infarcts on MRI were associated with presence of CMLs, which is in line with prior neuroimaging^{12,14,37}, and neuropathology studies.³⁹⁻⁴¹ Apart from lacunes of presumed

vascular origin, we did not find associations with CSVD markers such as WMH, microbleeds or brain atrophy. Associations of CMLs with WMH have been found in several studies^{12–14}, but were absent in others.^{6–8,37} Associations with cerebral microbleeds were similarly inconsistent^{7,8,11,12,14}, as are the few results for brain atrophy.^{8,11,37} An explanation for these inconsistencies could be that most evidence is based on studies with small to modest sample sizes, studies conducted in different settings and study populations, examining different determinants and neuroimaging markers. In this study we used accurate and comprehensive methods to assess CMLs and their risk factors, potential etiologies, and cognitive consequences in a large and generalizable study population to increase the consistency of evidence.

We observed strong associations between markers of extracranial atherosclerosis and presence of CMLs in a subcohort of persons with manifest arterial disease. These results are in concordance with prior studies, although associations of CMLs with cMT and ABI have not been previously studied. These associations are likely a reflection of the systemic nature of atherosclerosis that is in line with the well-established association between CMLs and intracranial atherosclerosis.^{12,37,42,43} Furthermore, we observed an association between lower cerebral blood flow and presence of CMLs, which is in line with a recent study in memory clinic patients.¹⁶ Lower CBF is regarded a proxy of cerebral hypoperfusion, one of the proposed etiologies of CMLs.² However, CBF can be low due to a problem with supply or due to decreased metabolic demand from diseased or injured tissue.⁴⁴ Since we do not have data on cerebral metabolism, we cannot make this distinction. Hence, the current finding may also represent decreased metabolic demand. Overall, CMLs showed consistent associations with markers of large arterial disease and not with specific small vessel disease lesions. Although the association with lacunes might be regarded as discrepant, lacunes are caused by small and large vessel disease.⁴⁵

Concerning the cognitive outcomes of CMLs, we observed that presence of more than 2 CMLs was associated with lower cognitive performance, most evident for global cognitive functioning. Our findings suggest that especially executive functioning and working memory might be affected due to high CML burden. These findings are in concordance with most *in vivo* studies.^{7,11,12,14} The small number of participants with 1 and more than 2 CMLs might have unpowered the analyses of specific cognitive domains, nonetheless, the estimated effect sizes were similar to prior studies.^{11,12,14} Our findings suggest that CMLs are one of the pathways through which large vessel disease could contribute to cognitive decline, which is potentially modifiable.

In conclusion, CMLs on 7T MRI were observed in vascular and memory clinic patients with similar frequency, but they were less frequent than reported in previous studies. Our results suggest that CMLs are a manifestation of the severity of systemic arterial disease, possibly through the pathways of hypoperfusion and microemboli. In addition, presence of more than two CMLs was associated with significantly poorer global cognitive functioning, suggesting that CMLs could be an important vascular contributor to cognitive decline.

References

1. Van Veluw SJ, Zwanenburg JJM, Engelen-Lee J, Spliet WGM, Hendrikse J, Luijten PR, et al. In vivo detection of cerebral cortical microinfarcts with high-resolution 7T MRI. *J Cereb Blood Flow Metab* 2013; 33: 322–9.
2. van Veluw SJ, Shih AY, Smith EE, Chen C, Schneider JA, Wardlaw JM, et al. Detection, risk factors, and functional consequences of cerebral microinfarcts. *Lancet Neurol* 2017; 16: 730–40.
3. Smith EE, Schneider JA, Wardlaw JM, Greenberg SM. Cerebral microinfarcts: the invisible lesions. *Lancet Neurol* 2012; 11: 272–82.
4. van Veluw SJ, Heringa SM, Kuijf HJ, Koek HL, Luijten PR, Biessels GJ. Cerebral cortical microinfarcts at 7 Tesla MRI in patients with early Alzheimer's disease. *J Alzheimers Dis* 2014; 39: 163–7.
5. van Rooden S, Goos JDC, Van Opstal AM, Versluis MJ, Webb AG, Blauw GJ, et al. Increased number of microinfarcts in Alzheimer disease at 7-T MR imaging. *Radiology* 2014; 270: 205–11.
6. Van Dalen JW, Scuric EEMM, van Veluw SJ, Caan MWA, Nederveen AJ, Biessels GJ, et al. Cortical microinfarcts detected in vivo on 3 tesla MRI: Clinical and radiological correlates. *Stroke* 2015; 46: 255–7.
7. Wang Z, van Veluw SJ, Wong A, Liu W, Shi L, Yang J, et al. Risk factors and cognitive relevance of cortical cerebral microinfarcts in patients with ischemic stroke or transient ischemic attack. *Stroke* 2016; 47: 2450–5.
8. Xiong L, van Veluw SJ, Bounemia N, Charidimou A, Pasi M, Boulouis G, et al. Cerebral cortical microinfarcts on magnetic resonance imaging and their association with cognition in cerebral amyloid angiopathy. *Stroke* 2018; 49: 2330–6.
9. van den Brink H, Zwiers A, Switzer AR, Charlton A, McCreary CR, Goodyear BG, et al. Cortical microinfarcts on 3T magnetic resonance imaging in cerebral amyloid angiopathy. *Stroke*. 2018; 49: 1899–1905.
10. Kovari E, Herrmann FR, Hof PR, Bouras C, Kövari E, Herrmann FR, et al. The relationship between cerebral amyloid angiopathy and cortical microinfarcts in brain ageing and Alzheimer's disease. *Neuropathol Appl Neurobiol* 2013; 39: 498–509.
11. Van Veluw SJ, Hilal S, Kuijf HJ, Ikram MK, Xin X, Yeow TB, et al. Cortical microinfarcts on 3T MRI: Clinical correlates in memory-clinic patients. *Alzheimers Dement* 2015; 11: 1500–9.
12. Hilal S, Sicking E, Shaik MA, Chan QL, Van Veluw SJ, Vrooman H, et al. Cortical cerebral microinfarcts on 3T MRI: A novel marker of cerebrovascular disease. *Neurology* 2016; 87: 1583–90.
13. Oliveira-Filho J, Ay H, Shoamanesh A, Park KY, Avery R, Sorgun M, et al. Incidence and etiology of microinfarcts in patients with ischemic stroke. *J Neuroimaging* 2018; 28:406–11.
14. Ferro DA, van Veluw SJ, Koek HL, Exalto LG, Biessels GJ, Utrecht Vascular Cognitive Impairment (VCI) study group. Cortical cerebral microinfarcts on 3 Tesla MRI in patients with vascular cognitive impairment. *J Alzheimers Dis* 2017; 60:1443–50.
15. Lauer A, van Veluw SJ, William CM, Charidimou A, Roongpiboonsopit D, Vashkevich A, et al. Microbleeds on MRI are associated with microinfarcts on autopsy in cerebral amyloid angiopathy. *Neurology* 2016; 87: 1488–92.
16. Ferro DA, Mutsaerts HJJM, Hilal S, Kuijf HJ, Petersen ET, Petr J, et al. Cortical microinfarcts in memory clinic patients are associated with reduced cerebral perfusion. *J Cereb Blood Flow Metab* 2020; 40: 1869–78.
17. Gwon JG, Kwon TW, Cho YP, Kang DW, Han Y, Noh M. Analysis of risk factors for cerebral microinfarcts after carotid endarterectomy and the relevance of delayed cerebral infarction. *J Clin Neurol* 2017; 13: 32–7.
18. Wisse LEM, Biessels GJ, Stegenga BT, Kooistra M, Van Der Veen PH, Zwanenburg JJM, et al. Major depressive episodes over the course of 7 years and hippocampal subfield volumes at 7 tesla MRI: The PREDICT-MR study. *J Affect Disord* 2015; 175: 1–7.
19. Appelman APA, Van Der Graaf Y, Vincken KL, Tiehuis AM, Witkamp TD, Mali WPTMP, et al. Total cerebral blood flow, white matter lesions and brain atrophy: the SMART-MR study. *J Cereb Blood Flow Metab* 2008; 28: 633–9.
20. Blom K, Koek HL, Zwartbol MHT, Ghaznawi R, Kuijf HJ, Witkamp TD, et al. Vascular Risk Factors of Hippocampal Subfield Volumes in Persons without Dementia: The Medea 7T Study. *J Alzheimers Dis* 2020; 77: 1223–39.
21. McKhann G, Drachman D, Folstein M, Katzman R, Price D, Stadlan EM. Clinical diagnosis of Alzheimer's disease: report of the NINCDS-ADRDA Work Group under the auspices of Department of Health and Human Services Task Force on Alzheimer's Disease. *Neurology* 1984; 34: 939–44.
22. Petersen RC, Smith GE, Waring SC, Ivnik RJ, Tangalos EG, Kokmen E. Mild cognitive impairment: Clinical characterization and outcome. *Arch Neurol* 1999; 56: 303–8.

23. Wardlaw JM, Smith EE, Biessels GJ, Cordonnier C, Fazekas F, Frayne R, et al. Neuroimaging standards for research into small vessel disease and its contribution to ageing and neurodegeneration. *Lancet Neurol* 2013; 12: 822–38.
24. Gregoire SM, Chaudhary UJ, Brown MM, Yousry TA, Kallis C, Jäger HR, et al. The Microbleed Anatomical Rating Scale (MARS): Reliability of a tool to map brain microbleeds. *Neurology* 2009; 73: 1759–66.
25. Gaser C, Dahnke R. CAT-A computational anatomy toolbox for the analysis of structural MRI data. *BioRxiv* 2022.
26. Schmidt P, Gaser C, Arsic M, Buck D, Förchler A, Berthele A, et al. An automated tool for detection of FLAIR-hyperintense white-matter lesions in Multiple Sclerosis. *Neuroimage* 2012; 59: 3774–83.
27. Simons PCG, Algra A, Van De Laak MF, Grobbee DE, Van Der Graaf Y. Second manifestations of ARterial disease (SMART) study: Rationale and design. *Eur J Epidemiol* 1999; 15: 773–81.
28. Brand N, Jolles J. Learning and retrieval rate of words presented auditorily and visually. *J Gen Psychol* 1985; 112: 201–10.
29. Osterrieth P. Filetest de copie d'une figure complexe: contribution a l'etude de la perception et de la memoire [The test of copying a complex figure: a contribution to the study of perception and memory]. *Arch Psychol* 1944; 30: 286–356.
30. Robertson IH, Ward T, Ridgeway V, Nimmo-Smith I. The structure of normal human attention: The Test of Everyday Attention. *J Int Neuropsychol Soc* 1996; 2: 525–34.
31. Burgess PW, Shallice T. Bizarre responses, rule detection and frontal lobe lesions. *Cortex* 1996; 32: 241–59.
32. Wilkins AJ, Shallice T, McCarthy R. Frontal lesions and sustained attention. *Neuropsychologia* 1987; 25: 359–65.
33. Wechsler D. Wechsler Adult Intelligence Scale—Fourth Edition. 4th ed. San Antonio, TX: Pearson; 2008.
34. Lezak M, Howieson D, Loring D. Neuropsychological Assessment. 4th ed. New York: Oxford University Press; 2004.
35. Neuhaus JM, Jewell NP. A geometric approach to assess bias due to omitted covariates in generalized linear models. *Biometrika* 1993; 80: 807–15.
36. West RR, Evans DA. Lifestyle changes in long term survivors of acute myocardial infarction. *J Epidemiol Community Health* 1986; 40: 103–9.
37. Hilal S, Chai YL, van Veluw S, Shaik MA, Ikram MK, Venketasubramanian N, et al. Association between subclinical cardiac biomarkers and clinically manifest cardiac diseases with cortical cerebral microinfarcts. *JAMA Neurology* 2017; 74: 403–10.
38. Brundel M, Reijmer YD, van Veluw SJ, Kuijff HJ, Luijten PR, Kappelle LJ, et al. Cerebral microvascular lesions on high-resolution 7-Tesla MRI in patients with type 2 diabetes. *Diabetes* 2014; 63: 3523–9.
39. Arvanitakis Z, Leurgans SE, Barnes LL, Bennett DA, Schneider JA. Microinfarct pathology, dementia, and cognitive systems. *Stroke* 2011; 42: 722–7.
40. Longstreth WT, Sonnen JA, Koepsell TD, Kukull WA, Larson EB, Montine TJ. Associations between microinfarcts and other macroscopic vascular findings on neuropathologic examination in 2 databases. *Alzheimer Dis Assoc Disord* 2009; 23: 291–4.
41. Schneider JA, Arvanitakis Z, Bang W, Bennett DA. Mixed brain pathologies account for most dementia cases in community-dwelling older persons. *Neurology* 2007; 69: 2197–204.
42. De Reuck JL, Deramecourt V, Auger F, Durieux N, Cordonnier C, Devos D, et al. The significance of cortical cerebellar microbleeds and microinfarcts in neurodegenerative and cerebrovascular diseases. A post-mortem 7.0-tesla magnetic resonance study with neuropathological correlates. *Cerebrovasc Dis* 2015; 39: 138–43.
43. Dieleman N, van der Kolk AG, van Veluw SJ, Frijns CJM, Hartevelde AA, Luijten PR, et al. Patterns of intracranial vessel wall changes in relation to ischemic infarcts. *Neurology* 2014; 83: 1316–20.
44. Frackowiak RSJ, Pozzilli C, Legg NJ, Boulay GHD, Marshall J, Lenzi GL, et al. Regional cerebral oxygen supply and utilization in dementia: A clinical and physiological study with oxygen-15 and positron tomography. *Brain* 1981; 104: 753–78.
45. Wardlaw JM, Smith C, Dichgans M. Mechanisms of sporadic cerebral small vessel disease: Insights from neuroimaging. *Lancet Neurol* 2013; 12: 483–97.

Supplemental Table 1. Association between CMIs and cognitive functioning in subcohorts.

| | Medea-7T (n = 368) | SMART-MR (n = 213) | Memory clinics (n = 35) | General practice (n = 70) | PREDICT-MR (n = 50) |
|--|------------------------|-----------------------|----------------------------|------------------------------|------------------------|
| CMIs (%) | 9.5% | 13% | 13% | 3% | 1% |
| Global cognition (z-score) ^a | 0±1 | -0.04±1.00 | -1.15±1.11 | 0.34±1.04 | 0.48±0.93 |
| Executive functioning (z-score) ^a | 0±1 | -0.06±1.19 | -0.75±1.44 | 0.30±1.70 | 0.36±1.00 |
| Working memory (z-score) ^a | 0±1 | -0.02±1.00 | -0.42±0.88 | 0.25±1.08 | 0.04±0.87 |
| CMIs vs. global cognitive functioning (b, (95% CI)) ^b | -0.08 (-0.15 to -0.01) | -0.07 (-0.15 to 0.01) | -0.06 (-0.22 to 0.10) | N/A | N/A |
| CMIs vs. executive functioning (b, (95% CI)) ^b | -0.08 (-0.16 to 0.00) | -0.08 (-0.16 to 0.01) | -0.05 (-0.25 to 0.15) | N/A | N/A |
| CMIs vs. working memory (b, (95% CI)) ^b | -0.08 (-0.15 to -0.01) | -0.08 (-0.17 to 0.02) | -0.08 (-0.22 to 0.07) | N/A | N/A |

^a presented as mean ± standard deviation.

^b linear regression analysis with number of cortical cerebral microinfarcts (CMIs) as independent variable and cognitive domain as dependent variable, adjusted for age, sex and educational level.

N/A. No valid analyses possible due to low frequency of CMIs.



7

Microinfarcts in the deep gray matter on 7 tesla MRI: Risk factors, MRI correlates and relation to cognitive functioning. The SMART-MR study

Rashid Ghaznawi, Maarten H.T. Zwartbol, Jeroen de Bresser, Hugo J. Kuijf,
Koen L. Vincken, Ina Rissanen, Mirjam I. Geerlings, Jeroen Hendrikse, on behalf of
the UCC-SMART Study Group

Published in *American Journal of Neuroradiology* 2022; 43: 829-36
doi: 10.3174/ajnr.A7512

Abstract

The clinical relevance of cortical microinfarcts has recently been established, however studies on microinfarcts in the deep gray matter are lacking. We examined the risk factors and MRI correlates of microinfarcts in the deep gray matter on 7T MRI and their relation to cognitive functioning.

Within the SMART-MR study, 213 patients (68 ± 8 years) had risk factor assessment, a 7T and 1.5T brain MRI, and cognitive examination. Microinfarcts on 7T MRI were defined as lesions $< 5\text{mm}$. Regression models were used to examine the age-adjusted associations between risk factors, MRI markers and microinfarcts. Cognitive function was summarized as composite and domain-specific z-scores.

A total of 47 microinfarcts were found in 28 patients (13%), most commonly in the thalamus. Older age, history of stroke, hypertension and intima-media thickness were associated with microinfarcts. On 1.5T MRI, cerebellar infarcts ($RR = 2.75$, 95% CI: 1.4-5.33), lacunes in the white ($RR = 3.28$, 95% CI: 3.28-6.04) and deep gray matter ($RR = 3.06$, 95% CI: 1.75-5.35) were associated with microinfarcts, and on 7T MRI cortical microinfarcts ($RR = 2.33$, 95% CI: 1.32-4.13). Microinfarcts were also associated with poorer global cognitive functioning (mean difference in global z-score between patients with multiple microinfarcts vs. none = -0.97 , 95% CI: -1.66 to -0.28 , $p = 0.006$) and across all cognitive domains.

Microinfarcts in the deep gray matter on 7T MRI were associated with worse cognitive functioning and risk factors and MRI markers of small vessel and large vessel disease. Our findings suggest that microinfarcts in the deep gray matter may represent a novel imaging marker of vascular brain injury.

Introduction

Cerebral microinfarcts are a common neuropathological finding in older individuals.¹⁻³ Conventionally, they are defined as small ischemic lesions that are not visible to the naked eye on gross pathology and can range from 100 μm to a few mm in size.² Although small, microinfarcts often occur in large numbers and their effect is thought to extend well beyond their lesion boundaries.^{2,4} Associations with cognitive impairment and dementia have been reported, and microinfarcts may play an important role in silent cerebrovascular disease.⁴

Recently, cortical microinfarcts have been identified *in vivo* using 7T MRI.² Subsequent neuroimaging studies reported that the causes of cortical microinfarcts are heterogeneous, and their occurrence has been associated with both small vessel and large vessel disease, microemboli and hypoperfusion.⁵⁻⁸ The clinical importance of cortical microinfarcts has been demonstrated by their association with worse cognitive functioning.⁹ *In vivo* data on the prevalence and risk factors of microinfarcts in the deep gray matter, however, is lacking. Moreover, it is not known to what extent microinfarcts in the deep gray matter are related to cognitive functioning. Previous histopathologic studies reported that microinfarcts as well as lacunes in the deep gray matter were associated with worse antemortem cognitive performance.¹⁰⁻¹² Identifying the risk factors and MRI markers associated with microinfarcts in the deep gray matter is of importance as these may provide clues to their underlying etiology and may provide potential targets for intervention. Examining the association with cognitive functioning is important as it will provide evidence whether microinfarcts in the deep gray matter are structural correlates of impaired cognitive performance.

In the current study, we examined the frequency and distribution of microinfarcts in the caudate nucleus, lentiform nucleus and thalamus on 7T MRI in a large sample of older persons with a history of arterial disease. In addition, we examined whether microinfarcts in the deep gray matter were associated with risk factors, MRI markers of cerebrovascular disease and cognitive functioning.

Methods

Study population

Data were used from the Second Manifestations of ARterial disease-Magnetic Resonance (SMART-MR) study, a prospective cohort study at the University Medical Center Utrecht with the aim to investigate risk factors and consequences of brain changes on MRI in patients with symptomatic atherosclerotic disease.¹³ In brief, between 2001 and 2005, 1309 middle-aged and older adult persons newly referred to the University Medical Center Utrecht for treatment of symptomatic atherosclerotic disease (coronary artery disease,

cerebrovascular disease, peripheral arterial disease or abdominal aortic aneurysm) were included for baseline measurements. During a one-day visit to our medical center, a physical examination, ultrasonography of the carotid arteries to measure the intima-media thickness (mm), blood and urine samplings, neuropsychological assessment and a 1.5T brain MRI scan were performed. The height and weight were measured, and the body mass index (kg/m^2) was calculated. Questionnaires were used for the assessment of demographics, risk factors, medical history, medication use and cognitive and physical functioning.

Of the 1309 persons included, 754 had follow-up measurements after an average of four years between January 2006 and May 2009. From November 2013, all patients alive were invited for a second follow-up, including a 7T brain MRI. Of the 329 persons included between November 2013 and October 2017, 213 had a 7T MRI scan and these patients formed the current study sample. A participation flowchart of the SMART-MR study is shown in Supplementary Figure 1.

In the present study, we used the 1.5T brain MRI, cognitive functioning and vascular risk factor data obtained during follow-up. Due to logistic reasons, however, the 1.5T brain MRI and cognitive function measurements were obtained prior to the 7T brain MRI in 97 patients (median 1.5 years; range 0.6-2.7 years), whereas in 116 patients these examinations were obtained on the same day. Also, vascular risk factor assessment was performed prior to the 7T brain MRI in 163 patients (median 2.3 years; range 0.6-9.4 years), whereas in 50 patients vascular risk factors were obtained concurrently with the 7T brain MRI.

The SMART-MR study was approved by the medical ethics committee of the University Medical Center Utrecht according to the guidelines of the Declaration of Helsinki of 1975 and written informed consent was obtained from all patients.

Vascular risk factors

Baseline smoking habits and alcohol intake were assessed with questionnaires. Packyears of smoking was calculated and alcohol intake was categorized as 'no or <1 unit per week', '1-10 units per week', and '≥11 units per week'. Height and weight were measured, and the body mass index (BMI) was calculated (kg/m^2). Systolic blood pressure (SBP) (mmHg) and diastolic blood pressure (DBP) (mmHg) were measured three times with a sphygmomanometer, and the average of these measures was calculated. Hypertension was defined as a mean SBP of > 140 mmHg, a mean DBP of > 90 mmHg or self-reported use of antihypertensive drugs. An overnight fasting venous blood sample was taken to determine glucose, lipids, total homocysteine and apolipoprotein-B levels. Diabetes mellitus was defined as fasting serum glucose levels of ≥ 7.0 mmol/l, and/or use of glucose-lowering medication, and/or a known history of diabetes. Hyperlipidemia was considered if the serum cholesterol was ≥5.0 mmol/l, a low-density lipoprotein cholesterol of >3.2 mmol/l, or if the patient was using lipid lowering medication. History of stroke was based on a composite scoring made of neurologist-verified self-reported symptoms of previous stroke, previous

history of carotid artery operation, or a physician diagnosis at study inclusion of the following conditions: transient ischemic attack, brain infarct, ischemic stroke, cerebral ischemia, amaurosis fugax or retinal infarction. Mean carotid intima-media thickness (in mm) was calculated for the left and right common carotid arteries based on six far-wall measurements on ultrasound. Ankle brachial index measurements were made using a Vasoguard Doppler probe (8 MHz) and measurement techniques have been described in detail elsewhere.¹⁴ Metabolic syndrome was determined by the National Cholesterol Education Program Adult Treatment Panel III criteria.¹⁵ Genotyping for apolipoprotein-E (Apo-E) was performed on coded DNA specimens and has been described in detail elsewhere.¹⁶

MRI protocol

High-field imaging of the brain was performed on a whole-body 7T MR system (Philips Healthcare, Cleveland, OH, USA) with a volume transmit and 32-channel receive head coil (Nova Medical, Wilmington, MA, USA). The standardized scan protocol is described in detail in previous publications.^{17, 18}

Conventional MR imaging of the brain was performed on a 1.5T whole-body system (Gyrosan ACS-NT, Philips Medical Systems, Best, the Netherlands) using a standardized scan protocol described in detail in previous work.^{13, 19}

Assessment of MRI markers of cerebrovascular disease

Brain infarcts (cortical, cerebellar or brain stem), lacunes of presumed vascular origin, and white matter hyperintensity (WMH) and brain volumes were determined using 1.5T MRI data. Cortical microinfarcts and cerebral microbleeds were rated on 7T MRI data due to the enhanced conspicuity of these lesions at higher field strengths.^{18, 20} All ratings were performed blinded to patient characteristics.

Brain infarcts (cortical, cerebellar or brainstem) and lacunes were visually rated by an experienced rater (MHTZ) with 6 years of experience in neuroradiology on the T1-weighted, T2-weighted and FLAIR images of the 1.5T MRI scans. Lacunes were rated according to the STRIVE criteria as round or ovoid, subcortical, fluid-filled cavities (signal similar to cerebrospinal fluid) of 3-15mm in diameter, in the territory of one perforating arteriole.²¹ Uncertain lesions were discussed during a consensus meeting (MHTZ) to reach agreement.

WMH and brain volumes were obtained using an automated segmentation program on the T1-weighted, FLAIR, and T1-weighted inversion recovery sequences of the 1.5T MR scans. A probabilistic segmentation technique was performed with *k*-nearest neighbor classification distinguishing gray matter, white matter, cerebrospinal fluid and lesions.²² Brain infarcts, including lacunes and their hyperintense rim, were manually segmented. All WMH segmentations were visually checked by an investigator (RG) using an image processing framework (MeVisLab 2.7.1., MeVis Medical Solutions AG, Bremen, Germany) to ensure that brain infarcts were correctly removed from the WMH segmentations.

Periventricular WMH were defined as adjacent to or within 1 cm of the lateral ventricles and deep WMH were defined as located in the deep white matter tracts that may or may not have adjoined periventricular WMH. Total brain volume was calculated by summing the volumes of gray matter, white matter, total WMH and, if present, the volumes of brain infarcts. Total intracranial volume (ICV) was calculated by summing the cerebrospinal fluid volume and total brain volume.

Phase-contrast MR angiography was used to measure total cerebral blood flow, as this method has been demonstrated to be a fast, reproducible, and noninvasive method to measure total cerebral blood flow in large cohorts.²³ Previous studies established that phase-contrast MR angiography correlates well with arterial spin-labeled perfusion MRI, although estimates tend to be somewhat higher and more variable than arterial spin-labeled perfusion MRI.²⁴ Post-processing of the cerebral blood flow measurements was performed by one investigator (MHTZ). The flow through the basilar artery and the left and right internal carotid arteries was summed to calculate the total cerebral blood flow (ml/min). Total cerebral blood flow was expressed per 100 ml brain parenchymal volume to obtain parenchymal cerebral blood flow (pCBF).

Cortical microinfarcts were visually rated by a rater (MHTZ) on the 3D T1-weighted, 3D T2-weighted and 3D FLAIR sequences of the 7T MRI scans according to criteria previously described.² Cerebral microbleeds were rated by a rater (MHTZ) using the minimum intensity projection images and source images of the 7T SWI sequence. Microbleeds were labeled as lobar or deep using the Microbleed Anatomical Rating Scale.²⁵

We considered cortical, cerebellar and brain stem infarcts rated on 1.5T MRI as markers of large vessel disease²⁶, whereas lacunes of presumed vascular origin, white matter hyperintensities and microbleeds were considered markers of small vessel disease, consistent with the STRIVE criteria.²¹

Assessment of cognitive functioning

All patients underwent neuropsychological assessment for memory, executive functioning, information processing speed and working memory.

Memory was assessed with the 15 Word Learning Test using a composite score of the immediate and delayed recall based on five trials, and the Rey-Osterrieth Complex figure test.^{27, 28} Executive functioning was assessed with the Verbal Fluency test using animals as categories (2 minutes) and the letter A (1 minute); the Visual Elevator test (10 trials), and the Brixton Spatial Anticipation test.²⁹⁻³¹ Working memory was assessed with the combined longest span scores and total span scores of the Forward Digit Span and Backward Digit Span.³² Processing speed was assessed with the Digit Symbol Substitution Test (120 seconds).³³

Domain-specific z scores were calculated by converting raw test scores to standardized z scores and averaging these for each domain prior to the final z transformation. A global cognitive functioning composite z score was calculated by standardizing the averaged domain-specific z scores.

Assessment of microinfarcts in the deep gray matter

First, all available 7T MRI scans were screened by an experienced neuroradiologist. All lesions hypointense on T1-weighted images, hyperintense on T2-weighted images, and either hyperintense or hypointense with a hyperintense rim on FLAIR images consistent with the imaging criteria set forth in our previous work¹⁸ were rated as possible microinfarcts. The lesions were restricted to the caudate nucleus, lentiform nucleus or thalamus and not appearing as a perivascular space, artery, vein or microbleed on the SWI sequence. In addition, the lesion had to be detectable in the axial, coronal, and sagittal views. Uncertain lesions were discussed during a consensus meeting to reach agreement. Next, all identified possible microinfarcts were inspected by an investigator (RG) using MR imaging software and the largest diameter of each lesion was determined on the FLAIR sequence. Lesions <5mm in their largest diameter were accepted as microinfarcts as this value has been suggested by previous studies on cortical microinfarcts.^{6, 34-38} Presence and number of lesions ≥5mm in the deep gray matter were also recorded as these may act as potential confounders in the relation between microinfarcts and cognitive functioning.

Statistical analysis

First, vascular risk factors and MRI markers of cerebrovascular disease were calculated of patients with and without microinfarcts in the deep gray matter on 7T MRI, and of the entire study sample. Second, relative risks for presence of microinfarcts in the deep gray matter were estimated for vascular risk factors and MRI markers of cerebrovascular disease using log-binomial regression, adjusted for age. For continuous variables, a relative risk for presence of microinfarcts was estimated for one standard deviation increase. For dichotomous variables, a relative risk for microinfarcts was calculated for presence of a vascular risk factor or MRI marker. Third, to examine the association between microinfarcts in the deep gray matter and cognitive functioning, analysis of covariance (ANCOVA) was used to estimate age and education level adjusted cognitive functioning z scores for patients without microinfarcts, with a single microinfarcts and with multiple microinfarcts. Age and education level were entered as covariates as these represent the most important potential confounders in the relation between microinfarcts and cognitive functioning.

We repeated the abovementioned analyses with additional adjustment for number of infarcts ≥5mm in the deep gray matter on 7T MRI. Statistical significance was set at a *p* value of <0.05.

Results

A total of 47 deep gray matter microinfarcts (caudate nucleus; $n = 17$, lentiform nucleus; $n = 9$, thalamus; $n = 21$) were identified in 28 patients on 7T MRI (range 1-6 microinfarcts). A single microinfarct was seen in 19 patients (68%), while multiple microinfarcts were seen in 9 patients (32%). Size of microinfarcts ranged from 2.1 to 4.8mm (caudate nucleus; 2.1 to 4.7mm, lentiform nucleus; 2.7 to 4.1mm, thalamus; 2.4 to 4.8mm). Of patients with microinfarcts ($n = 28$), twelve patients (42%) also showed infarcts ≥ 5 mm in the deep gray matter on 7T MRI (Table 1). Examples of deep gray matter microinfarcts are shown in Figure 1. Twenty-six patients showed a total of 33 infarcts ≥ 5 mm in the deep gray matter on 7T MRI, ranging from 6.7 to 15.7mm in size (Table 1). Of these 33 lesions, 18 (55%) were rated as lacunes in the deep gray matter on the corresponding 1.5T MRI scans.

Baseline characteristics and MRI markers of patients with microinfarcts in the deep gray matter ($n = 28$), those without microinfarcts ($n = 185$) and in the total study sample ($n = 213$) are shown in Tables 2 and 3, respectively.

Compared to baseline (2001-2005) characteristics of patients without a 7T brain MRI, patients in the study sample with a 7T brain MRI were younger, had more often current alcohol intake, less often diabetes mellitus, and showed a slightly lower intima-media thickness and a slightly higher ankle brachial index (Supplementary Table 1).

Vascular risk factors

Higher age was associated with presence of microinfarcts in the deep gray matter (RR per year increase = 1.05, 95% CI: 1.02 to 1.08, $p = 0.001$). In addition, after adjusting for age, a history of stroke (RR=2.88, 95% CI: 1.24 to 6.67, $p = 0.01$), hypertension (RR=3.16, 95% CI: 1.30 to 7.65, $p = 0.01$) and a higher intima-media thickness (RR per 1 SD increase = 1.29, 95% CI: 1.04 to 1.61, $p = 0.02$) were associated with microinfarcts. Number of smoking pack years (RR per SD increase = 1.11, 95% CI: 0.87 to 1.42, $p = 0.40$), carotid artery stenosis $\geq 50\%$ (RR = 1.39, 95% CI: 0.70 to 2.75, $p = 0.34$) and presence of metabolic syndrome (RR = 1.47, 95% CI: 0.74 to 2.91, $p = 0.27$) were not significantly associated with presence of microinfarcts in the deep gray matter after adjusting for age (Table 2).

After additionally adjusting for number of infarcts ≥ 5 mm in the deep gray matter on 7T MRI, higher age (RR per year increase = 1.04, 95% CI: 1.01 to 1.07, $p = 0.01$) and hypertension (RR = 5.25, 95% CI: 1.43 to 19.28, $p = 0.01$) remained associated with microinfarcts, whereas a history of stroke (RR = 2.37, 95% CI: 0.94 to 5.79, $p = 0.07$) and a higher intima-media thickness (RR per 1 SD increase = 1.25, 95% CI: 0.98 to 1.57, $p = 0.07$) lost statistical significance.

MRI markers of cerebrovascular disease

For cerebrovascular markers on 1.5T MRI, cerebellar infarcts (RR = 2.18, 95% CI: 1.23 to 3.87, $p = 0.008$), lacunes in the white matter (RR = 3.28, 95% CI: 1.79 to 6.04, $p < 0.0001$) and lacunes in the deep gray matter (RR = 3.93, 95% CI: 1.99 to 7.78, $p < 0.0001$) were associated



Figure 1. Examples of microinfarcts in the deep gray matter on 7T MRI. A: Microinfarct with a diameter of 2.3 mm (arrow) in the left thalamus of a 73-year-old female on transversal 7T FLAIR. B: Microinfarct with a diameter of 2.9 mm (arrow) in the left caudate nucleus of a 64-year-old male on sagittal 7T FLAIR. C: Two microinfarcts with diameters of 3.0 mm and 3.2 mm (arrows) in the left putamen of a 65-year-old male on coronal 7T FLAIR. Note that the gliotic rim extends into the adjacent external capsule.

Table 1. Frequency of patients with microinfarcts and with infarcts $\geq 5\text{mm}$ in the deep gray matter on 7T MRI.

| Microinfarct (<5mm) | Infarct $\geq 5\text{mm}$ | | |
|---------------------|---------------------------|-----|-------|
| | No | Yes | Total |
| No | 171 | 14 | 185 |
| Yes | 16 | 12 | 28 |
| Total | 187 | 26 | 213 |

with presence of microinfarcts in the deep gray matter, after adjusting for age. For cerebrovascular markers on 7T MRI, cortical microinfarcts (RR = 2.33, 95% CI: 1.32 to 4.13, $p = 0.004$) were associated with microinfarcts in the deep gray matter after adjusting for age. Although the RR was increased, cortical infarcts (RR = 1.64, 95% CI: 0.76 to 3.51, $p = 0.21$), brainstem infarcts (RR = 3.37, 95% CI: 0.95 to 12.0, $p = 0.07$) and periventricular WMH volume (RR per SD increase = 1.14, 95% CI: 0.95 to 1.37, $p = 0.16$) on 1.5T MRI were not significantly associated with presence of microinfarcts in the deep gray matter after adjusting for age. Deep microbleeds (RR = 1.60, 95% CI: 0.70 to 3.68, $p = 0.27$) and lobar microbleeds (RR = 1.27, 95% CI: 0.59 to 2.72, $p = 0.54$) on 7T MRI were also not significantly associated with microinfarcts in the deep gray matter after adjusting for age (Table 3).

After additionally adjusting for number of infarcts $\geq 5\text{mm}$ in the deep gray matter on 7T MRI, lacunes in the white matter on 1.5T MRI (RR = 2.76, 95% CI: 1.45 to 5.27, $p = 0.002$), cerebellar infarcts on 1.5T MRI (RR = 2.05, 95% CI: 1.13 to 3.73, $p = 0.02$) and cortical microinfarcts on 7T MRI (RR = 2.16, 95% CI: 1.20 to 3.90, $p = 0.01$) remained associated with microinfarcts.

Table 2. Association of vascular risk factors and presence of microinfarcts in the deep gray matter on 7T MRI.

| | Patients with microinfarcts in the deep gray matter (n = 28) | Patients without microinfarcts in the deep gray matter (n = 185) | All patients (n = 213) | Microinfarct (presence vs. absence) RR (95% CI) ^a |
|---------------------------------|--|--|------------------------|--|
| Age (years) | 70 ± 7 | 64 ± 9 | 64 ± 9 | 1.05 (1.02 to 1.08) ^{b*} |
| Sex, % men | 85.7 | 82.2 | 82.6 | 0.78 (0.30 to 2.02) ^c |
| History of stroke, % | 50.0 | 23.2 | 26.8 | 2.88 (1.24 to 6.67) [*] |
| BMI (kg/m ²) | 28 ± 4 | 27 ± 4 | 27 ± 4 | 1.20 (0.87 to 1.65) |
| Smoking, packyears ^d | 27 (0, 56) | 20 (0, 47) | 22 (0, 49) | 1.11 (0.87 to 1.42) |
| Alcohol intake | | | | |
| No or <1 unit/week, % | 22.2 | 26.5 | 25.9 | 1 (reference) |
| 1–10 units/week, % | 59.3 | 41.1 | 43.4 | 1.55 (0.67 to 3.61) |
| ≥11 units/week, % | 18.5 | 32.4 | 30.7 | 0.65 (0.22 to 1.98) |
| Hypertension, % | 96.4 | 72.4 | 75.6 | 3.16 (1.30 to 7.65) [*] |
| Diabetes mellitus, % | 14.3 | 16.2 | 16.0 | 0.85 (0.32 to 2.21) |
| Carotid stenosis ≥50%, % | 17.9 | 7.6 | 8.9 | 1.39 (0.70 to 2.75) |
| Hypercholesterolemia, % | 77.8 | 86.4 | 85.3 | 1.33 (0.86 to 2.05) |
| IMT (mm) | 1.0 ± 0.3 | 0.8 ± 0.2 | 0.9 ± 0.2 | 1.29 (1.04 to 1.61) [*] |
| ABI | 1.1 ± 0.2 | 1.1 ± 0.1 | 1.1 ± 0.2 | 0.86 (0.67 to 1.11) |
| Homocysteine (μmol/l) | 13.0 ± 5.2 | 12.5 ± 4.3 | 12.5 ± 4.4 | 1.07 (0.40 to 2.82) |
| Apo-B (g/l) | 0.8 ± 0.2 | 0.8 ± 0.2 | 0.8 ± 0.2 | 0.84 (0.58 to 1.23) |
| Metabolic syndrome, % | 60.7 | 51.4 | 52.6 | 1.47 (0.74 to 2.91) |
| ≥1 Apo-E ε4 allele, % | 35.7 | 28.1 | 29.1 | 1.58 (0.79 to 3.20) |

Characteristics are presented as mean ± SD or %. RR represents the relative risk for microinfarcts in the presence of a risk factor (in case of a dichotomous variable) or for 1 SD increase in the risk factor (in case of a continuous variable).

^a Log-binomial regression with adjustment for age.

^b Per year increase.

^c Men vs. women.

^d Median (10th percentile, 90th percentile). Natural log-transformed due to a non-normal distribution in the analysis.

**p* < 0.05

BMI: body mass index; LDL: low density lipoprotein; HDL: high density lipoprotein; IMT: intima-media thickness; ABI: ankle brachial index; Apo-B: apolipoprotein B; Apo-E: apolipoprotein E; SD: standard deviation; CI: confidence interval.

Table 3. Association of MRI markers of cerebrovascular disease and presence of microinfarcts in the deep gray matter on 7T MRI.

| | Patients with microinfarcts in the deep gray matter (n = 28) | Patients without microinfarcts in the deep gray matter (n = 185) | All patients (n = 213) | Microinfarct (presence vs. absence) RR (95% CI) ^a |
|---|--|--|------------------------|--|
| Infarcts on 1.5T MRI, % | | | | |
| Cortical | 21 | 11 | 12 | 1.64 (0.76 to 3.51) |
| Cerebellar | 32 | 9 | 12 | 2.18 (1.23 to 3.87)* |
| Brainstem | 7 | 1 | 2 | 3.37 (0.95 to 12.0) |
| Lacunes in the white matter on 1.5T MRI, % | 32 | 6 | 9 | 3.28 (1.79 to 6.04)* |
| Lacunes in the deep gray matter on 1.5T MRI, % | 43 | 8 | 12 | 3.93 (1.99 to 7.78)* |
| WMH volumes on 1.5T MRI, ml ^b | | | | |
| Total | 3.3 (0.9, 32.5) | 2.0 (0.3, 9.3) | 2.0 (0.4, 10.0) | 1.13 (0.93 to 1.38) ^c |
| Periventricular | 2.9 (0.7, 31.7) | 1.4 (0.2, 8.3) | 1.4 (0.3, 9.0) | 1.14 (0.95 to 1.37) ^c |
| Deep | 0.2 (0.1, 0.9) | 0.3 (0.0, 1.5) | 0.2 (0.0, 1.4) | 0.67 (0.38 to 1.16) ^c |
| Total brain volume, ml | 1104.9 ± 116.5 | 1125.3 ± 104.3 | 1122.7 ± 105.9 | 0.84 (0.56 to 2.72) ^d |
| Total intracranial volume, ml | 1449.2 ± 114.7 | 1452.6 ± 126.4 | 1452.16 ± 128.5 | 1.21 (0.85 to 1.73) |
| Parenchymal CBF, ml/min per 100 ml brain volume | 50.5 ± 16.8 | 48.2 ± 12.0 | 48.5 ± 12.7 | 1.13 (0.93 to 1.38) |
| Cortical microinfarcts on 7T MRI, % | 32 | 9 | 12 | 2.33 (1.32 to 4.13)* |
| Deep microbleeds on 7T MRI, % | 21 | 10 | 12 | 1.60 (0.70 to 3.68) |
| Lobar microbleeds on 7T MRI, % | 36 | 26 | 27 | 1.27 (0.59 to 2.72) |

Characteristics are presented as mean ± SD or %. RR represents the relative risk for microinfarcts in the presence of an MRI marker (in case of a dichotomous variable) or for 1 SD increase in the MRI marker (in case of a continuous variable).

^a Log-binomial regression with adjustment for age.

^b Median (10th percentile, 90th percentile).

^c Natural log-transformed due to a non-normal distribution and normalized for total intracranial volume.

^d Adjusted for age and total intracranial volume.

**p* < 0.05

WMH: white matter hyperintensity; CBF: cerebral blood flow; SD: standard deviation; CI: confidence interval

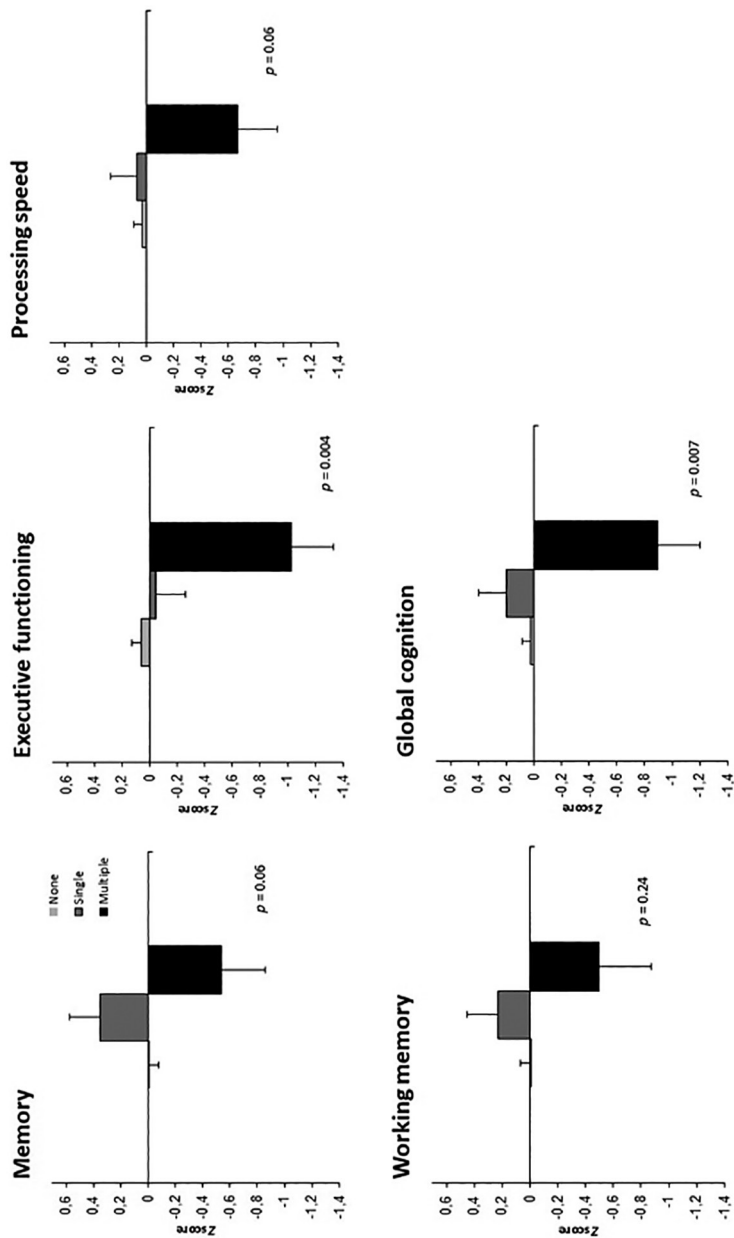


Figure 2. Association between microinfarcts in the deep gray matter and global and domain-specific cognitive functioning z-scores. Values are mean \pm standard error z-scores, adjusted for age and educational level. Memory: none; -0.01 ± 0.07 , single; 0.35 ± 0.22 , multiple; -0.54 ± 0.32 . Executive functioning: none; 0.05 ± 0.07 , single; -0.05 ± 0.21 , multiple; -1.02 ± 0.31 . Processing speed: none; 0.02 ± 0.06 , single; 0.07 ± 0.20 , multiple; -0.67 ± 0.29 . Working memory: none; -0.01 ± 0.07 , single; 0.22 ± 0.22 , multiple; -0.50 ± 0.37 . Global cognition: none; 0.02 ± 0.06 , single; 0.20 ± 0.20 , multiple; -0.90 ± 0.30 .

Cognitive functioning

Global cognitive functioning z scores differed significantly between patients without (n = 185), with a single (n = 19) and with multiple microinfarcts (n = 9) in the deep gray matter (ANCOVA $p = 0.007$), adjusted for age and education level. Specifically, presence of multiple microinfarcts in the deep gray matter was associated with worse global cognitive functioning compared to absence of microinfarcts or presence of a single microinfarct (mean difference in z-score = -0.92, 95% CI: -1.53 to -0.31, $p = 0.003$; -1.10, 95% CI: -1.81 to -0.39, $p = 0.002$, respectively). This pattern was observed for each cognitive domain. The mean estimates of domain-specific z-scores were lower for patients with multiple microinfarcts compared to patients with none or a single microinfarct for memory, executive functioning, information processing speed and working memory (Figure 2).

After additionally adjusting for number of infarcts $\geq 5\text{mm}$ in the deep gray matter on 7T MRI, the association between microinfarcts and global cognitive functioning persisted (ANCOVA $p = 0.01$; mean difference in z-score between patients with multiple microinfarcts versus none = -0.97, 95% CI: -1.66 to -0.28, $p = 0.006$; versus a single microinfarct = -1.13, 95% CI: -1.88 to -0.39, $p = 0.003$).

Discussion

In this cohort of patients with a history of arterial disease, microinfarcts in the deep gray matter on 7T MRI were detected in 13% of patients. These lesions were associated with older age, a history of stroke, hypertension and a higher intima-media thickness. With regard to MRI markers, they were associated with lacunes and cerebellar infarcts on 1.5T MRI, and with cortical microinfarcts on 7T MRI. Presence of multiple microinfarcts in the deep gray matter was associated with worse global cognitive functioning independent of age, education level and number of infarcts $\geq 5\text{mm}$.

We previously reported that small infarcts in the caudate nucleus on 7T MRI can be detected with excellent intra-rater and inter-rater agreement, and that the imaging characteristics of these lesions are similar to those in the cerebral cortex.¹⁸ The present study extends our previous findings and emphasizes the potential clinical importance of these lesions, which is in accordance with autopsy studies that reported associations between microinfarcts in the deep gray matter and ante-mortem cognitive impairment.^{10, 12} In addition, we found that the majority of patients with microinfarcts in the deep gray matter did not show larger infarcts in the deep gray matter on 7T MRI and, importantly, that the relationship between microinfarcts and worse global cognitive functioning was independent of infarcts $\geq 5\text{mm}$. These findings suggest that microinfarcts in the deep gray matter are structural correlates of impaired cognitive functioning that are largely undetected on conventional MRI.¹

The association between microinfarcts and worse cognitive functioning may be explained by the important role that the basal ganglia play in cognition through receiving and processing cortical information in the caudate and lentiform nuclei and sending information back to the cerebral cortex through the thalamus.^{39, 40} Damage to this neuronal network may compromise cognition.⁴¹ However, we did not find significant differences in cognition between patients without microinfarcts and patients with a single microinfarct, suggesting that the impact of a single microinfarct on cognition may be weak, contrary to the presence of multiple lesions. A possible explanation is that the damage associated with a single microinfarct is insufficient to affect neural network integrity and therefore result in lower cognitive performance, whereas this may be the case for multiple microinfarcts. Alternatively, it may be that patients with multiple microinfarcts are also more likely to have smaller lesions that are not discernible on 7T MRI.⁴²

The associations of microinfarcts in the deep gray matter with older age, hypertension, a higher intima-media thickness, lacunes and cerebellar infarcts suggest that small vessel and large vessel disease may be involved in the pathogenesis of these lesions. Support for this notion is provided by a large postmortem study in which atherosclerosis and arteriolosclerosis were associated with subcortical microinfarcts.⁴³ However, as the *in vivo* associations presented in this study are novel, further studies in different populations are needed to identify risk factors of microinfarcts that may pose potential targets for intervention.

Strengths of our study include the large sample size for a 7T MRI study and the detailed information available on vascular risk factors, MRI markers of cerebrovascular disease and cognitive functioning that enabled us to examine these relationships within one study. A limitation of this study is that microinfarcts in the deep gray matter, cortical microinfarcts and microbleeds were rated on 7T MRI data whereas other MRI markers were evaluated on 1.5T MRI data. Several remarks have to be made with respect to this matter. First, we obtained brain volumes from 1.5T MRI data due to a lack of robust and validated brain segmentation software for 7T MRI data. Second, cerebral blood flow measurements were obtained from 1.5T MRI data because our standardized 7T MRI protocol did not contain phase contrast sequences. Third, it should be noted that the greatest added value of ultra-high field 7T MRI lies in its ability to visualize the smallest cerebrovascular lesions (i.e., microinfarcts and microbleeds) due to the higher signal-to-noise ratio compared to conventional 1.5T MRI. Although it would be preferable to determine all cerebrovascular lesions on the 7T MRI scans for consistency, it is unlikely that 7T MRI yields a greater detection rate for larger lesions such as cortical infarcts. Another limitation is the potential overlap that may occur between microinfarcts and lacunes of presumed vascular origin in the deep gray matter. According to the STRIVE criteria, lacunes of presumed vascular origin are defined as small subcortical infarcts ranging from 3 to 15mm in size.²¹ As microinfarcts were previously defined as lesions <5mm, it is possible

that larger microinfarcts in the range of 4mm may have been classified as lacunes on 1.5T MRI. The potential overlap however was limited as the majority of patients with microinfarcts did not show lacunes in the deep gray matter on 1.5T MRI. In addition, we controlled for the effects of infarcts $\geq 5\text{mm}$ in the analyses. Another possible limitation of this study is that the sample consisted of patients who completed two follow-up measurements and these patients represent a slightly healthier subset. This may have led to an underestimation of the association of microinfarcts with vascular risk factors, MRI markers of cerebrovascular disease and cognitive functioning. A further limitation of this study is that in some patients the 7T brain MRI did not coincide with the 1.5T brain MRI, cognitive function measurements and vascular risk factor assessment. Especially for the vascular risk factor assessment the interval was quite large in some patients. Due to logistical reasons, we were not able to repeat the measurement of vascular risk factors at the time of the brain MRI and cognitive assessment in these patients, which may have under- or overestimated the associations. However, in a previous analysis⁴⁴ we did not see major changes in the relationship with 7T MRI outcomes when adjusting for the time interval between vascular risk factor assessment and 7T brain MRI.

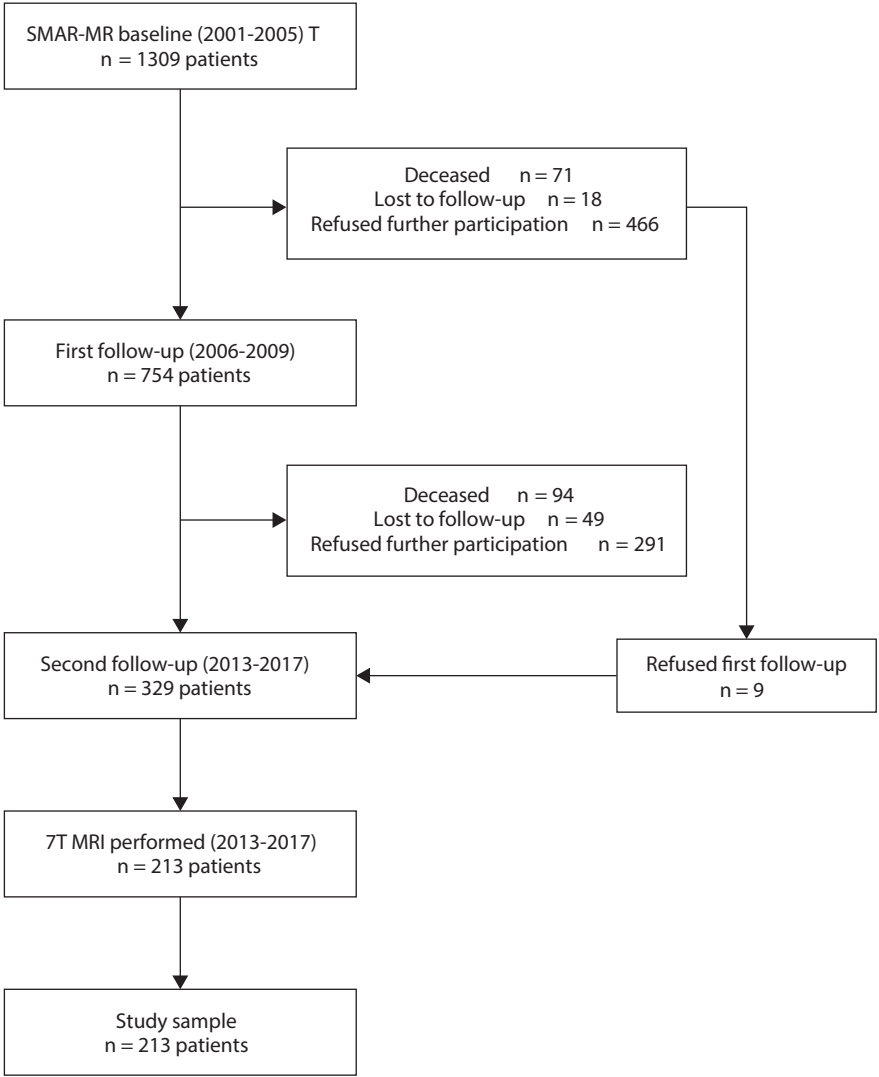
Conclusions

Our findings demonstrate that microinfarcts in the deep gray matter on 7T MRI are associated with worse cognitive functioning and vascular risk factors and MRI markers of small vessel and large vessel disease in patients with a history of arterial disease. These results suggest that microinfarcts in the deep gray matter may be relevant imaging markers of vascular brain injury that, together with cortical microinfarcts, could be a potential target for future prevention strategies of vascular cognitive impairment.

References

1. Smith EE, Schneider JA, Wardlaw JM, Greenberg SM. Cerebral microinfarcts: the invisible lesions. *Lancet Neurol* 2012; 11:272–82.
2. van Veluw SJ, Shih AY, Smith EE, Chen C, Schneider JA, Wardlaw JM, et al. Detection, risk factors, and functional consequences of cerebral microinfarcts. *Lancet Neurol* 2017; 16: 730–40.
3. Brundel M, de Bresser J, van Dillen JJ, Kappelle LJ, Biessels GJ. Cerebral microinfarcts: a systematic review of neuropathological studies. *J Cereb Blood Flow Metab* 2012; 32: 425–36.
4. Summers PM, Hartmann DA, Hui ES, Nie X, Deardorff RL, McKinnon ET, et al. Functional deficits induced by cortical microinfarcts. *J Cereb Blood Flow Metab* 2017; 37: 3599–614.
5. Wang Z, van Veluw SJ, Wong A, Liu W, Shi L, Yang J, et al. Risk Factors and Cognitive Relevance of Cortical Cerebral Microinfarcts in Patients With Ischemic Stroke or Transient Ischemic Attack. *Stroke* 2016; 47: 2450–5.
6. van Dalen JW, Sciric EE, van Veluw SJ, Caan MW, Nederveen AJ, Biessels GJ, et al. Cortical microinfarcts detected in vivo on 3 Tesla MRI: clinical and radiological correlates. *Stroke* 2015; 46: 255–7.
7. van Veluw SJ, Hilal S, Kuijff HJ, Ikram MK, Xin X, Yeow TB, et al. Cortical microinfarcts on 3T MRI: Clinical correlates in memory-clinic patients. *Alzheimers Dement* 2015; 11: 1500–9.
8. Hilal S, Chai YL, van Veluw S, Shaik MA, Ikram MK, Venketasubramanian N, et al. Association Between Subclinical Cardiac Biomarkers and Clinically Manifest Cardiac Diseases With Cortical Cerebral Microinfarcts. *JAMA Neurology* 2017; 74: 403–10.
9. Hilal S, Sikking E, Shaik MA, Chan QL, van Veluw SJ, Vrooman H, et al. Cortical cerebral microinfarcts on 3T MRI: A novel marker of cerebrovascular disease. *Neurology* 2016; 87: 1583–90.
10. Troncoso JC, Zonderman AB, Resnick SM, Crain B, Pletnikova O, O'Brien RJ. Effect of infarcts on dementia in the Baltimore longitudinal study of aging. *Ann Neurol* 2008; 64: 168–76.
11. Gold G, Kovari E, Herrmann FR, Canuto A, Hof PR, Michel JP, et al. Cognitive consequences of thalamic, basal ganglia, and deep white matter lacunes in brain aging and dementia. *Stroke* 2005; 36: 1184–8.
12. White L, Petrovitch H, Hardman J, Nelson J, Davis DG, Ross GW, et al. Cerebrovascular pathology and dementia in autopsied Honolulu-Asia Aging Study participants. *Ann N Y Acad Sci* 2002; 977: 9–23.
13. Geerlings MI, Appelman AP, Vincken KL, Algra A, Witkamp TD, Mali WP, van der Graaf Y. Brain volumes and cerebrovascular lesions on MRI in patients with atherosclerotic disease. The SMART-MR study. *Atherosclerosis* 2010; 210: 130–6.
14. Hendriks EJ, Westerink J, de Jong PA, de Borst GJ, Nathoe HM, Mali WP, et al. Association of High Ankle Brachial Index With Incident Cardiovascular Disease and Mortality in a High-Risk Population. *Arterioscler Thromb Vasc Biol* 2016; 36: 412–7.
15. Third Report of the National Cholesterol Education Program (NCEP) Expert Panel on Detection, Evaluation, and Treatment of High Blood Cholesterol in Adults (Adult Treatment Panel III) final report. *Circulation* 2002; 106: 3143–421.
16. Jochemsen HM, Muller M, van der Graaf Y, Geerlings MI. APOE ϵ 4 differentially influences change in memory performance depending on age. The SMART-MR study. *Neurobiol Aging* 2012; 33: 832.e15–22.
17. Visser F, Zwanenburg JJ, Hoogduin JM, Luijten PR. High-resolution magnetization-prepared 3D-FLAIR imaging at 7.0 Tesla. *Magn Reson Med* 2010; 64: 194–202.
18. Ghaznawi R, de Bresser J, van der Graaf Y, Zwartbol MH, Witkamp TD, Geerlings MI, Hendrikse J. Detection and characterization of small infarcts in the caudate nucleus on 7 Tesla MRI: The SMART-MR study. *J Cereb Blood Flow Metab* 2018; 38: 1609–17.
19. Ghaznawi R, Geerlings MI, Jaarsma-Coes MG, Zwartbol MH, Kuijff HJ, van der Graaf Y, et al. The association between lacunes and white matter hyperintensity features on MRI: The SMART-MR study. *J Cereb Blood Flow Metab* 2019; 39: 2486–96.
20. Conijn MM, Geerlings MI, Biessels GJ, Takahara T, Witkamp TD, Zwanenburg JJ, et al. Cerebral microbleeds on MR imaging: comparison between 1.5 and 7T. *AJNR Am J Neuroradiol* 2011; 32: 1043–9.
21. Wardlaw JM, Smith EE, Biessels GJ, Cordonnier C, Fazekas F, Frayne R, et al. Neuroimaging standards for research into small vessel disease and its contribution to ageing and neurodegeneration. *Lancet Neurol* 2013; 12: 822–38.

22. Anbeek P, Vincken KL, van Bochove GS, van Osch MJ, van der Grond J. Probabilistic segmentation of brain tissue in MR imaging. *Neuroimage* 2005; 27: 795–804.
23. Spilt A, Box FM, van der Geest RJ, Reiber JH, Kunz P, Kamper AM, et al. Reproducibility of total cerebral blood flow measurements using phase contrast magnetic resonance imaging. *J Magn Reson Imaging* 2002; 16: 1–5.
24. Dolui S, Wang Z, Wang DJJ, Mattay R, Finkel M, Elliott M, et al. Comparison of non-invasive MRI measurements of cerebral blood flow in a large multisite cohort. *J Cereb Blood Flow Metab* 2016; 36: 1244–56.
25. Gregoire SM, Chaudhary UJ, Brown MM, Yousry TA, Kallis C, Jager HR, Werring DJ. The Microbleed Anatomical Rating Scale (MARS): reliability of a tool to map brain microbleeds. *Neurology* 2009; 73: 1759–66.
26. De Cocker LJ, Kloppenborg RP, van der Graaf Y, Luijten PR, Hendrikse J, Geerlings MI. Cerebellar Cortical Infarct Cavities: Correlation With Risk Factors and MRI Markers of Cerebrovascular Disease. *Stroke* 2015; 46: 3154–60.
27. Lu PH, Boone KB, Cozolino L, Mitchell C. Effectiveness of the Rey-Osterrieth Complex Figure Test and the Meyers and Meyers recognition trial in the detection of suspect effort. *Clinical Neuropsych* 2003; 17: 426–40.
28. Brand N, Jolles J. Learning and retrieval rate of words presented auditorily and visually. *J Gen Psychol* 1985; 112: 201–10.
29. Wilkins AJ, Shallice T, McCarthy R. Frontal lesions and sustained attention. *Neuropsychologia* 1987; 25: 359–65.
30. Robertson IH, Ward T, Ridgeway V, Nimmo-Smith I. The structure of normal human attention: The Test of Everyday Attention. *J Int Neuropsychol Soc* 1996; 2: 525–34.
31. Burgess PW, Shallice T. Bizarre responses, rule detection and frontal lobe lesions. *Cortex* 1996; 32: 241–59.
32. Wechsler D. *Wechsler Adult Intelligence Scale—Fourth Edition*. 4th ed. San Antonio, TX: Pearson; 2008.
33. Lezak M, Howieson D, Loring D. *Neuropsychological Assessment*. 4th ed. New York: Oxford University Press; 2004.
34. Takasugi J, Miwa K, Watanabe Y, Okazaki S, Todo K, Sasaki T, et al. Cortical Cerebral Microinfarcts on 3T Magnetic Resonance Imaging in Patients With Carotid Artery Stenosis. *Stroke* 2019; 50: 639–44.
35. Sagnier S, Okubo G, Catheline G, Munsch F, Bigourdan A, Debruxelles S, et al. Chronic Cortical Cerebral Microinfarcts Slow Down Cognitive Recovery After Acute Ischemic Stroke. *Stroke* 2019; 50: 1430–6.
36. li Y, Maeda M, Ishikawa H, Ito A, Matsuo K, Umino M, et al. Cortical microinfarcts in patients with multiple lobar microbleeds on 3T MRI. *J Neurol* 2019; 266: 1887–96.
37. Fu R, Wang Y, Wang Y, Liu L, Zhao X, Wang DZ, et al. The Development of Cortical Microinfarcts Is Associated with Intracranial Atherosclerosis: Data from the Chinese Intracranial Atherosclerosis Study. *J Stroke Cerebrovasc Dis* 2015; 24: 2447–54.
38. van Rooden S, Goos JD, van Opstal AM, Versluis MJ, Webb AG, Blauw GJ, et al. Increased number of microinfarcts in Alzheimer disease at 7-T MR imaging. *Radiology* 2014; 270: 205–11.
39. Alexander GE. Basal ganglia-thalamocortical circuits: their role in control of movements. *J Clin Neurophysiol* 1994; 11: 420–31.
40. Alexander GE, Crutcher MD. Functional architecture of basal ganglia circuits: neural substrates of parallel processing. *Trends Neurosci* 1990; 13: 266–71.
41. Leh SE, Petrides M, Strafella AP. The neural circuitry of executive functions in healthy subjects and Parkinson's disease. *Neuropsychopharmacology* 2010; 35: 70–85.
42. Auriel E, Westover MB, Bianchi MT, Reijmer Y, Martinez-Ramirez S, Ni J, et al. Estimating Total Cerebral Microinfarct Burden From Diffusion-Weighted Imaging. *Stroke* 2015; 46: 2129–35.
43. Arvanitakis Z, Capuano AW, Leurgans SE, Buchman AS, Bennett DA, Schneider JA. The Relationship of Cerebral Vessel Pathology to Brain Microinfarcts. *Brain Pathol* 2017; 27: 77–85.
44. Zwartbol MHT, van der Kolk AG, Ghaznavi R, van der Graaf Y, Hendrikse J, Geerlings MI, Group SS. Intracranial Vessel Wall Lesions on 7T MRI (Magnetic Resonance Imaging). *Stroke* 2019; 50: 88–94.



Supplementary Figure 1. Participation flowchart of the SMART-MR study.

Supplementary Table 1. Baseline vascular risk factors of the study population (n = 1309) according to presence or absence of 7T brain MRI data.

| | Patients with a 7T brain MRI scan (n = 213) | Patients without a 7T brain MRI scan (n = 1096) | p value |
|----------------------------------|---|---|--------------------|
| Age (years) | 55 ± 8 | 59 ± 10 | <0.001 |
| Sex, % men | 82.6 | 79.1 | 0.242 |
| History of stroke, % | 24.4 | 22.8 | 0.611 |
| BMI (kg/m ²) | 27 ± 3 | 27 ± 4 | 0.628 |
| Smoking, pack years ^a | 21 (0, 47) | 23 (0, 52) | 0.772 ^b |
| Alcohol use, % current | 85 | 73 | <0.001 |
| Hypertension, % | 51.2 | 52.0 | 0.823 |
| Diabetes mellitus, % | 11.5 | 22.7 | <0.001 |
| Carotid artery stenosis ≥70%, % | 7.4 | 11.9 | 0.06 |
| IMT (mm) | 0.9 ± 0.2 | 1.0 ± 0.3 | <0.001 |
| ABI | 1.2 ± 0.2 | 1.1 ± 0.2 | <0.001 |

Characteristics are presented as mean ± SD or %.

^a Median (10th percentile, 90th percentile).

^b Natural log-transformed due to a non-normal distribution in the statistical analysis.

BMI: body mass index; SD: standard deviation; IMT: intima-media thickness; ABI: ankle brachial index.

PART III

White Matter Lesions, Cerebral Blood Flow and Brain Atrophy



8

White matter hyperintensity shape is associated with cognitive functioning – the SMART-MR study

Maarten H.T. Zwartbol, Rashid Ghaznawi, Myriam Jaarsma-Coes, Hugo J. Kuijf, Jeroen Hendrikse, Jeroen de Bresser, Mirjam I. Geerlings, on behalf of the UCC-SMART Study Group

Published in *Neurobiology of Aging* 2022; 120: 81-87
doi: 10.1016/j.neurobiolaging.2022.08.009

Abstract

White matter hyperintensity (WMH) shape has been associated with the severity of the underlying brain pathology, suggesting it is a potential neuroimaging marker of WMH impact on brain function.

In 563 patients with vascular disease (58 ± 10 years), we examined the relationship between WMH volume, shape and cognitive functioning. WMH volume and shape were automatically determined on 1.5T brain MRI data. Standardized linear regression analyses estimated the association between WMH volume and shape (concavity index, solidity, convexity, fractal dimension and eccentricity) and memory and executive functioning, adjusted for age, sex, educational level, and reading ability.

Larger WMH volumes were associated with lower executive functioning Z-scores (b (95% CI): -0.09 (-0.17 ; 0.01)). Increased shape complexity of periventricular/confluent WMH associated with lower executive functioning (concavity index +1SD: -0.13 (-0.20 ; 0.06); solidity -1SD: -0.09 (-0.17 ; 0.02)) and lower memory function (fractal dimension +1SD: -0.10 (-0.18 ; 0.02)). Of note, the association between concavity index and executive functioning was independent of WMH volume (-0.12 (-0.19 ; 0.04)).

Our results suggest that WMH shape contains additional information about WMH burden, not otherwise captured by WMH volume.

Introduction

White matter hyperintensities of presumed vascular origin (WMH) are a common finding on magnetic resonance imaging (MRI) of the aging brain and represent a key imaging feature of cerebral small vessel disease (CSVD).^{1,2} CSVD comprises a group of neuropathological disease processes with various etiologic and pathologic correlates and neuroimaging features.³

Previous studies have shown that increased WMH volume is associated with worse cognitive functioning, but the effect sizes on individual cognitive domains are relatively small.^{4,5} An explanation for these small effect sizes could be that WMH volume is a relatively crude metric that does not fully capture the heterogeneity of the underlying pathology.²

Histopathologic studies have shown that WMH shape is related to the underlying pathology, e.g., smooth periventricular WMH are associated with mild, non-ischemic, parenchymal changes, whereas confluent and irregular WMH are associated with more severe changes, such as spongiosis and necrosis.² This suggests that, compared to volume, WMH shape may be a more important determinant of the functional consequences of WMH.

Recently, we showed that WMH shape can be automatically determined on magnetic resonance imaging (MRI) data.^{6,7} Furthermore, we showed that WMH shape is associated with different underlying etiology⁶, and that a more complex WMH shape is associated with presence of lacunes⁷ and with physical frailty.⁸ Another study has shown that the irregularity of WMH was related to mental speed and fluid abilities, where in this study WMH volume was not.⁹ This suggests that WMH shape could show a better potential as a descriptor of the relation between WMH and certain cognitive functions.⁹

Therefore, in the current study we examined the relationship between WMH volume and shape and cognitive functioning in a large group of patients with vascular disease.

Methods

Study sample

The Second Manifestations of ARterial disease-Magnetic Resonance (SMART-MR) study is a prospective cohort study at the University Medical Center Utrecht with the objective to study determinants and clinical correlates of brain changes on MRI in patients with vascular disease.¹⁰ From May 2001 to December 2005, patients newly referred to the University Medical Center Utrecht with coronary artery disease, cerebrovascular disease, peripheral arterial disease, or an abdominal aortic aneurysm, and without MRI contraindications, were asked to participate. A total of 1309 patients were enrolled during this period. On a single visit to the University Medical Center Utrecht all patients underwent: a physical examination, carotid ultrasound, blood and urine samplings, and 1.5T brain MR imaging.

Questionnaires were used for the assessment of demographics, risk factors, medical history, medication use and cognitive and physical functioning. Neuropsychological assessment was introduced in the study in 2003 and performed on the same day as the other examinations.

For the current analysis, we had to exclude patients because of missing MRI data of one or more MRI sequences due to motion artifacts or logistic reasons ($n = 239$), irretrievable MRI data ($n = 19$), unreliable brain volume data due to motion artifacts in all three MRI sequences ($n = 44$), severe undersegmentation of WMH by the automated segmentation program ($n = 4$), and no WMH greater than five voxels ($n = 4$). Moreover, because of the later introduction of neuropsychological assessment during the enrollment period, data on cognitive functioning was not available in all patients, leaving 563 patients for the current study.

The SMART-MR study was approved by the medical ethics committee of the University Medical Center Utrecht according to the guidelines of the Declaration of Helsinki of 1975 and written informed consent was obtained from all patients.

Vascular risk factors

Questionnaires were used to assess smoking habits, alcohol intake, medication use and educational level. An overnight fasted venous blood sample was used to determine glucose and lipid levels. Height and weight were measured, and the body mass index (BMI) was calculated (kg/m^2). Systolic blood pressure (mmHg) and diastolic blood pressure (mmHg) were measured twice with a sphygmomanometer, and the averages of the two measures were calculated. Hypertension was defined as a mean systolic blood pressure of ≥ 160 mmHg, a mean diastolic blood pressure of ≥ 95 mmHg, self-reported use of antihypertensive drugs, or a known history of hypertension at inclusion. Diabetes mellitus was defined as use of glucose-lowering drugs, a history of diabetes mellitus, or a fasting plasma glucose level of > 11.1 mmol/l. Hyperlipidemia was defined as a total cholesterol of > 5.0 mmol/l, a low-density lipoprotein cholesterol of > 3.2 mmol/l, use of lipid-lowering drugs, or a known history of hyperlipidemia.

Neuropsychological assessment

Neuropsychological tests were used to assess memory and executive functioning.¹¹ Memory was assessed with the 15 Word Learning Test (a modification of the Rey Auditory Verbal Learning test) using a composite score of: the immediate recall based on 5 trials, the delayed recall and the retention score; and the delayed recall of the Rey-Osterrieth Complex figure test.^{12,13} Executive functioning was assessed with the Visual Elevator test, the Brixton Spatial Anticipation test, and the Verbal Fluency test using the letter *n*.^{14–16} Natural logarithm transformation was applied to the Visual Elevator test scores, because of non-normal distribution. For the Visual Elevator test and the Brixton Spatial Anticipation test, scores were multiplied by -1 to ensure that lower scores represented worse performance. Lastly, composite domain-specific Z-scores were calculated. Reading ability, a measure of

premorbid intellectual functioning, was assessed using the Dutch version of the National Adult Reading Test.¹⁷ Educational level was divided into 7 categories: graded from primary school (around 6 years of education) to academic degree (around 16 years of education), according to the Dutch educational system.

Brain MRI

Brain MRI scans were performed on a 1.5 T whole-body system (Gyrosan ACS-NT, Philips Medical Systems, Best, The Netherlands). The standardized scan protocol consisted of four two-dimensional sequences (transversal acquisition, 38 contiguous slices, and 1.0x1.0x4.0 mm³ voxel size): T1-weighted [repetition time (TR) = 235 ms; echo time (TE) = 2 ms], T1-weighted inversion recovery [TR = 2900 ms; TE = 22 ms; TI = 410 ms], T2-weighted [TR = 2200 ms; TE = 11 ms], and fluid-attenuated inversion recovery (FLAIR) images [TR = 6000 ms; TE = 100 ms; inversion time (TI) = 2000 ms].

Image processing of brain volumes and WMH volume and type

A probabilistic segmentation method using *k*-nearest neighbor classification was used to segment gray matter, white matter, cerebrospinal fluid and WMH¹⁸ using the T1-weighted, FLAIR, and T1-weighted inversion recovery sequences of the MRI scans. Cerebral infarcts were manually segmented. Segmentation of WMH was checked by an investigator (RG) blinded to patient characteristics using an image processing framework (MeVisLab 2.7.1., MeVis Medical Solutions AG, Bremen, Germany), and corrected if needed.

Segmentation of the lateral ventricles was performed using the automated lateral ventricle delineation (ALVIN) algorithm in Statistical Parametric Mapping 8 (SPM8, Wellcome Trust Centre for Neuroimaging, University College London, London, UK) for Matlab (The MathWorks, Inc., Natick, Massachusetts, United States).^{7,19} The ALVIN mask was used to establish the margins of the lateral ventricles.

WMH probability data were processed into binary data using a threshold of 0.10. The arbitrary chosen threshold of 0.1 resulted in a good balance between retaining information and introduction of noise. A WMH lesion was defined as a group of voxels with touching corners, edges or faces. We labeled WMH lesions as periventricular, confluent or deep, based on their contiguity with the ventricular margins and depth of extension into the white matter.⁷ Periventricular WMH were defined as lesions contiguous with the margins of the lateral ventricles and extending up to 10 mm from the lateral ventricles. Confluent WMH were defined as lesions contiguous with the margins of the lateral ventricles and extending more than 10 mm from the lateral ventricles. Deep WMH were defined as lesions that were not contiguous with the lateral ventricles (regardless of their distance to the ventricular margins). Labels were visually checked by an investigator (MJC) blinded to patient characteristics and corrected if needed.

Total periventricular, confluent and deep WMH volumes were obtained by summing all WMH lesion volumes per type. Total WMH volume was calculated by summing all WMH

lesion volumes. Total brain volume was calculated by summing the volumes of gray matter, white matter, total WMH and other brain lesions. Intracranial volume was calculated by summing the cerebrospinal fluid volume and total brain volume.¹⁰

Image processing of WMH shape

We analyzed WMH shape with the use of shape features.⁶ Shape features were calculated from the binary WMH segmentation data using Matlab.

The selection of WMH shape features has been described in detail in a prior study.⁷ In short, we first examined which shape features are able to describe the complexity of periventricular, confluent and deep WMHs.⁷ Next, the shape features were graded using the following criteria: comprehensibility (the ability to relate the shape feature output to the visual interpretation of WMH shape on MRI), usability on 1.5T MRI resolution, volume dependence (the degree to which a shape feature is correlated with WMH volume), robustness (the degree to which WMH positioning influences the shape feature), presence of a flooring effect (the minimum measured value is close to or similar to the smallest possible value of the shape feature) and presence of a ceiling effect (the maximum measured value is close to or similar to the highest possible value of the shape feature).⁷

The shape features with the best combination of criteria (e.g., high comprehensibility, limited volume dependence, usability on 1.5T MRI data, adequate robustness, limited flooring and/or ceiling effect) were selected. The selected shape features and their definitions are presented in Supplemental Table 1.

We decided to group the periventricular WMH and confluent WMH together into periventricular/confluent WMH. Although confluent WMH is a more heterogeneous group than periventricular WMH (because it contains periventricular WMHs which extend into the deep white matter but also deep WMH which extend into the periventricular white matter to the ventricular wall), they can be regarded as ends on the same spectrum (Fazekas 1/2 vs. Fazekas 3), are morphologically more similar (compared to deep WMH) and well-described by the same shape features.

We analyzed periventricular and confluent WMHs by calculating their convex hulls and obtaining volume and surface area ratios. Convexity was obtained by dividing the area of the convex hull by the WMH lesion's surface area. Solidity was calculated by dividing the volume of the WMH lesion by the volume of its hull. The concavity and solidity of a WMH lesion was used to calculate its concavity index.²⁰

We analyzed deep WMHs by dividing their minor axis by their major axis, which presents their eccentricity.

Lastly, fractal dimension was calculated for periventricular, confluent and deep WMHs. It was calculated with the box-counting method (Minkowski-Bouligand dimension) (Supplemental Table 1) as implemented in Matlab by Frederic Moisy.²¹ We chose for box-counting because it is a straightforward and robust method which can be applied easily to a large variety of shapes. The algorithm works as follows. As a general step, the

binarized WHM image is partitioned into square boxes of size $r \times r \times r$ and the number of boxes ($n(r)$) containing a portion of the shape are counted. The algorithm starts with the smallest box fitting the entire binarized WHM and being a 2 multiple of the voxel size. Next, r is divided by two and the process repeated, each time dividing r by two until the voxel size is reached. The fractal dimension is calculated as the absolute value of the slope of the line obtained from the linear regression of the $(\log(n(r)), \log(1/r))$ curve. Visual examples of this calculation are shown in Supplemental Figure 1. The images show an excellent correlation between the input data and the fitted linear regression, indicating that the FD computation is valid. In addition, the code was verified using an artificial 'Menger Sponge', which resulted in the expected value of 2.7.

All shape values were expressed as mean values per patient with only fractal dimension having separate mean values per WHM subgroup (periventricular, confluent and deep WHM).

The reproducibility of the WMH shape feature calculation was examined because of the potential influence of manual infarct segmentation. In a random dataset of 15 persons with infarcts a second rater repeated the process of automatic brain segmentation, manual infarct segmentation and WMH shape feature calculation. Spearman's ρ was used to test for correlations between the initial and second segmentations. With a correlation coefficient of 1.0 for each of the WMH shape features, the reproducibility of the shape feature calculation was regarded as excellent.

How to interpret WMH shape parameters

We use the term 'complexity' to denote roughness of a shape.

Solidity and convexity both measure roughness, solidity on a morphological level and convexity on a textural level.²⁰ As can be derived from Supplemental Table 1, lower solidity and convexity indicate a more complex shape. E.g., a WMH with several long protrusions will likely have a relatively large convex hull volume compared to the contained WMH volume, which will cause solidity to trend downward.

Concavity index is a compound parameter which combines the information from solidity and convexity into a single parameter.²⁰ As shown in Supplemental Table 1, a lower solidity and/or convexity will lead to a higher concavity index. Hence, higher concavity index correlates with a more complex shape.

Fractal dimension is another measure of textural roughness and higher values indicate a more geometrically complex surface area of a WMH lesion.^{22,23}

Eccentricity measures the form of a shape.^{24,25} A lower eccentricity means a more elongated lesion, while a higher eccentricity means a relatively round WMH lesion.

Of note, for convexity and solidity lower values indicate higher complexity whereas for concavity index and fractal dimension higher values indicate higher complexity. We have clarified this in the results section with the use of negative or positive standard deviations.

Statistical analysis

Baseline characteristics and WMH volume and shape features were calculated for the study sample.

Standardized linear regression analyses were used to estimate the association between total WMH volume Z-scores and WMH shape feature Z-scores with Z-scores of memory and executive functioning. WMH volume was natural-log transformed, to achieve a normal distribution, and expressed as a percentage of intracranial volume (%ICV), to adjust for variations in head size. All analyses were adjusted for age, sex, level of education and reading ability (model 1). The analyses of WMH shape features were additionally adjusted for natural-log transformed total WMH volume (%ICV) (model 2) to test if the associations were independent of WMH volume. The covariates were added because of their known influence on cognitive functioning and/or for being a potential confounder.

A *p*-value of < 0.05 was considered to be statistically significant. SPSS 25.0 for Windows (Chicago, IL, USA) was used to analyze the data.

Results

Characteristics of the 563 patients in our study sample (58 ± 10 years; 76% male) are presented in Table 1. The total WMH volume and WMH shape features are shown in Table 2. The median (10th; 90th percentile) total WMH volume was 0.81 ml (0.17; 5.51).

Larger total WMH volume Z-scores were associated with lower executive functioning Z-scores ($b = -0.09$; 95% CI -0.17 to -0.01) after adjusting for age, sex, educational level, and reading ability (Table 3). The adjusted R^2 of this model was 0.34. Larger total WMH volume Z-scores were also associated with lower memory Z-scores, but this association did not reach statistical significance ($b = -0.08$; 95% CI -0.16 to 0.00; $p = 0.06$).

A more complex shape of periventricular/confluent WMH was associated with lower executive functioning Z-scores (concavity index +1SD: $b = -0.13$; 95% CI -0.20 to -0.06; solidity -1SD: $b = -0.09$; 95% CI -0.17 to -0.02) after adjusting for age, sex, educational level, and reading ability (Table 3). After additional adjustment for total WMH volume, the association between concavity index and executive functioning remained significant (concavity index +1SD: $b = -0.12$; 95% CI -0.19 to -0.04), showing that this association was independent of WMH volume. The adjusted R^2 of the latter model was 0.351 whereas the model without WMH volume adjustment had an adjusted R^2 of 0.350. This shows that WMH volume does not explain additional variation in executive functioning, compared to concavity index. Furthermore, it suggests that concavity index explains a little bit more variation in executive functioning compared to WMH volume alone, shown by the adjusted R^2 of 0.34.

Table 1. Characteristics of the study sample (n = 563).

| | |
|--------------------------------|------------------|
| Age (years) | 58.1 ± 10.2 |
| Sex, % male | 76 |
| Educational level (range 0-7) | 3 (1-6) |
| Reading ability (range 0-100) | 83 (56-97) |
| Alcohol use, % current | 75 |
| Cigarette smoking (pack-years) | 18.2 (0.0; 50.4) |
| Hypertension, % | 55 |
| Diabetes, % | 19 |
| Hyperlipidemia, % | 79 |
| History of arterial disease | |
| Coronary heart disease, % | 58 |
| Cerebrovascular disease, % | 20 |
| Peripheral artery disease, % | 25 |
| Abdominal aortic aneurysm, % | 8 |

Characteristics are presented as mean±SD, % or median (10th, 90th percentile).

Table 2. WMH volume and shape features of the study sample (n = 563).

| | |
|--|-------------------|
| WMH volume (ml) | |
| Total WMH | 0.81 (0.17; 5.51) |
| Periventricular/confluent WMH | 0.66 (0.12; 4.86) |
| Deep WMH | 0.06 (0.01; 0.75) |
| Periventricular/confluent WMH shape features | |
| Solidity | 0.63 (0.24; 0.91) |
| Convexity | 1.03 (0.91; 1.28) |
| Concavity index | 1.04 (0.94; 1.17) |
| Fractal dimension | 1.22 (0.96; 1.51) |
| Deep WMH shape features | |
| Eccentricity | 0.47 (0.30; 0.67) |
| Fractal dimension | 1.44 (1.29; 1.63) |

Values are median (10th; 90th percentile).

WMH: white matter hyperintensities.

Table 3. Association between WMH volume, shape and cognitive functioning.

| | Model | Memory (Z-score) <i>b</i> (95% CI) | Executive functioning (Z-score) <i>b</i> (95% CI) |
|--|-------|---------------------------------------|---|
| Total WMH volume (Z-score) ^a | 1 | -0.08 (-0.16 to 0.00) | -0.09 (-0.17 to -0.01)* |
| Periventricular/confluent WMH shape features (Z-scores) ^b | | | |
| Solidity, per -1 SD | 1 | -0.08 (-0.16 to 0.00) | -0.09 (-0.20 to -0.02)* |
| | 2 | -0.04 (-0.17 to 0.09) | -0.07 (-0.20 to 0.06) |
| Convexity, per -1 SD | 1 | 0.02 (-0.05 to 0.09) | -0.02 (-0.09 to 0.05) |
| | 2 | 0.00 (-0.07 to 0.08) | -0.04 (-0.12 to 0.03) |
| Concavity index, per +1 SD | 1 | -0.06 (-0.13 to 0.02) | -0.13 (-0.20 to -0.06)*** |
| | 2 | -0.04 (-0.12 to 0.04) | -0.12 (-0.19 to -0.04)** |
| Fractal dimension, per +1 SD | 1 | -0.10 (-0.18 to -0.02)* | -0.06 (-0.14 to 0.01) |
| | 2 | -0.16 (-0.36 to 0.03) | 0.07 (-0.12 to 0.25) |
| Deep WMH shape features (Z-scores) ^{b, c} | | | |
| Eccentricity, per +1 SD | 1 | 0.07 (-0.02 to 0.16) | 0.03 (-0.06 to 0.13) |
| | 2 | 0.07 (-0.03 to 0.16) | 0.02 (-0.07 to 0.11) |
| Fractal dimension, per +1 SD | 1 | 0.05 (-0.05 to 0.15) | 0.04 (-0.06 to 0.13) |
| | 2 | 0.05 (-0.04 to 0.15) | 0.04 (-0.05 to 0.14) |

b values are unstandardized linear regression coefficients with 95% confidence intervals.

Model 1: adjusted for age, sex, educational level, and reading ability. Model 2: model 1 with additional adjustment for natural log-transformed total WMH volume (%ICV).

WMH: white matter hyperintensities; %ICV: percentage of intracranial volume; SD: standard deviation.

^a Natural log-transformed total WMH volume (%ICV).

^b The +1 or -1 change in standard deviation denotes the direction of increasing shape complexity. E.g., lower solidity and higher concavity both indicate increasing shape complexity.

^c Analysis performed only in patients with deep WMH lesions (*n* = 340).

* $p \leq 0.05$; ** $p \leq 0.01$; *** $p \leq 0.001$.

A more complex shape of periventricular/confluent WMH was also associated with lower memory Z-scores (fractal dimension +1SD: $b = -0.10$; 95% CI -0.18 to -0.02) after adjusting for age, sex, educational level and reading ability. This association lost statistical significance after additional adjustment for total WMH volume (fractal dimension +1SD: $b = -0.16$; 95% CI -0.36 to 0.03; $p = 0.10$). Figure 1 shows an example of WMH in two patients (A and B) with similar WMH volume (A = 11.4 ml; B = 12.2 ml), but a more than 2 standard deviation difference in concavity index (concavity index Z-score: A = 1.06; B = 2.82). No associations were found between shape of deep WMH (i.e., eccentricity, fractal dimension) and cognitive functioning (Table 3).

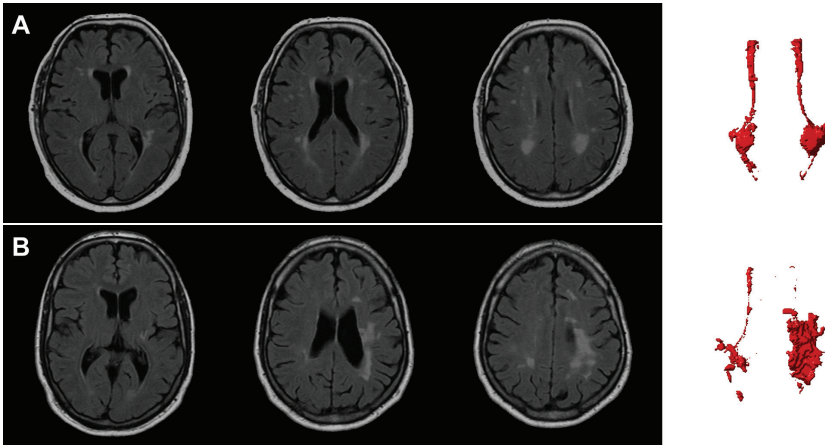


Figure 1. Example of WMH shape difference in two patients (A, B) with comparable WMH volume (11.4 ml vs. 12.2 ml, respectively) but a 2.7 SD difference (Z-scores: 0.10 vs. 2.82, respectively) in concavity index. The three leftmost images in each row are axial FLAIR images at three different levels. The rightmost image is a top-down view of a volumetric rendering of the periventricular/confluent WMH segmentation. Note, the more complex shape of the periventricular/confluent WMH in the patient with the highest concavity index (B).

We repeated the analyses for each vascular disease group separately (Supplemental Table 2 and 3). For memory function the results were fairly similar although the effect estimates varied somewhat across disease groups, but confidence intervals showed considerable overlap. This was also found for executive functioning, except for the AAA group where associations with periventricular/confluent WMH shape features were stronger, although it should be noted that this group was rather small.

Discussion

In this large cohort study among patients with a history of vascular disease, a larger total WMH volume was associated with decreased executive functioning, but not with memory performance. A more complex shape of periventricular/confluent WMH was associated with both decreased executive functioning and decreased memory performance. Furthermore, the association between WMH shape measured by the concavity index and executive functioning was independent of WMH volume. We did not find an association between deep WMH shape and cognitive functioning.

Only few studies have been published on WMH shape analysis in CSVD.^{6–9,26} To the best of our knowledge, only one study has examined the relationship between WMH

shape and cognitive functioning.⁹ This study found that in two heterogeneous samples largely consisting of patients with cognitive impairment of various etiologies (e.g. Alzheimer's disease, vascular dementia, mixed-type), a more irregular shape of WMH (expressed by the "confluency sum score") was associated with a decrease in mental speed, executive functioning and mini-mental state examination performance.⁹ Notably, these associations were also independent of WMH volume, which is in agreement with our findings. Additionally, our study shows that this association already exists in persons with preclinical cognitive decline. We also show that within this population the association more specifically pertains to periventricular/confluent WMH and not to deep WMH, whereas Lange et al. examined shape of WMHs as a whole.

A wide variety of shape features and shape analysis methods exist.^{7,9,26,27} Because WMH shape analysis in CSVD is a new area of research, it is unclear which shape features best capture the relevant shape variation of WMH. Gwo et al. examined the applicability of Zernike polynomials of WMH lesions, which describe both lower order features such as gross shape and global contour and higher order features such as fine topological details.^{26,28} Although they were able to quantify shape, and cluster WMH lesions into distinctive groups, associations with determinants and outcomes were not assessed. We previously performed a broad exploration of available shape features to determine the most optimal features that capture the possible variations in WMH shape best.^{6,7} However, examining the relation of these features with determinants and outcomes is also important to determine which variations in shape of WMHs are clinically relevant.

Meta-analyses have shown that WMHs have a small and global detrimental effect on cognitive functioning.^{4,26} We found an association between WMH volume and executive functioning and memory, although the latter was not statistically significant. For WMH shape, we found that concavity index was associated with executive functioning but not with memory, and fractal dimension was associated with memory but not executive functioning. A hypothetical explanation for this, is that WMH shape is not only related to the underlying pathology of WMHs, but also to their etiology, and different small vessel etiologies are known to have different effects on cognitive functioning.

Several mechanisms have been suggested for the relation between WMHs and cognitive functioning, all of which revolve around disruption of brain pathways.³⁰ However, the extent of disruption for different underlying pathological changes (e.g. non-ischemic changes to necrosis) can vary², which might explain the variable relationship of WMH volume with cognitive functioning in previous studies.^{4,29} Shape irregularity and confluency of WMH have been linked to the severity of WMH pathology.^{2,31} This suggests that WMH shape may be a better determinant of cognitive functioning, compared to WMH volume. Our results seem to give support to this hypothesis, since the association between WMH shape (measured by concavity index) and cognitive functioning was independent of WMH volume.

We think there are two likely explanations for this which partially overlap: WMH shape correlates with differences in etiology and/or pathological severity, which in turn differentially relate to cognitive functioning. As mentioned previously, this has been shown in periventricular WMH, where irregular (complex) shape is related to ischemia and more severe tissue damage, and smooth “caps and bands” to non-ischemic causes and more benign tissue changes.³⁰ The exact mechanisms which lead to complex shape remains to be researched. However, a general observation of human pathophysiology suggests that — in general — benign processes are often controlled whereas less benign processes show loss of control and develop more irregular boundaries (e.g., neoplasms). The same may hold true for WMH pathophysiology.

Strengths of our study are the large size of the cohort, the semi-automatic WMH segmentation and automated image processing techniques to determine WMH shape features automatically, and the examination of two cognitive domains. Furthermore, the adjustment of our analyses for WMH volume allowed us to estimate if the association of WMH shape with cognitive functioning was independent of WMH volume. Moreover, the use of neuropsychological tests that are sensitive to mild impairments in cognitive functioning and the available data on premorbid cognitive functioning allowed detection of more subtle associations.

A limitation is that all participants had one or more vascular diseases, which might limit generalizability of our results to the general population. However, vascular disease is linked to the development of WMH and therefore these findings are especially of interest to this population. Another limitation is the use of 2-dimensional FLAIR MRI images with anisotropic voxels, which could have resulted in a less accurate approximation of WMH shape compared to the use of 3-dimensional FLAIR images with isotropic voxel size. However, even with use of these 2-dimensional FLAIR MRI images we were able to find relevant associations with WMH shape. Lastly, values of fractal dimension were very low. On 3-dimensional data values between 2 and 3 are expected whereas in our data the 90th percentile was already below 2. A likely explanation is that the implementation of box-counting that we use is suboptimal for WMH morphology and is better fitted for cubic shapes. Nonetheless, FD did differ between WMH lesions and showed a relation with cognitive functioning before WMH volume correction, suggesting that some relevant information about WMH lesions is captured.

Our findings are relevant because they suggest that WMH shape may be a new method to characterize the impact of WMHs on cognitive function. WMHs are highly prevalent in the older population, but their effect size on cognitive functioning is small, possibly because conventional methods (e.g., volumetry, Fazekas score) do not correlate with the severity of underlying pathology. New methods to better characterize WMHs, e.g., with shape features, will help in the study of risk factors and differential cognitive outcomes of WMHs.

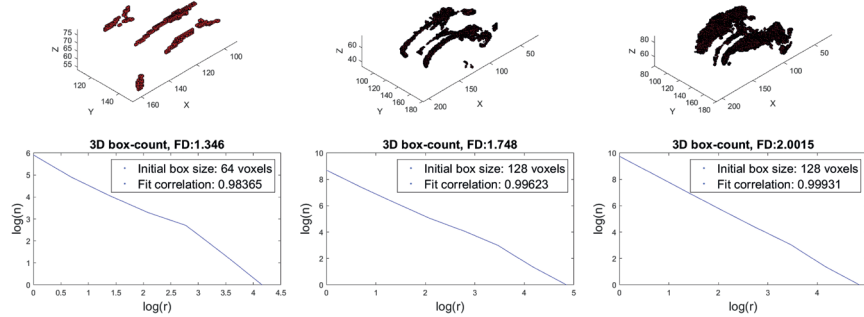
In conclusion, WMH shape is associated with cognitive functioning in patients with vascular disease. Our results suggest that WMH shape contains additional information about WMH burden, not otherwise captured by WMH volume.

References

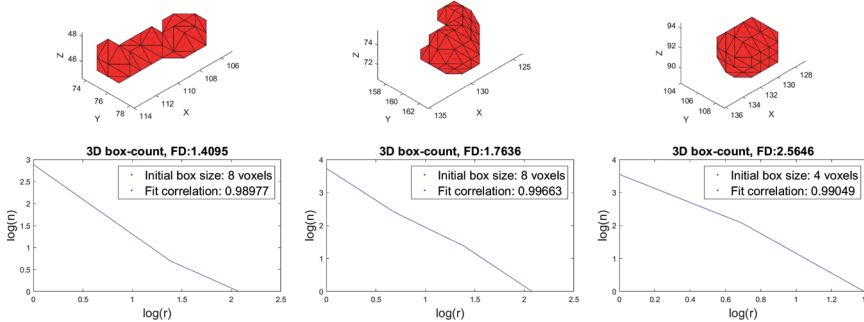
1. Wardlaw JM, Smith EE, Biessels GJ, Cordonnier C, Fazekas F, Frayne R, et al. Neuroimaging standards for research into small vessel disease and its contribution to ageing and neurodegeneration. *Lancet Neurol* 2013; 12: 822–38.
2. Gouw AA, Seewann A, Van Der Flier WM, Barkhof F, Rozemuller AM, Scheltens P, et al. Heterogeneity of small vessel disease: A systematic review of MRI and histopathology correlations. *J Neurol Neurosurg Psychiatry* 2011; 82: 126–35.
3. Pantoni L. Cerebral small vessel disease: from pathogenesis and clinical characteristics to therapeutic challenges. *Lancet Neurol* 2010; 9: 689–701.
4. Kloppenborg RP, Nederkoorn PJ, Geerlings MI, Van Den Berg E. Presence and progression of white matter hyperintensities and cognition: A meta-analysis. *Neurology* 2014; 82: 2127–38.
5. Vogels RL, Oosterman JM, van Harten B, Gouw AA, Schroeder-Tanka JM, Scheltens P, et al. Neuroimaging and correlates of cognitive function among patients with heart failure. *Dement Geriatr Cogn Disord* 2007; 24: 418–23.
6. de Bresser J, Kuijf HJ, Zaenen K, Viergever MA, Hendrikse J, Biessels GJ, et al. White matter hyperintensity shape and location feature analysis on brain MRI; Proof of principle study in patients with diabetes. *Sci Rep* 2018; 8: 1–10.
7. Ghaznawi R, Geerlings MI, Jaarsma-Coes MG, Zwartbol MHT, Kuijf HJ, van der Graaf Y, et al. The association between lacunes and white matter hyperintensity features on MRI: The SMART-MR study. *J Cereb Blood Flow Metab* 2019; 39: 2486–96.
8. Kant IMJ, Mutsaerts HJMM, van Montfort SJT, Jaarsma-Coes MG, Witkamp TD, Winterer G, et al. The association between frailty and MRI features of cerebral small vessel disease. *Sci Rep* 2019; 9: 1–9.
9. Lange C, Suppa P, Mäurer A, Ritter K, Pietrzyk U, Steinhagen-Thiessen E, et al. Mental speed is associated with the shape irregularity of white matter MRI hyperintensity load. *Brain Imaging Behav* 2017; 11: 1720–30.
10. Geerlings MI, Appelman AP, Vincken KL, Algra A, Witkamp TD, Mali WP, et al. Brain volumes and cerebrovascular lesions on MRI in patients with atherosclerotic disease. The SMART-MR study. *Atherosclerosis* 2010; 210: 130–6.
11. Muller M, Appelman AP, van der Graaf Y, Vincken KL, Mali WP, Geerlings MI. Brain atrophy and cognition: interaction with cerebrovascular pathology? *Neurobiol Aging* 2011; 32: 885–93.
12. Brand N, Jolles J. Learning and retrieval rate of words presented auditorily and visually. *J Gen Psychol* 1985; 112: 201–10.
13. Osterrieth P. Fildetest de copie d'une figure complex: contribution a l'etude de la perception et de la memoire [The test of copying a complex figure: a contribution to the study of perception and memory]. *Arch Psychol* 1944; 30: 286–356.
14. Robertson IH, Ward T, Ridgeway V, Nimmo-Smith I. The structure of normal human attention: The Test of Everyday Attention. *J Int Neuropsychol Soc* 1996; 2: 525–34.
15. Burgess PW, Shallice T. Bizarre responses, rule detection and frontal lobe lesions. *Cortex* 1996; 32: 241–59.
16. Wilkins AJ, Shallice T, McCarthy R. Frontal lesions and sustained attention. *Neuropsychologia* 1987; 25: 359–65.
17. Schmand B, Geerlings MI, Jonker C, Lindeboom J. Reading Ability as an Estimator of Premorbid Intelligence : Does It Remain Stable in Emergent Dementia ? Reading Ability as an Estimator of Premorbid Intelligence : Does It Remain Stable in Emergent Dem. *J Clin Exp Neuropsychol* 1998; 20: 42–51.
18. Anbeek P, Vincken KL, van Osch MJ, Bisschops RH, van der Grond J. Probabilistic segmentation of white matter lesions in MR imaging. *Neuroimage* 2004; 21: 1037–44.
19. Kempton MJ, Underwood TSA, Brunton S, Stylios F, Ettinger U, Smith MS, et al. A comprehensive testing protocol for MRI neuroanatomical segmentation techniques: Evaluation of a novel lateral ventricle segmentation method. *Neuroimage* 2013; 58: 1051–9.
20. Liu EJ, Cashman K V, Rust AC. Optimising shape analysis to quantify volcanic ash morphology. *GeoResJ* 2015; 8: 14–30.
21. Moisy F. boxcount [Internet]. MathWorks File Exchange. 2008. Available from: <https://www.mathworks.com/matlabcentral/fileexchange/13063-boxcount>
22. Esteban FJ, Sepulcre J, de Miras JR, Navas J, de Mendizábal NV, Goñi J, et al. Fractal dimension analysis of grey matter in multiple sclerosis. *J Neurol Sci* 2009; 282: 67–71.

23. Zhang L, Liu JZ, Dean D, Sahgal V, Yue GH. A three-dimensional fractal analysis method for quantifying white matter structure in human brain. *J Neurosci Methods* 2006; 150: 242–53.
24. Loizou CP, Petroudi S, Seimenis I, Pantziaris M, Pattichis CS. Quantitative texture analysis of brain white matter lesions derived from T2-weighted MR images in MS patients with clinically isolated syndrome. *J Neuroradiol* 2015; 42: 99–114.
25. Murphy K, van Ginneken B, Schilham AMR, de Hoop BJ, Gietema HA, Prokop M. A large-scale evaluation of automatic pulmonary nodule detection in chest CT using local image features and k-nearest-neighbour classification. *Med Image Anal* 2009; 13: 757–70.
26. Gwo CY, Zhu DC, Zhang R. Brain White Matter Hyperintensity Lesion Characterization in T2 Fluid-Attenuated Inversion Recovery Magnetic Resonance Images: Shape, Texture, and Potential Growth. *Front Neurosci* 2019; 13: 1–15.
27. Li S, Tavares JMRS. *Shape Analysis in Medical Image Analysis*. 1st ed. Switzerland: Springer International Publishing; 2014.
28. Gwo CY, Wei CH. Shoeprint retrieval: Core point alignment for pattern comparison. *Sci Justice* 2016; 56: 341–50.
29. Debetto S, Markus HS. The clinical importance of white matter hyperintensities on brain magnetic resonance imaging: Systematic review and meta-analysis. *BMJ* 2010; 341: c3666.
30. Prins ND, Scheltens P. White matter hyperintensities, cognitive impairment and dementia: An update. *Nat Rev Neurol* 2015; 11: 157–65.
31. Fazekas F, Schmidt R, Scheltens P. Pathophysiologic mechanisms in the development of age-related white matter changes of the brain. *Dement Geriatr Cogn Disord* 1998; 9(Suppl 1): 2–5.

A. PWMH & CWMH



B. DWMH



Supplemental Figure 1. Examples of fractal dimension calculation using the box-counting method. The colored meshes are the 3d segmented WMH lesions with below the corresponding graph showing results from the fractal dimension calculation with the box size (r) on the x-axis and the number of filled boxes (n) on the y-axis. The absolute directional coefficient of the line representing the fractal the dimension is shown in the chart title. All fits show an excellent correlation coefficient between the result of the linear regression computation and the input. Clear differences can be observed between the PWMH and CWMH lesions with the low volume and relative smooth lesions at the upper left showing a low FD compared to the rough and high-volume lesion in the upper right corner.

Supplemental Table 1. Definitions of the WMH shape features.

| Name | Formula |
|-------------------------------------|--|
| Convexity (C) ^a | $C = \frac{\text{Convex hull area}}{\text{Area}}$ |
| Solidity (S) ^b | $S = \frac{\text{Volume}}{\text{Convex hull volume}}$ |
| Concavity index (CI) ^c | $CI = \sqrt{(2 - C)^2 + (1 - S)^2}$ |
| Fractal dimension (FD) ^d | $FD = \lim_{r \rightarrow x_{xyz}} \frac{\log(n_r)}{\log\left(\frac{1}{r}\right)}$ |
| Eccentricity (E) ^e | $E = \frac{\text{Minor axis}}{\text{Major axis}}$ |

^a Area represents the surface area of the WMH lesion and convex hull area the surface area of the convex hull.^{1,2} The convex hull is the smallest convex set that contains the WMH lesion.

^b Volume represents the volume of the WMH lesion and convex hull volume the volume of the corresponding convex hull.²

^c C represents the convexity of the lesion and S the solidity.²

^d Fractal dimension is calculated with the box-counting (Minkowski-Bouligand dimension) method, in which n is the number of boxes, x_{xyz} is the voxel size and r is the box size.^{3–5}

^e Major axis represents the largest diameter of the lesion in three dimensions and minor axis the smallest diameter orthogonal to the major axis.^{3,6,7}

Supplemental Table 2. Association between WMH volume, shape and memory function per vascular disease.

| | Model | Total sample (n = 563) | Memory function (Z-score) | | | |
|--|-------|---------------------------|--|---|---|--|
| | | | Coronary heart disease (n = 324) | Cerebrovascular disease (n = 111) | Peripheral artery disease (n = 138) | Abdominal aortic aneurysm (n = 45) |
| Total WMH volume (Z-score) ^a | 1 | -0.08 (-0.16 to 0.00) | -0.11 (-0.22 to 0.00) | 0.08 (-0.10 to 0.26) | -0.06 (-0.25 to 0.13) | -0.21 (-0.56 to 0.14) |
| Periventricular/confluent WMH shape features (Z-scores) ^b | | | | | | |
| Solidity, per -1 SD | 1 | -0.08 (-0.16 to 0.00) | -0.11 (-0.22 to 0.00) | -0.01 (-0.18 to 0.16) | -0.03 (-0.21 to 0.15) | -0.25 (-0.61 to 0.11) |
| | 2 | -0.04 (-0.17 to 0.09) | -0.06 (-0.23 to 0.12) | -0.21 (-0.50 to 0.09) | 0.04 (-0.25 to 0.32) | -0.20 (-0.81 to 0.41) |
| Convexity, per -1 SD | 1 | 0.02 (-0.05 to 0.09) | 0.04 (-0.06 to 0.14) | -0.00 (-0.17 to 0.16) | 0.00 (-0.15 to 0.16) | 0.05 (-0.27 to 0.37) |
| | 2 | 0.00 (-0.07 to 0.08) | 0.00 (-0.10 to 0.11) | -0.00 (-0.17 to 0.17) | -0.01 (-0.16 to 0.15) | 0.05 (-0.27 to 0.37) |
| Concavity index, per +1 SD | 1 | -0.06 (-0.13 to 0.02) | -0.05 (-0.15 to 0.05) | -0.02 (-0.19 to 0.15) | -0.06 (-0.22 to 0.10) | -0.14 (-0.44 to 0.16) |
| | 2 | -0.04 (-0.12 to 0.04) | -0.03 (-0.13 to 0.08) | -0.09 (-0.30 to 0.12) | -0.05 (-0.22 to 0.13) | -0.04 (-0.43 to 0.36) |
| Fractal dimension, per +1 SD | 1 | -0.10 (-0.18 to -0.02)* | -0.12 (-0.23 to -0.01)* | 0.05 (-0.13 to 0.22) | -0.14 (-0.31 to 0.04) | -0.20 (-0.56 to 0.16) |
| | 2 | -0.16 (-0.36 to 0.03) | -0.11 (-0.37 to 0.14) | -0.30 (-0.90 to 0.30) | -0.36 (-0.73 to 0.00) | -0.01 (-0.93 to 0.91) |
| Deep WMH shape features (Z-scores) ^b | | | | | | |
| Eccentricity, per +1 SD | 1 | 0.07 (-0.02 to 0.16) | 0.06 (-0.07 to 0.19) | 0.12 (-0.07 to 0.30) | 0.11 (-0.11 to 0.32) | 0.06 (-0.32 to 0.43) |
| | 2 | 0.07 (-0.03 to 0.16) | 0.43 (-0.10 to 0.17) | 0.14 (-0.04 to 0.33) | 0.11 (-0.11 to 0.32) | 0.05 (-0.34 to 0.44) |
| Fractal dimension, per +1 SD | 1 | 0.05 (-0.05 to 0.15) | -0.02 (-0.16 to 0.11) | 0.19 (-0.02 to 0.40) | 0.21 (0.00 to 0.42)* | -0.02 (-0.39 to 0.34) |
| | 2 | 0.05 (-0.04 to 0.15) | -0.02 (-0.15 to 0.12) | 0.19 (-0.02 to 0.39) | 0.21 (0.01 to 0.42)* | -0.02 (-0.39 to 0.36) |

Values are unstandardized linear regression coefficients with 95% confidence intervals.

Model 1: adjusted for age, sex, educational level, and reading ability. Model 2: model 1 with additional adjustment for natural log-transformed total WMH volume (%ICV).

WMH: white matter hyperintensities; %ICV: percentage of intracranial volume; SD: standard deviation.

^a Natural log-transformed total WMH volume (%ICV).

^b The +1 or -1 change in standard deviation denotes the direction of increasing shape complexity. E.g., lower solidity and higher concavity both indicate increasing shape complexity.

* $p \leq 0.05$.

Supplemental Table 3. Association between WMH volume, shape and executive functioning per vascular disease.

| | | Executive functioning (Z-score) | | | | |
|--|-------|---------------------------------|-------------------------------------|--------------------------------------|--|---------------------------------------|
| | Model | Total sample (n = 563) | Coronary heart disease (n = 324) | Cerebrovascular disease (n = 111) | Peripheral artery disease (n = 138) | Abdominal aortic aneurysm (n = 45) |
| Total WMH volume (Z-score) ^a | 1 | -0.09 (-0.17 to -0.01)* | 0.00 (-0.11 to 0.10) | -0.09 (-0.26 to 0.09) | -0.14 (-0.32 to 0.04) | -0.15 (-0.44 to 0.15) |
| Periventricular/confluent WMH shape features (Z-scores) ^b | | | | | | |
| Solidity, per -1 SD | 1 | -0.09 (-0.20 to -0.02)* | -0.04 (-0.14 to 0.06) | -0.12 (-0.29 to 0.05) | -0.08 (-0.25 to 0.10) | 0.19 (-0.13 to 0.51) |
| | 2 | -0.07 (-0.20 to 0.06) | -0.10 (-0.26 to 0.06) | -0.15 (-0.44 to 0.14) | 0.07 (-0.20 to 0.35) | 0.82 (0.37 to 1.26)*** |
| Convexity, per -1 SD | 1 | -0.02 (-0.09 to 0.05) | -0.00 (-0.09 to 0.09) | -0.10 (-0.26 to 0.06) | -0.02 (-0.17 to 0.14) | -0.42 (-0.66 to -0.19)*** |
| | 2 | -0.04 (-0.12 to 0.03) | -0.00 (-0.10 to 0.09) | 0.10 (-0.06 to 0.26) | -0.04 (-0.19 to 0.12) | -0.42 (-0.65 to -0.18)*** |
| Concavity, per +1 SD | 1 | -0.13 (-0.20 to -0.06)*** | -0.05 (-0.14 to 0.04) | -0.21 (-0.37 to -0.05)* | -0.15 (-0.30 to 0.01) | -0.30 (-0.53 to -0.06)* |
| | 2 | -0.12 (-0.19 to -0.04)** | -0.05 (-0.15 to 0.04) | -0.24 (-0.44 to -0.04)* | -0.12 (-0.29 to 0.05) | -0.39 (-0.70 to -0.07)* |
| Fractal dimension, per +1 SD | 1 | -0.06 (-0.14 to 0.01) | -0.01 (-0.11 to 0.09) | -0.04 (-0.21 to 0.14) | -0.11 (-0.28 to 0.06) | 0.05 (-0.27 to 0.36) |
| | 2 | 0.07 (-0.12 to 0.25) | -0.02 (-0.26 to 0.21) | 0.53 (-0.05 to 1.10) | 0.03 (-0.33 to 0.38) | 1.04 (0.37 to 1.70)** |
| Deep WMH shape features (Z-scores) ^b | | | | | | |
| Eccentricity, per +1 SD | 1 | 0.03 (-0.06 to 0.13) | 0.02 (-0.10 to 0.13) | -0.22 (-0.30 to 0.08) | 0.15 (-0.06 to 0.36) | 0.05 (-0.30 to 0.40) |
| | 2 | 0.02 (-0.07 to 0.11) | 0.01 (-0.11 to 0.13) | -0.13 (-0.32 to 0.07) | 0.13 (-0.08 to 0.34) | 0.02 (-0.33 to 0.38) |
| Fractal dimension, per +1 SD | 1 | 0.04 (-0.06 to 0.13) | 0.05 (-0.07 to 0.17) | -0.07 (-0.29 to 0.14) | 0.13 (-0.08 to 0.33) | -0.21 (-0.54 to 0.12) |
| | 2 | 0.04 (-0.05 to 0.14) | 0.05 (-0.07 to 0.17) | -0.07 (-0.29 to 0.15) | 0.15 (-0.06 to 0.35) | -0.19 (-0.52 to 0.15) |

Values are unstandardized linear regression coefficients with 95% confidence intervals.

Model 1: adjusted for age, sex, educational level, and reading ability. Model 2: model 1 with additional adjustment for natural log-transformed total WMH volume (%ICV).

WMH: white matter hyperintensities; %ICV: percentage of intracranial volume; SD: standard deviation.

^a Natural log-transformed total WMH volume (%ICV).

^b The +1 or -1 change in standard deviation denotes the direction of increasing shape complexity. E.g., lower solidity and higher concavity both indicate increasing shape complexity.

* $p \leq 0.05$; ** $p \leq 0.01$; *** $p \leq 0.001$.

Supplemental references

1. Zimmer Y, Tepper R, Akselrod S. An improved method to compute the convex hull of a shape in a binary image. *Pattern Recognit* 1997; 30: 397–402.
2. Liu EJ, Cashman KV, Rust AC. Optimising shape analysis to quantify volcanic ash morphology. *GeoResJ* 2015; 8: 14–30.
3. de Bresser J, Kuijff HJ, Zaanen K, Viergever MA, Hendrikse J, Biessels GJ, et al. White matter hyperintensity shape and location feature analysis on brain MRI; Proof of principle study in patients with diabetes. *Sci Rep* 2018; 8: 1–10.
4. Esteban FJ, Sepulcre J, de Miras JR, Navas J, de Mendizábal NV, Goñi J, et al. Fractal dimension analysis of grey matter in multiple sclerosis. *J Neurol Sci* 2009; 282: 67–71.
5. Zhang L, Liu JZ, Dean D, Sahgal V, Yue GH. A three-dimensional fractal analysis method for quantifying white matter structure in human brain. *J Neurosci Methods* 2006; 150: 242–53.
6. Murphy K, van Ginneken B, Schilham AMR, de Hoop BJ, Gietema HA, Prokop M. A large-scale evaluation of automatic pulmonary nodule detection in chest CT using local image features and k-nearest-neighbour classification. *Med Image Anal* 2009; 13: 757–70.
7. Loizou CP, Petroudi S, Seimenis I, Pantziaris M, Pattichis CS. Quantitative texture analysis of brain white matter lesions derived from T2-weighted MR images in MS patients with clinically isolated syndrome. *J Neuroradiol* 2015; 42: 99–114.



9

Reduced parenchymal cerebral blood flow is associated with greater progression of brain atrophy. The SMART-MR study

Rashid Ghaznawi, Maarten H.T. Zwartbol, Nicolaas P.A. Zuithoff, Jeroen de Bresser, Jeroen Hendrikse, Mirjam I. Geerlings, on behalf of the UCC-SMART Study Group

Published in *Journal of Cerebral Blood Flow and Metabolism* 2021; 41: 1229-39
doi: 10.1177/0271678X20948614

Abstract

Global cerebral hypoperfusion may be involved in the etiology of brain atrophy, however long-term longitudinal studies on this relationship are lacking. We examined whether reduced cerebral blood flow was associated with greater progression of brain atrophy.

Data was used of 1165 patients (61 ± 10 years) from the SMART-MR study, a prospective cohort study of patients with arterial disease, of whom 689 participated after 4 years and 297 again after 12 years. Attrition was substantial. Total brain volume and total cerebral blood flow were obtained from MRI scans and expressed as brain parenchymal fraction (BPF) and parenchymal cerebral blood flow (pCBF).

Mean decrease in BPF per year was 0.22 % total intracranial volume (95% CI:-0.23 to -0.21). Mean decrease in pCBF per year was 0.24 ml/min per 100 ml brain volume (95% CI:-0.29 to -0.20). Using linear mixed models, lower pCBF at baseline was associated with a greater decrease in BPF over time ($p = 0.01$). Lower baseline BPF, however, was not associated with a greater decrease in pCBF ($p = 0.43$).

These findings indicate that reduced cerebral blood flow is associated with greater progression of brain atrophy and provide further support for a role of cerebral blood flow in the process of neurodegeneration.

Introduction

Brain atrophy is a common finding on magnetic resonance imaging (MRI) in older individuals and individuals with manifest arterial disease.¹⁻³ Although brain atrophy occurs with normal ageing, previous studies have demonstrated that accelerated brain atrophy is associated with cognitive decline and dementia.⁴⁻⁸ The underlying causes that can lead to progression of brain atrophy, however, remain largely unknown.⁹

Reduced cerebral blood flow has been postulated as a possible risk factor for brain tissue loss.^{2, 10-13} In physiological conditions, cerebral blood flow is regulated by the cerebral vasculature in order to maintain an adequate delivery of oxygen and nutrients to the brain.¹⁴ Failure of these mechanisms can lead to a reduced cerebral blood flow, which has been associated with mortality and an increased risk of dementia in large cohort studies.^{15, 16} Whether these relationships are mediated by progression of brain atrophy is not known as few studies have reported on the relationship between cerebral blood flow and brain atrophy.^{2, 10-12} In addition, there is some evidence to suggest that the relationship between cerebral blood flow and brain atrophy may be bidirectional, such that smaller brain volumes are a risk factor for greater decline in cerebral blood flow.¹¹ Examining the long-term longitudinal relationship between cerebral blood flow and brain atrophy is of importance as cerebral blood flow can be modified and may pose a potential target for future prevention strategies of brain atrophy and dementia.¹⁷⁻¹⁹

In the current study, we examined the longitudinal relationship between cerebral blood flow and brain atrophy in a large cohort of patients with manifest arterial disease over 12 years of follow-up.

Methods

Study population

Data were used from the Second Manifestations of ARterial disease-Magnetic Resonance (SMART-MR) study, a prospective cohort study at the University Medical Center Utrecht with the aim to investigate risk factors and consequences of brain changes on MRI in patients with symptomatic arterial disease.²⁰ Between 2001 and 2005, 1309 middle-aged and older adult individuals newly referred to the University Medical Center Utrecht for treatment of symptomatic atherosclerotic disease (manifest coronary artery disease (59%), cerebrovascular disease (23%), peripheral arterial disease (22%) or abdominal aortic aneurysm (9%)) were included for baseline measurements, including a 1.5T brain MRI. Presence of neurodegenerative disease was not considered an exclusion criterion. Of these, 754 persons had follow-up measurements four years later between January 2006 and May 2009. During a one-day visit to our medical center, a physical examination, ultrasonography of the carotid arteries to measure the intima-media thickness (mm), blood

and urine samplings, neuropsychological assessment and a 1.5T brain MRI scan were performed. The height and weight were measured, and the body mass index (kg/m^2) was calculated. Questionnaires were used for the assessment of demographics, risk factors, medical history, medication use and cognitive and physical functioning. Since November 2013, all patients alive were invited for a second follow-up, including a 1.5T brain MRI, of which 329 persons had second follow-up measurements between November 2013 and October 2017. A flowchart of the SMART-MR study is shown in Figure 1.

The SMART-MR study was approved by the medical ethics committee of the University Medical Center Utrecht according to the guidelines of the Declaration of Helsinki of 1975 and written informed consent was obtained from all patients.

Vascular risk factors

At baseline, age, sex, smoking habits and alcohol intake were assessed with questionnaires. Height and weight were measured, and the body mass index (BMI) was calculated (kg/m^2). Systolic blood pressure (SBP) (mmHg) and diastolic blood pressure (DBP) (mmHg) were measured three times with a sphygmomanometer, and the average of these measures was calculated. Hypertension was defined as a mean SBP of >160 mmHg, a mean DBP of >95 mmHg or self-reported use of antihypertensive drugs. An overnight fasting venous blood sample was taken to determine glucose and lipids. Diabetes mellitus was defined as fasting serum glucose levels of ≥ 7.0 mmol/l, and/or use of glucose-lowering medication, and/or a known history of diabetes. Ultrasonography was performed with a 10MHz linear-array transducer (ATL Ultramark 9) and the degree of the carotid artery stenosis at both sides was assessed with color Doppler-assisted duplex scanning. The severity of carotid artery stenosis was evaluated on the basis of blood flow velocity patterns and the greatest stenosis observed on the right or the left side of the common or internal carotid artery was taken to determine the severity of carotid artery disease. Carotid artery stenosis $\geq 70\%$ was defined as peak systolic velocity >210 cm/s.²¹

MRI protocol

MR imaging of the brain was performed on a 1.5T whole-body system (Gyrosan ACS-NT, Philips Medical Systems, Best, the Netherlands) using a standardized scan protocol.²⁰ Transversal T1-weighted [repetition time (TR) = 235 ms; echo time (TE) = 2 ms], T2-weighted [TR = 2200 ms; TE = 11 ms], fluid-attenuated inversion recovery (FLAIR) [TR = 6000 ms; TE = 100 ms; inversion time (TI) = 2000 ms] and T1-weighted inversion recovery images [TR = 2900 ms; TE = 22 ms; TI = 410 ms] were acquired with a voxel size of $1.0 \times 1.0 \times 4.0$ mm³ and contiguous slices. For cerebral blood flow measurements, a 2-dimensional phase-contrast section was positioned at the level of the skull base to measure the volume flow in the basilar artery and in the internal carotid arteries on the basis of a localizer MR angiographic slab in the sagittal plane.²² The 2-dimensional phase-contrast section was positioned through the basilar artery and the internal carotid arteries (TR/TE, 16/9 milliseconds;

flip angle 75°; FOV 250 x 250 mm; matrix size 256 x 256; slice thickness 5.0 mm; 8 acquired signals; velocity sensitivity 100 cm/s).

Cerebral blood flow measurements

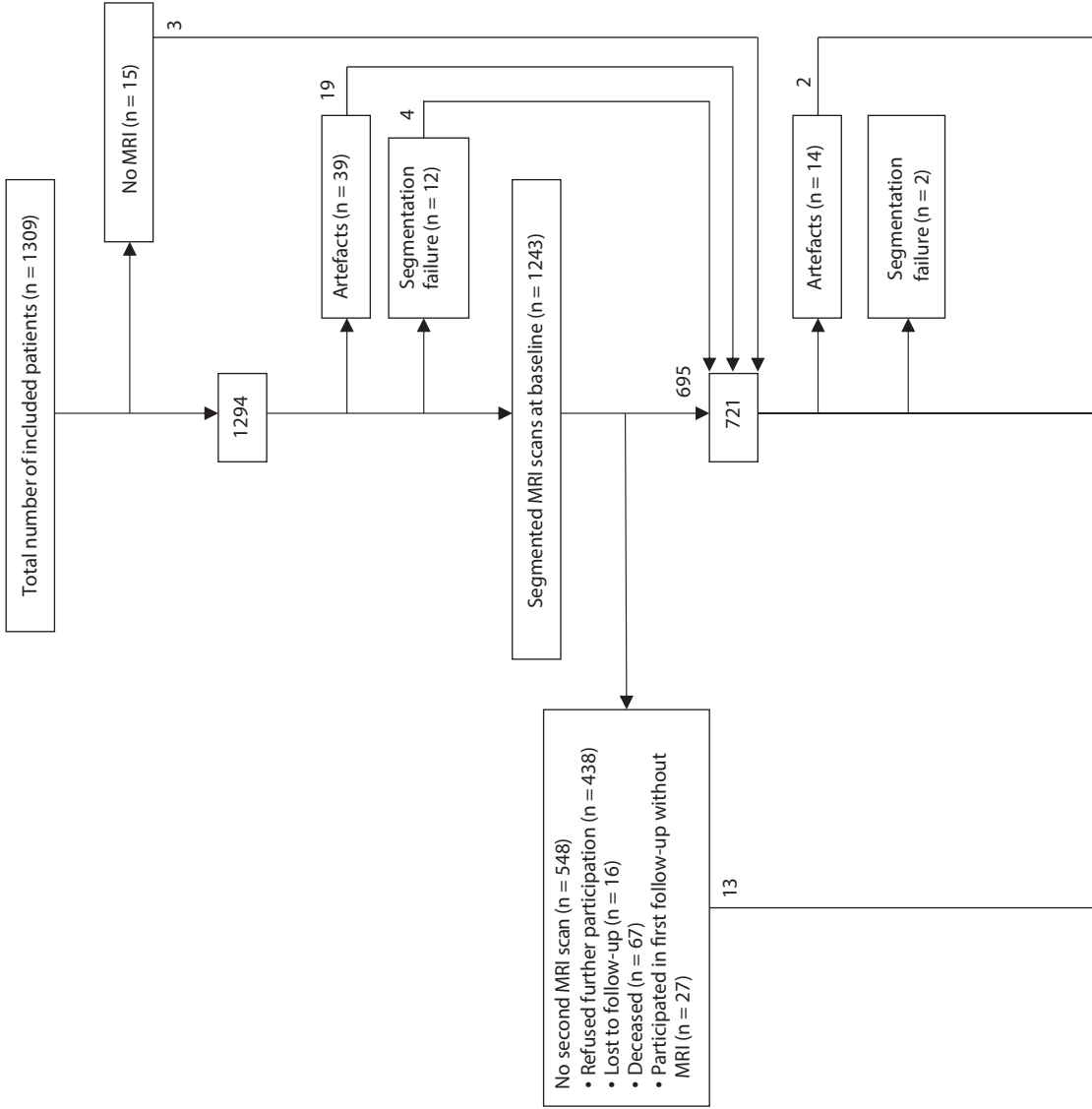
Phase-contrast MR angiography was used to measure total cerebral blood flow, as this method has been demonstrated to be a fast, reproducible, and noninvasive method to measure total cerebral blood flow in large cohorts.^{23, 24} Previous studies established that phase-contrast MR angiography correlates well with arterial spin-labeled perfusion MRI, although estimates tend to be somewhat higher and more variable than arterial spin-labeled perfusion MRI.²⁵ Post processing of the flow measurements was performed by investigators blinded to patient characteristics. The flow through the basilar and internal carotid arteries was summed to calculate the total cerebral blood flow. Total cerebral blood flow was expressed per 100 ml brain parenchymal volume to obtain parenchymal cerebral blood flow (pCBF).¹⁶ Parenchymal CBF was measured at baseline, and at the first and second follow-up visits.

Brain volume measurements

White matter hyperintensity (WMH) volumes and brain volumes were obtained using the *k*-nearest neighbor (kNN) automated segmentation program on the T1-weighted, FLAIR, and T1-weighted inversion recovery sequences of the MRI scans.²⁶ The kNN segmentation method has been shown to be suitable for detecting longitudinal brain volume changes.^{20, 27} All WMH segmentations were visually checked by an investigator (RG) using an image processing framework (MeVisLab 2.7.1., MeVis Medical Solutions AG, Bremen, Germany) to ensure that brain infarcts were correctly removed from the WMH segmentations. Incorrectly segmented voxels were added to the correct segmentation volumes using the image processing framework. Periventricular WMH were defined as lesions ≤1 cm of the lateral ventricles and deep WMH were defined as lesions that were located >1 cm of the lateral ventricles. Total brain volume was calculated by summing the volumes of gray matter, white matter, total WMH and, if present, the volumes of brain infarcts. Total intracranial volume (ICV) was calculated by summing the total brain volume and the volume of the cerebrospinal fluid. Total brain volume was normalized for ICV and expressed as brain parenchymal fraction (BPF). Brain volumes were measured at baseline, and at the first and second follow-up visits.

Brain infarcts

Brain infarcts were visually rated by a neuroradiologist blinded to patient characteristics on the T1-weighted, T2-weighted and FLAIR images of the MRI scans. Lacunes were defined as focal lesions between 3 to 15 mm according to the STRIVE criteria²⁸, whereas non-lacunar lesions were divided into large infarcts (i.e. cortical infarcts and subcortical infarcts not involving the cerebral cortex) and those located in the cerebellum or brain stem.



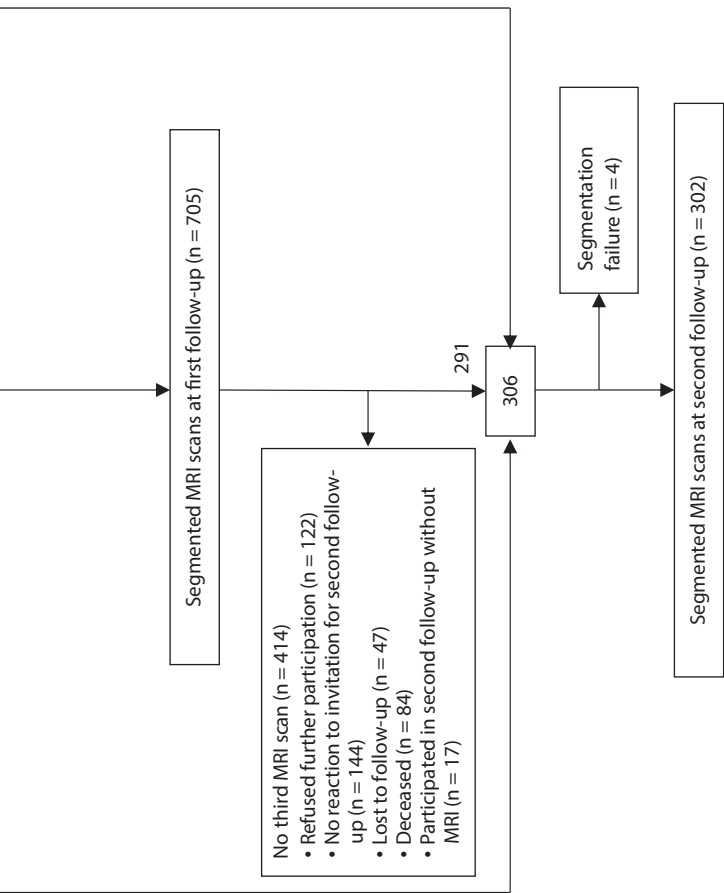


Figure 1. MRI participation flowchart of the SMART-MR study. Numbers in the boxes represent the numbers of patients who underwent a 1.5T MRI at each time point.

Study sample

At baseline, 1165 patients had both pCBF and BPF measurements, whereas this was the case for 689 and 297 patients at the first and second follow-up, respectively. The study sample included patients with consecutive and non-consecutive pCBF and/or BPF measurements.

Statistical analysis

Baseline characteristics of patients with BPF and pCBF measurements at baseline ($n = 1165$) were reported as means or percentages where applicable. Baseline characteristics of patients with follow-up measurements and those without were compared using an independent samples *t*-test and Chi square test for continuous and dichotomous variables, respectively.

Linear mixed models were used to analyze change in BPF and change in pCBF over time.^{29, 30} As the time intervals between MRI measurements differed between patients, the age of patients at the MRI measurements was chosen as the time variable. Age was centered on 61 years, the mean value at which the first MRI measurement was performed. BPF and pCBF were analyzed per standard deviation decrease. To minimize the risk of bias due to complete case analysis, chained equations imputation was performed on missing covariates to generate 10 imputed datasets using SPSS 25.0 (Chicago, IL, USA).³¹ The statistical analyses were performed on these datasets and pooled results were presented. In chained equations imputation, linear and logistic regression is used to impute continuous and categorical covariates, respectively, using other covariates as predictors.³¹

First, we modeled longitudinal measurements of BPF (dependent variable) with pCBF as time-varying predictor, with age at time of MRI as the time-scale and adjusted for baseline age and sex. In a second model, we additionally adjusted for large infarcts, lacunes and WMH volume on MRI, diastolic blood pressure, hypertension, carotid stenosis $\geq 70\%$, body mass index and smoking pack years at baseline. To determine whether baseline pCBF was a risk factor for subsequent BPF decline, we modeled change in BPF with baseline pCBF. Baseline pCBF, time, baseline age, sex and the interaction between baseline pCBF and time were entered in a model. Next, we additionally adjusted for large infarcts, lacunes and WMH volume on MRI, hypertension, diabetes mellitus, carotid stenosis $\geq 70\%$, body mass index and smoking pack years at baseline.

Second, we modeled longitudinal measurements of pCBF (dependent variable) with BPF as time-varying predictor with age at time of MRI as the time-scale and adjusted for baseline age and sex. In a second model, we additionally adjusted for large infarcts, lacunes and WMH volume on MRI, hypertension, diabetes mellitus, carotid stenosis $\geq 70\%$, body mass index and smoking pack years at baseline. To determine whether baseline BPF was a risk factor for subsequent pCBF decline, we modeled change in pCBF with baseline BPF. Next, we additionally adjusted for large infarcts, lacunes and WMH volume on MRI, hypertension, diabetes mellitus, carotid stenosis $\geq 70\%$, body mass index and smoking pack years at baseline.

In all models, a random intercept and random slope with time was assumed, meaning that the models accounted for individual variation in the starting level of BPF or pCBF (intercept) and in change of BPF or pCBF over time (slope), respectively. Adequacy of all models was determined by examining the residuals for homoscedasticity and normality.³² We concluded that model assumptions were adequately met. Statistical significance was set at $p \leq 0.05$. Due to the exploratory nature of the analyses, no adjustment of p values was made for multiple comparison. SAS 9.4 (SAS Institute, Cary, NC, USA) and SPSS 25.0 (Chicago, IL, USA) were used to perform the statistical analyses.

As sensitivity analyses, we assumed a fixed slope with time and repeated the analyses with baseline pCBF as predictor and change in BPF as outcome, and with baseline BPF as predictor and change in pCBF as outcome. In addition, to examine whether multiple imputation affected the results, we repeated the analyses in patients without missing data (i.e., complete case analysis). Lastly, to examine the effect of attrition on the results of the longitudinal analyses, we hypothesized that dropout due to death may represent a form of informative dropout. We examined the effect of dropout due to death on the results of the linear mixed models using a joint modelling approach that includes a time-to-event submodel.³³ For the time-to-event submodel, data on occurrence of death and survival times was obtained from questionnaires that patients received biannually. Acquisition of data relating to occurrence of death and survival times is described in detail elsewhere.³⁴ The JM package for R version 3.6.3 (R Core Team, 2019) was used to perform the joint model analysis.³³

Results

Baseline characteristics of the study sample ($n = 1165$) are shown in Table 1. The mean age at baseline was 61 ± 10 years and 80% was male. Mean pCBF was 51.4 ± 10.6 ml/min per 100 ml brain volume.

Mean time between baseline and first follow-up measurements for patients with available pCBF and BPF data ($n = 689$) was 3.9 ± 0.4 years (range 2.9 – 5.8 years). Mean time between the first follow-up and second follow-up measurements for patients with available pCBF and BPF data ($n = 297$) was 8.2 ± 0.4 years (range 7.3 – 9.5 years). Mean time between baseline and the second follow-up measurements was 12.0 ± 0.4 years (range 11.1 – 13.5 years) for patients with available pCBF and BPF data on the second follow-up ($n = 297$). Mean decrease in BPF per year for the study sample was 0.22 % ICV (95% CI: -0.23 to -0.21). Mean decrease in pCBF per year was 0.24 ml/min per 100 ml brain volume (95% CI: -0.29 to -0.20).

Patients with follow-up measurements ($n = 754$) were younger ($p < 0.001$), more often male ($p = 0.011$), had more often current alcohol use ($p = 0.001$), had less often hypertension ($p = 0.001$), diabetes mellitus ($p < 0.001$) and carotid artery stenosis $\geq 70\%$ ($p = 0.04$), and had a

Table 1. Characteristics of the study population with available pCBF and BPF data at baseline (n = 1165).

| | |
|--------------------------------------|----------------|
| Age (years) | 61 ± 10 |
| Sex, % men | 80.3 |
| History of stroke, % | 23.3 |
| BMI (kg/m ²) | 27 ± 4 |
| Smoking, pack years ^a | 19 (0, 50) |
| Alcohol use, % | |
| Current | 75.0 |
| Former | 8.7 |
| Never | 16.3 |
| Hypertension, % | 50.9 |
| Diabetes mellitus, % | 20.6 |
| Carotid artery stenosis ≥70%, % | 10.6 |
| Infarcts on MRI, % | |
| Large | 12.2 |
| Cerebellar | 4.0 |
| Brainstem | 2.9 |
| Lacunes on MRI, % | 18.5 |
| WMH volumes on MRI, ml ^a | |
| Total | 0.9 (0.2, 6.5) |
| Periventricular | 0.6 (0.1, 4.2) |
| Deep | 0.3 (0.0, 2.5) |
| BPF, % ICV | 79.0 ± 2.9 |
| pCBF, ml/min per 100 ml brain volume | 51.4 ± 10.6 |

Characteristics are presented as mean ± SD or %.

^a Median (10th percentile, 90th percentile).

BMI: body mass index; SD: standard deviation; WMH: white matter hyperintensity; BPF: brain parenchymal fraction; ICV: total intracranial volume; pCBF: parenchymal cerebral blood flow.

greater BPF ($p < 0.001$) and smaller WMH volumes on MRI ($p < 0.001$) compared to patients without follow-up measurements (n = 555) (Table 2).

Time-varying pCBF as a predictor of time-varying BPF

Lower pCBF was associated with lower BPF at baseline and follow-up, adjusted for age and sex. Specifically, each standard deviation decrease in pCBF at a given time point was associated with an additional 0.10 % ICV lower BPF at that given time point (95% CI: -0.17

Table 2. Baseline characteristics of the study population (n = 1309) according to participation in follow-up visits.

| | Patients with one or two follow-up visits (n = 754) | Patients without follow-up visits (n = 555) | p value |
|--------------------------------------|---|---|---------------------|
| Age (years) | 58 ± 9 | 60 ± 11 | <0.001 |
| Sex, % men | 82.1 | 76.4 | 0.011 |
| History of stroke, % | 23.7 | 22.2 | 0.503 |
| BMI (kg/m ²) | 27 ± 4 | 27 ± 4 | 0.568 |
| Smoking, pack years ^a | 20 (0, 49) | 17 (0, 53) | 0.253 ^b |
| Alcohol use, % current | 79 | 70 | 0.001 |
| Hypertension, % | 47.9 | 57.3 | 0.001 |
| Diabetes mellitus, % | 16.3 | 27.1 | <0.001 |
| Carotid artery stenosis ≥70%, % | 9.6 | 13.3 | 0.04 |
| Infarcts on MRI, % | | | |
| Large | 11.3 | 14.0 | 0.152 |
| Cerebellar | 3.8 | 4.5 | 0.528 |
| Brainstem | 2.7 | 3.2 | 0.490 |
| Lacunes on MRI, % | 17.3 | 20.7 | 0.117 |
| WMH volumes on MRI, ml ^a | | | |
| Total | 0.8 (0.2, 4.8) | 1.1 (0.3, 8.8) | <0.001 ^b |
| Periventricular | 0.5 (0.1, 3.0) | 0.8 (0.1, 5.7) | <0.001 ^b |
| Deep | 0.2 (0.0, 2.1) | 0.3 (0.0, 3.6) | <0.001 ^b |
| BPF, % ICV | 79.3 ± 2.6 | 78.5 ± 3.2 | <0.001 |
| pCBF, ml/min per 100 ml brain volume | 51.6 ± 10.4 | 51.0 ± 10.9 | 0.336 |

Characteristics are presented as mean ± SD or %.

^a Median (10th percentile, 90th percentile).

^b Natural log-transformed due to a non-normal distribution in the statistical analysis.

BMI: body mass index; SD: standard deviation; WMH: white matter hyperintensity; BPF: brain parenchymal fraction; ICV: total intracranial volume; pCBF: parenchymal cerebral blood flow.

to -0.04, $p = 0.001$). This relationship remained statistically significant after adjusting for large infarcts, lacunes and WMH volume on MRI, hypertension, diabetes mellitus, carotid stenosis ≥70%, body mass index, alcohol use and smoking pack years at baseline ($B = -0.09$ % ICV, 95% CI: -0.15 to -0.03, $p = 0.005$).

Baseline pCBF as a predictor of longitudinal BPF

Adjusted for age and sex, lower baseline pCBF was associated with greater subsequent decreases in BPF. Specifically, each standard deviation decrease in baseline pCBF was associated with an additional 0.01 % ICV decrease per year in BPF (95% CI: -0.02 to -0.004, $p = 0.004$) (Table 3). This relationship remained statistically significant after adjusting for large infarcts, lacunes and WMH volume on MRI, hypertension, diabetes mellitus, carotid stenosis $\geq 70\%$, body mass index, alcohol use and smoking pack years at baseline ($B = -0.01$ % ICV, 95% CI: -0.02 to -0.003, $p = 0.010$).

Time-varying BPF as a predictor of time-varying pCBF

Lower BPF was associated with lower pCBF at baseline and follow-up, adjusted for age and sex. Each standard deviation decrease in BPF at a given time point was associated with an additional 0.90 ml/min per 100 ml brain volume lower pCBF at that given time point (95% CI: -1.57 to -0.24, $p = 0.008$). The estimate attenuated and lost statistical significance after adjusting for large infarcts, lacunes and WMH volume on MRI, hypertension, diabetes mellitus, carotid stenosis $\geq 70\%$, body mass index, alcohol use and smoking pack years at baseline ($B = -0.58$ ml/min per 100 ml brain volume, 95% CI: -1.28 to 0.12, $p = 0.104$).

Baseline BPF as a predictor of longitudinal pCBF

Adjusted for age and sex, lower baseline BPF was not associated with greater subsequent decreases in pCBF ($B = 0.02$ ml/min per 100 ml brain volume, 95% CI: -0.03 to 0.07, $p = 0.439$) (Table 4). This relationship did not change after adjusting for large infarcts, lacunes and WMH volume on MRI, hypertension, diabetes mellitus, carotid stenosis $\geq 70\%$, body mass index, alcohol use and smoking pack years at baseline ($B = 0.02$ ml/min per 100 ml brain volume, 95% CI: -0.03 to 0.07, $p = 0.429$).

Sensitivity analyses

Lower baseline pCBF was associated with a greater subsequent decrease in BPF when assuming a fixed slope with time or when performing the analysis only in patients without missing data, adjusted for age, sex, large infarcts, lacunes and WMH volume on MRI, hypertension, diabetes mellitus, carotid stenosis $\geq 70\%$, body mass index, alcohol use and smoking pack years at baseline (Supplementary Table 1 and Supplementary Table 2, respectively). Baseline BPF was not associated with change in pCBF over time when assuming a fixed slope with time or when performing the analysis only in patients without missing data.

A total of 167 patients (14%) died during the study. Accounting for dropout due to death, lower baseline pCBF was associated with a greater subsequent decline in BPF ($B = -0.02$, 95% CI: -0.03 to -0.002, $p = 0.009$) in a joint model that included age, sex, large infarcts, lacunes, WMH volume, hypertension, diabetes mellitus, carotid stenosis $\geq 70\%$,

Table 3. Results of the linear mixed model with BPF as dependent variable and baseline pCBF as independent variable. Estimates represent fixed effects of the linear mixed model with their 95% confidence intervals for a 1 unit increase of a continuous variable or presence of a dichotomous variable unless stated otherwise.

| | Model 1 | | Model 2 | |
|--------------------------------|-------------------------|---------|-------------------------|---------|
| | Estimate (95% CI) | p value | Estimate (95% CI) | p value |
| Intercept | 78.50 (78.35 to 78.64) | <0.001 | 78.61 (77.71 to 79.51) | <0.001 |
| Baseline pCBF ^a | -0.19 (-0.32 to -0.07) | 0.002 | -0.12 (-0.24 to 0.00) | 0.051 |
| Rate of change | | | | |
| Time ^b | -0.24 (-0.25 to -0.22) | <0.001 | -0.23 (-0.25 to -0.22) | <0.001 |
| Time x baseline pCBF | -0.01 (-0.02 to -0.004) | 0.004 | -0.01 (-0.02 to -0.003) | 0.010 |
| Age ^b | -0.04 (-0.06 to -0.03) | <0.001 | -0.05 (-0.07 to -0.04) | <0.001 |
| Sex ^c | 0.90 (0.59 to 1.21) | <0.001 | 0.86 (0.55 to 1.17) | <0.001 |
| Large infarcts on MRI | - | | -0.61 (-1.00 to -0.20) | 0.003 |
| Lacunes on MRI | - | | -0.60 (-0.94 to -0.26) | <0.001 |
| WMH volume on MRI ^d | - | | -0.01 (-0.11 to 0.09) | 0.836 |
| Hypertension | - | | -0.19 (-0.43 to 0.05) | 0.117 |
| Diabetes mellitus | - | | -1.05 (-1.35 to -0.74) | <0.001 |
| Carotid stenosis ≥70% | - | | -0.17 (-0.61 to 0.27) | 0.460 |
| Body mass index | - | | 0.03 (-0.01 to 0.06) | 0.109 |
| Smoking pack years | - | | -0.01 (-0.02 to -0.01) | <0.001 |
| Alcohol use | | | | |
| Current | - | | 0 (reference) | - |
| Former | - | | -0.41 (-0.84 to 0.01) | 0.056 |
| Never | - | | 0.06 (-0.28 to 0.40) | 0.728 |

Model 1: adjusted for age and sex.

Model 2: additionally adjusted for large infarcts on MRI, lacunes on MRI, WMH volume on MRI, hypertension, diabetes mellitus, carotid stenosis ≥70%, body mass index, alcohol use and smoking pack years at baseline. ICC model 1: 0.87. ICC model 2: 0.86. Marginal R² Model 1: 0.48. Conditional R² Model 1: 0.94. Marginal R² Model 2: 0.53. Conditional R² Model 2: 0.94.

^a Per standard deviation decrease.

^b Per year increase.

^c Females vs. males.

^d Natural log-transformed due to a non-normal distribution and normalized for total intracranial volume.

BPF: brain parenchymal fraction, pCBF: parenchymal cerebral blood flow, CI: confidence interval, WMH: white matter hyperintensity.

Table 4. Results of the linear mixed model with pCBF as dependent variable and baseline BPF as independent variable. Estimates represent fixed effects of the linear mixed model with their 95% confidence intervals for a 1 unit increase of a continuous variable or presence of a dichotomous variable unless stated otherwise.

| | Model 1 | | Model 2 | |
|--------------------------------|------------------------|---------|------------------------|---------|
| | Estimate (95% CI) | p value | Estimate (95% CI) | p value |
| Intercept | 50.31 (49.57 to 51.06) | <0.001 | 51.56 (47.46 to 55.67) | <0.001 |
| Baseline BPF ^a | -0.48 (-1.20 to 0.37) | 0.185 | -0.06 (-0.80 to 0.67) | 0.868 |
| Rate of change | | | | |
| Time ^b | -0.35 (-0.45 to -0.26) | <0.001 | -0.36 (-0.45 to -0.27) | <0.001 |
| Time x baseline BPF | 0.02 (-0.03 to 0.07) | 0.439 | 0.02 (-0.03 to 0.07) | 0.429 |
| Age ^b | -0.18 (-0.30 to -0.07) | <0.001 | -0.22 (-0.34 to -0.11) | <0.001 |
| Sex ^c | 3.56 (2.22 to 4.89) | <0.001 | 4.17 (2.78 to 5.55) | <0.001 |
| Large infarcts on MRI | - | | -1.40 (-3.17 to 0.37) | 0.121 |
| Lacunes on MRI | - | | 0.68 (-0.81 to 2.17) | 0.371 |
| WMH volume on MRI ^d | - | | -0.50 (-0.97 to -0.04) | 0.034 |
| Hypertension | - | | -1.32 (-2.39 to -0.24) | 0.016 |
| Diabetes mellitus | - | | -0.36 (-1.74 to 1.02) | 0.609 |
| Carotid stenosis ≥70% | - | | -4.98 (-6.88 to -3.08) | <0.001 |
| Body mass index | - | | -0.06 (-0.21 to 0.08) | 0.410 |
| Smoking pack years | - | | 0.02 (-0.01 to 0.04) | 0.184 |
| Alcohol use | | | | |
| Current | - | | 0 (reference) | |
| Former | - | | -1.28 (-3.21 to 0.64) | 0.191 |
| Never | - | | 0.45 (-1.05 to 1.96) | 0.556 |

Model 1: adjusted for age and sex.

Model 2: additionally adjusted for large infarcts on MRI, lacunes on MRI, WMH volume on MRI, hypertension, diabetes mellitus, carotid stenosis ≥70%, body mass index, alcohol use and smoking pack years at baseline. ICC model 1: 0.54. ICC model 2: 0.52. Marginal R² Model 1: 0.27. Conditional R² Model 1: 0.65. Marginal R² Model 2: 0.33. Conditional R² Model 2: 0.65.

^a Per standard deviation decrease.

^b Per year increase.

^c Females vs. males.

^d Natural log-transformed due to a non-normal distribution and normalized for total intracranial volume.

pCBF: parenchymal cerebral blood flow, BPF: brain parenchymal fraction, CI: confidence interval, WMH: white matter hyperintensity.

body mass index, alcohol use and smoking pack years at baseline as covariates in the linear mixed and time-to-event submodels.

Discussion

In this cohort of patients with manifest arterial disease, we observed that a reduced pCBF was associated with smaller total brain volumes, and that smaller total brain volumes were associated with reduced pCBF throughout the follow-up period of 12 years. Reduced pCBF at baseline was associated with a greater subsequent decline in BPF in a model that controlled for sex, cardiovascular risk factors, brain infarcts and small vessel disease. However, reduced BPF at baseline was not associated with a greater decline in pCBF.

Our finding that lower pCBF was associated with lower BPF at baseline and at follow-up is in line with previous cross-sectional studies that reported smaller total brain volumes in patients with reduced cerebral blood flow.^{12, 13, 35} A study in patients with a history of arterial disease found a significant correlation between total cerebral blood flow measured using phase-contrast MR angiography and total brain volume.¹³ Similarly, a smaller population-based study revealed that decreased total brain perfusion measured using arterial spin labeling MRI was associated with smaller total brain volumes.¹² A study comparing patients with Alzheimer's disease with age-matched controls showed that reduced total cerebral blood flow was associated with smaller total brain volumes only in patients with Alzheimer's disease, whereas this relation was not found in the control group.³⁵ To our knowledge, only one previous study reported on the longitudinal relationship between cerebral blood flow and total brain volume.¹¹ In this population-based cohort study, reduced total cerebral blood flow was associated with greater progression of brain atrophy only in older patients, whereas a smaller brain volume at baseline was associated with a steeper decrease in total cerebral blood flow in the whole population.¹¹ Direct comparison with the findings of the present study, however, is only possible to a limited extent due to the shorter follow-up period and the use of total cerebral blood flow instead of pCBF.

We found that reduced baseline pCBF was significantly associated with greater decline in BPF, however the effect size was modest when taking into account the estimated mean annual decline in BPF. A number of remarks should be made with respect to this finding. First, the volumetric technique used in our study did not allow us to measure region-specific brain volume changes. Recent cross-sectional studies using arterial spin labeling and dynamic-susceptibility contrast MRI reported regional effects of reduced cerebral blood flow on specific brain volumes, predominantly the temporal lobes.^{12, 35, 36} Similarly, the use of phase-contrast MR angiography did not allow us to measure region-specific cerebral blood flow. It is therefore possible that the association between pCBF and progression of brain atrophy in the present study reflects regional effects of

cerebral blood flow on specific brain regions. Second, the longitudinal analysis included patients with multiple BPF measurements, and these patients may represent a healthier group, which may have led to an underestimation of the association of pCBF with progression of brain atrophy. Nonetheless, the significant longitudinal relationship between pCBF and BPF in the present study supports a role of cerebral blood flow in the process of neurodegeneration and, from a clinical perspective, strengthens the notion that cerebral blood flow could be a potential target for future prevention strategies of brain atrophy.¹⁷⁻¹⁹

In the present study, we chose a bidirectional modelling approach between pCBF and BPF for the following reasons. First, although experimental studies using animal models suggest that reduced cerebral blood flow may be a risk factor for brain tissue loss³⁷, some studies hypothesized that smaller brain volumes may lead to reduced metabolic demand, which in turn may lead to a greater decrease in cerebral blood flow over time.³⁸ Second, a previous longitudinal study with a shorter follow-up period reported that smaller brain volumes at baseline were associated with a greater decline in cerebral blood flow.¹¹ The results of the present study, however, provide support for the notion that reduced pCBF is a risk factor for greater subsequent brain atrophy.

Strengths of the present study are the longitudinal design with pCBF and BPF measurements at three time points, the large sample size and the relatively long follow-up period. In addition, the detailed information on cardiovascular risk factors and cerebrovascular lesions allowed us to adjust for these possible confounders in the association between pCBF and BPF over time. Also, we used a statistical modelling approach that allowed patients to have a variable number of measurements and accounted for differences in time intervals between measurements.

Limitations are, first, that cerebral autoregulatory mechanisms to maintain adequate cerebral blood flow and cardiac output were not considered in this study, which is a major limitation. Second, as mentioned above, the volumetric technique used in our study did not allow us to measure region-specific brain volume changes and phase-contrast MR angiography did not allow region-specific assessment of blood flow, which is likely more sensitive in detecting associations with brain atrophy. Third, volumetry was performed on MRI sequences with a slice thickness of 4 mm instead of 1 mm, which is more sensitive in detecting brain volume changes. Fourth, our study sample consisted of mostly males with a relatively young age and a history of arterial disease, which may limit the generalizability of our results. Lastly, although the MRI scan protocol did not change throughout the study, each patient was not necessarily scanned using the exact same MRI scanner over time and scanner stability was not determined.

In conclusion, our findings demonstrate that reduced parenchymal cerebral blood flow is independently associated with greater progression of brain atrophy in patients with manifest arterial disease. These findings provide further support for a role of cerebral blood flow in the process of neurodegeneration.

References

1. Resnick SM, Pham DL, Kraut MA, et al. Longitudinal magnetic resonance imaging studies of older adults: a shrinking brain. *J Neurosci* 2003; 23: 3295–3301.
2. Appelman AP, van der Graaf Y, Vincken KL, et al. Total cerebral blood flow, white matter lesions and brain atrophy: the SMART-MR study. *J Cereb Blood Flow Metab* 2008; 28: 633–39.
3. Enzinger C, Fazekas F, Matthews PM, et al. Risk factors for progression of brain atrophy in aging: six-year follow-up of normal subjects. *Neurology* 2005; 64: 1704–11.
4. Jack CR, Jr, Shiung MM, Gunter JL, et al. Comparison of different MRI brain atrophy rate measures with clinical disease progression in AD. *Neurology* 2004; 62: 591–600.
5. Jack CR, Jr, Shiung MM, Weigand SD, et al. Brain atrophy rates predict subsequent clinical conversion in normal elderly and amnesic MCI. *Neurology* 2005; 65: 1227–31.
6. Kramer JH, Mungas D, Reed BR, et al. Longitudinal MRI and cognitive change in healthy elderly. *Neuropsychology* 2007; 21: 412–18.
7. Silbert LC, Quinn JF, Moore MM, et al. Changes in premorbid brain volume predict Alzheimer's disease pathology. *Neurology* 2003; 61: 487–92.
8. Fox NC, Scahill RI, Crum WR, et al. Correlation between rates of brain atrophy and cognitive decline in AD. *Neurology* 1999; 52: 1687–89.
9. Raz N, Kennedy KM. *A Systems Approach to the Aging Brain: Neuroanatomic Changes, Their Modifiers, and Cognitive Correlates, in Imaging the Aging Brain*. New York: Oxford Academic; 2010.
10. Kitagawa Y, Meyer JS, Tanahashi N, et al. Cerebral blood flow and brain atrophy correlated by xenon contrast CT scanning. *Comput Radiol* 1985; 9: 331–40.
11. Zonneveld HI, Loehrer EA, Hofman A, et al. The bidirectional association between reduced cerebral blood flow and brain atrophy in the general population. *J Cereb Blood Flow Metab* 2015; 35: 1882–87.
12. Alosco ML, Gunstad J, Jerskey BA, et al. The adverse effects of reduced cerebral perfusion on cognition and brain structure in older adults with cardiovascular disease. *Brain Behav* 2013; 3: 626–36.
13. van Es AC, van der Grond J, ten Dam VH, et al. Associations between total cerebral blood flow and age related changes of the brain. *PLoS One* 2010; 5: e9825.
14. van Beek AH, Claassen JA, Rikkert MG, et al. Cerebral autoregulation: an overview of current concepts and methodology with special focus on the elderly. *J Cereb Blood Flow Metab* 2008; 28: 1071–85.
15. Sabayan B, van der Grond J, Westendorp RG, et al. Total cerebral blood flow and mortality in old age: a 12-year follow-up study. *Neurology* 2013; 81: 1922–29.
16. Wolters FJ, Zonneveld HI, Hofman A, et al. Cerebral Perfusion and the Risk of Dementia: A Population-Based Study. *Circulation* 2017; 136: 719–28.
17. Espeland MA, Luchsinger JA, Neiberg RH, et al. Long Term Effect of Intensive Lifestyle Intervention on Cerebral Blood Flow. *J Am Geriatr Soc* 2018; 66: 120–26.
18. Muller M, van der Graaf Y, Visseren FL, et al. Hypertension and longitudinal changes in cerebral blood flow: the SMART-MR study. *Ann Neurol* 2012; 71: 825–33.
19. de la Torre JC. Cerebral Perfusion Enhancing Interventions: A New Strategy for the Prevention of Alzheimer Dementia. *Brain Pathol* 2016; 26: 618–31.
20. Geerlings MI, Appelman AP, Vincken KL, et al. Brain volumes and cerebrovascular lesions on MRI in patients with atherosclerotic disease. The SMART-MR study. *Atherosclerosis* 2010; 210: 130–36.
21. Muller M, van der Graaf Y, Algra A, et al. Carotid atherosclerosis and progression of brain atrophy: the SMART-MR study. *Ann Neurol* 2011; 70: 237–44.
22. Bakker CJ, Kouwenhoven M, Hartkamp MJ, et al. Accuracy and precision of time-averaged flow as measured by nontriggered 2D phase-contrast MR angiography, a phantom evaluation. *Magn Reson Imaging* 1995; 13: 959–65.
23. Vernooij MW, van der Lugt A, Ikram MA, et al. Total cerebral blood flow and total brain perfusion in the general population: the Rotterdam Scan Study. *J Cereb Blood Flow Metab* 2008; 28: 412–19.
24. Spilt A, Box FM, van der Geest RJ, et al. Reproducibility of total cerebral blood flow measurements using phase contrast magnetic resonance imaging. *J Magn Reson Imaging* 2002; 16: 1–5.

25. Dolui S, Wang Z, Wang DJJ, et al. Comparison of non-invasive MRI measurements of cerebral blood flow in a large multisite cohort. *J Cereb Blood Flow Metab* 2016; 36: 1244–56.
26. Anbeek P, Vincken KL, van Bochove GS, et al. Probabilistic segmentation of brain tissue in MR imaging. *Neuroimage* 2005; 27: 795–804.
27. de Boer R, Vrooman HA, Ikram MA, et al. Accuracy and reproducibility study of automatic MRI brain tissue segmentation methods. *Neuroimage* 2010; 51: 1047–56.
28. Wardlaw JM, Smith EE, Biessels GJ, et al. Neuroimaging standards for research into small vessel disease and its contribution to ageing and neurodegeneration. *Lancet Neurol* 2013; 12: 822–38.
29. Carmichael O, Schwarz C, Drucker D, et al. Longitudinal changes in white matter disease and cognition in the first year of the Alzheimer disease neuroimaging initiative. *Arch Neurol* 2010; 67: 1370–78.
30. Benedictus MR, Leeuwis AE, Binnewijzend MA, et al. Lower cerebral blood flow is associated with faster cognitive decline in Alzheimer's disease. *Eur Radiol* 2017; 27: 1169–75.
31. White IR, Royston P and Wood AM. Multiple imputation using chained equations: Issues and guidance for practice. *Stat Med* 2011; 30: 377–99.
32. Singer JD and Willett JB. *Applied longitudinal data analysis : modeling change and event occurrence*. Oxford: Oxford University Press, 2003.
33. Rizopoulos D. JM: An R Package for the Joint Modelling of Longitudinal and Time-to-Event Data. *Journal of Statistical Software*; Vol 1, Issue 9 (2010) 2010.
34. Goessens BM, Visseren FL, Kappelle LJ, et al. Asymptomatic carotid artery stenosis and the risk of new vascular events in patients with manifest arterial disease: the SMART study. *Stroke* 2007; 38: 1470–75.
35. Benedictus MR, Binnewijzend MAA, Kuijer JPA, et al. Brain volume and white matter hyperintensities as determinants of cerebral blood flow in Alzheimer's disease. *Neurobiol Aging* 2014; 35: 2665–70.
36. Wirth M, Pichet Binette A, Brunecker P, et al. Divergent regional patterns of cerebral hypoperfusion and gray matter atrophy in mild cognitive impairment patients. *J Cereb Blood Flow Metab* 2017; 37: 814–24.
37. Washida K, Hattori Y and Ihara M. Animal Models of Chronic Cerebral Hypoperfusion: From Mouse to Primate. *Int J Mol Sci* 2019; 20: 6176.
38. Shaw TG, Mortel KF, Meyer JS, et al. Cerebral blood flow changes in benign aging and cerebrovascular disease. *Neurology* 1984; 34: 855–62.

Supplementary Table 1. Results of the linear mixed model with BPF as dependent variable and baseline pCBF as independent variable assuming a fixed slope with time. Estimates represent fixed effects of the linear mixed model with their 95% confidence intervals for a 1 unit increase of a continuous variable or presence of a dichotomous variable unless stated otherwise.

| | Estimate (95% CI) | p value |
|--------------------------------|-------------------------|---------|
| Intercept | 78.40 (77.50 to 79.30) | <0.001 |
| Baseline pCBF ^a | -0.10 (-0.22 to 0.02) | 0.096 |
| Rate of change | | |
| Time ^b | -0.23 (-0.24 to -0.22) | <0.001 |
| Time x baseline pCBF | -0.01 (-0.02 to -0.003) | 0.007 |
| Age ^b | -0.05 (-0.07 to -0.03) | <0.001 |
| Sex ^c | 0.84 (0.53 to 1.15) | <0.001 |
| Large infarcts on MRI | -0.64 (-1.04 to -0.25) | 0.001 |
| Lacunes on MRI | -0.54 (-0.87 to -0.21) | 0.001 |
| WMH volume on MRI ^d | -0.02 (-0.12 to 0.09) | 0.748 |
| Hypertension | -0.21 (-0.45 to 0.03) | 0.087 |
| Diabetes mellitus | -1.04 (-1.34 to -0.74) | <0.001 |
| Carotid stenosis ≥70% | -0.16 (-0.59 to 0.27) | 0.465 |
| Body mass index | 0.03 (-0.00 to 0.06) | 0.082 |
| Smoking pack years | -0.01 (-0.02 to -0.01) | <0.001 |
| Alcohol use | | |
| Current | 0 (reference) | - |
| Former | -0.44 (-0.86 to -0.01) | 0.043 |
| Never | 0.11 (-0.22 to 0.44) | 0.522 |

^a Per standard deviation decrease.

^b Per year increase.

^c Females vs. males.

^d Natural log-transformed due to a non-normal distribution and normalized for total intracranial volume. BPF: brain parenchymal fraction, pCBF: parenchymal cerebral blood flow, CI: confidence interval, WMH: white matter hyperintensity.

Supplementary Table 2. Results of the linear mixed model with BPF as dependent variable and baseline pCBF as independent variable in patients without missing data. Estimates represent fixed effects of the linear mixed model with their 95% confidence intervals for a 1 unit increase of a continuous variable or presence of a dichotomous variable unless stated otherwise.

| | Estimate (95% CI) | p value |
|--------------------------------|-------------------------|---------|
| Intercept | 78.69 (77.75 to 79.62) | <0.001 |
| Baseline pCBF ^a | -0.12 (-0.25 to 0.00) | 0.053 |
| Rate of change | | |
| Time ^b | -0.24 (-0.25 to -0.22) | <0.001 |
| Time x baseline pCBF | -0.01 (-0.02 to -0.003) | 0.011 |
| Age ^b | -0.05 (-0.07 to -0.03) | <0.001 |
| Sex ^c | 0.75 (0.43 to 1.08) | <0.001 |
| Large infarcts on MRI | -0.65 (-1.07 to -0.22) | 0.003 |
| Lacunes on MRI | -0.56 (-0.91 to -0.21) | 0.002 |
| WMH volume on MRI ^d | -0.01 (-0.11 to 0.10) | 0.907 |
| Hypertension | -0.17 (-0.42 to 0.08) | 0.171 |
| Diabetes mellitus | -1.09 (-1.40 to -0.77) | <0.001 |
| Carotid stenosis ≥70% | -0.15 (-0.60 to 0.30) | 0.509 |
| Body mass index | 0.02 (-0.01 to 0.06) | 0.150 |
| Smoking pack years | -0.01 (-0.02 to -0.01) | <0.001 |
| Alcohol use | | |
| Current | 0 (reference) | - |
| Former | -0.44 (-0.86 to 0.01) | 0.054 |
| Never | 0.09 (-0.25 to 0.44) | 0.596 |

^a Per standard deviation decrease.

^b Per year increase.

^c Females vs. males.

^d Natural log-transformed due to a non-normal distribution and normalized for total intracranial volume.

BPF: brain parenchymal fraction, pCBF: parenchymal cerebral blood flow, CI: confidence interval, WMH: white matter hyperintensity.



10

General discussion

General discussion

The main goal of this thesis was to study the characteristics, determinants, and cognitive correlates of several emergent MRI markers of cerebrovascular disease, seeking to explore the relationship between intracranial atherosclerosis (ICAS) and cerebral small vessel disease (CSVD).

Part I. Vessel Wall Lesions and Intracranial Atherosclerosis on 7T MRI

The term “intracranial vessel wall lesions” has been used to describe focal or more diffuse thickening of the vessel wall visualized on vessel wall MR imaging (VW-MRI).^{1,2} Vessel wall lesions are a promising MRI marker of ICAS, offering several benefits over conventional markers like arterial stenosis or calcification.^{3–5} Specifically, the ability of VW-MRI to visualize more subtle plaques, but also severe plaques without stenosis — due to positive remodeling.^{6,7} Studies show that 7T MRI outperforms 3T MRI in visualizing these plaques, primarily due to its increased spatial resolution and contrast-to-noise ratio.^{8,9} Consequently, 7T VW-MRI should improve ICAS burden assessment, aiding in improving our understanding of this disease.

In **Chapter 2** through **Chapter 5** we examined the frequency, determinants, and outcomes of intracranial vessel wall lesions in 130 persons from the SMART-MR study that underwent 7T brain MRI.

In **Chapter 2**, we found that intracranial vessel wall lesions occurred in >95% of persons with manifest arterial disease, with a mean of 8.6 ± 5.7 lesions, and a maximum of 32 lesions. A higher ICAS burden (i.e., total number of lesions) was found in persons with prior stroke, compared to persons without stroke. In addition, we observed associations with vascular risk factors such as older age, increased systolic blood pressure, diabetes, increased glycated hemoglobin (HbA1c), apolipoprotein-B and C-reactive protein. To date, only a few studies have reported thoroughly on the epidemiological characteristics of intracranial vessel wall lesions.^{10,11} The Atherosclerosis Risk in Communities study observed a 36% prevalence in a population-based cohort.¹⁰ A different 7T MRI study from our group found a prevalence of 84% in ischemic stroke patients.¹¹ Studies based on conventional ICAS measures have reported estimates of 13–21% in cardiovascular high-risk persons, increasing to 40–67% in persons with ischemic stroke.¹² Our higher estimate can likely be explained by the use of 7T VW-MRI in combination with our study population, consisting of older persons with various manifestations of arterial disease. Notably, our results are in line with prior autopsy studies that report estimates approaching 100% in older age.¹³ In addition, the observed risk factors were largely in concordance with prior studies based on detection of arterial stenosis and with data from vessel wall MRI studies.^{11,14,15} Our results support the hypothesis of the atherosclerotic origin of these lesions. In addition, it indicates that risk factors for stenotic lesions are comparable to those for the complete spectrum of vessel wall lesions.

In **Chapter 3**, we examined the relationship between ICAS and markers of extracranial atherosclerosis. Our interest in this relationship was triggered by only modest post-mortem correlations between intra- and extracranial atherosclerosis, suggesting these two entities may have differing etiologies.^{16,17} Additionally, *in vivo* studies exploring their relationship are limited, and have focused primarily on calcification.^{17,18} A strong association could suggest a shared etiology. We found a clear association between increased ICAS burden and extracranial carotid disease, peripheral artery disease, and decreased renal function. Notably, ICAS burden did not significantly differ between different manifest arterial diseases. Our results support the hypothesis that atherosclerosis is a systemic disease, with different manifestations throughout the arterial system. In addition, it further solidifies the atherosclerotic origin of these lesions, and further validates their use as an MRI marker of ICAS.

As previously noted, cerebrovascular disease is a significant contributor to cognitive decline and dementia.¹⁹ ICAS likely plays an important role in this process. Several studies have reported associations between intracranial stenosis and cognitive impairment and dementia.^{20–23} However, these studies predominantly examined the more severe manifestations of both conditions, leaving the association in the early or ‘premorbid’ stages of cognitive decline unexplored. Furthermore, the question remains whether the correlation between ICAS and cognitive functioning is universally present across all arteries or predominantly rooted in the impairment of a specific artery. Considering that vessel wall lesions represent a broader spectrum of disease, they may serve as a more sensitive tool for identifying these potentially subtler associations. In **Chapter 4**, we examined this premise and found associations between the ICAS burden of the posterior cerebral artery and memory and executive functioning. Additionally, while there were observable trends, the associations between the overall ICAS burden and memory, as well as the ICAS burden in the anterior cerebral artery and both memory and executive functioning, were not significant. Collectively, these findings hint at an artery-specific susceptibility in these cognitive domains, potentially owing to the localization of strategic brain regions within the arterial territories of the posterior and anterior cerebral artery.

In **Chapter 5**, we studied the relationship between ICAS and various CSVD-associated parenchymal lesions. ICAS likely plays a role in the pathogenesis of certain parenchymal lesions associated with CSVD.²⁴ Yet, its precise contribution remains a subject of debate. A better understanding of this relationship could help elucidate the heterogeneity in both the etiology and outcomes of CSVD. Additionally, it would broaden our understanding regarding the implications of ICAS. In our study, we found associations between ICAS and lacunes of presumed vascular origin, periventricular and total white matter hyperintensity volume, as well as cortical microinfarcts. These findings align largely with the limited number of studies that have previously been published on this topic.^{4,25–29} Although causality cannot be inferred from these associations, one possible mechanistic link between ICAS and these parenchymal lesions could be ICAS-induced microemboli or

arterial steno-occlusion, particularly of the subcortical perforator arteries, leading to hemodynamic-impairment, ischemia, and infarction. This also provides a potential explanation for the lack of association with microbleeds, which are typically caused by hemorrhage due to intrinsic small vessel disease.

Our findings in **Chapter 2** through **Chapter 5** have several implications. First, our data shows that ICAS is highly prevalent in persons with manifest arterial disease, also in persons without a prior cerebrovascular event. Second, ICAS correlates with measures of extracranial atherosclerosis, suggesting those measures could be used to gauge the quality of the cerebral vasculature. Third, ICAS correlates with large brain infarcts but also with parenchymal lesions conventionally ascribed to CSVD. This suggests that ICAS might play a role in their etiology, signifying the (clinical) importance of ICAS. Furthermore, the clinical relevance of ICAS has been further highlighted by its association with premorbid cognitive decline.

Part II. Cerebral Microinfarcts on 7T MRI

In the second part of this thesis, we focused on cerebral microinfarcts, an emergent MRI marker of cerebrovascular disease, which has gained increased recognition in the past decade.³⁰

Cerebral microinfarcts, small-scale areas of brain necrosis due to ischemia, are the most widespread form of brain infarction.³⁰ They associate with cognitive decline and dementia, independent from Alzheimer's disease and large infarcts.^{30,31} Consequently, they might represent a prospective target for preventing vascular cognitive impairment. Their small size long represented a challenge to their detection on conventional MRI, earning them the nickname 'the invisible lesion'.³¹ As a result, most of our understanding of these lesions is based on post-mortem neuropathological studies. A pivotal moment arrived in 2013 with the pioneering work of Van Veluw et al., who first identified microinfarcts in the cerebral cortex on 7T brain MRI.³² This innovation facilitated their detection on conventional MRI and catalyzed their study in living subjects. Since then, cortical microinfarcts have been the subject of various studies in living persons. However, most studies are restricted by small sample sizes and specific settings, which limits the generalizability of their findings. As a result, uncertainties persist regarding their determinants, etiology, and association with cognitive performance, thereby questioning their relevance in living individuals. Additionally, most larger studies have utilized low to high field strength MRI, leading to a limited assessment of cortical microinfarcts. This approach may underestimate the microinfarct burden when compared to assessments using ultra-high field 7T MRI. Therefore, in **Chapter 6**, we merged various 7T brain MRI cohorts, constructing the largest 7T brain MRI study to date, to study their frequency, determinants, and MRI and cognitive correlates. The study population consisted of a diverse cohort of 386 older persons with normal cognition, patients with manifest arterial disease from the SMART-MR study, and memory clinic patients. We found that cortical

microinfarcts occurred with a similar frequency of around 13% in patients with manifest arterial disease and memory clinic patients. Furthermore, we found that they primarily associated with MRI markers of large vessel disease, and less with markers of small vessel disease. Importantly, we found that presence of more than two cortical microinfarcts is associated with poorer global cognitive functioning.

Although cortical microinfarcts have received significant attention in the past decade, there is a shortage of studies focusing on subcortical microinfarcts. However, subcortical microinfarcts may be even more clinically relevant and intriguing due to their strategic localization. We know from post-mortem studies that subcortical microinfarcts associate with ante-mortem cognitive dysfunction.^{33,34} One factor impeding research in this area was the lack of imaging criteria. However, we recently demonstrated that the criteria for subcortical microinfarcts are similar to those of cortical microinfarcts, and that inter- and intra-rater agreement is excellent.³⁵ In **Chapter 7**, we used these imaging criteria to rate microinfarcts in the deep gray matter on 7T brain MRI data in 213 patients from the SMART-MR study. We found that they occurred in approximately 13% of the population, comparable to cortical microinfarcts, were most often observed in the thalami, and were mainly associated with MRI markers of large vessel disease. Interestingly, they were also associated with presence of cortical microinfarcts, which could indicate shared etiology. Lastly, they were associated with worse cognitive performance across all tested cognitive domains.

Taken together, the findings from **Chapter 6** and **Chapter 7** serve as a valuable addition to the current literature regarding cerebral microinfarcts in living individuals. First, we showed that they are mainly associated with MRI markers of large vessel disease. Although they do associate with lacunes, significant associations with white matter hyperintensities and microbleeds are absent, leaving little evidence to support a CSVD-related etiology. Second, their association with poorer cognitive functioning, especially for subcortical microinfarcts, suggests that these lesions are clinically relevant. Consequently, they may be an important “missing link” between large vessel disease and cognitive decline, and as such, an interesting target for prevention.

Part III. White Matter Lesions, Cerebral Blood Flow and Brain Atrophy

In the final part of this thesis, we examined the association between white matter hyperintensity (WMH) shape and cognitive functioning. Furthermore, we explored the bidirectional association between cerebral blood flow and brain atrophy.

In the aging brain, WMH, a key feature of CSVD, is a common MRI finding.³⁶ Generally, the severity of WMH is graded using qualitative scales (e.g. Fazekas) or by automatic MRI segmentation techniques that can accurately determine regional and total WMH volumes.^{37,38} Studies have shown that WMH volume is linked to cognitive deterioration.³⁹ However, the effects on individual cognitive domains are modest, possibly due to the volume metric’s inability to fully encapsulate the underlying pathology’s heterogeneity.⁴⁰

Recent research has demonstrated that WMH shape, which can be automatically determined using MRI data, might serve as a more effective determinant of functional consequences, as it is linked with varying underlying etiologies and pathologies.^{41–43} In **Chapter 8**, we tested this hypothesis by investigating the association between several shape features of WMH and executive functioning and memory. We found that increased complexity of WMH shape was associated with worse executive functioning and memory. Interestingly, the association of “Concavity Index” (one of the WMH shape parameters used in our study) and executive functioning was independent of WMH volume. This suggests that shape of WMH could potentially serve as a more sensitive and nuanced marker for cognitive impairment in CSVD than WMH volume alone. In addition, this may refine current diagnostic procedures and assist in early detection of cognitive impairment.

In **Chapter 9**, we examined the bidirectional relationship between cerebral blood flow and cerebral atrophy. Accelerated cerebral atrophy, beyond normal age-related shrinkage, is associated with cognitive decline and dementia.^{44,45} Cardiovascular risk factors and disease have been associated with cerebral atrophy.^{46–50} However, the pathways through which atherosclerosis might lead to brain atrophy remain elusive. One hypothesis postulates that reductions in cerebral perfusion, possibly due to factors such as carotid stenosis or heart failure, could lead to progressive brain atrophy.^{51–53} This is akin to a plant which, without necessary hydration, would wilt and eventually die. While existing studies have identified links between parenchymal cerebral blood flow (pCBF) and atrophy, a lack of longitudinal studies has hampered the study of causality. To explore this hypothesis, we examined the bidirectional association between pCBF and brain volume in a longitudinal study design. We used data from 1165 subjects participating in the baseline SMART-MR study, of whom 689 participated after 4 years of follow-up, and 297 participated at the last follow-up at 12 years. We found a consistent association between reduced pCBF and smaller total brain volumes at every data point. Notably, a lower baseline pCBF indicated a more substantial decline in total brain volume during the 12-year follow-up. Conversely, however, smaller initial brain volumes were not associated with a greater decrease in pCBF. This study adds depth to existing research on the relationship between cerebral blood flow and brain atrophy. Specifically, our results indicate that cerebral hypoperfusion likely plays a role in the onset of brain atrophy. Furthermore, they lend credence to the idea that cerebral blood flow, modifiable via lifestyle changes and pharmacological interventions, could be a viable target for preventing brain atrophy in the future.

Opportunities for future research

There are various opportunities for further research going forward. In this section, we will focus on a select few that seem like the next logical steps and require further clarification. Vessel wall lesions are an emergent and interesting MRI marker of vascular brain health. To clarify their utility, we need to gain a better understanding of their development,

prevalence, and progression in different populations. A population of significant interest could be patients from memory clinics in various stages of cognitive impairment. Vessel wall lesions may precede brain parenchymal lesions which suggests they could be an early marker of vascular cognitive impairment. Catching these patients early may give an opportunity to prevent further cognitive decline. Another focus of interest should be radio-pathologic correlation studies. Although we assume vessel wall lesions are ICAS, based on correlation with vascular risk factors and extracranial atherosclerosis, pathological validation is still lacking. Although ICAS is the dominant large vessel vasculopathy in the brain, there are other forms of vasculopathy such as arterial stiffening (seen in hypertension and diabetes) which may also lead to slight wall thickening.

Second, our understanding of cerebral microinfarcts would greatly benefit from longitudinal MRI studies in various populations, including the general population, with comprehensive data on frequency, determinants, and outcomes. Furthermore, our (and other) studies suggest that the pathophysiological mechanisms underlying cerebral microinfarcts differ across study populations. Studies could examine if certain microinfarct characteristics (e.g., size, distribution, cavitation) can be correlated with the underlying pathophysiology. This could also help clarify if the mechanisms underlying subcortical microinfarcts are the same as those underlying cortical lesions.

Third, there are several technical developments which could facilitate the abovementioned studies. A major advancement would be further improvement of 3T VW-MRI sequences, which are more feasibly implemented in large-scale studies compared to 7T MRI. Furthermore, the development of semi-automated segmentation of vessel wall lesions should improve both the reproducibility and validity of the 'ICAS burden' metric. Moreover, a similar semi-automated detection technique for microinfarcts would facilitate their study in large MRI studies.

Fourth, the link between large vessel disease and small vessel disease needs further exploration. Our study is part of the increasing evidence on the association between large and small vessel disease. However, there remain various unclarities about their relationship. A major hiatus is whether there is causality; larger and longitudinal studies could investigate this. Once this is clarified, it could help explain the heterogeneous etiology of CSVD. For instance, one could implement VW-MRI in CSVD studies to distinguish whether MRI markers of CSVD are more likely to be caused by ICAS or intrinsic small vessel abnormalities. This would help clarify the etiology and clinical consequences of CSVD.

Lastly, over the past few decades, neuroimaging studies have primarily focused on cerebrovascular lesions visible on structural MRI sequences. However, at this stage the damage to the brain is already done and often irreversible. To address this limitation, studies should shift their focus to the earlier, premorbid stages of ICAS and CSVD. Application of more advanced or functional MRI sequences might help elucidate the preceding stage. An example of this is MRI-based measurement of blood flow in the small subcortical arteries, which can forego CSVD-associated parenchymal lesions.⁵⁴

Furthermore, changes in white matter integrity on diffusion tensor imaging have been shown to precede the formation of white matter hyperintensities.⁵⁵ This could provide insight into which persons are at risk of developing ICAS or CSVD and help in development of risk-stratified preventive strategies.

Conclusion

This thesis has yielded new insights into several emergent MRI markers of cerebrovascular disease, regarding their characteristics, determinants, and association with cognitive functioning. In addition, these insights give a better understanding of the relationship between MRI markers of large and small vessel disease.

Key findings

- Intracranial vessel wall lesions associate with MRI markers of large and small vessel disease and with premorbid cognitive decline.
- Microinfarcts in the cortical and deep gray matter are primarily associated with MRI markers of large vessel disease and with decreased cognitive functioning.
- WMH shape has emerged as an intriguing metric for white matter hyperintensities and has potential clinical relevance in relation to cognitive functioning.
- Reduced cerebral blood flow is associated with greater progression of brain atrophy.

As we look ahead, the emphasis in research should be on comprehensive longitudinal MRI studies. Such studies will be pivotal in uncovering the determinants, understanding the clinical consequences, and formulating potential therapeutic and preventive measures. Additionally, a concentrated effort on the earlier premorbid phases of ICAS and CSVD is needed to develop strategies to prevent vascular brain damage.

References

1. Hartevelde AA, Van Der Kolk AG, Van Der Worp HB, Dieleman N, Zwanenburg JJM, Luijten PR, et al. Detecting Intracranial Vessel Wall Lesions with 7T-Magnetic Resonance Imaging: Patients with Posterior Circulation Ischemia Versus Healthy Controls. *Stroke* 2017; 48: 2601–4.
2. van der Kolk AG, Zwanenburg JJM, Brundel M, Biessels GJ, Visser F, Luijten PR, et al. Distribution and natural course of intracranial vessel wall lesions in patients with ischemic stroke or TIA at 7.0 tesla MRI. *Eur Radiol* 2015; 25: 1692–700.
3. Mandell DM, Mossa-Basha M, Qiao Y, Hess CP, Hui F, Matouk C, et al. Intracranial Vessel Wall MRI: Principles and Expert Consensus Recommendations of the American Society of Neuroradiology. *AJNR Am J Neuroradiol* 2016; 38: 218–29.
4. Dieleman N, Van Der Kolk AG, Zwanenburg JJM, Brundel M, Hartevelde AA, Biessels GJ, et al. Relations between location and type of intracranial atherosclerosis and parenchymal damage. *J Cereb Blood Flow Metab* 2016; 36: 1271–80.
5. Bash S, Villablanca JP, Jahan R, Duckwiler G, Tillis M, Kidwell C, et al. Intracranial vascular stenosis and occlusive disease: Evaluation with CT angiography, MR angiography, and digital subtraction angiography. *AJNR Am J Neuroradiol* 2005; 26: 1012–21.
6. Alexander MD, Yuan C, Rutman A, Tirschwell DL, Gandhi D, Sekhar LN, et al. Beyond the Lumen. *J Neurol Neurosurg Psychiatry* 2017; 87: 589–97.
7. Qiao Y, Anwar Z, Intrapromkul J, Liu L, Zeiler SR, Leigh R, et al. Patterns and Implications of Intracranial Arterial Remodeling in Stroke Patients. *Stroke* 2016; 47: 434–40.
8. Hartevelde AA, van der Kolk AG, van der Worp HB, Dieleman N, Siero JCW, Kuijff HJ, et al. High-resolution intracranial vessel wall MRI in an elderly asymptomatic population: comparison of 3T and 7T. *Eur Radiol* 2017; 27: 1585–95.
9. van der Kolk AG, Zwanenburg JJM, Brundel M, Biessels GJ, Visser F, Luijten PR, et al. Intracranial vessel wall imaging at 7.0-T MRI. *Stroke* 2011; 42: 2478–84.
10. Qiao Y, Guallar E, Suri FK, Liu L, Zhang Y, Anwar Z, et al. MR Imaging Measures of Intracranial Atherosclerosis in a Population-based Study. *Radiology* 2016; 280: 860–8.
11. Lindenholtz A, van der Kolk AG, van der Schaaf IC, van der Worp HB, Hartevelde AA, Dieleman N, et al. Intracranial atherosclerosis assessed with 7-T MRI: Evaluation of patients with ischemic stroke or transient ischemic attack. *Radiology* 2020; 295: 162–70.
12. Gorelick P, Wong KS, Liu L. Epidemiology. *Front Neurol Neurosci*. 2016;40:34–46.
13. Resch JA, Baker AB. Etiologic Mechanisms in Cerebral Atherosclerosis: Preliminary Study of 3,839 Cases. *Arch Neurol* 1964; 10: 617–28.
14. Uehara T, Bang OY, Kim JS, Minematsu K, Sacco R. Risk Factors. *Front Neurol Neurosci* 2017; 40: 47–57.
15. Qiao Y, Suri FK, Zhang Y, Liu L, Gottesman R, Alonso A, et al. Racial differences in prevalence and risk for intracranial atherosclerosis in a US community-based population. *JAMA Cardiol* 2017; 2: 1341–8.
16. Sternby NH. Atherosclerosis in a defined population. An autopsy survey in Malmö, Sweden. *Acta Pathol Microbiol Scand* 1968;Suppl 194:5+.
17. Bos D, Ikram MA, Elias-Smale SE, Krestin GP, Hofman A, Witteman JCMM, et al. Calcification in major vessel beds relates to vascular brain disease. *Arterioscler Thromb Vasc Biol* 2011; 31: 2331–7.
18. Odink AE, van der Lugt A, Hofman A, Hunink MGM, Breteler MMB, Krestin GP, et al. Association between calcification in the coronary arteries, aortic arch and carotid arteries: The Rotterdam study. *Atherosclerosis* 2007; 193: 408–13.
19. Iadecola C, Duering M, Hachinski V, Joutel A, Pendlebury ST, Schneider JA, et al. Vascular Cognitive Impairment and Dementia: JACC Scientific Expert Panel. *J Am Coll Cardiol* 2019; 73: 3326–44.
20. Zhu J, Wang Y, Li J, Deng J, Zhou H. Intracranial artery stenosis and progression from mild cognitive impairment to Alzheimer disease. *Neurology* 2014; 82: 842–9.
21. Hilal S, Xu X, Ikram MK, Vrooman H, Venketasubramanian N, Chen C. Intracranial stenosis in cognitive impairment and dementia. *J Cereb Blood Flow Metab* 2017; 37: 2262–9.

22. Bos D, Vernooij MW, De Bruijn RFAG, Koudstaal PJ, Hofman A, Franco OH, et al. Atherosclerotic calcification is related to a higher risk of dementia and cognitive decline. *Alzheimers Dement* 2015; 11: 639–647.e1.
23. Dearborn JL, Zhang Y, Qiao Y, Suri MFK, Liu L, Gottesman RF, et al. Intracranial atherosclerosis and dementia. *Neurology* 2017; 88: 1556–63.
24. Wardlaw JM, Smith C, Dichgans M. Mechanisms of sporadic cerebral small vessel disease: Insights from neuroimaging. *Lancet Neurol* 2013; 12: 483–97.
25. Nam KWW, Kwon HMM, Jeong HYY, Park JHH, Kim SSHS, Jeong SMM, et al. Cerebral white matter hyperintensity is associated with intracranial atherosclerosis in a healthy population. *Atherosclerosis* 2017; 265: 179–83.
26. Park JHH, Kwon HMM, Lee J, Kim DSS, Ovbiagele B. Association of intracranial atherosclerotic stenosis with severity of white matter hyperintensities. *Eur J Neurol*. 2015; 22: 44–52.
27. Lee SJ, Kim JS, Chung SW, Kim BS, Ahn KJ, Lee KS. White matter hyperintensities (WMH) are associated with intracranial atherosclerosis rather than extracranial atherosclerosis. *Arch Gerontol Geriatr* 2011; 53: e129–32.
28. Chung JW, Kim BJ, Sohn CH, Yoon BW, Lee SH. Branch Atheromatous Plaque: A Major Cause of Lacunar Infarction (High-Resolution MRI Study). *Cerebrovasc Dis Extra* 2012; 2: 36–44.
29. Degnan AJ. Underestimating the importance of middle cerebral artery atherosclerosis in lacunar stroke. *Cerebrovasc Dis* 2011; 32: 301.
30. van Veluw SJ, Shih AY, Smith EE, Chen C, Schneider JA, Wardlaw JM, et al. Detection, risk factors, and functional consequences of cerebral microinfarcts. *Lancet Neurol* 2017; 16: 730–40.
31. Smith EE, Schneider JA, Wardlaw JM, Greenberg SM. Cerebral microinfarcts: the invisible lesions. *Lancet Neurol* 2012; 11: 272–82.
32. Van Veluw SJ, Zwanenburg JJM, Engelen-Lee J, Spliet WGM, Hendrikse J, Luijten PR, et al. In vivo detection of cerebral cortical microinfarcts with high-resolution 7T MRI. *J Cereb Blood Flow Metab* 2013; 33: 322–9.
33. Gold G, Kövari E, Herrmann FR, Canuto A, Hof PR, Michel JP, et al. Cognitive consequences of thalamic, basal ganglia, and deep white matter lacunes in brain aging and dementia. *Stroke* 2005; 36: 1184–8.
34. White L, Petrovitch H, Hardman J, Nelson J, Davis DG, Ross GW, et al. Cerebrovascular Pathology and Dementia in Autopsied Honolulu-Asia Aging Study Participants. *Ann N Y Acad Sci* 2002; 977: 9–23.
35. Ghaznawi R, de Bresser J, van der Graaf Y, Zwartbol MHT, Witkamp TD, Geerlings MI, et al. Detection and characterization of small infarcts in the caudate nucleus on 7 Tesla MRI: The SMART-MR study. *J Cereb Blood Flow Metab* 2018; 38: 1609–17.
36. Wardlaw JM, Valdés Hernández MC, Muñoz-Maniega S. What are white matter hyperintensities made of? Relevance to vascular cognitive impairment. *J Am Heart Assoc*. 2015; 4: 001140.
37. Kuijf HJ, Casamitjana A, Collins DL, Dadar M, Georgiou A, Ghafoorian M, et al. Standardized Assessment of Automatic Segmentation of White Matter Hyperintensities and Results of the WMH Segmentation Challenge. *IEEE Trans Med Imaging*. 2019; 38: 2556–68.
38. Fazekas F, Kleinert R, Offenbacher H, Payer F, Schmidt R, Kleinert G, et al. The morphologic correlate of incidental punctate white matter hyperintensities on MR images. *AJNR Am J Neuroradiol* 1991; 12: 915–21.
39. Kloppenborg RP, Nederkoorn PJ, Geerlings MI, Van Den Berg E. Presence and progression of white matter hyperintensities and cognition: A meta-analysis. *Neurology* 2014; 82: 2127–38.
40. Gouw AA, Seewann A, Van Der Flier WM, Barkhof F, Rozemuller AM, Scheltens P, et al. Heterogeneity of small vessel disease: A systematic review of MRI and histopathology correlations. *J Neurol Neurosurg Psychiatry* 2011; 82: 126–35.
41. de Bresser J, Kuijf HJ, Zaanen K, Viergever MA, Hendrikse J, Biessels GJ, et al. White matter hyperintensity shape and location feature analysis on brain MRI; Proof of principle study in patients with diabetes. *Sci Rep*. 2018; 8:1–10.
42. Ghaznawi R, Geerlings MI, Jaarsma-Coes MG, Zwartbol MHT, Kuijf HJ, van der Graaf Y, et al. The association between lacunes and white matter hyperintensity features on MRI: The SMART-MR study. *J Cereb Blood Flow Metab* 2019; 39: 2486–96.
43. Lange C, Suppa P, Mäurer A, Ritter K, Pietrzyk U, Steinhagen-Thiessen E, et al. Mental speed is associated with the shape irregularity of white matter MRI hyperintensity load. *Brain Imaging Behav* 2017; 11: 1720–30.
44. Mungas D, Harvey D, Reed BR, Jagust WJ, DeCarli C, Beckett L, et al. Longitudinal volumetric MRI change and rate of cognitive decline. *Neurology* 2005; 65: 565–71.

45. Jack CR, Shiung MM, Weigand SD, O'Brien PC, Gunter JL, Boeve BF, et al. Brain atrophy rates predict subsequent clinical conversion in normal elderly and amnesic MCI. *Neurology* 2005; 65: 1227–31.
46. Muller M, van der Graaf Y, Algra A, Hendrikse J, Mali WP, Geerlings MI, et al. Carotid atherosclerosis and progression of brain atrophy: the SMART-MR study. *Ann Neurol* 2011; 70: 237–44.
47. Jochemsen HM, Muller M, Visseren FL, Scheltens P, Vincken KL, Mali WP, et al. Blood pressure and progression of brain atrophy: the SMART-MR Study. *JAMA Neurol.* 2013; 70: 1046–53.
48. Alosco ML, Hayes SM. Structural brain alterations in heart failure: a review of the literature and implications for risk of Alzheimer's disease. *Heart Fail Rev* 2015; 20: 561.
49. Goh FQ, Kong WKF, Wong RCC, Chong YF, Chew NWS, Yeo TC, et al. Cognitive Impairment in Heart Failure—A Review. *Biology (Basel).* 2022; 11: 179.
50. Knopman DS, Mosley TH, Catellier DJ, Sharrett AR. Cardiovascular risk factors and cerebral atrophy in a middle-aged cohort. *Neurology* 2005; 65: 876–81.
51. Appelman APA, Van Der Graaf Y, Vincken KL, Tiehuis AM, Witkamp TD, Mali WPTMP, et al. Total cerebral blood flow, white matter lesions and brain atrophy: the SMART-MR study. *J Cereb Blood Flow Metab* 2008; 28: 633–9.
52. Kitagawa Y, Stirling Meyer J, Tanahashi N, Rogers RL, Tachibana H, Kandula P, et al. Cerebral blood flow and brain atrophy correlated by xenon contrast CT scanning. *Comput Radiol* 1985; 9: 331–40.
53. Alosco ML, Gunstad J, Jerskey BA, Xu X, Clark US, Hassenstab J, et al. The adverse effects of reduced cerebral perfusion on cognition and brain structure in older adults with cardiovascular disease. *Brain Behav* 2013; 3: 626–36.
54. van den Brink H, Doubal FN, Duering M. Advanced MRI in cerebral small vessel disease. *Int J Stroke* 2023; 18: 28–35.
55. Van Leijsen EMC, Bergkamp MI, Van Uden IWM, Ghafoorian M, Van Der Holst HM, Norris DG, et al. Progression of white matter hyperintensities preceded by heterogeneous decline of microstructural integrity. *Stroke* 2018; 49: 1386–93.

APPENDICES

Nederlandse samenvatting

About the author

List of publications

Dankwoord

Nederlandse samenvatting

Cerebrovasculaire ziekten omvatten diverse afwijkingen die invloed hebben op de bloedvaten en bloedcirculatie van de hersenen. Het meest voorkomende en ernstige gevolg hiervan is een beroerte, een urgente medische situatie die zich manifesteert als neurologische uitval, veroorzaakt door het blokkeren of barsten van een hersenbloedvat. Een beroerte is één van de belangrijkste wereldwijde oorzaken van overlijden en invaliditeit. Daarnaast zijn cerebrovasculaire ziekten geassocieerd met een verhoogd risico op cognitieve achteruitgang en dementie.

Cerebrovasculaire ziekten worden vaak onderverdeeld in grote en kleine vaatziekten. De meest voorkomende grote vaatziekte in de hersenen is atherosclerose van de grote hersenslagaders, ook bekend als intracraniale atherosclerose (ICAS). Kleine vaatziekten, vaak aangeduid als 'cerebral small vessel disease' (CSVD), omvatten aandoeningen die de kleinere slagaders en aderen in de hersenen beïnvloeden, de meest voorkomende is vasculair risicofactor geassocieerde-CSVD. Ondanks de classificatie als twee afzonderlijke entiteiten, toont post-mortem onderzoek een significante overlap en relatie tussen deze aandoeningen.

De afwijkingen die deze ziektes veroorzaken in de bloedvaten en het hersenparenchym kunnen worden gevisualiseerd door middel van MRI. De toepassing van MRI is cruciaal geweest voor onze kennis over het ontstaan, de progressie en het gevolg van cerebrovasculaire aandoeningen. Echter, er zijn enkele relatief recent beschreven MRI afwijkingen, ook wel 'MRI markers' genoemd, waar nog veel over onbekend is.

Het doel van dit proefschrift is om de karakteristieken, determinanten en relatie met cognitieve functies van deze MRI markers te onderzoeken, om zo de relatie tussen ICAS en CSVD beter te begrijpen.

Deel I van dit proefschrift omvat vier studies naar intracraniale vaatwandlaesies, een 7 tesla (7T) MRI marker van ICAS. Deze studies werden uitgevoerd onder 130 patiënten met manifest arterieel vaatlijden uit de Second Manifestations of ARterial disease-Magnetic Resonance (SMART-MR) studie, een single-center prospectief cohortonderzoek onder patiënten met manifest arterieel vaatlijden die zijn doorverwezen naar het Universitair Medisch Centrum Utrecht.

In **Hoofdstuk 2** worden de karakteristieken en determinanten van deze MRI marker beschreven. Uit het onderzoek bleek dat intracraniale vaatwandlaesies voorkwamen bij >95% van de studiepopulatie, met een gemiddeld aantal van $8,6 \pm 5,7$ laesies en een maximum van 32 laesies. Een hogere 'ICAS burden' (i.e. totaal aantal vaatwandlaesies) werd gevonden bij personen met een eerdere beroerte. Ook waren vaatwandlaesies geassocieerd met vasculaire risicofactoren zoals oudere leeftijd, verhoogde systolische bloeddruk, diabetes, verhoogd geglyceerd hemoglobine, apolipoproteïne-B en C-reactief eiwit. **Hoofdstuk 3** beschrijft de relatie tussen ICAS burden en verschillende vormen van

extracraniele atherosclerose. Uit de analyses bleek een duidelijk relatie tussen een hogere ICAS burden en aanwezigheid van ernstige halsslagaderziekte, perifere arteriële ziekte en een verlaagde nierfunctie. Deze bevindingen versterken het bewijs voor de atherosclerotische origine van vaatwandlaesies, een punt waarover bij 7T MRI nog enige onzekerheid bestaat. In **Hoofdstuk 4** wordt gekeken naar de relatie tussen ICAS burden, op globaal en territoriaal niveau, en cognitief functioneren. Een hogere ICAS burden van de arteria cerebri posterior bleek geassocieerd met een verminderd geheugen en executief functioneren. Hoewel er ook relaties zichtbaar waren met de ICAS burden van de arteria cerebri anterior en de globale ICAS burden, waren deze niet statistisch significant. **Hoofdstuk 5** richt zich op de relatie tussen ICAS burden en MRI markers van CSVD. Een hogere ICAS burden bleek geassocieerd te zijn met lacunes van veronderstelde vasculaire origine, periventriculair en totaal volume van witte stofafwijkingen, evenals corticale microinfarcten.

De resultaten van deze hoofdstukken tonen dat ICAS zeer prevalent is onder personen met manifest arterieel vaatlijden en mogelijk van grotere klinische betekenis is dan tot nu toe werd gedacht, gezien de relatie met premorbide cognitieve functie en CSVD. Een verduidelijking van de relatie met CSVD zou mogelijk een deel van de klinische heterogeniteit van deze aandoening kunnen verklaren.

In **Deel II** wordt de aandacht verlegd naar cerebrale microinfarcten, geëvalueerd op 7T MRI, met specifieke aandacht voor hun frequentie, etiologie en relatie met cognitief functioneren.

In **Hoofdstuk 6** wordt gekeken naar de frequentie en determinanten van corticale microinfarcten, en hun relatie met vasculaire MRI markers en cognitieve functie. Deze studie werd uitgevoerd in het Memory Depression and Aging (Medea) 7T cohort, een heterogeen cohort van 386 oudere personen. Uit de analyses bleek dat corticale microinfarcten met een vergelijkbare frequentie van rond de 13% voorkwamen bij personen met manifest arterieel vaatlijden en patiënten van de geheugenpoli. Verder waren ze voornamelijk geassocieerd met MRI markers van grote vaatziekte en minder met MRI markers van kleine vaatziekte. Ook was aanwezigheid van meer dan twee corticale microinfarcten geassocieerd met slechtere globale cognitieve functie.

In **Hoofdstuk 7** wordt de focus verlegd naar microinfarcten in de diepe grijze stof. Een studie onder 213 personen met manifest arterieel vaatlijden uit het SMART-MR cohort, toonde dat deze geassocieerd zijn met risicofactoren en MRI markers van zowel grote als kleine vaatziekte. Ook hier bleek de aanwezigheid van meerdere microinfarcten geassocieerd te zijn met een slechtere globale cognitieve functie.

De bevindingen uit deze hoofdstukken suggereren een belangrijke rol voor grote vaatziekte in de etiologie van microinfarcten. Daarnaast benadrukt hun relatie met cognitief functioneren de klinische relevantie van deze laesies.

In **Deel III** van dit proefschrift wordt gekeken naar de relatie tussen de vorm van witte-stofafwijkingen en cognitief functioneren, evenals de tweerichtingsrelatie tussen cerebrale doorbloeding en hersenatrofie. Deze studies werden uitgevoerd in het SMART-MR cohort.

Hoofdstuk 8 gaat in op de relatie tussen de verschillende vormkenmerken van witte-stofafwijkingen en cognitieve functie. Analyse onder 563 personen met manifest arterieel vaatlijden toonde dat de complexiteit van de vorm van wittestofafwijkingen samenhangt met slechter executief functioneren en geheugen, los van het volume van de wittestofafwijkingen, wat suggereert dat de vorm van wittestofafwijkingen een gevoeliger marker kan zijn voor cognitieve achteruitgang bij CSVD.

Hoofdstuk 9 beschrijft de resultaten van een longitudinaal onderzoek naar de relatie tussen cerebrale doorbloeding en hersenatrofie onder 1165 personen met manifest arterieel vaatlijden. Uit de analyses bleek dat verminderde cerebrale doorbloeding op baseline geassocieerd was met een sterkere mate van hersenatrofie over de tijd, terwijl aanwezigheid van hersenatrofie op baseline niet geassocieerd was met een sterkere afname van de cerebrale doorbloeding over de tijd. Dit suggereert dat therapie gericht op het verbeteren van de cerebrale doorbloeding de progressie van hersenatrofie mogelijk kan afremmen.

Samenvattend biedt dit proefschrift nieuwe inzichten in de karakteristieken en determinanten van enkele nieuwe MRI markers van ICAS en CSVD, evenals in hun relatie met cognitief functioneren. Ook bieden de resultaten een dieper inzicht in de onderlinge verbanden tussen deze aandoeningen.

About the author

Maarten Zwartbol was born on October 2nd, 1985 in Meppel, the Netherlands. After graduating from C.S.G. Dingstede in 2003, he started his studies in Biology at the University of Groningen, but switched to Medicine in his third year, graduating in 2012.

In February 2013, he started as a resident in radiology at the Haga Teaching Hospital in The Hague under the supervision of Dr. Hans van Overhagen and Dr. Ad van Gils. He further specialized in neuroradiology during internships at the Haaglanden Medical Center and Leiden University Medical Center. After completing his residency in 2019, he pursued additional specialization as a neuroradiologist during a one-year fellowship.



In January 2016, he started as a part-time researcher in the research group of Prof. Dr. Jeroen Hendrikse at the Department of Radiology of the University Medical Center in Utrecht. In 2017, he seized the opportunity to begin his Ph.D. candidacy and work as a full-time researcher for a year. During this period, his research primarily focused on exploring the connection between large and small vessel disease of the brain, with a particular emphasis on 7T MRI, under the co-supervision of Dr. Mirjam Geerlings and Dr. Anja van der Kolk.

Since March 2021, Maarten has been working as a radiologist at the Martini Hospital in Groningen.

List of publications

Twait EL, Blom K, Koek HL, **Zwartbol MHT**, Ghaznawi R, Hendrikse J, Gerritsen L, Geerlings MI. Psychosocial factors and hippocampal subfields: The Medea-7T study. *Human Brain Mapping*. 2023; 44(5): 1964–84.

Ghaznawi R, Vonk MJM, **Zwartbol MHT**, de Bresser J, Rissanen I, Hendrikse J, Geerlings MI. Low-grade carotid artery stenosis is associated with progression of brain atrophy and cognitive decline. The SMART-MR study. *Journal of Cerebral Blood Flow and Metabolism*. 2023; 43(2): 309–18.

Zwartbol MHT, Ghaznawi R, Jaarsma-Coes MGM, Kuijff HJ, Hendrikse J, de Bresser J, Geerlings MI. White matter hyperintensity shape is associated with cognitive functioning – the SMART-MR study. *Neurobiology of Aging*. 2022; 120: 81–87.

Ghaznawi R, **Zwartbol MHT**, de Bresser J, Kuijff HJ, Vincken KL, Rissanen I, Geerlings MI, Hendrikse J. Microinfarcts in the Deep Gray Matter on 7T MRI: Risk Factors, MRI Correlates, and Relation to Cognitive Functioning-The SMART-MR Study. *American Journal of Neuroradiology*. 2022; 43(6): 829–36.

Vonk MJM, Ghaznawi R, **Zwartbol MHT**, Stern Y, Geerlings MI. The role of cognitive and brain reserve in memory decline and atrophy rate in mid and late-life: The SMART-MR study. *Cortex*. 2022; 148: 204–14.

Zwartbol MHT, Rissanen I, Ghaznawi R, de Bresser J, Kuijff HJ, Blom K, Witkamp TD, Koek HL, Biessels GJ, Hendrikse J, Geerlings MI. Cortical cerebral microinfarcts on 7T MRI: Risk factors, neuroimaging correlates and cognitive functioning – The Medea-7T study. *Journal of Cerebral Blood Flow and Metabolism*. 2021; 41(11): 3127–38.

Polak SB, Huybregts JGJ, **Zwartbol MHT**, Hammer S, Lycklama à Nijeholt GJ, Broekman MLD. Uw diagnose? *Tijdschrift voor Neurologie & Neurochirurgie*. 2021; 122(2): 84.

Zwartbol MHT, van der Kolk AG, Ghaznawi R, Witkamp TD, Hendrikse J, Geerlings MI. Intracranial Vessel Wall Lesions on 7T MRI and MRI features of Cerebral Small Vessel Disease: The SMART-MR study. *Journal of Cerebral Blood Flow and Metabolism*. 2020; 41(6): 1219–28.

Blom K, Koek HL, **Zwartbol MHT**, Ghaznawi R, Kuijff HJ, Witkamp TD, Hendrikse J, Biessels GJ, Geerlings MI. Vascular risk factors of hippocampal subfield volumes in persons without dementia: the Medea 7T study. *Journal of Alzheimer's Disease*. 2020; 77(3): 1223–39.

Zwartbol MHT, Verbist BM. A jugular foramen schwannoma with multiple lower cranial nerve palsies. ECR Quiz cases of the day 2020. *EuroRad*. 2020. <https://www.eurorad.org/case/16776>

Zwartbol MHT, Navas Cañete A. Ossifying fibromyxoid tumor of the cervical spine: a rare case. *EuroRad*. 2020. <https://www.eurorad.org/case/16881>

Ghaznawi R, **Zwartbol MHT**, Zuithoff NP, de Bresser J, Hendrikse J, Geerlings MI. Reduced parenchymal cerebral blood flow is associated with greater progression of brain atrophy: The SMART-MR study. *Journal of Cerebral Blood Flow and Metabolism*. 2021; 41(6): 1229–39.

Zwartbol MHT, van der Kolk AG, Ghaznawi R, van der Graaf Y, Hendrikse J, Geerlings MI. Intracranial Atherosclerosis on 7T MRI and Cognitive Functioning - the SMART-MR study. *Neurology*. 2020; 95(10): e1351–e1361.

Zwartbol MHT, van der Kolk AG, Geerlings MI. Reply. *American Journal of Neuroradiology*. 2019; 41(5): e32.

Zwartbol MHT, Geerlings MI, Ghaznawi R, Hendrikse J, van der Kolk AG. Intracranial atherosclerotic burden on 7T MRI is associated with markers of extracranial atherosclerosis: The SMART-MR study. *American Journal of Neuroradiology*. 2019; 40(12): 2016–22.

Blom K, Koek HL, **Zwartbol MHT**, van der Graaf Y, Kesseler L, Biessels GJ, Geerlings MI. Subjective cognitive decline, brain imaging biomarkers, and cognitive functioning in patients with a history of vascular disease: the SMART-Medea study. *Neurobiology of Aging*. 2019; 84: 33–40.

Blom K, Koek HL, van der Graaf Y, **Zwartbol MHT**, Wisse LEM, Hendrikse J, Biessels GJ, Geerlings MI. Hippocampal sulcal cavities: prevalence, risk factors and association with cognitive performance. The SMART-Medea study and PREDICT-MR study. *Brain Imaging and Behavior*. 2019; 13(4): 1093–1102.

Zwartbol MHT, van der Kolk AG, Ghaznawi R, van der Graaf Y, Hendrikse J, Geerlings MI. Intracranial Vessel Wall Lesions on 7T MRI: Occurrence and Vascular Risk Factors: The SMART-MR Study. *Stroke*. 2019; 50(1): 88–94.

Ghaznawi R, Geerlings MI, Jaarsma-Coes MGM, **Zwartbol MHT**, Kuijff HJ, van der Graaf Y, Witkamp TD, Hendrikse J, de Bresser J. The association between lacunes and white matter hyperintensity features on MRI. The SMART-MR study. *Journal of Cerebral Blood Flow and Metabolism*. 2018; 39(12): 2486–96.

De Cocker LJ, Lindenholz A, Zwanenburg JJ, van der Kolk AG, **Zwartbol MHT**, Luijten PR, Hendrikse J. Clinical vascular imaging in the brain at 7T. *NeuroImage*. 2018; 168: 452–458.

Ghaznawi R, de Bresser J, van der Graaf Y, **Zwartbol MHT**, Witkamp TD, Geerlings MI, Hendrikse J. Detection and characterization of small infarcts in the caudate nucleus on 7 Tesla MRI: The SMART-MR study. *Journal of Cerebral Blood Flow and Metabolism*. 2018; 38(9): 1609–17.

Zwartbol MHT, Hammer S. Beeldvorming bij epilepsie. Speuren naar het epileptogene focus. *Nervus*. 2017; 4: 52–58.

van Hulsteijn LT, Mieog JSD, **Zwartbol MHT**, Merkus JWS, van Nieuwkoop C. Appendicitis presenting as cellulitis of the right leg. *Journal of Emergency Medicine*. 2017; 52(1): e1-e3.

Lu B, Yu H, **Zwartbol MHT**, Ruifrok WP, van Gilst WH, de Boer RA, Silljé HHW. Identification of hypertrophy and heart failure-associated genes by combining in vitro and in vivo models. *Physiological Genomics*. 2012; 44(8): 443–54.

Dankwoord

In de illustratie op de cover van dit proefschrift prijkt een boom (dank Ammie ♥), die als metafoor dient voor de vitale relatie tussen de vaten en het weefsel in onze hersenen. Zoals een boom niet zonder zijn netwerk van wortels kan — die voeding en stabiliteit verschaffen — zo zou mijn werk niet mogelijk zijn geweest zonder de voedende bijdragen en onwrikbare steun van velen onder jullie. Jullie zijn de wortels die niet alleen mijn onderzoek, maar ook mijn groei en ontwikkeling als onderzoeker hebben gevoed. Aan iedereen die een deel van deze voedende bodem vormde, mijn diepste dank!

In dit hoofdstuk wil ik een aantal mensen in het bijzonder bedanken.

Ten eerste wil ik alle deelnemers aan de SMART-MR studie bedanken voor de tijd en moeite die zij hebben gestoken in het participeren in de vele onderzoeken, waaronder het ondergaan van een 1.5T en 7T MRI scan van de hersenen. Jullie gegevens liggen ten grondslag aan vele wetenschappelijke artikelen over de relatie tussen arteriële vaatziekte, het hersenparenchym en hersenfunctie. Hiermee is een significante bijdrage geleverd aan dit onderzoeksveld. Daarnaast gaat mijn dank uit naar de leden van de UCC-SMART studiegroep en naar de ondersteuning vanuit de SMART office.

Prof. dr. J. Hendrikse, beste Jeroen, toen ik in 2015 op de Radiologendagen in De Doelen met je in gesprek raakte, had ik al de ambitie om te promoveren binnen de neuroradiologie. Na dat gesprek was ik geïnspireerd door je kijk op onderzoek en je scala aan ideeën. Bedankt voor de kans en het vertrouwen dat je mij hebt gegeven, en voor de vrijheid en mogelijkheden die je tijdens mijn promotietraject ter beschikking hebt gesteld. Het is een lang maar vruchtbaar traject geworden!

Dr. M.I. Geerlings, beste Mirjam, wat ben ik dankbaar dat ik jou als mijn meest intensieve supervisor heb gehad. Je bent echt een toponderzoeker, heel scherp en kritisch maar ook met een bepaalde ontspanning waarmee je mij altijd vertrouwen wist te geven. Jouw epidemiologische kennis en feedback zijn essentieel geweest voor dit proefschrift, en voor mijn vorming als onderzoeker. Ook kijk ik met een warm gevoel terug op onze koffiemomenten en onze gezamenlijke VasCog in Hongkong. Het was een mooie tijd. Veel succes met het uitzetten van onderzoekslijnen bij het Amsterdam UMC!

Dr. A.G. van der Kolk, beste Anja, jouw promotieonderzoek staat aan de basis van het onderzoek naar intracraniale atherosclerose en 7T vaatwand MR imaging in het UMC Utrecht. Inmiddels zijn hier al meerdere proefschriften uit voortgekomen en is het ook een belangrijke pijler in mijn proefschrift. Bedankt voor je begeleiding bij mijn vaatwandartikelen en het hiermee op de rit brengen van mijn promotietraject. Ook wil ik je bedanken voor je pragmatische en optimistische adviezen waar ik als beginnende onderzoeker veel aan heb gehad. Veel succes in het Radboud UMC!

Rashid, dr. Choliño, ik weet niet meer hoe onze eerste ontmoeting is gegaan maar volgens mij was er vrijwel direct een klik. Dank voor je humor, vergelijkbare obscure interesses, en de daaruit ontstane vriendschap. Je stond altijd klaar voor hulp en advies, en doordat je iets op mij voorliep, kon ik gebruik maken van jouw ervaring. Ik had me geen betere onderzoeks-partner kunnen wensen. Veel succes komend jaar als fellow neuro-interventie!

Bonne, sjefke, bedankt dat je mijn paranimf wil zijn. Ik weet dat je er al jaren naar uitkijkt, nu is het eindelijk zover! We hebben elkaar ontmoet in het onderzoek, dus je zou kunnen zeggen dat de cirkel nu rond is. Uiteraard S.O. naar de Podssee. Dank voor jullie vriendschap, wederzijdse interesse en de mooie momenten.

Geachte leden van de beoordelingscommissie: prof. dr. G.J. Biessels, prof. dr. M.H. Emmelot-Vonk, prof. dr. ir. M.J.P. van Osch, prof. dr. B.K. Velthuis, prof. dr. A. van der Zwan, hartelijk dank voor de tijd en moeite die jullie hebben gestoken in het kritisch lezen en beoordelen van mijn proefschrift. Ook gaat mijn dank uit naar prof. dr. ir. M.A. Viergever voor het voorzitterschap tijdens mijn verdediging, en aan dr. W. van der Zwaag en dr. ir. J.J.M. Zwanenburg voor het deelnemen aan de oppositie.

Graag zou ik kort een aantal mensen willen bedanken die een belangrijke bijdrage hebben geleverd aan de totstandkoming van dit proefschrift. Allereerst dr. Kuijf, beste Hugo, dank voor je technische ondersteuning op allerlei vlakken, maar specifiek voor de MRI segmentaties. Ten tweede, dr. Blom, beste Kim, dank voor je prettige samenwerking, met name binnen de Medea-7T studie. Ten derde, dr. de Bresser, beste Jeroen, het heeft even geduurd maar uiteindelijk kwam ons paper in *Neurobiology of Aging* er toch, en over een innovatief onderwerp! Fourth, dr. Risannen, dear Ina, thanks for all your help and critical remarks on several of my papers and my thesis. We still have one to go! Ten vijfde, dr. ir. Siero en dr. ir. Zwanenburg, beste Jeroen en Jaco, dank voor de uitleg over 7T MRI en neurovasculaire beeldvorming die ik in de eerste jaren van jullie heb gekregen. Ten zesde, dr. Jaarsma-Coes, beste Myriam, dank voor al je hulp bij het WMH shape artikel, zonder jou was het nooit zo goed geworden! Tot slot, prof. dr. Y. van der Graaf, beste Yolanda, dank voor je kritische blik op enkele van mijn artikelen en je bemoedigende woorden.

Vakgroep Radiologie van het HagaZiekenhuis, en specifiek dr. Ad van Gils, dank voor de ruimte die ik heb gekregen om het onderzoek naast mijn opleiding te doen. Ad bedankt voor je interesse en waardering die ik tijdens mijn opleiding heb ervaren.

Vakgroep Radiologie en Nucleaire Geneeskunde van het Martini Ziekenhuis, ik had mij geen leukere groep mensen kunnen wensen om samen een praktijk mee te runnen en het vak uit te oefenen. Bedankt ook voor de hulp die ik heb gekregen bij de laatste loodjes!

Lieve Augustinus en Gea, dank voor al jullie hulp en aanwezigheid de afgelopen jaren. Als jullie er zijn is het altijd gezellig. Jullie zijn echte toppers!

Lieve papa en mama, bedankt voor jullie liefde en steun. Mam, bedankt voor alle keren dat jij, en jullie, hebben opgepast zodat ik kon schrijven, het is een gouden zet geweest. Het is nu klaar, je hoeft me niet meer achter mijn broek aan te zitten.

Lief gezin, wat ik ben ik blij met jullie als mijn liefdevolle basis. Lieve Zeger, ons kleine "gekkie" en part-time klusser. Bedankt voor de lol die je brengt, je fantasie en nieuwsgierigheid. Lieve Rijk, kleine sloopkogel en knuffelbeer. Bedankt voor je vrolijke en tomeloze energie. Lieve Am, het is eindelijk volbracht! De tijd van snordrukken is voorbij. Ik heb veel van je gevraagd de afgelopen jaren en het leek vaak een gebed zonder einde. Bedankt voor je liefde, steun en eindeloze geduld. You're the best! Ik waardeer je enorm om de persoon die je bent en het leven dat we samen delen. Samen maken we er wat moois van!

